
BIOLOGICAL RESPONSE MODELS

Predicting Injury and Mortality of Fish During Downstream Passage through Hydropower Facilities

November 2020

Brett D. Pflugrath, Ryan K. Saylor, Kristin Engbrecht, Robert P. Mueller,
John R. Stephenson, Mark Bevelhimer, Brenda M. Pracheil, Alison H. Colotelo

BIOLOGICAL RESPONSE MODELS

Predicting Injury and Mortality of Fish During Downstream Passage through Hydropower Facilities

November 2020

Brett D. Pflugrath¹, Ryan K. Saylor², Kristin Engbrecht¹, Robert P. Mueller¹, John R. Stephenson¹, Mark Bevelhimer², Brenda M. Pracheil², Alison H. Colotelo¹

¹ Pacific Northwest National Laboratory

² Oak Ridge National Laboratory

Prepared for
the U.S. Department of Energy
under Contract DE-AC05-76RL01830

Available to DOE and DOE contractors from the
Office of Scientific and Technical Information,
P.O. Box 62, Oak Ridge, TN 37831-0062;
ph: (865) 576-8401
fax: (865) 576-5728
email: reports@adonis.osti.gov

Available to the public from the National Technical Information Service
5301 Shawnee Rd., Alexandria, VA 22312
ph: (800) 553-NTIS (6847)
email: orders@ntis.gov <<https://www.ntis.gov/about>>
Online ordering: <http://www.ntis.gov>

DISCLAIMER

This report was prepared as an account of work sponsored by an agency of the United States Government. Neither the United States Government nor any agency thereof, nor Battelle Memorial Institute, nor any of their employees, makes any warranty, express or implied, or assumes any legal liability or responsibility for the accuracy, completeness, or usefulness of any information, apparatus, product, or process disclosed, or represents that its use would not infringe privately owned rights. Reference herein to any specific commercial product, process, or service by trade name, trademark, manufacturer, or otherwise does not necessarily constitute or imply its endorsement, recommendation, or favoring by the United States Government or any agency thereof, or Battelle Memorial Institute. The views and opinions of authors expressed herein do not necessarily state or reflect those of the United States Government or any agency thereof.

U.S. DEPARTMENT OF
ENERGY

Energy Efficiency &
Renewable Energy



 **OAK RIDGE**
National Laboratory

HYDROPASSAGE
U.S. DEPARTMENT OF ENERGY

ABSTRACT

This report describes the U.S. Department of Energy's HydroPASSAGE project efforts to develop and collect biological response models for integration into the Biological Performance Assessment (BioPA) toolset and the Hydropower Biological Evaluation Toolset (HBET). These models help understand how fish are likely to respond during dam passage when exposed to hydraulic and physical stressors associated with turbines and other hydropower structures.

When fish pass through hydropower facilities, they may encounter several stressors, of which the three most common are collision, rapid decompression, and fluid shear. Specialized equipment has been used to develop 99 biological response models for exposure to blade strike, rapid decompression, or fluid shear. The models were gathered from the literature or developed as part of this effort and include models for 31 different species of fish that have various predicted endpoints (i.e., injury or mortality). Among these models, considerable variation in susceptibility to the stressors has been observed from one species to another, and a species' susceptibility to one stressor does not necessarily indicate similar susceptibility to another. Although several species have been examined, it is still unclear how many other species, which may have different morphological traits, may respond to these stressors, so further examination of the different species is needed.

These models can and have been applied in several different cases, often using the BioPA toolset and HBET, to better understand the potential for injury and mortality that may occur during fish passage at hydropower facilities, including specific applications, such as turbine replacement, the installation of new turbines, or changing operations of currently installed turbines. As hydropower is continually developed to meet the electricity needs of society, tools such as HBET and BioPA, used with the integrated biological response models, will aid in the development of technologies and strategies that avoid, minimize, mitigate, or manage environmental effects.



SUMMARY

Since 2014, the U.S. Department of Energy's Water Power Technologies Office has been funding the HydroPASSAGE (formerly BioDE [Biologically Based Design and Evaluation Tools for Hydropower Turbines]) project, which is conducted by Pacific Northwest National Laboratory and Oak Ridge National Laboratory. The project has been developing tools that the hydropower industry can use to mitigate the environmental impacts of dam passage on fish nationwide. These tools include biological response models—or dose-response models—that are used to predict the likelihood that an organism will respond in a particular way to a stimulus or stressor.

Ninety-nine biological response models for exposure to blade strike, fluid shear, or rapid decompression have been developed or collected from the literature, including models for 31 different species of fish.

The biological response models have been collected from the literature about research conducted under the HydroPASSAGE project or developed for integration into two software tools—the Biological Performance Assessment (BioPA) toolset and Hydropower Biological Evaluation Toolset (HBET). The BioPA toolset uses computational fluid dynamics (CFD) models to estimate the likelihood that a fish will be exposed to a stressor at a specific magnitude and applies the biological response models to estimate the probability of injury or mortality. HBET functions similarly to BioPA, but rather than using CFD, HBET uses Sensor Fish—an autonomous sensor package deployed through hydropower facilities to quantify the stressors fish may experience—to predict the stressors and the magnitudes to which fish may be exposed. Biological response models reviewed in this report are focused on predicting the effects of exposure to three main stressors when passing downstream through hydropower facilities—collision, rapid decompression, and fluid shear.

The use of biological response models, integrated with the HBET and BioPA software tools, provides valuable information for the design and operation of hydropower that will promote the safe passage of fish. Ninety-nine biological response models for exposure to blade strike, fluid shear, or rapid decompression have been developed or collected from the literature, including models for 31 different species of fish that have various predicted endpoints (i.e., injury or mortality; see Table S1 at the end of this summary).



Collision refers to instances when fish physically contact part of the structure such as colliding with the stay vanes, wicket gates, or screens and includes blade strike where fish are struck by the turbine runner blade. Biological response models for collision are based on blade strike experiments and models.



Exposure to **rapid decompression** occurs when fish experience a rapid (<1 s) decrease in pressure that has the potential to cause barotrauma (injuries caused by changes in pressure).



Fluid shear refers to instances when fish pass through an interface of water masses that are moving in different directions and/or at different velocities. This interface has a shearing effect that can injure fish.

BLADE STRIKE

Blade strike testing is conducted using a specially designed blade strike apparatus by which anesthetized fish are suspended inside a tank or flume and struck with an artificial turbine blade. Testing is conducted over a range of blade velocities and often using several blades of varying thicknesses. Many of the studies also include additional variables such as the location of the strike on the body and the orientation of the fish when struck. Biological response models are then developed to estimate the probability of injury and mortality as a function of blade velocity and thickness. These models have been developed for nine fish species (Figure S1).

In general, thinner faster blades are more likely to cause injury or mortality in fish than thicker slower blades.

Key findings are as follows:

- Fish have the highest rates of injury and mortality when they are struck by a blade at a 90° angle near the center of the fish (mid-body) and from the side (lateral). However, the probability that a fish will be struck by a turbine blade at different locations and angles is currently unknown and is likely dependent upon turbine design. Consequently, for models for which multiple body locations and strike angles were examined, an even distribution of strike locations and angles is assumed. As more studies are conducted on strike location and fish orientation, the distribution can be adjusted as necessary.
- When blade velocities exceeded 10 m s⁻¹ for blade thicknesses ranging from 26–76 mm, all currently tested species, except for American eel, experienced 100% mortality when struck on the mid-body in the lateral orientation at 90°.
- In general, relatively thinner faster blades are more likely to cause injury or mortality in fish than relatively thicker slower blades. Differences in injury or mortality rates have been observed when blade thickness was changed by as little as 10 mm.

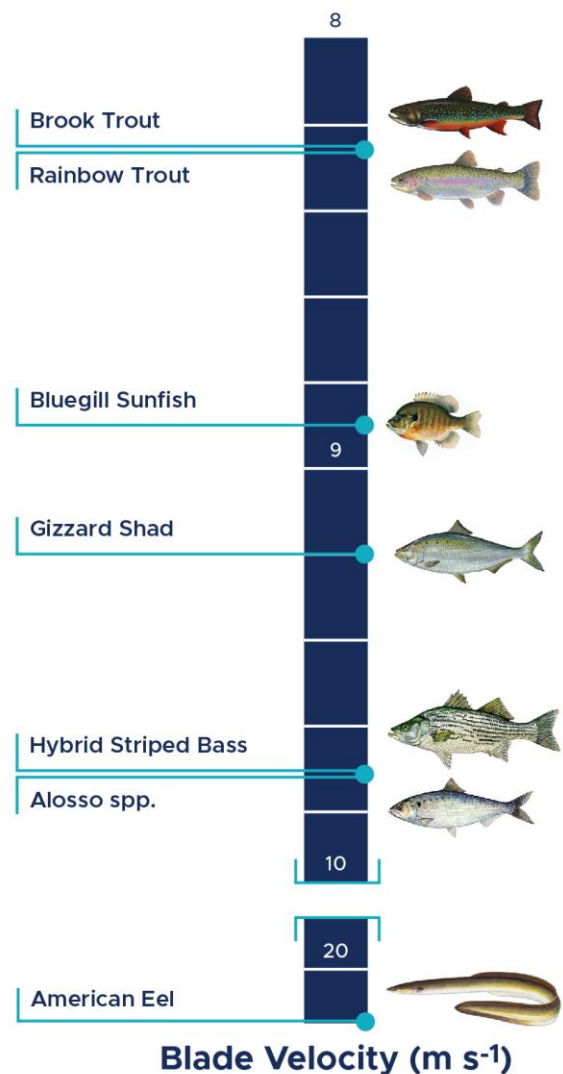


Figure S1. The blade velocity (m s⁻¹) at which LD₅₀ (lethal dose, 50%) occurs (mortality based on fish sustaining injuries likely to cause mortality) for various fish species. More susceptible species are located at the top and less susceptible at the bottom.

Modifications to turbines should include designs that have shallower impact angles, which would likely result in more strikes being deflected away from the fish's center of mass, thereby decreasing the rate of severe injury and increasing passage survival. As further research is conducted on the effects of collision and blade strike on fish, it is recommended that fish orientation and behavior within the turbine environment be further examined, particularly the

likelihood of fish being struck at different angles and orientations. In addition, there is a need to test different types of fish that have different morphological and physiological traits that may make them more or less susceptible to blade strike.

RAPID DECOMPRESSION

To develop biological response models for rapid decompression, fish are placed into water-filled pressure chambers that allow researchers to expose fish to pressures above and below atmospheric pressure and rapidly change the pressure to simulate passage through a hydropower facility. Fish are then examined for injury and mortality so that biological response models can be developed to estimate the probability of injury or mortality related to exposure to different severities of rapid decompression. Forty-six rapid decompression biological response models have been developed for 16 fish species, each of which predicts either the probability of injury, mortal injury (injuries statistically determined to be highly associated with and significant predictors of mortality; Figure S2), or mortality for an individual species.

The swim bladder (a gas-filled buoyancy-regulating organ within the body cavity of a fish) is a major driving force of barotrauma, because gas within the swim bladder expands when a fish is decompressed.

Key findings are as follows:

- These models have demonstrated that different species can have varying susceptibility to rapid decompression (Figure S2).
- In general, as the ratio of pressure change (RPC) increases, fish are more likely to sustain injury or mortality when passing through hydropower facilities. The RPC is the ratio of acclimation pressure (the water

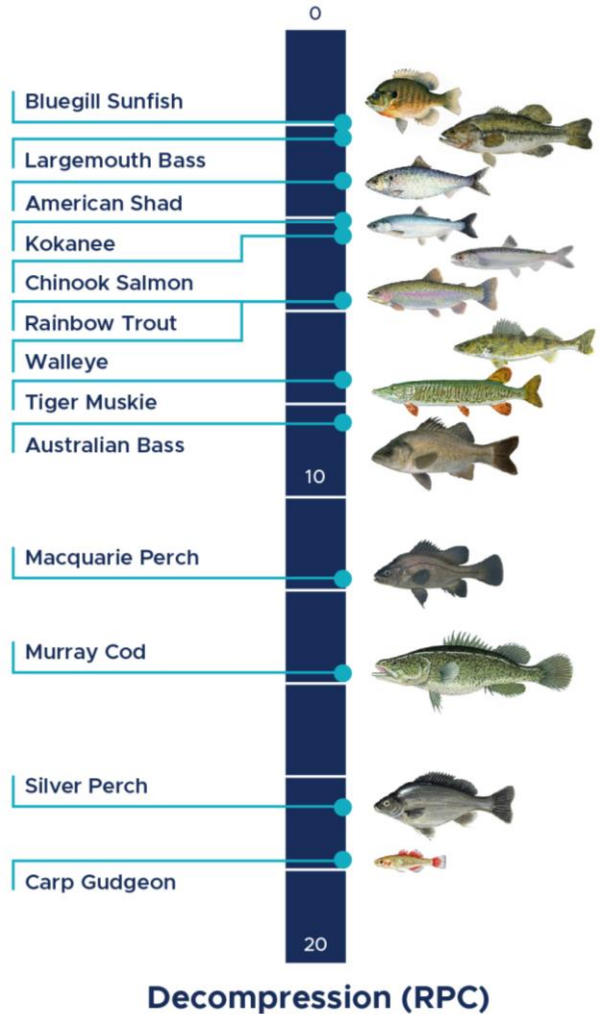


Figure S2. Decompression, quantified as the ratio of pressure change (RPC), at which LD₅₀ (lethal dose, 50%) occurs (mortality based on fish sustaining injuries likely to cause mortality) for various fish species. More susceptible species are located at the top and less susceptible at the bottom.

pressure at which a fish resides and to which it is acclimated prior to decompression) to nadir pressure (the lowest pressure the fish experiences during decompression). RPC increases as the nadir pressure decreases and/or the acclimation pressure increases.

- The swim bladder (a gas-filled buoyancy-regulating organ within the body cavity of a fish) is a major driving force of barotrauma, because gas within the swim bladder expands when a fish is decompressed. There are three general categories of fish related to swim

bladders—those that have open swim bladders (physostomous), those that have closed swim bladders (physoclistous), and those that do not have swim bladders.

- For fish species without swim bladders (e.g., common sole, Pacific lamprey, and western brook lamprey), barotrauma is not likely to occur as a result of the rapid decompression associated with passage through hydropower facilities.
- Physoclistous fish (e.g., largemouth bass, and bluegill) cannot rapidly remove gas from the swim bladder and are often more susceptible to barotrauma than physostomous fish (e.g., Chinook salmon, American eel, and American shad), which are able to rapidly expel gas from the swim bladder. However, research indicates some physoclistous species, such as the tested Australian species, are hardier and although they may be more likely to be injured, they are able to sustain those injuries without mortality.

As research to better quantify the effects of rapid decompression on fish continues, several topics need to be addressed. These topics include several variables that may affect a fish's susceptibility to rapid decompression such as the effect of multiple exposures, rates of decompression, temperature, swimming activity during decompression, and reproductive success after exposure to rapid decompression. Research is also needed on additional species that have traits that are morphometrically different than those previously examined so that inferences can be made about other species that possess these traits but have not been tested. These include cyprinids, the most diverse family of fish, which have been minimally researched. Further understanding of these variables will help turbine designers and hydropower owners and operators design and operate hydropower in ways that promote safe fish passage and are tailored to the needs of local fish species.

FLUID SHEAR

Biological response models for fluid shear are developed by introducing fish into a shear

environment created by a water jet in a large tank. Testing is done using a range of jet velocities, and fish are examined after exposure to fluid shear for injuries and mortality. Biological response models are then developed to predict the probability of injuries or mortality for individual fish species as a function of strain rate (change in velocity over distance) or acceleration (change in velocity over time). Forty-five fluid shear biological response models have been developed for 16 fish species (19 when including subspecies).

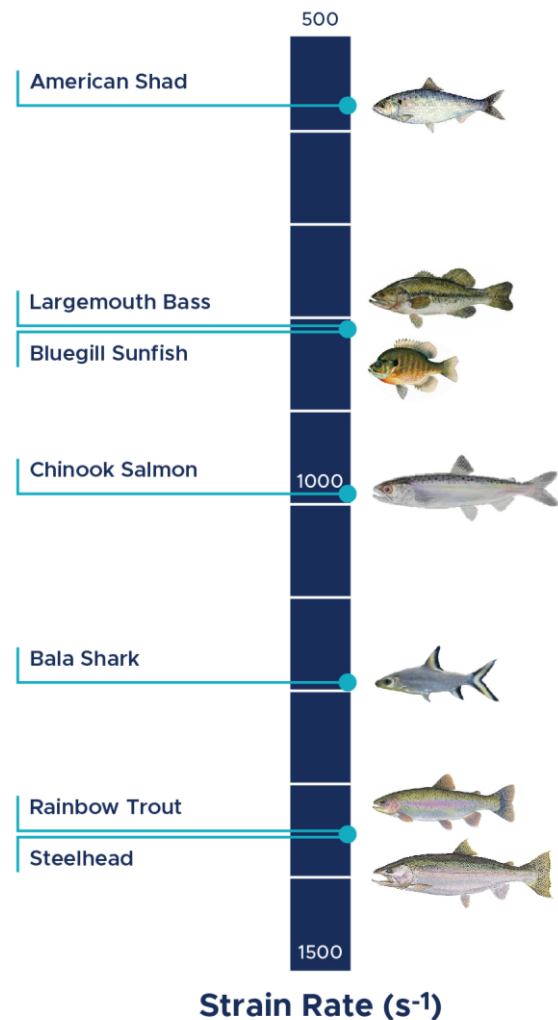


Figure S3. The strain rate (s⁻¹) at which LD₅₀ (lethal dose, 50%) occurs (mortality based on fish sustaining injuries likely to cause mortality) for various fish species. More susceptible species are located at the top and less susceptible at the bottom.

Fish are more susceptible to injury or mortality as strain rate or acceleration increases.

Key findings are as follows:

- Overall, fish are more susceptible to injury or mortality as strain rate or acceleration increases.
- Response to fluid shear can vary significantly between different species (Figure S3).
 - Eel and lamprey have little to no susceptibility to fluid shear, because they have no or very small integrated scales and lack or have reduced sizes of vulnerable structures regularly injured by shear such as opercula, gills, and eyes.
 - Fish with elongated, fusiform (i.e., torpedo-shaped) bodies, such as salmonids, tend to experience increased bruising and lacerations, and fish laterally compressed with truncated bodies, such as bluegill and American shad, appear to be more susceptible to descaling and operculum damage.

Testing additional, more morphologically diverse fish would help acquire deeper understanding of how specific traits (such as scale morphology and body shape) affect the susceptibility of different fish groups. Future research should focus on the effects of multiple fluid shear exposures, selecting appropriate surrogates for testing, examining more of the physiological effects caused by fluid shear, and understanding the indirect effects of fluid shear, like potential increased predation.

APPLICATION

Biological response models incorporated into HBET and the BioPA toolset can and have been applied in several different cases to better understand the potential for injury and mortality that may occur during fish passage at hydropower facilities. This includes specific applications, such as turbine replacement, the installation of new turbines, or changing

operations for currently installed turbines. Although these tools were primarily developed for use with turbines, they can also be applied for any other instances where exposure to stressors may be of concern, such as spillways, weirs, and bypasses at both powered and non-powered dams.

CONCLUSIONS

Several general conclusions prevailed throughout the research:

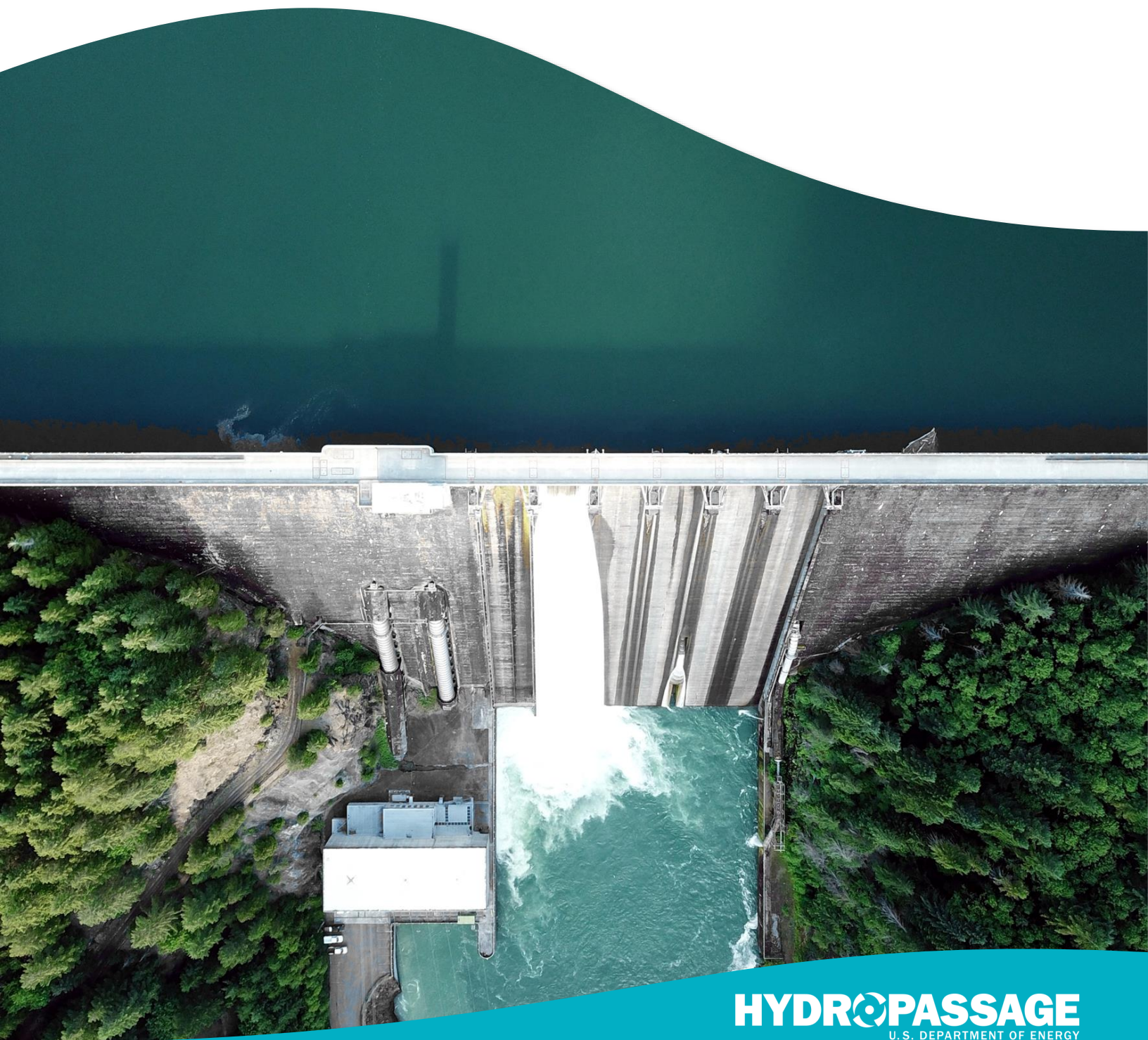
- Considerable variation in susceptibility from one species to another has been reported for fish exposure to blade strike, rapid decompression, and fluid shear.
- A fish species' susceptibility to one stressor (i.e., blade strike, rapid decompression, or fluid shear) does not necessarily indicate similar susceptibility to another stressor.
- Biological response models can and have been applied through HBET and the BioPA toolset for numerous situations to accurately characterize the potential for injury and mortality to occur during fish passage through turbines and other water management structures.
- Future research related to these stressors is recommended for additional species (such as cyprinids) that have different morphological traits and to determine how different environmental and physical variables may affect the occurrence or severity of injuries caused by these stressors. Morphological traits that are of particular importance for one stressor do not necessarily apply to other stressors; for instance, a swim bladder is very important for rapid decompression, whereas scale and operculum morphology is very important for fluid shear.

As hydropower is continually developed to meet the electricity needs of society, tools such as HBET and the BioPA toolset, used with the integrated biological response models (Table S1), will aid in the development of technologies and strategies that avoid, minimize, mitigate, or manage environmental effects.

Table S1. List of all the species for which a biological response model has been developed for blade strike, rapid decompression, or fluid shear. The table includes citations for the models or for the data from which the models were derived.

Species	Scientific Name	Model	Citation
American eel	<i>Anguilla rostrata</i>	Blade Strike	Saylor et al. (2019)
		Decompression	Pflugrath et al. (2019)
		Fluid Shear	Pflugrath et al. (in prep-c)
American shad and blueback herring	<i>Alosa</i> spp.	Blade Strike	Saylor et al. (2020)
American shad	<i>Alosa sapidissima</i>	Decompression	Pflugrath et al. (2020b)
		Fluid Shear	Pflugrath et al. (2020b)
Atlantic herring	<i>Clupea harengus</i>	Fluid Shear	Turnpenny et al. (1992)
Atlantic salmon	<i>Salmo salar</i>	Fluid Shear	Turnpenny et al. (1992)
Australian bass	<i>Percales novemaculeata</i>	Decompression	Pflugrath et al. (2018)
Bala shark	<i>Balantiocheilos melanopterus</i>	Fluid Shear	Baumgartner et al. (2017)
Blue gourami	<i>Trichopodus trichopterus</i>	Fluid Shear	Colotelo et al. (2018)
Bluegill & pumpkinseed	<i>Lepomis macrochirus</i> and <i>L. gibbosus</i>	Fluid Shear	Engbrecht et al. (in prep)
Bluegill sunfish	<i>Lepomis macrochirus</i>	Blade Strike	Saylor et al. (2019)
		Decompression	Pflugrath et al. (in prep-b)
Brook trout	<i>Salvelinus fontinalis</i>	Blade Strike	Saylor et al. (2020)
Brown Trout	<i>Salmo trutta</i>	Fluid Shear	Turnpenny et al. (1992)
Carp gudgeon	<i>Hypseleotris</i> sp.	Decompression	Pflugrath et al. (2018)
Chinook salmon	<i>Oncorhynchus tshawytscha</i>	Decompression	Brown et al. (2012a)
		Fluid Shear	Neitzel et al. (2004)
Coho salmon	<i>Oncorhynchus kisutch</i>	Fluid Shear	Johnson (1972)
Common sole	<i>Solea solea</i>	Decompression	Turnpenny et al. (1992)
		Fluid Shear	Turnpenny et al. (1992)
European eel	<i>Anguilla anguilla</i>	Fluid Shear	Turnpenny et al. (1992)
Gizzard shad	<i>Dorosoma cepedianum</i>	Blade Strike	Saylor et al. (2020)
Golden gray mullet	<i>Chelon aurata</i>	Decompression	(Turnpenny et al. 2000)
Hybrid striped bass	<i>Morone saxatilis</i> x <i>M. chrysops</i>	Blade Strike	Bevelhimer et al. (2019)
Iridescent shark	<i>Pangasianodon hypophthalmus</i>	Fluid Shear	Colotelo et al. (2018)
Kokanee	<i>Oncorhynchus nerka</i>	Decompression	Beirão et al. (2020)
Largemouth bass	<i>Micropterus salmoides</i>	Decompression	Pflugrath et al. (in prep-b)
		Fluid Shear	Engbrecht et al. (in prep)
Macquarie perch	<i>Macquaria australasica</i>	Decompression	Pflugrath et al. (in prep-a)
Murray cod	<i>Maccullochella peelii</i>	Decompression	Pflugrath et al. (2018)
Pacific lamprey	<i>Entosphenus tridentatus</i>	Decompression	Colotelo et al. (2012)
		Fluid Shear	Moursund et al. (2000)
Rainbow trout/ steelhead	<i>Oncorhynchus mykiss</i>	Blade Strike	EPRI (2011, 2008); Saylor et al. (2020); Amaral et al. (2020)
		Decompression	Beirão et al. (2020)
		Fluid Shear	Neitzel et al. (2004)
Silver perch	<i>Bidyanus bidyanus</i>	Decompression	Pflugrath et al. (2018)

Species	Scientific Name	Model	Citation
Tiger muskie	<i>Esox masquinongy</i> x <i>E. lucius</i>	Decompression	Brown et al. (2016)
Walleye	<i>Sander vitreus</i>	Decompression	Brown et al. (2016)
Western brook lamprey	<i>Lampetra planeri</i>	Decompression	Colotelo et al. (2012)
White sturgeon	<i>Acipenser transmontanus</i>	Decompression	Brown et al. (2016)



ACKNOWLEDGMENTS

Funding for this report was provided by the U.S. Department of Energy, Energy Efficiency and Renewable Energy, Water Power Technologies Office under the HydroPASSAGE project (previously called BioDE). The authors' views expressed in this publication do not necessarily reflect the views of Water Power Technologies Office or the United States government. Pacific Northwest National Laboratory is operated for U.S. Department of Energy by Battelle Memorial Institute under Contract DE-AC05-76RLO 1830.

The authors thank Lara Aston, Brandon Boehnke, Lysel Garavelli, Megan Nims, David Geist, and Julie Snook of Pacific Northwest National Laboratory, and Dustin Sterling, Allison Fortner, Kendra Deck of Oak Ridge National Laboratory for contributing their diverse professional expertise to the success of this study. All research under the HydroPASSAGE project was conducted in compliance with a protocol approved by PNNL or ORNL Institutional Animal Care and Use Committee.



ACRONYMS AND ABBREVIATIONS

3D	three-dimensional
BioPA	Biological Performance Assessment
CFD	Computational fluid dynamic
DOE	U.S. Department of Energy
FL	fork length
FSTF	Fluid Shear Testing Facility
GUI	graphical user interface
HBET	Hydropower Biological Evaluation Toolset
IUCN	International Union for Conservation of Nature
LD ₅₀	Lethal Dose, 50%
LRP	log ratio pressure
NSW DPI	New South Wales Department of Primary Industry
ORNL	Oak Ridge National Laboratory
PNNL	Pacific Northwest National Laboratory
RPC	Ratio of pressure change
RPM	rotations per minute
spp.	abbreviation for species that indicates multiple known species
TDG	total dissolved gas
TL	total length
U.S.	United States
USACE	U.S. Army Corps of Engineers
WPTO	Water Power Technologies Office

CONTENTS

Abstract.....	ii
Summary	iii
Acknowledgments.....	x
Acronyms and Abbreviations	xi
Contents	xii
1.0 Introduction	1
1.1 Purpose and Scope.....	1
1.2 Background	2
1.3 Report Contents and Organization.....	3
2.0 Predicting the Effects of Exposure to Blade Strike on Fish.....	5
2.1 Blade Strike through Turbines.....	6
2.1.1 Turbine Type	6
2.1.2 Blade Characteristics.....	7
2.1.3 Site of Impact.....	9
2.2 Developing Biological Response Models for Blade Strike	12
2.2.1 Mortality Rates.....	12
2.2.2 Developing Biological Response Models for Blade Strike.....	12
2.2.3 Whole-fish Biological Response Model Derivation	13
2.2.4 Blade Strike Biological Response Models for the BioPA Toolset and HBET	17
2.2.5 Fish Species Examined for Susceptibility to Blade Strike	18
2.2.6 Probability of Mortality Due to Blade Strike	22
2.2.7 Use of Surrogacy for Blade Strike	23
2.3 Traits Affecting Susceptibility to Blade Strike	24
2.3.1 Fish Shape	24
2.3.2 Center of Gravity	25
2.3.3 Biomechanical Traits	25
2.3.4 Fish Size.....	26
2.4 Blade Strike Discussion	29
2.4.1 Data Limitations.....	29
2.4.2 Future Research Needs for Blade Strike.....	30
2.5 Blade Strike Conclusions	31
3.0 Predicting the Effects of Exposure to Rapid Decompression on Fish.....	33
3.1 Decompression Through Turbines and Other Hydro Structures	34
3.2 Developing Biological Response Models for Rapid Decompression.....	35
3.2.1 Fish Species Examined for Susceptibility to Rapid Decompression	36

3.2.2	Rapid Decompression Biological Response Models	51
3.3	Traits Affecting Barotrauma.....	56
3.3.1	Swim Bladder Morphology.....	56
3.3.2	Life Stage	58
3.3.3	Rapid Decompression Surrogacy.....	58
3.4	Rapid Decompression Discussion.....	59
3.4.1	Limitations of Current Rapid Decompression Data.....	59
3.4.2	Future Research Needs for Rapid Decompression	59
3.5	Rapid Decompression Conclusions	62
4.0	Predicting the Effects of Exposure to Fluid Shear on Fish.....	64
4.1	Fluid Shear Through Turbines and Other Hydro Structures.....	65
4.2	Developing Biological Response Models for Exposure to Fluid Shear	65
4.2.1	Fish Species Examined for Susceptibility to Fluid Shear.....	66
4.2.2	Fluid Shear Biological Response Models	74
4.3	Traits and Variables Affecting Shear-related Trauma	80
4.3.1	Morphology	81
4.3.2	Scales.....	81
4.3.3	Eyes and Opercula	81
4.3.4	Body Shape and Overall Trends	82
4.3.5	Life Stage	82
4.3.6	Fish Length.....	83
4.3.7	Fish Orientation and Susceptibility During Exposure.....	83
4.3.8	Fluid Shear Surrogacy	85
4.4	Fluid Shear Discussion.....	85
4.4.1	Fluid Shear Limitations of the Current Data.....	85
4.4.2	Future Research Needs for Fluid Shear	86
4.5	Fluid Shear Conclusions	86
5.0	Application of Biological Response Mode	88
5.1	HydroPASSAGE Tool Example.....	88
6.0	Conclusion	92
7.0	References.....	93
Appendix A – Experimental Apparatuses		A.1

FIGURES

Figure S1.	The blade velocity (m s^{-1}) at which LD_{50} (lethal dose, 50%) occurs (mortality based on fish sustaining injuries likely to cause mortality) for various fish species.	iv
Figure S2.	Decompression, quantified as the ratio of pressure change (RPC), at which LD_{50} (lethal dose, 50%) occurs (mortality based on fish sustaining injuries likely to cause mortality) for various fish species.	v
Figure S3.	The strain rate (s^{-1}) at which LD_{50} (lethal dose, 50%) occurs (mortality based on fish sustaining injuries likely to cause mortality) for various fish species.	vi
Figure 1.	Sensor Fish (right) and Sensor Fish Mini (left).	2
Figure 2.	Flow chart of the most common applications of the HBET and BioPA software toolsets.	4
Figure 3.	Diagram of a Francis and a Kaplan turbine.	7
Figure 4.	High-speed video images of subadult rainbow trout being struck with a 26 (top panel) and 52 mm (bottom panel) turbine blade.	8
Figure 5.	Simplified diagram showing blade strike impact characteristics related to the fish itself including (A) body location, (B) body orientation, and (C) angle of impact.	10
Figure 6.	Diagram of potential blade strike impact angles according to the body location (A) and orientation (B) of the fish.	11
Figure 7.	Diagram depicting the 12 major areas that we defined to represent all location and orientation possibilities during derivation of our whole-fish dose-response model for each species.	13
Figure 8.	Example diagram, using hybrid striped bass, depicting nine mathematical models created to represent the 12 major body areas defined on most species of fish.	14
Figure 9.	Graph depicting the whole-fish dose-response curve, i.e., probability of mortality versus strike velocity (m s^{-1}), for hybrid striped bass.	16
Figure 10.	Example of the curvilinear blade strike model (gray line) fit to data exported from the whole-fish biological response model (black circles).	18
Figure 11.	A summary plot of all species dose-response curves available to date for mid-body lateral strikes at 90° with a 52 mm blade.	20
Figure 12.	Comparison of the curvilinear biological response models for various species that have been integrated into the BioPA toolset and HBET.	24
Figure 13.	Results of blade strike impact trials on 10 juvenile (small, $\text{TL} = 10.1\text{--}14.9$ cm; top panel) and 10 subadult (large $\text{TL} = 20.1\text{--}31.6$ cm; bottom panel) rainbow trout.	26
Figure 14.	Comparison of L/t ratio for all published rainbow trout data, presented with original data from EPRI (2008).	28
Figure 15.	Estimated 95% confidence intervals versus the relative sample size of each treatment group.	30
Figure 16.	Median (solid dots) and range (open dots) of nadir pressures recorded during Sensor Fish releases through Francis turbines (dark blue) at Arrowrock, Detroit, and Cougar Dams, and an advanced hydropower Kaplan turbine (light blue) at Wanapum Dam.	35

Figure 17. Neutrally buoyant (black line) juvenile Chinook salmon are more susceptible to rapid decompression than negatively buoyant (gray line) due to the amount of gas held within the swim bladder.	40
Figure 18. The results from three studies conducted on the susceptibility of largemouth bass to rapid decompression reported rates.	43
Figure 19. Probability of injury biological response models for rapid decompression using coefficients from Table 11 with Equation (12).	52
Figure 20. Probability of mortal injury biological response models for rapid decompression using the coefficients from Table 12 and Equation (12).	54
Figure 21. Probability of immediate mortality biological response models for rapid decompression using the coefficients from Table 13 and Equation (12).	56
Figure 22. The relationship between pressure reduction and gas volume according to Boyle's law under constant temperature.	62
Figure 23. Jet velocity correlates to strain rate and acceleration measured by Sensor Fish for exposure to fluid shear.	67
Figure 24. Probability of injury biological response models for exposure to fluid shear using the coefficients from Table 14 and Equation (14).	76
Figure 25. Probability of major injury biological response models for exposure to fluid shear using the coefficients from Table 15 and Equation (14).	78
Figure 26. Probability of mortality biological response models for exposure to fluid shear using the coefficients from Table 16 and Equation (14).	80
Figure 27. Probability of exposure distributions of rapid decompression (nadir), fluid shear (strain rate), and collision (impact velocity) for fish passing through generalized Kaplan (gray bars) and Francis (light blue bars) turbines.	89
Figure 28. Comparison of the probability of adverse passage for bluegill, rainbow trout, and American eel passing through a generic Kaplan and Francis turbine.	90
Figure 29. BioPA PQI scores (relative performance scores) for bluegill, rainbow trout, and American eel passing through a generic Kaplan and Francis turbine.	91

TABLES

Table S1.	List of all the species for which a biological response model has been developed for blade strike, rapid decompression, or fluid shear.	viii
Table 1.	Detailed summary of our whole-fish dose-response model produced for each species.	16
Table 2.	State of the science for the blade strike-related level of understanding of each species.	19
Table 3.	Multiple linear regression model coefficients for predicting the probability of mortal injury as a function of strike velocity (m s^{-1}) and L/t ratio (Fish length to blade thickness ratio) for rainbow trout. Coefficients are to be used for the various L/t ratios with Equation (8).	22
Table 4.	Logistic regression biological response models for two species that have been integrated into the BioPA toolset and HBET. Coefficients are to be used with Equation (9). Models that do not use L/t ratio as a predictor variable do not have a coefficient for β_2 .	23
Table 5.	Curvilinear biological response models for various species that have been integrated into the BioPA toolset and HBET. Coefficients are to be used with Equation (10).	23
Table 6.	Percent mortality of bluegill resulting from exposure to simulated turbine passage pressures at various acclimation and nadir pressures and total dissolved gas levels. Sixty fish were tested under each treatment.	38
Table 7.	Percent mortality of fall Chinook salmon resulting from exposure to simulated turbine passage pressures at various acclimation and nadir pressures, and total dissolved gas levels. Sixty fish were tested under each treatment. Recreated from Abernethy et al. (2001).	39
Table 8.	Mortality rates reported by Hogan (1941) for various fish species exposed to a vacuum simulating passage through a siphon tube.	47
Table 9.	Mortality rates reported by Tsvetkov et al. (1972) for several species exposed to varying rapid decompression treatments. Fish were decompressed to surface pressure (≈ 101 kPa) from acclimation pressures ranging from 200–700 kPa.	48
Table 10.	Mortality rates and rates for specific observed injuries, including swim bladder rupture (SB rupture, eye hemorrhage (eye hem), and fin hemorrhage (fin hem), reported by Turnpenny et al. (1992) for several fish species exposed to rapid decompression simulating passage through a tidal power turbine.	50
Table 11.	Coefficients for rapid decompression biological response models predicting the probability of injury. Model coefficients to be used with Equation (12).	51
Table 12.	Coefficients for rapid decompression biological response models predicting the probability of mortal injury. Model coefficients to be used with Equation (12).	53
Table 13.	Coefficients for rapid decompression biological response models predicting the probability of immediate mortality. Model coefficients to be used with Equation (12).	55
Table 14.	Probability of injury due to exposure to fluid shear (strain rate: s^{-1}) biological response model coefficients to be used with Equation (14).	75
Table 15.	Probability of major injury due to exposure to fluid shear biological response model coefficients to be used with Equation (14).	77
Table 16.	Probability of mortality due to exposure to fluid shear biological response model coefficients to be used with Equation (14).	79



1.0 INTRODUCTION

Since 2014, the HydroPASSAGE project (formerly the Biologically Based Design and Evaluation Tools for Hydropower Turbines [BioDE] project) has been funded by the U.S. Department of Energy's (DOE's) Water Power Technologies Office (WPTO) to provide information and tools to increase fish survival through turbines and other hydropower structures across the United States (U.S.) and around the world. This research builds on more than 25 years of DOE-supported basic and applied research aimed at understanding the impacts of hydropower on fish. This research and development project is a collaboration between engineers and biologists at the DOE's Pacific Northwest National Laboratory (PNNL) and Oak Ridge National Laboratory (ORNL).

As part of this project, numerous biological response models have been developed for several fish species. These models can be applied as stand-alone models, but under this

project, the primary intention of developing and collecting these models is for their integration into two software tools: the Hydropower Biological Evaluation Toolset (HBET) and the Biological Performance Assessment (BioPA). These tools enable the quantification of the physical stressors at hydropower dams and assess fish biological responses to these stressors. Ultimately, these tools support downstream passage evaluations to compare the impacts of different hydropower turbine designs and operation schemes on fish species of concern.

1.1 PURPOSE AND SCOPE

This report provides a review of the research conducted on the development of biological response models to predict the probability of injuries or mortality when fish are exposed to stressors during passage through turbines or other hydropower structures. It is based on a

review of the available literature and research conducted under the HydroPASSAGE project.

1.2 BACKGROUND

When fish pass downstream through hydropower facilities, either through turbines, spillways, or other pathways, they may be exposed to physical and hydraulic stressors. Three main stressors are of particular concern: collision, rapid decompression, and fluid shear (Čada 1997). Collision refers to instances in which fish physically contact part of the structure, such as colliding with the stay vanes, wicket gates, or screens, and includes blade strikes during which fish are struck by the turbine runner blade. Exposure to rapid decompression occurs when fish experience a rapid (<1 s) decrease in pressure and it has the potential to cause barotrauma (injuries caused by changes in pressure). Fluid shear refers to instances during which fish pass through an interface of water masses that are moving in different directions and/or velocities. This interface has a shearing effect that can injure fish. These three stressors have the potential to not only cause direct mortality because of injuries sustained during exposure to the stressor, but also indirect mortality by increasing fish susceptibility to disease and predation (Pracheil et al. 2016a).

To better understand the potential for turbines and other structures within a hydropower facility to cause fish injury or mortality, two software tools have been developed: HBET (Hou et al. 2018) and the BioPA toolset (Richmond et al. 2014b; Richmond et al. 2014a). These tools have a similar function because they combine the biological response models with the probability that fish will be exposed to various magnitudes of a stressor when passing the hydropower facility. The key difference between the two tools is that HBET relies on *in situ* data gathered from Sensor Fish, whereas the BioPA toolset applies data exported from computational fluid dynamic (CFD) models.

The Sensor Fish (Figure 1) is an autonomous sensor package that is deployed through a hydropower structure and rapidly records various physical events that affect the device, such as

pressure, three-dimensional (3D) acceleration, and 3D rotational velocity, which can be used to predict the likelihood that fish will be exposed to the three focal stressors (Deng et al. 2014). The Sensor Fish was designed to have a size and density similar to a yearling salmon smolt and is nearly neutrally buoyant in freshwater. A smaller version of the Sensor Fish, known as Sensor Fish Mini, was recently developed for studying small hydropower turbines with small clearances between the turbine blades (Salalila et al. 2019).



Figure 1. Sensor Fish (right) and Sensor Fish Mini (left).

The BioPA toolset acquires similar data by running thousands of particle trajectories through a CFD model and collecting the physical data from each trajectory for rapid decompression, strike or collision, fluid shear, and turbulence (Richmond et al. 2014b). Once exposure distributions are produced by the software tools for each focal stressor, the distributions are combined with biological response models to predict the probability that injury or mortality will occur for fish passing the structure. These probabilities are limited to each stressor because the compounding effect of exposure to multiple stressors or repeated sublethal exposures is currently unknown. The BioPA toolset does, however, allow for combining the probabilities using adjustable weighting to create a relative performance score. The results for individual stressors from each toolset and the performance score from the BioPA toolset can be used to make relative comparisons. Several types of comparisons can be made using these tools, such as comparing different designs or

operations for turbines, spillways, or other hydropower facilities (e.g., fish bypass systems).

The biological response models are a key component of each toolset and are established for individual species because different species have been observed to respond very differently to the stressors. The response models are developed by conducting laboratory testing on fish across a range of magnitudes for each stressor. After the fish are exposed, they are examined for behavioral changes, injuries, and mortality. Examination data (observation and necropsy) are then used to develop the biological response models to predict the probability of various endpoints of injury and mortality. The development of these biological response models for blade strikes, rapid decompression, and fluid shear are detailed in this report.

There are a number of ways that these biological response models can be applied using HBET and the BioPA toolset to assess the impacts of hydropower development on fish in hopes of using the resulting information to reduce those impacts (Figure 1). The most common applications are for when facilities are being upgraded, such as when new or replacement turbines are being installed, and when facility operations may be altered. For instance, in the case of replacing a turbine, the BioPA toolset can be used to compare the previously installed turbine design with new turbine designs. Once the new turbine is installed, HBET can be used to compare Sensor Fish results related to the

previously installed turbine with those related to the newly installed turbine. In addition, either of these tools can be used to compare different operations for a single turbine. If CFD models have been generated for the turbine, the BioPA toolset could be run for different operations. Otherwise, Sensor Fish can be deployed while operating the turbine under the desired settings and the results of each operation can be compared using HBET. These tools can also be used for cases in which the status of the current operation may need to be confirmed. This method has been applied at Ice Harbor Dam on the Snake River in Washington State, where a newly designed turbine was examined using HBET to confirm design improvements for fish passage.

1.3 REPORT CONTENTS AND ORGANIZATION

This report summarizes the work conducted under the HydroPASSAGE project (Section 1.0) to develop or assemble biological response models for fish exposed to blade strike (Section 2.0), rapid decompression (Section 3.0), and fluid shear (Section 4.0). An example of the application of these models using the software tools developed under the HydroPASSAGE project is provided in Section 5.0, and conclusions gathered from this assemblage of research are included in Section 6.0. In addition, descriptions of the apparatuses used to collect experimental data to develop the biological response models are included in Appendix A.

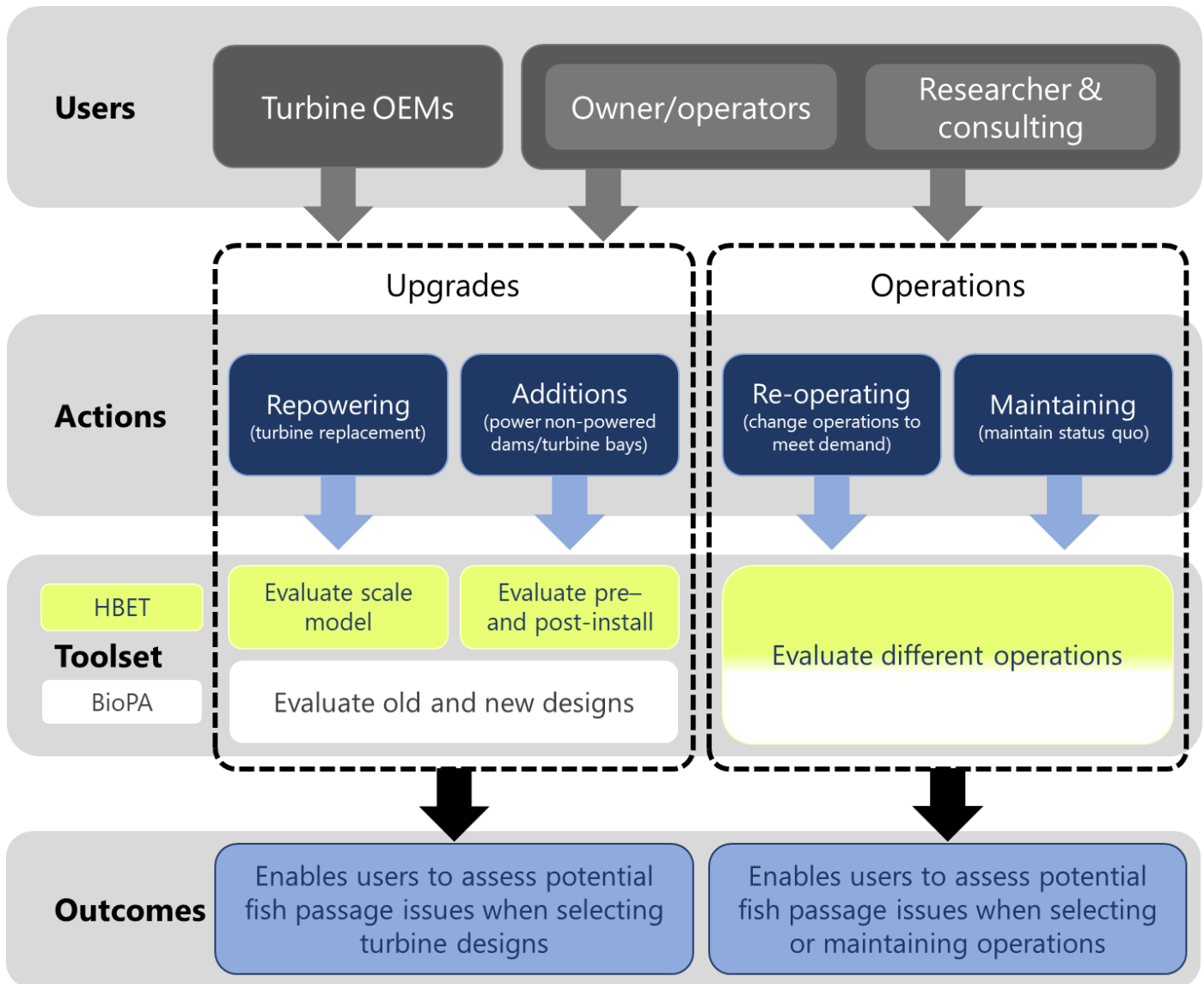


Figure 2. Flow chart of the most common applications of the HBET and BioPA software toolsets. This chart shows how various users would apply the software tools for different hydropower development needs.



2.0 PREDICTING THE EFFECTS OF EXPOSURE TO BLADE STRIKE ON FISH

Chapter authors: Ryan Saylor, Mark Bevelhimer, and Brenda Pracheil

Turbine blade strike can be a significant source of fish injury and mortality during passage through hydroelectric turbines, particularly for larger fish (Coutant and Whitney 2000; Pracheil et al. 2016a). Physical blade strike discussed here is considered separate from other collisions of the fish with non-rotating structures (e.g., stay vanes, wicket gates) or pinching between the tip of a turbine blade runner and a discharge ring wall. Field trials have confirmed that fish passing through turbines experience a wide range of traumatic injuries (Mathur et al. 1996; Mathur et al. 2000; Hostetter et al. 2011; Mueller et al. 2017), but linking the exact stressor to each injury is not often possible because some stressors

cause similar injuries. For example, scale and mucus loss may result from both shear stress and blade strike impact or exophthalmia, which has been linked to exposure to fluid shear, barotrauma, and blade strike impact. Scale turbine models are also used to test passage survival, and the ability to control passage conditions may provide additional insights about passage injuries not possible from field trials (Amaral et al. 2003; Cook et al. 2003; Hecker and Cook 2005). Amaral et al. (2003) were able to remove wicket gates from their model so that injuries and mortalities were more directly linked to the physical impacts of the runner. Injuries included contusions, lacerations, amputations,

eye damage, and descaling, but contusions were the most common injury observed in all species tested (Amaral et al. 2003). All injuries for both field and scale-model hydropower studies are limited to post passage assessments, which makes it difficult to determine the exact cause of death. Furthermore, field and scale-model studies are unable to control every aspect of the exposure conditions (stressor magnitude), including exposure to non-blade strike stressors. Therefore, inferences about fish injuries in these studies must be confirmed by controlled laboratory experiments that include internal necropsies.

Controlled laboratory experiments involving blade strike form the bulk of current knowledge about injuries caused by blade strike impact. Early insights from laboratory studies confirmed that scale and mucus loss, contusions, and eye trauma could be linked to blade strike impacts (Turnpenny et al. 1992; Turnpenny 1998). Other signs of severe trauma included internal hemorrhaging, crushing of the body, and spinal damage assumed to be fractures (Turnpenny et al. 1992). Likewise, additional research performed more than 15 years later found similar external injuries, confirmed contusions were the most prevalent, and also observed lacerations (EPRI 2008). More detailed injury descriptions have now been published and also include internal necropsies to better link mortality with a cause of death. Similar external injuries were also observed in these studies, but hyperpigmentation near the impact site, damage to the gills, and eye amputation were noted as well (Bevelhimer et al. 2019; Saylor et al. 2019; Saylor et al. 2020). Nearly every internal organ has at some point been observed to have signs of trauma, including hemorrhaging, clotting, lacerations, and in severe cases avulsion or rupture. The most common organ injuries were linked to the liver, heart, swim bladder, and kidney; damage to other organs has occurred but is rare (Saylor et al. 2019; Bevelhimer et al. 2019). Internal hemorrhaging and clotting were also observed frequently and are likely linked with other trauma observed in test fish. Skeletal fracture of the ribs was common but nonlethal, whereas vertebral fractures and internal decapitation (separation of atlas vertebrae from the cranium) occurred frequently

and were often associated with moribund behavior or immediate mortality (Saylor et al. 2019; Saylor et al. 2020). In most cases, rib and vertebral fractures also led to more severe damage to the kidney and surrounding musculature (Bevelhimer et al. 2019). The most severe injuries noted were in fish that had up to three or more separate vertebral fractures, which may also have included internal decapitation. While many injuries have been noted, nearly every fish that was considered dead had a broken vertebral column, suggesting these fractures were the most likely cause of death. No other general injury trends were apparent among species that have been examined during laboratory testing, and species-specific descriptions are provided later (Section 2.2.5).

2.1 BLADE STRIKE THROUGH TURBINES

The type of turbines and the characteristics of turbine blades are linked to rates of fish injury and mortality.

The design characteristics of the Francis turbine fixed runner blades—that feature radial water flow entering and axial flows exiting the turbine and varying blade leading-edge thickness and velocity along the meridional length of the runner—are likely why Francis turbines have the highest incidences of fish passage mortality; estimates of mortality for Francis turbines can be as low as 5% but as high as 75% for some projects.

2.1.1 TURBINE TYPE

Rates of injury and mortality among fish are closely linked to the type of turbine installed at each hydroelectric dam, and the Francis and Kaplan turbines represent the most common types installed in the U.S. (Uria-Martinez et al. 2018). Francis turbines (Figure 3) have the most installed capacity to date (~66%), but have been installed less frequently at new hydropower plants (~33%; Uria-Martinez et al. 2018). Francis turbines are ideally installed where there is

between 10 to 550 m or more of head and are best for systems with water flows between 0.5 to 25 m³ s⁻¹ (Ghosh and Prelas 2011; Fu et al. 2016). Design characteristics include 9 to 25 fixed runner blades (Ghosh and Prelas 2011) with radial water flow entering and axial flows exiting the turbine (Fu et al. 2016). Blade leading-edge thickness and velocity vary along the meridional length of the runner with blade thickness ranging between 10 to 25 mm (Çelebioğlu and Kaplan 2019) and velocities between 3.0 to 23.0 m s⁻¹ (Andritz Hydro, *personal communication*). All these design characteristics are likely why Francis turbines have the highest incidences of fish passage mortality; however, exact mortality varies by project based on operational regimes and local hydrology. Nonetheless, estimates of mortality for Francis turbines can be as low as 5% but as high as 75% for some projects (Calles and Greenberg 2009; Fu et al. 2016; Pracheil et al. 2016a; Martinez et al. 2019).

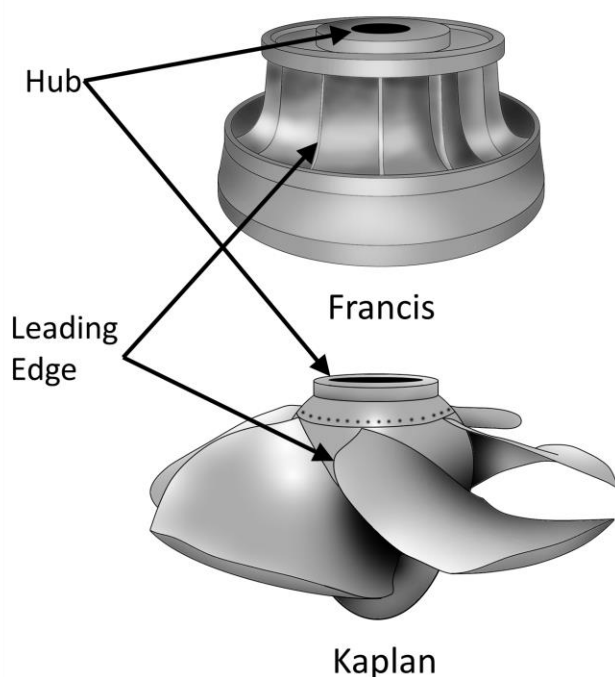


Figure 3. Diagram of a Francis and a Kaplan turbine. The hub and leading edge are identified for each turbine.

Kaplan turbines (Figure 3) form a group of slightly different but related propeller-type turbines, most notably characterized by fewer blades and

considered to be more fish friendly overall. Kaplan turbines (including both horizontal and vertical units) are mostly installed at sites that have fairly low heads (i.e., 2 to 50 m) over a much wider range of flow rates between 0.2 to 50 m³ s⁻¹ (Ghosh and Prelas 2011). In addition to fewer runner blades (i.e., three to eight), wicket gates and runners may be adjustable, which allows dam operators to optimize performance (Martinez et al. 2019; Ghosh and Prelas 2011). Additional modifications, such as minimum gap runners designed to avoid grinding-type injuries, are becoming standard features in new turbine designs to increase fish survival (Čada 2001). The blades of modern Kaplan turbines are also larger and have more pronounced variation in leading-edge thickness along the meridional length—the thickest part of the blade is located near the hub and the thinnest at the tip (Bevelhimer et al. 2019). In addition, the velocity of the blade changes along the same continuum because of the rate of rotation and change in radius from the center of rotation. Thus, the thicker portion of the blades moves slower than the fast-moving, thin sections of the blade at the periphery at the maximum extent of the radius and therefore risk to fish increases as they pass further from the hub. Modifications like fewer, adjustable blades and minimum gap runners are likely why Kaplan turbines have noticeably higher fish survival rates (88 to 96%) than Francis turbines (Fu et al. 2016). Strikes of sufficient magnitude do occur and are likely responsible for some instances of mortality among fish passing through them (Martinez et al. 2019).

2.1.2 BLADE CHARACTERISTICS

Two of the most prominent factors linked to rates of injury and mortality among fish exposed to blade strike are the blade leading-edge shape and thickness. The exact shapes of turbine blades are proprietary, but previous laboratory studies have shown blades that have semicircular leading edges limit hydrodynamic drag, which suggests they are better suited to simulating turbine blades than elliptical shapes (EPRI 2008). Information regarding leading-edge blade thicknesses is also not widely distributed because industry developers consider the blade geometry to be proprietary. In addition, insights from one

turbine are difficult to apply to all turbines of a specific type because each has been engineered according to project-specific parameters (Bevelhimer et al. 2019). While available information about blade design in turbines is lacking, valuable insights have been gained about the biological response of fish to leading-edge blade thickness and design. In general, regardless of species, controlled laboratory studies have shown that thinner blades tend to have higher rates of fish injury and mortality (Turnpenny et al. 1992; EPRI 2008; Bevelhimer et al. 2019). To date, laboratory studies involving blade strike have found the same trends across a range of leading-edge widths from as low as 10 mm to up to 150 mm (EPRI 2008, 2011). The

disparity between 0% and 100% mortality is quite dramatic across small increases in blade thickness when strike velocity is the same. High-speed video footage has shown that the “bow wave” of thinner blades is less pronounced and does not cause pre-bending or movement prior to actual blade strike (Figure 4). Presumably, curvature occurs over a smaller section of the fish body and the maximum curvature of impact is

Turbine blade impact velocity is especially lethal as it reaches 10.0 m s^{-1} for most species, but the exact velocity range depends on species and blade thickness.

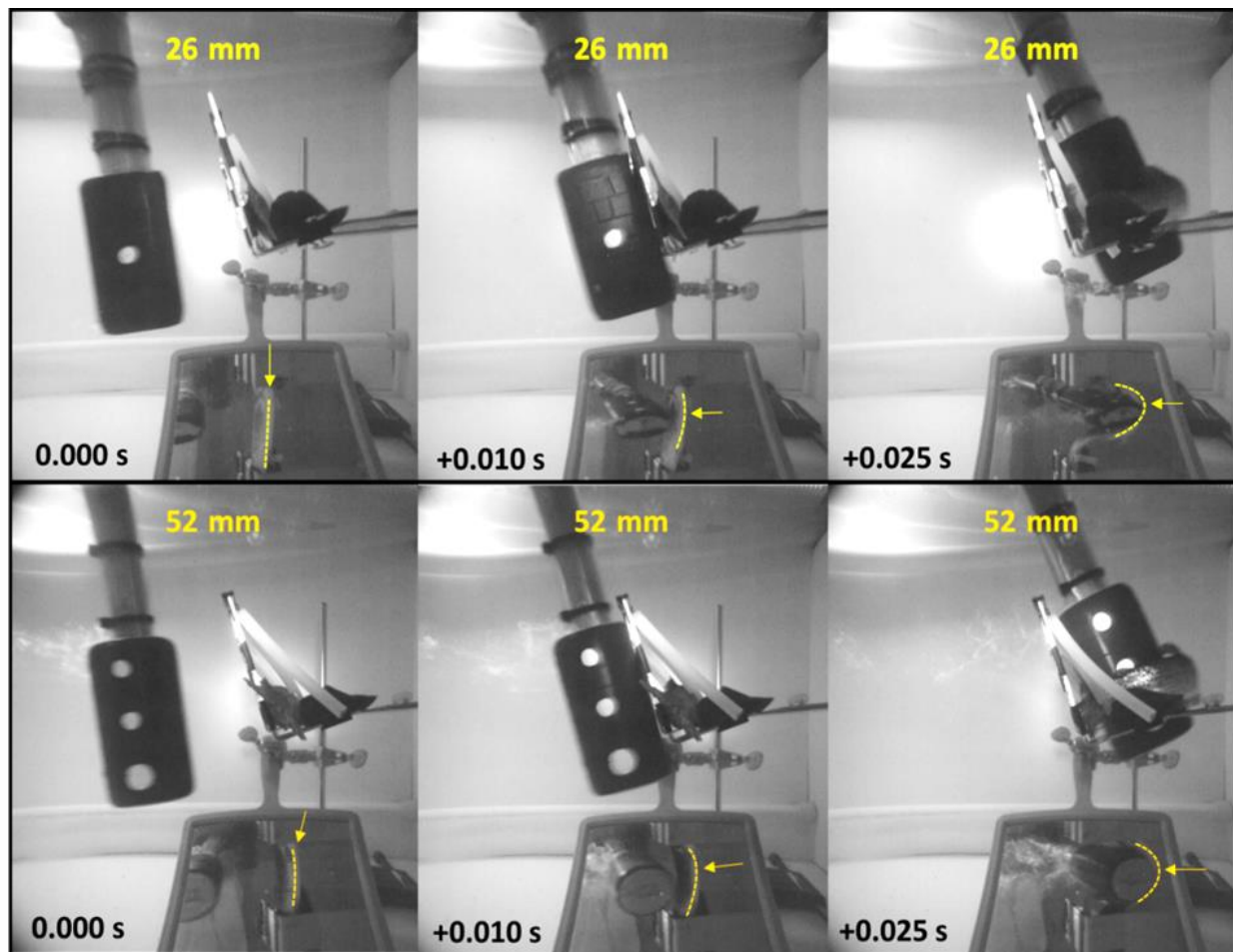


Figure 4. High-speed video images of subadult rainbow trout being struck with a 26 (top panel) and 52 mm (bottom panel) turbine blade. Dashed lines and arrows in the mirrored image were included to show the trout's body curvature along the ventral surface in each frame, including the blade approach (0.000 s; reference), just before contact (+0.010 s), and through the maximum curvature after impact (+0.025 s). Both fish were struck at approximately the same position on the mid-body, lateral surface at 90° with an impact velocity of 6.6 m s^{-1} .

more pronounced (EPRI 2008; Turnpenny et al. 1992). In contrast, a thicker blade will visibly cause the entire fish to begin bending well before impact, and the maximum curvature is also notably less than that associated with a thinner blade (EPRI 2008). Thinner blades would also cause the energy of the strike to be transferred over a much smaller surface relative to larger blades, which would also lead to higher rates of injury and mortality. The presence of a strong bow wave effect that decreased the maximum body curvature during strike, and energy that dissipated over a larger surface area, may explain why mortality is significantly lower with thicker blades.

The second and equally important characteristic to consider is blade strike velocity, i.e., the velocity at which the blade makes physical contact with the fish body. The actual or realized impact velocity is determined by accounting for both the angular velocity of the blade at the radius where the strike occurs and that of the fish. Because the velocity of a fish passing through the turbine is difficult to ascertain or model, the water velocity is often used as a surrogate. Rotational velocity is a function of turbine revolutions per minute (RPMs), which in turn varies by turbine, operational conditions, and the radius from the center of rotation. Across all turbine types, RPMs may range from 50 to 900 with Francis turbines operating at higher RPMs than Kaplan-type turbines (Bevelhimer et al. 2019). Water velocity is related directly to flow rate (discharge; which can range from 0.2 to 50 m³ s⁻¹ (Ghosh and Prelas 2011), cross-sectional surface area of the turbine inlet, and subsequent water passage through the distributor, runner, and draft tube. Water velocity is important because we assumed fish move in the same direction as water flow after reaching critical swimming speeds, fatigue, and succumb to water movement. The orientation of the fish entering the turbine is not known and we also assumed that the water (and fish) moves in the same direction as the turbine blades, which simplified realized impact velocity calculations. If these assumptions are true, the realized impact velocity would be the difference between the runner and water velocity vectors; however, this may be a low estimate, which would increase because the angular velocity vectors of water flow change direction relative to the turbine runner

(Bevelhimer et al. 2019). Like blade width, realized impact velocity would change along the meridional length of each turbine blade. In Francis turbines, the velocity may increase in the crown (uppermost portion) to band (lowermost portion) direction, and velocities as low as 3.0 m s⁻¹ near the crown or in excess of 20.0 m s⁻¹ near the band would be possible (Andritz Hydro, *personal communication*). In contrast, Kaplan turbines would have the slowest velocities near the hub, fastest near the tip, and form a continuum between the hub and tip along the leading edge of the blade. In general, higher impact velocities cause significantly higher rates of injury and mortality—impact velocity becomes especially lethal as it reaches 10.0 m s⁻¹ for most species during direct hits, but the exact velocity range depends on species and blade thickness.

2.1.3 SITE OF IMPACT

When a fish enters a turbine, impact could occur anywhere along the length of the fish, from head to tail, and risk of injury or mortality is dependent on the impact location along the body of a fish. Estimates of injury and mortality are often first linked to strikes that occur on the head, mid-body, or tail (Figure 5A). The head refers to the area between the snout and trailing edge of the operculum, but the exact proportion of the head relative to total length varies by species. The “mid-body” or trunk generally includes the fish body between the trailing edge of the operculum and leading edge of the anal fin. Caudal or tail regions of fish are generally considered any location posterior of the anal fin for most fishes at risk of passing through turbines. For most fishes, this breaks the body surface into roughly equal thirds (except for the American eel [Section 2.2.5.1] and paddlefish [Section 2.2.5.7]).

Injury and mortality rates are generally higher in individuals struck on the mid-body for all species tested to date (Turnpenny et al. 1992; EPRI 2008, 2011; Amaral et al. 2020; Saylor et al. 2019; Bevelhimer et al. 2019; Saylor et al. 2020). Mid-body strikes are likely worse because this area includes the location of most internal organs and the vertebral column. In addition, the center of mass is found in the mid-body region (Amaral et al. 2020), and strikes on areas with more mass

likely transfer more energy to the fish. In contrast, tail strikes are associated with low rates of mortality (generally <20%) at velocities up to 12.0 m s⁻¹, because the fish's body deflects away from the blade following impact (Bevelhimer et al. 2019). In addition, the tail region has few internal organs present (i.e., posterior edge of kidney or swim bladder), is dominated by the musculoskeletal system, and has much less mass compared to the rest of the body. Head strikes lead to higher rates of mortality than tail strikes and likely result from the greater relative mass of the head, which may often lead to internal decapitation. Strikes to the head may also be deflected away from the blade when the impact occurs at angles other than perpendicular to the body (Figure 5C).

The orientation of the fish body when it is struck is also an important factor in injury and mortality risk. Fish orientation can be defined by three distinct body surfaces—dorsal, lateral, and ventral (Figure 5B). The dorsal (upper side or back) and ventral (bottom side or belly) surfaces correspond to less surface area than the two lateral (side) surfaces of laterally compressed fishes. As fish dimensions change the amount of surface area also changes and may become more equally distributed between all three surfaces. Similarly, the probability of strike at any

orientation is assumed to be equal for all three orientations; however, lateral strikes are more likely because fish have two sides. Strikes on the left versus right lateral surface were considered to have the same effect on fish injury and mortality because fish are bilaterally symmetrical along the medial or mid-sagittal plane. Strikes on the lateral surface were also associated with the highest rates of severe injury and mortality, which often reached 100% at or below 10.0 m s⁻¹ strike velocity across all species regardless of blade leading-edge thickness (EPRI 2008, 2011; Saylor et al. 2019; Bevelhimer et al. 2019). Lateral strikes often correspond to the highest incidence of rib and vertebral fractures, though damage to the liver and kidney are also common (Saylor et al. 2019; Bevelhimer et al. 2019). Dorsal strikes also cause injury (e.g., vertebral fractures), but the related mortality rate is typically lower than that for lateral strikes. Ventral strikes often caused injuries to soft tissues (organs and musculature), had the lowest incidence of mortality, and observations of skeletal fractures were uncommon.

Strikes on the lateral surface of fish were associated with the highest rates of severe injury and mortality.

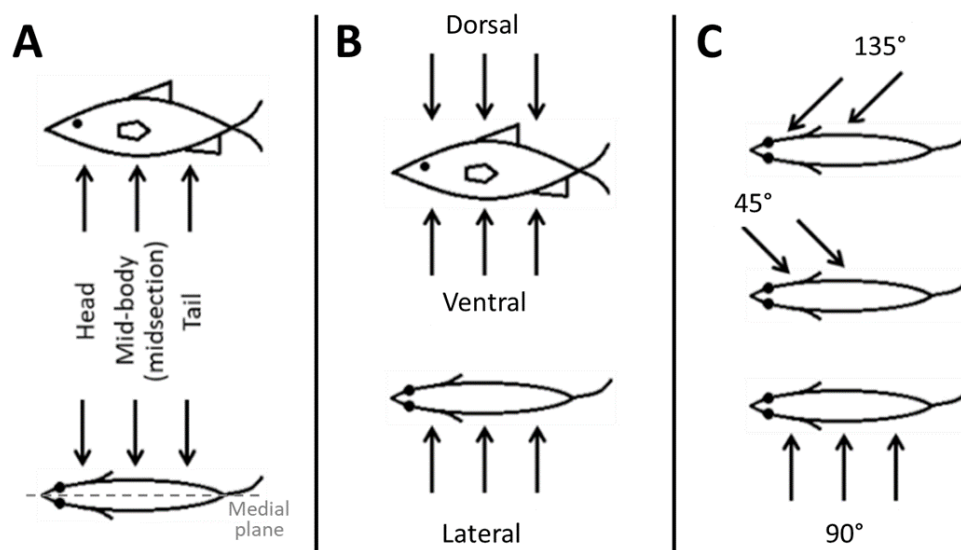


Figure 5. Simplified diagram showing blade strike impact characteristics related to the fish itself including (A) body location, (B) body orientation, and (C) angle of impact. The medial plane (i.e., mid-sagittal plane) is labeled in (A).

Like location and orientation, the exact angle at which the turbine blade impacts passing fishes is not known, but rates of severe injury and death are affected by the impact angle. The angle of impact is a more challenging variable to define because each fish could conceivably be struck at any angle (0–180°) on each surface and location (Figure 5C and Figure 6). The total number of exposure conditions a fish may encounter is nearly infinite, which makes it impossible to test them all. After initial trials, 0 and 180° (i.e., direct head and tail strikes, respectively) were not considered because of the low probability of a blade contacting the fish from these angles and the high likelihood of deflection for these strikes. Further testing revealed that strikes perpendicular to the mid-sagittal axis (i.e., 90°) were the most injurious impact angles for all species (Saylor et al. 2019; Bevelhimer et al. 2019; EPRI 2011).

Mortality at this angle often reaches 100% and is also associated with the highest incidence of severe injuries including spinal fractures at velocities near 10.0 m s⁻¹.

Additional trials included 45 and 135° blade strike impacts to better approximate the probability of mortality associated with blade strike (Saylor et al. 2019; Bevelhimer et al. 2019; EPRI 2011). Strikes at 45° are defined by any impact that occurs in a head to tail direction. Excluding hits to the tail, head strikes at 45° caused more severe injuries because the blade traveled toward the mid-body after contact where it could transfer more energy to the soft tissue and the musculoskeletal system. Most 45° strikes to the mid-body did not cause severe injuries or mortalities because the body of the fish deflected toward the caudal fin away from the blade after

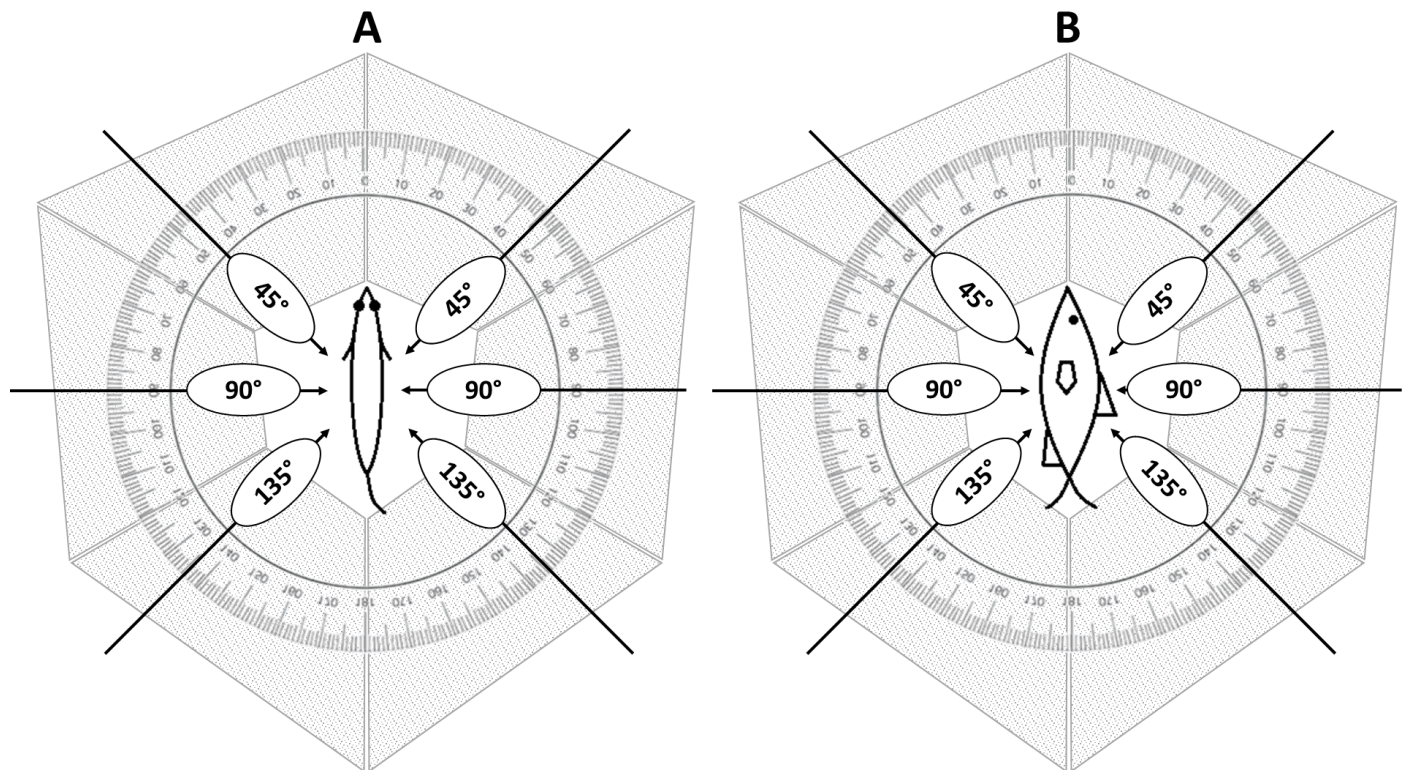


Figure 6. Diagram of potential blade strike impact angles according to the body location (A) and orientation (B) of the fish. The impact angles that have been tested are indicated by black arrows. Strikes at 90° occurred perpendicular to the mid-sagittal axis of the fish. Strikes at 45° occurred in a head to tail direction, while 135° was defined by a tail to head strike. Not shown in this image are the same angled strikes for each location and orientation, which were also possible. The grey trapezoids indicate each of six 60° areas that are represented by each 45, 90, or 135° strike angles. See text for more detail.

initial contact. The 135° strikes had the opposite effect because mid-body strikes had the highest incidence of severe injury and death. We believe these strikes were more injurious because the blade travels toward the head after initial contact, where it is more likely to transfer energy to the mid-body, operculum, and gills. All 135° strikes to the head caused the fish to immediately deflect away from the blade after initial contact. Recently, Amaral et al. (2020) reported that 60° and 75° strikes had rates of mortality between estimates for 45° and 90°, which suggests mortality rate may increase with impact angle; however, these angles have not been tested extensively and the previous study did include 120° or 150° strikes and used a blade that had a markedly different shape. To that end, it is assumed that most strikes would result in deflections based on how the fish body moved after strikes at 45° or 135°.

2.2 DEVELOPING BIOLOGICAL RESPONSE MODELS FOR BLADE STRIKE

Biological response models have been created to predict fish mortality rates related to blade strike impacts. Fish response differs greatly based on the blade strike location and fish orientation; therefore, the most useful blade strike response models are those that estimate the mortality for each species using a response equation that accounts for location, orientation, and angle of impact. For species without biological response data, whole-fish biological response models from taxonomically similar species may be used as surrogates for the desired species. The predictive biological response models for blade strike impact have all been integrated into HBET and the BioPA toolset, as described in the following sections.

2.2.1 MORTALITY RATES

The baseline estimate of mortality includes any fish that is moribund or dies during a 1 hr observation period, though this may underestimate actual mortality. Early work at ORNL found little difference in mortality rates for 1 and 48 hr post exposure so only 1 hr mortality rates were assessed for most species (Bevelhimer et al. 2017; Bevelhimer et al. 2019).

In contrast, research performed by EPRI (2008, 2011) found that some fish held up to 96 hr would die after blade strike impact. Delayed mortality could increase the overall mortality rate (or decrease survival) by up to 25% for some treatments where fish were exposed to higher strike velocities (EPRI 2008, 2011). ORNL mortality estimates did not include delayed mortality, but necropsies were used to further refine estimates and account for severe injuries like vertebral fractures. Vertebral fractures including internal decapitation were assumed to be severe enough to limit the ability of fish to escape predators or acquire sufficient food, so they were classified as functional mortalities. Instantaneous mortality was combined with functional deaths in the mortality metrics because it is a more conservative estimate of mortality, much like the Electric Power Research Institute (EPRI)-adjusted rates of survival (EPRI (2008, 2011), which included delayed mortalities. Combining these two metrics is supported by the observation that the combined mortality rates for American eel (*Anguilla rostrata*; Section 2.2.5.1) were similar to adjusted survival rates (EPRI 2008; Saylor et al. 2019). Both estimates are comparable because spinal damage was observed in American eel during the 96 hr observation period, but this was not confirmed by necropsy (EPRI 2008).

2.2.2 DEVELOPING BIOLOGICAL RESPONSE MODELS FOR BLADE STRIKE

The ultimate goal of the laboratory research was to generate biological response models that predict a response (mortality) as a function of the dose (blade strike velocity; $m\ s^{-1}$) (Colotelo et al. 2017). Biological response models for blade strike were initially created from EPRI (2008, 2011) linear models of mortality versus blade strike velocity for each fish body length to blade width (L/t) ratio group (Figure 11; Section 2.2.4.1). These linear models did not separate treatment conditions (location, orientation, or impact angle), the number of data points for each L/t ratio were low, and no linear regression analyses were performed. Combined, these limitations suggest use of linear models to estimate mortality may actually underestimate survival for each L/t ratio group. The ORNL

biological responses were produced by modeling combined mortality rates relative to blade strike velocity for fish exposed to mid-body, lateral strikes at 90°. These conditions caused the highest mortality rates and were used to generate baseline biological response models for each species. Models were generated from four-parameter log-logistic regression given by the following equation (Ritz et al. 2015):

$$f(x; b, c, d, e) = c + \frac{d-c}{1+(\frac{x}{e})^b} \quad (1)$$

where $f(x)$ is the estimated mortality rate, x is strike velocity (m s⁻¹), b is the inclination point, c is the lower boundary for mortality rate and was fixed a 0.0, d is the upper boundary for mortality rate and was fixed at 1.0, and e is the effective dose (ED50) of velocity that would be expected to cause 50% mortality.

Ideally, separate curves could be created for each treatment scenario; however, doing so is not feasible because it is impractical to test all possible exposure conditions. Rather, biological response models were created for mid-body, lateral strikes at 90° (e.g., worse-case scenario) and were then modified to account for other conditions. In fact, it is easy to shift or translate the entire curve by changing coefficient e or to modify the slope by changing coefficient b based on fit with other treatment combinations (if available) or trends detected in more thoroughly tested species.

2.2.3 WHOLE-FISH BIOLOGICAL RESPONSE MODEL DERIVATION

Whole-body biological response models that estimate mortality caused by turbine blade strike are essential components of the BioPA toolset and HBET. A whole-fish biological response equation was developed that accounts for location (head: H , mid-body: M , and tail: T), orientation (dorsal: D , lateral: L , and ventral: V), and impact angle (45°, 90°, and 135°). The body of a fish was considered to have 12 distinct areas based on combinations of location and orientation, which were assumed to have equal

probability of being struck by a turbine blade (Figure 7). Ideally, there

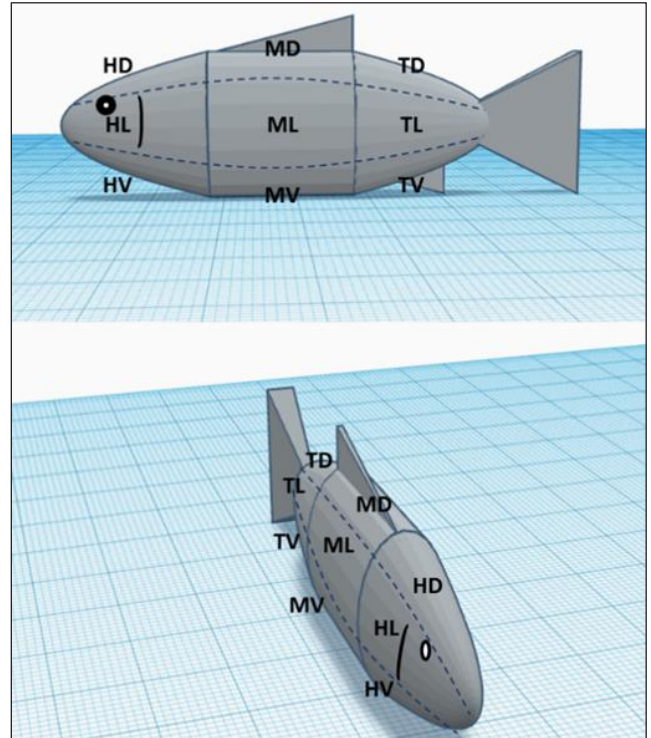


Figure 7. Diagram depicting the 12 major areas that we defined to represent all location and orientation possibilities during derivation of our whole-fish dose-response model for each species. The layout above is generally indicative of all species except American eel, which was mostly tail. See the text for detail and how these areas were used to produce a more broadly representative biological response model.

would be mortality rate estimates for all 12 areas given by:

$$P([M]) = \frac{(a_{HV}+2a_{HL}+a_{HD} + a_{MV}+2a_{ML}+a_{MD} + a_{TV}+2a_{TL}+a_{TD})}{12} \quad (2)$$

where α is the estimated mortality rate for each area (for example, HV = head, ventral) and the overall probability of mortality $P(M)$ would simply be the average rate for all 12 locations. Strikes to the left and right lateral sides were also assumed to be the same because fish are bilaterally symmetrical and were represented by doubling each term (e.g., $2HL$, $2ML$, and $2TL$). Each of the

12 strike areas could also be struck at any of the three impact angles tested. The 45°, 90°, and 135° angles were used to represent one of six 60° regions surrounding the fish on the lateral (Figure 5A) or dorsal and ventral (Figure 5B) surfaces. Angled strikes were not performed on the ventral and dorsal surfaces but were considered in the same manner as lateral strikes for the whole-fish estimate of mortality. With three possible strike angles for each of the 12 positions, the number of mortality rate parameters is 36, and the combined probability is calculated according to the following equation:

$$P(M) = \frac{\left(\sum_{i=1}^{3(\text{tail})} \sum_{j=1}^{4(\text{dorsal})} \sum_{k=1}^{3(135^\circ)} a_{ijk}\right)}{36} \quad (3)$$

where a_{ijk} is the estimated mortality rate at specific i location, j orientation, and k impact angle. Based on general findings that tail strikes at 45° and 90° and head strikes at 135° cause the least injury and mortality, 12 of the 36 terms in Equation (3) values can be consolidated into one term. Values for the remaining 24 parameters were based directly or indirectly (via extrapolation

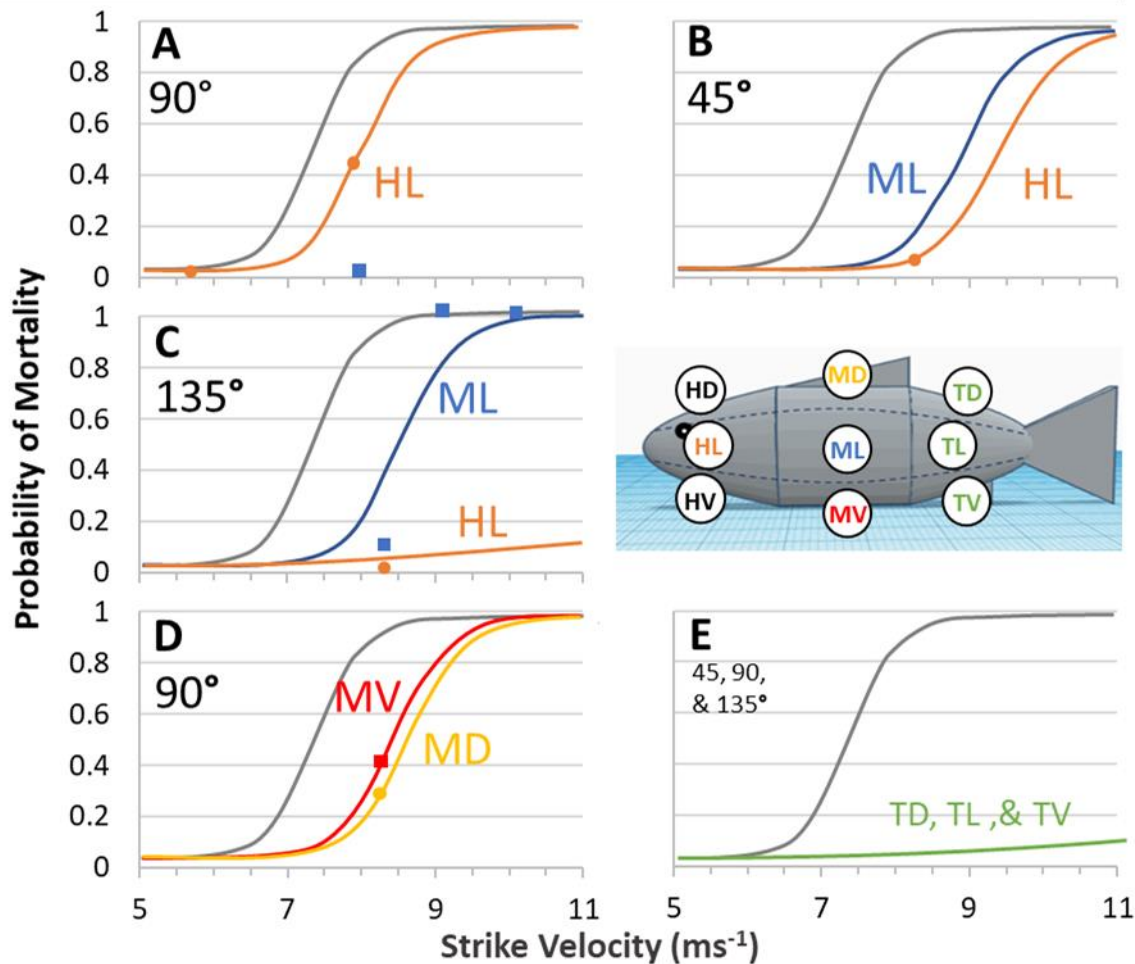


Figure 8. Example diagram, using hybrid striped bass, depicting nine mathematical models created to represent the 12 major body areas defined on most species of fish. The reference dose-response relationship curve (gray; displayed in each graph) was created from laboratory data generated from mid-body, lateral strikes at 90°. The whole-fish dose-response model includes (A) lateral strikes at 90° on the head (orange), (B) lateral strikes at 45° on the mid-body (blue) and head (orange), (C) lateral strikes at 135° on the mid-body (blue) and head (orange), (D) mid-body strikes at 90° on the dorsal (yellow) or ventral (red) surfaces, and (E) all strikes to the tail region including orientation and impact angles (green). See text for more specific details related to the exact model function used for each body area and the justification for its use.

or modification) on the most current laboratory-derived biological response models (Figure 8). Modified parameter values refer to the coefficients e and b produced from log-logistic regressions for mid-body, lateral strikes at 90° for each species (Equation (1)).

A total of 9 functions were produced that either incorporated log-logistic models or assumed a linear increase in mortality once a threshold velocity is reached (Table 1). The first equation (or reference model) accounts for two terms and was derived directly from laboratory response data (i.e., 2ML90). The next six equations (Table 1) were based on the severity of blade strike for each term (strike area) relative to the reference log-logistic model, and they were ranked from most (lowest E_{50}) to least (highest E_{50}) injurious, i.e., ML90 (reference) > ML135 > MD90 > ML45 > MV90 & HL90 > HL45. Equations (2) through (7) were derived from the reference model by adjusting the b and e coefficients to fit additional laboratory data if available or by following the severity scale above. The two remaining equations used a linear relationship because observed mortality rates were comparably low for head strikes at 135° (Equation (5)) and all tail-associated strikes (Equation (6)); Table 1). More specifically, no mortality was expected until velocities reached values greater than or equal to $e - 1$, which would increase by a factor of 0.02 as blade strike velocity increased thereafter. The final whole-fish biological response curve was then produced using the following equation for log-logistic models:

$$f(x)_y = \sum_{y=1}^7 \left[\frac{1}{\left(1 + \left(\frac{V}{e_y}\right)^{b_y}\right)} \right] \times m_y \quad (4)$$

where V is the blade strike velocity, y is the number of potential equations to use (1–7), and m is the number of strike areas (out of 36) each

function represents. The linear equations and coefficients were determined as follows:

$$f(1) = If V \geq (e_1 - 1) \quad (5)$$

$$Then (V - e_1 - 1) \times 0.02 \times l_1$$

$$f(2) = If V > e_1 \quad (6)$$

$$Then (V - e_1) \times 0.02 \times l_2$$

where l represents the number of strike areas each linear function represents. The first linear function included areas that would lead to slightly more severe rates of mortality so mortality would begin when velocity was greater than or equal to $e - 1$. The second linear equation represented strikes to tail areas, which were the least likely to cause injury, so mortality would not occur until strike velocity was greater than e (Table 1). If blade strike velocity is below thresholds for both linear models, then no mortality was predicted to occur. Finally, to produce a combined, whole-fish biological response model we used the following equation:

$$P(M) = \frac{\sum_{y=1}^7 f(x_y) + \sum_{x=1}^2 f(x)}{36} \quad (7)$$

where $P(M)$ is the whole-fish probability of mortality. Whole-fish probability of mortality can be plotted against a range of blade strike velocities for each blade leading-edge thickness (Figure 9). The only remaining variable to consider is blade leading-edge width, which can also be estimated by translating the curves by modifying all e -values. For example, a thicker blade will lead to less overall mortality at all blade strike velocities so that e -value is increased by 1.0 m s^{-1} , whereas the e will decrease by 1.0 m s^{-1} for thinner blades (Figure 9). This method likely best captures the disparities in estimated mortality for each blade strike exposure area, especially linear functions, which have particularly low mortality.

Table 1. Detailed summary of our whole-fish dose-response model produced for each species.

Eqn.	Type	<i>n</i> models	Blade Strike Areas Represented	Coefficients
1	Log-logistic	2	MLR90 & MLL90	b_1, e_1
2	Log-logistic	4	HLR90, HLL90, HD90, & HV90	b_2, e_2
3	Log-logistic	4	HLR45, HLL45, HD45, & HV45	b_3, e_3
4	Log-logistic	4	MLR45, MLL45, MD45, & MV45	b_4, e_4
5	Log-logistic	4	MLR135, MLL1355, MD135, & M1355	b_5, e_5
6	Log-logistic	1	MD90	b_6, e_6
7	Log-logistic	1	MV90	b_7, e_7
8	Linear	4	HLR135, HLL135, HD135, & HV135	l_1
9	Linear	12	TLR90, TLL90, TLR45, TLL45, TLR135, TLL135, TD90, TD45, TD135, TV90, TV45, & TV135	l_2
Total		36		16

Note: Areas include head (H), mid-body (M), tail (T), dorsal (D), lateral (L and left-L or right R), ventral (V) and impact angle 45, 90, or 135°. The coefficients *b* or inclination point and *e* or ED₅₀ value are derived from log-logistic regression of at least one reference set of dose-response data. The *l* coefficients are produced for areas on the first that are assumed to have a linear relationship.

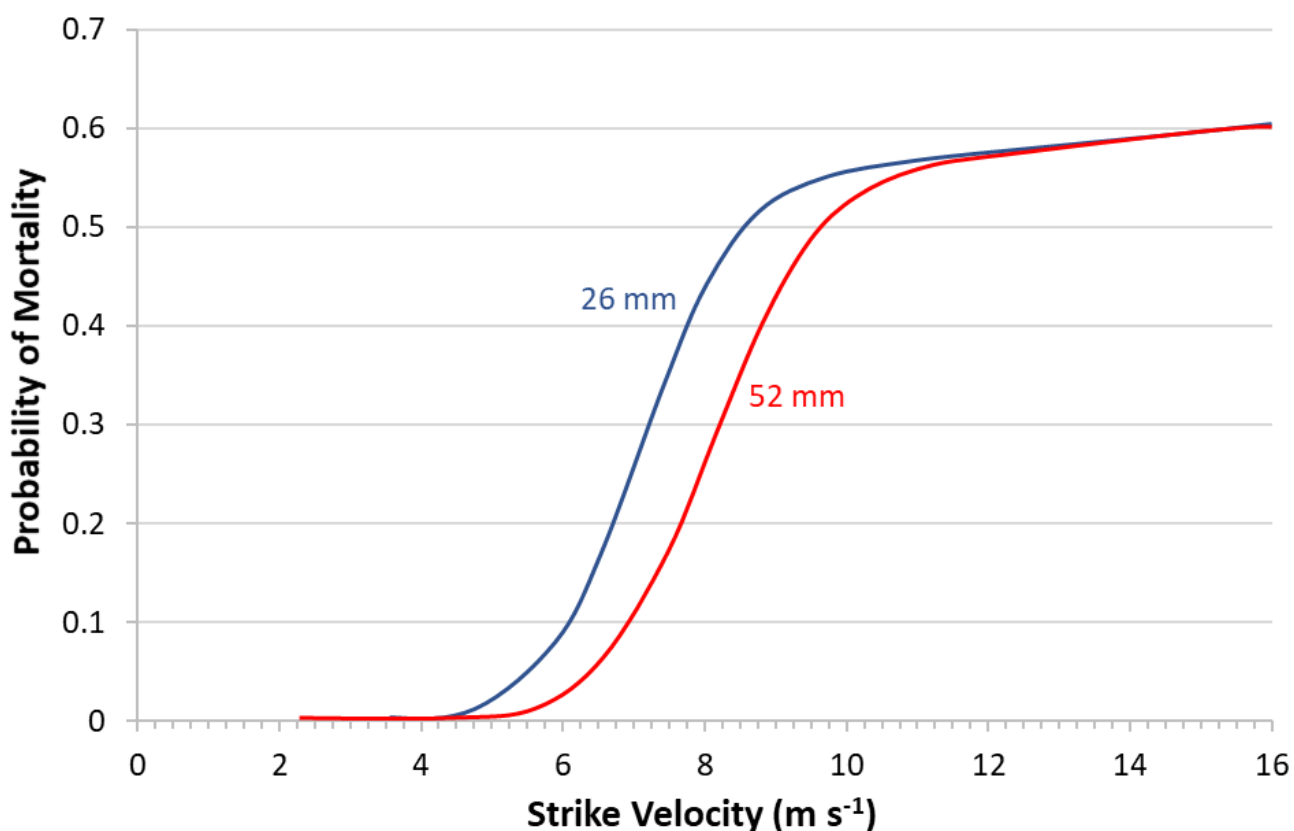


Figure 9. Graph depicting the whole-fish dose-response curve, i.e., probability of mortality versus strike velocity (m s^{-1}), for hybrid striped bass. The original model was built using log-logistic models for the 26 mm blade and the 52 mm curve was produced by modifying the reference log-logistic models.

2.2.4 BLADE STRIKE BIOLOGICAL RESPONSE MODELS FOR THE BIOPA TOOLSET AND HBET

A total of 11 blade strike biological response models have been integrated into HBET and the BioPA toolset. One of the biological response models is a multiple linear regression that predicts mortality as a function of strike velocity and the L/t ratio. Three of the 11 models use logistic regression, where the probability of mortality (immediate plus functional mortality) is a function of strike velocity and L/t ratio. The remaining seven models are fitted with curvilinear regression, where mortality is a function of strike velocity.

2.2.4.1 MULTIPLE LINEAR REGRESSION MODEL

Six linear regression relationships were combined to form the multiple linear regression model to predict mortality as a function of strike velocity ($m\ s^{-1}$) and the L/t ratio. Each linear relationship represents a different L/t ratio, ranging from 0.75 to 25.0. For each of these relationships, the probability of survival ($P(S)$) is expressed as a function of strike velocity (V):

$$P(S) = 1 + m(V - V_{crit}) \quad (8)$$

where m is the slope and is specific to each L/t ratio, and V_{crit} is the critical velocity, which designates the point at which survival begins to decrease. The model was bound to between 0 and 1, with any results less than or greater than this range being converted to 0 or 1, respectively.

2.2.4.2 LOGISTIC REGRESSION MODEL

Logistic regression models were also used to predict the probability of mortality ($P(M)$) as a function of strike velocity (V) and L/t ratio (L/t):

$$P(M) = \frac{e^{(\beta_0 + \beta_1 V + \beta_2 L/t)}}{1 + e^{(\beta_0 + \beta_1 V + \beta_2 L/t)}} \quad (9)$$

where β_0 – β_2 are species-specific coefficients. Not all models include the L/t ratio as a covariant and in these cases, β_2 and L/t are excluded from the equation.

2.2.4.3 CURVILINEAR MODEL

To facilitate the integration of the whole-fish biological response model, which was based on log-logistic and linear models, into the BioPA toolset and HBET, a simplified version was created. This was accomplished by fitting a curvilinear equation to the data for each species whole-fish biological response model. This reduced the number of coefficients from up to 28 to only 5. As with the previous model, the curvilinear model predicts the probability of mortality ($P(M)$) as a function of velocity (V):

$$\begin{aligned} \text{If } V \leq x: P(M) &= \frac{f}{1 + \left(\frac{V}{e}\right)^b} \\ \text{If } V > x: P(M) &= \frac{\beta_2}{1 + \left(\frac{V}{e}\right)^b} + m(V - x) \end{aligned} \quad (10)$$

where b , e , f , m , and x are specific coefficients associated with each species. This model splits the curvilinear relationship into two parts based on the x value—a logistic relationship for the lesser strike velocities followed by a linear relationship for the greater strike velocities. The shape of the logistic relationship is controlled by the first three coefficients where b designates the logistic growth rate (steepness of the curve), e designates the offset, and f designates the curves maximum value. The remaining two coefficients influence the linear relationship, where m designates the linear slope and x designates the linear intercept, i.e., the transition from logistic to linear relationship. The simplified model was fit to the previous model by using an iterative method to select the most accurate coefficients. The coefficient selection was conducted by running a script using MATLAB (v2019a; MathWorks, Natick, Massachusetts, USA), which selected and modified the coefficients until the best fit was achieved (Figure 10).

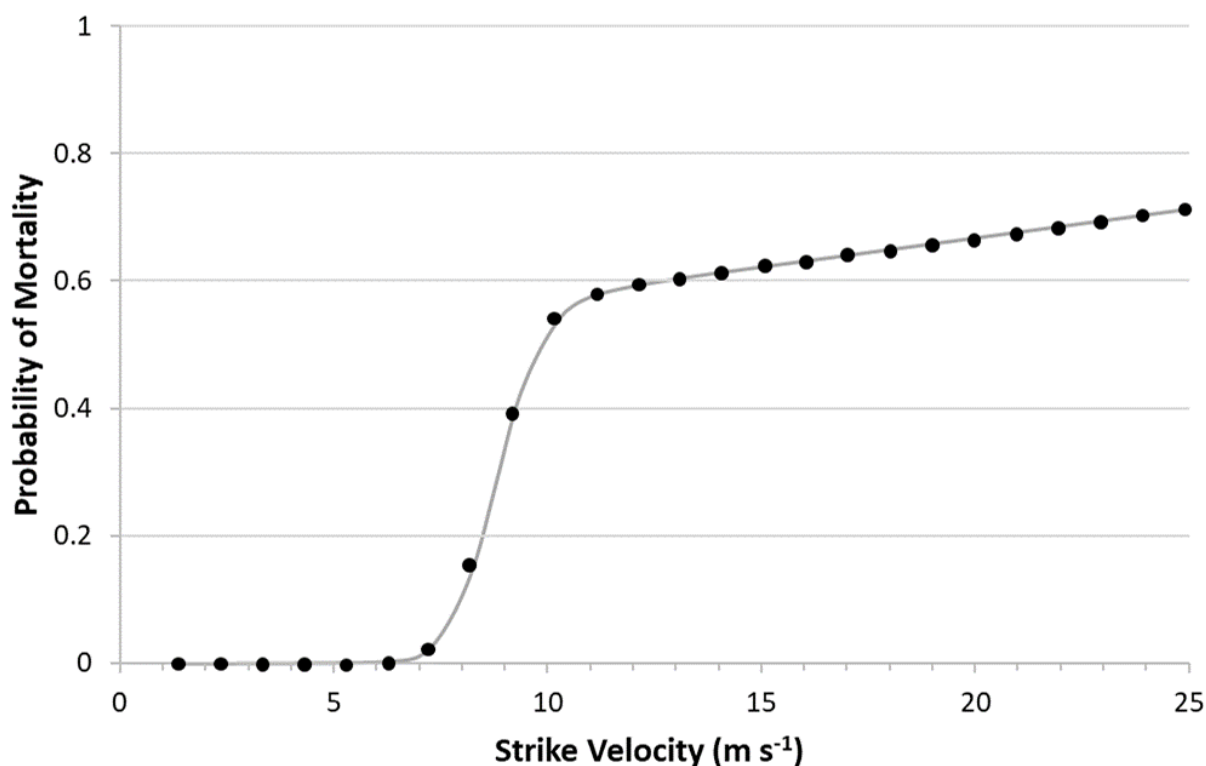


Figure 10. Example of the curvilinear blade strike model (gray line) fit to data exported from the whole-fish biological response model (black circles). This example uses models developed for hybrid striped bass.

2.2.5 FISH SPECIES EXAMINED FOR SUSCEPTIBILITY TO BLADE STRIKE

To date, blade strike trials have been performed on a total of 17 species that compose 9 different families of fishes. The blade strike data for most species have at least provided a baseline understanding of how physical impact affects mortality rates and have informed the general trends discussed in this report. Rainbow trout (*Oncorhynchus mykiss*) has served as the foundation of most blade strike studies because it has been included in most laboratory experiments completed in the last 25 years. Gizzard shad (*Dorosoma cepedianum*), hybrid striped bass (*Morone saxatilis* x *M. chrysops*), and bluegill sunfish (*Lepomis macrochirus*) are also well represented in terms of number of treatments and range of blade strike impact velocities tested (Table 2). The remaining species data for paddlefish (*Polyodon spathula*), American eel, American shad (*Alosa sapidissima*), blueback

herring (*Alosa aestivalis*), and brook trout (*Salvelinus fontinalis*) did not include as many treatment scenarios, but biological response models were successfully created for these species (Table 2; Figure 11). In the sections below, species accounts are provided for biological response models built from baseline (i.e., worst-case scenario) treatment groups (Figure 11). Species accounts are presented in phylogenetic order and are meant to provide general trends observed during blade strike trials that have not been discussed in previous sections. In addition, species accounts may contain descriptions of unique injuries observed during testing that do not apply to other species tested to date. Please note, biological response curves reported for each species are associated with a specific size known to pass through turbines; however, because size is often a variable that affects susceptibility, modeling biological responses of an entire population (of all sizes) using one curve should be approached with caution when considering certain species.

Table 2. State of the science for the blade strike-related level of understanding of each species.

Species	Data	Citation (s)
American eel (<i>Anguilla rostrate</i>)	○●	EPRI 2008; Saylor et al. 2019
American shad (<i>Alosa sapidissima</i>)	●	Saylor et al. 2020
Blueback herring (<i>Alosa aestivalis</i>)	●	Saylor et al. 2020
Bluegill sunfish (<i>Lepomis macrochirus</i>)	●●	Saylor et al. 2019
Brook trout (<i>Salvelinus fontinalis</i>)	●	Saylor et al. 2020
Gizzard shad (<i>Dorosoma cepedianum</i>)	●●	Bevelhimer et al. 2019; Saylor et al. 2020
Hybrid striped bass (<i>Morone saxatilis</i> × <i>M. chrysops</i>)	●●	Bevelhimer et al. 2019
Paddlefish ^(a) (<i>Polyodon spathula</i>)	●	Unpublished data
Rainbow trout (<i>Oncorhynchus mykiss</i>)	●●●	EPRI 2008; Bevelhimer et al. 2019; Saylor et al. 2020; Amaral et al. 2020

(a) Paddlefish data have not been published but have been integrated into HBET and the BioPA toolset.

Grey = Non-HydroPASSAGE project

Blue = HydroPASSAGE project

- Dose-response available; mortality includes individuals that survived exposure with severe injuries, likely functionally dead (unable to acquire nutrition or escape life-threatening stressors).
- No dose-response relationships were generated; project-specific metrics were described.
- Baseline understanding; dose-response models based mostly on worst-case scenario treatments.
- Satisfactory understanding; dose-response models also includes additional treatment scenarios.
- Comprehensive understanding; dose-response models covers most expected exposure scenarios.

2.2.5.1 AMERICAN EEL - *ANGUILLA ROSTRATA*

American eel (average total length [TL] = 53.9 cm; range = 45.7–67.5 cm) was the most resistant species tested, likely a result of their unique body shape, i.e., the eel body would mostly be considered tail. Mortalities in eels were not observed until velocities reached at least 12.0 m s⁻¹, but insufficient treatment groups were tested to determine the complete velocity exposure range (Saylor et al. 2019). No biological response model could be created directly for American eel and the whole-fish probability of mortality curve was based on slightly different assumptions. For example, eel was considered in fifths instead of in thirds like other species because of the large tail region of this species. In this way, up to 60% of the body was considered tail during model derivation and the influence of this linear model function was more pronounced in eel. Interestingly, dorsal strikes to the head were associated with much higher mortality rates

than both mid-body lateral and dorsal strikes in eel, which was not true for other species. Lateral and ventral mid-body strikes also caused traumatic injuries to the liver (e.g., the tissue fell apart) and in a few cases ruptured the gall bladder—all of which are probably related to their lack of ribs to protect internal organs.

2.2.5.2 AMERICAN SHAD AND BLUEBACK HERRING - *ALOSA* SPP.

Young of the year (average TL = 7.6 cm; range = 6.1 – 10.3 cm) American shad and blueback herring were analyzed and reported together as *Alosa* spp. (i.e., multiple known species of *Alosa*) because of the remarkable similarities in their body shapes and sizes that are at highest risk of turbine passage (Saylor et al. 2020). These clupeids are also notably resistant to blade strike impact; they have an ED₅₀ value (median effective dose producing 50% mortality) of 7.87 m s⁻¹ and

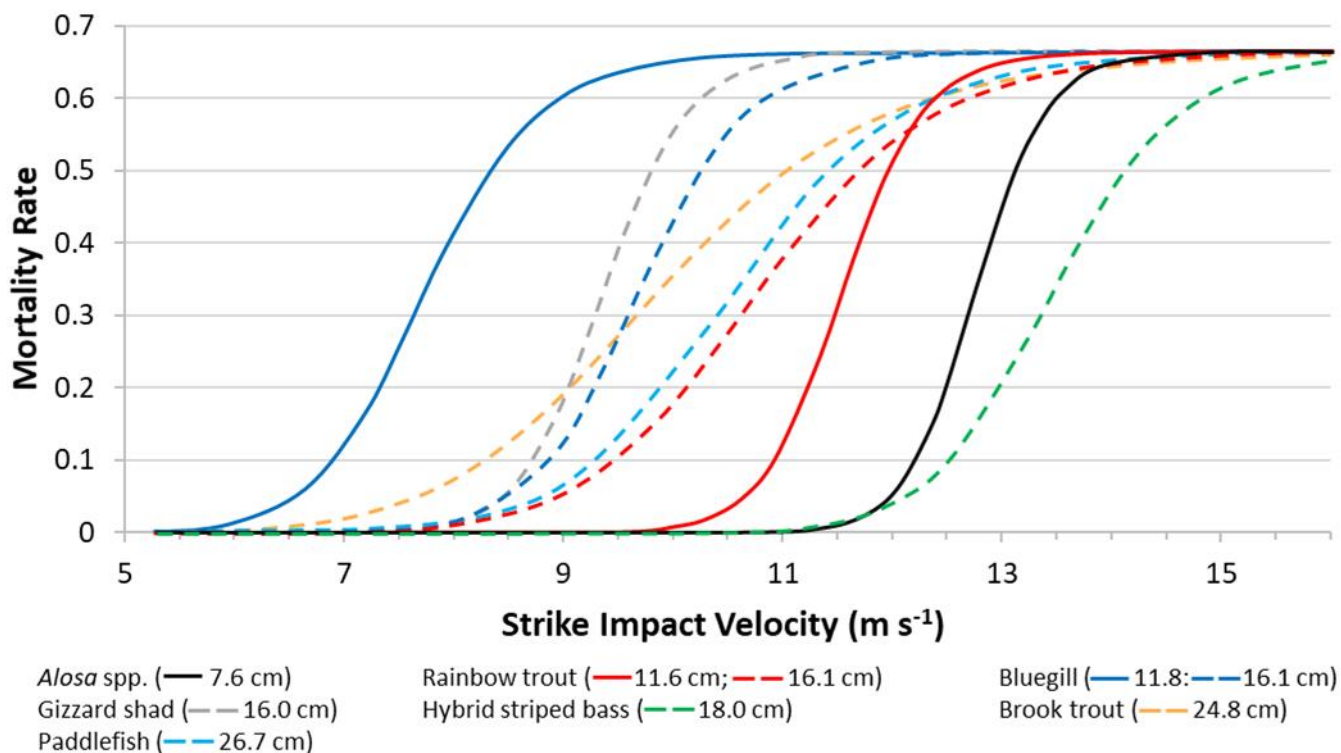


Figure 11. A summary plot of all species dose-response curves available to date for mid-body lateral strikes at 90° with a 52 mm blade. Fish sizes are shown in parenthesis in the figure legend. Similar colors correspond to the same species, while solid versus dashed lines represent smaller versus larger individuals, respectively. American eel is not included in this figure and the curve for hybrid striped bass was produced by modifying the log-logistic curve produced from 26 mm data. All response models were produced from at least four treatment groups that varied by strike impact velocity, except paddlefish, which was only based on three treatment groups.

formed the upper limit of biological response models with hybrid striped bass (Figure 11). The overall velocity exposure range was only about 2.0 m s⁻¹, and the steepness of the curve suggests the rate of mortality increase is faster than that of all other species tested (Saylor et al. 2020). Vertebral fractures were by far the most common injury observed, but eye amputation also occurred at the highest impact velocities and thinnest blade. Review of high-speed video showed that the approaching blade and bow wave had a profound effect on these fishes, which would begin to curve well before being struck. This was especially prominent for the largest, 76 mm blade, which would often push the fish aside and out of the impact zone. Turnpenny et al. (1992) observed a similar phenomenon in fish less than 20 g—both *Alosa* spp. tested here

were also well below 20 g in mass and had comparably high surface area-to-body ratios.

2.2.5.3 BLUEGILL SUNFISH - *LEPOMIS MACROCHIRUS*

Bluegill sunfish was the most susceptible species tested to date and size effects were exactly opposite of those described for rainbow trout. In fact, small bluegill (average TL = 11.8 cm; range = 9.0–14.7 cm) were markedly more susceptible than medium bluegill (average TL = 16.1 cm; 12.2–17.7 cm) and mortalities were observed at velocities below 4.0 m s⁻¹ (Saylor et al. 2019). The ED₅₀ values for both sizes also differed by more than 1.0 m s⁻¹, which was greater separation than observed for any other analysis that included within-species comparisons (Figure 11). Bluegill was also the first species for which

multiple vertebral fractures were confirmed; i.e., up to three separate fractures was not uncommon. Functional mortality rates were especially high among bluegill because many of the individuals of all sizes tested did not die as a result of skeletal fractures. Other injuries of note included lacerations and rupture of gonads for both sexes, but especially gravid females. This species is also the best represented relative to the number of different treatment scenarios investigated; many experiments were conducted on fish struck on the head, dorsal and ventral surfaces, and 45° and 135° strike angles (Saylor et al. 2019).

2.2.5.4 BROOK TROUT - *SALVELINUS CONFLUENTUS*

Brook trout (average TL = 24.8 cm; range = 19.3–29.3 cm) fell in the mid-range susceptibility of all the species tested and the biological response model covers a slightly wider velocity exposure range of 4.0–9.0 m s⁻¹ (Figure 11). The ED₅₀ for brook trout was ~6.0 m s⁻¹, which places it within the same range as medium-size bluegill and gizzard shad (Saylor et al. 2020). Dorsal, mid-body strikes at 90° had a higher rate of mortality than mid-body lateral strikes, which differs from most species tested to date. Mortality was observed in at least 13 brook trout exposed to lateral strikes to the head at 90°, but no apparent cause of death could be confirmed and none of these fish suffered vertebral fractures. Inflammation or other aspects of a fish's stress response to blade strike impact were suspected as the likely causes of death in these individuals (Debra Miller, DVM/PhD *personal communication*) and were not observed in any other species tested. Inclusion of biochemical indicators of stress, such as cortisol, glucose, or lactate, could be used to further elucidate mortality estimates in fish that have no obvious signs of impact-related trauma.

2.2.5.5 GIZZARD SHAD - *DOROSOMA CEPEDANIUM*

Gizzard shad (average TL = 16.0 cm; range = 14.3 – 17.2) were examined at ORNL and are one of the species most susceptible to blade strike impact tested so far (Figure 11). The ED₅₀

for gizzard shad was 5.66 m s⁻¹, which was the second lowest value recorded when compared to other species tested at ORNL. The velocity exposure range was between 5.0 to 8.0 m s⁻¹, which is comparable to most other species but a noticeably wider range than *Alosa* spp (Saylor et al. 2020). Direct comparisons with *Alosa* spp. described previously were not possible because the gizzard shad tested were noticeably larger. Much like other species, vertebral fractures were the most common severe wound observed. Interestingly, in nearly every fish of this species tested hemorrhaging, clotting, and sometimes avulsion of gill tissue was observed within the buccal cavity and operculum chamber.

2.2.5.6 HYBRID STRIPED BASS - *MORONE SAXATILIS* × *M. CHRYSOPS*

Hybrid striped bass was the second most resistant to blade strike of all the species tested, after American eel. This species had a predicted ED₅₀ value of 8.32 m s⁻¹, could potentially survive velocities above 9.0 m s⁻¹, and had a velocity exposure range of nearly 3 m s⁻¹ (7.2–9.6 m s⁻¹), but only one size group (average TL = 18.0 cm; range = 15.6 – 21.3 cm) was investigated (Figure 11). Please note, the biological response curve for hybrid striped bass was modeled for the 26 mm blade (Bevelhimer et al. 2019), but the curve shown in Figure 9 was approximated for the 52 mm blade. This curve was created by adjusting the ED₅₀ of the 26 mm curve by +1.0 m s⁻¹, which was used to help derive the whole-fish probability of mortality models described previously (Figure 9; Section 2.2.3).

2.2.5.7 PADDLEFISH - *POLYODON SPATHULA*

Paddlefish (average mid-eye to fork length = 27.8 cm; 21.2–33.8 cm) were also especially interesting because of their mostly cartilaginous endoskeleton, large protruding paddle, and mostly scale-less body. Resistance to blade strike impact for paddlefish appears to be nearly the same as that for subadult rainbow trout because the predicted ED₅₀ (e.g., 6.44 m s⁻¹) and velocity exposure range (5.0 to 8.0 m s⁻¹) nearly overlapped (Figure 11). Damage to the notochord was rarely observed in paddlefish, but forceful avulsion of the muscle from around the notochord

was often observed in moribund or mortally wounded fish. Paddlefish were also observed to have severe damage to their paddle, which was nearly amputated when struck on the lateral surface of the head at 90° with the 52 mm blade moving at 7.3 m s⁻¹. Injuries of this type have been observed in the field and many paddlefish collected in large rivers in the Midwest are often missing paddles (Pracheil et al. 2014; Hoover et al. 2019). Interestingly, while the damage to the paddle was quite severe, most of these individuals did not die from the trauma, suggesting their survivability is high. This is the first instance during laboratory tests at ORNL where field observations of previous trauma may be linked to blade strike impact during turbine passage.

2.2.5.8 RAINBOW TROUT - *ONCORHYNCHUS MYKISS*

Rainbow trout remain the most tested species with blade strike data over the last 25 years, but many insights are based on mid-body lateral strikes at 90° only (Turnpenny et al. 1992; EPRI 2008, 2011; Bevelhimer et al. 2019; Amaral et al. 2020; Saylor et al. 2020). The most recent study at ORNL included biological response data for both small (average TL = 11.6 cm; range = 10.1–14.9 cm) and large (average TL = 16.1 cm; range = 20.1–31.6 cm) fish to directly test the effect of fish size. The predicted ED₅₀ value for large trout was 6.59 m s⁻¹, which is slightly lower than small trout with 7.08 m s⁻¹ (Saylor et al. 2020). Both

small and large trout have a velocity exposure range of ~3.0 m s⁻¹, though the slope of the small trout curve indicates that the increase in mortality after 7.0 m s⁻¹ occurs quickly (Figure 11). Differences in the frequency and number of spinal fractures were also detected when small rainbow trout were not observed to have internal decapitation but large fish were (Section 2.3.2).

2.2.6 PROBABILITY OF MORTALITY DUE TO BLADE STRIKE

A total of 11 blade strike biological response models have been integrated into HBET and the BioPA toolset. The response model for rainbow trout used a multiple linear regression model based on data published by EPRI (2011) (Table 3). The models for bluegill (both small and medium sized fish) and hybrid striped bass used logistic regression models from data published by Saylor et al. (2019) and Bevelhimer et al. (2019), respectively (Table 4). The remaining seven models for American eel, *Alosa* spp (American shad and blueback herring), bluegill sunfish, brook trout, gizzard shad, hybrid striped bass, and rainbow trout used curvilinear models originally created from the whole-fish biological response model (Table 5; Figure 12). These models predict the probability of mortality as a function of strike velocity (m s⁻¹) and in some cases, when sufficient fish size range and blade thicknesses are examined, also used the L/t ratio as a predictor variable for mortality.

Table 3. Multiple linear regression model coefficients for predicting the probability of mortal injury as a function of strike velocity (m s⁻¹) and L/t ratio (Fish length to blade thickness ratio) for rainbow trout. Coefficients are to be used for the various L/t ratios with Equation (8).

Species	Scientific Name	Coefficients			Citation
		L/t Ratio	β_0	β_1	
Rainbow trout	<i>Oncorhynchus mykiss</i>	0	100.0	0.00	EPRI (2011)
		0.75	10.0	-0.01	
		1	7.5	-0.05	
		2	5.0	-0.06	
		4	4.9	-0.11	
		10	4.8	-0.90	
		25	4.8	-0.21	

Table 4. Logistic regression biological response models for two species that have been integrated into the BioPA toolset and HBET. Coefficients are to be used with Equation (9). Models that do not use L/t ratio as a predictor variable do not have a coefficient for β_2 .

Species	Scientific Name	Coefficients			Response	Citation
		β_0	β_1	β_2		
Bluegill sunfish	<i>Lepomis macrochirus</i>	-11.11	2.10	-	Functional Mortality	Saylor et al. (2019)
Bluegill sunfish	<i>Lepomis macrochirus</i>	-10.78	1.76	-	Combined Mortality	Saylor et al. (2019)
Hybrid striped bass	<i>Morone saxatilis</i> x <i>M. chrysops</i>	-26.93	0.47	2.88	Combined Mortality	Bevelhimer et al. (2019)

Table 5. Curvilinear biological response models for various species that have been integrated into the BioPA toolset and HBET. Coefficients are to be used with Equation (10).

Species	Scientific Name	Coefficients					Citation
		<i>b</i>	<i>e</i>	<i>f</i>	<i>m</i>	<i>x</i>	
American eel	<i>Anguilla rostrata</i>	-26.90	14.20	0.38	0.0119	11.4	Saylor et al. (2019)
American shad and blueback herring	<i>Alosa</i> spp.	-14.07	8.50	0.55	0.0089	6.64	Saylor et al. (2020)
Bluegill sunfish	<i>Lepomis macrochirus</i>	-10.00	7.50	0.55	0.0089	5.20	Saylor et al. (2019)
Brook trout	<i>Salvelinus fontinalis</i>	-7.99	6.56	0.52	0.0089	2.81	Saylor et al. (2020)
Gizzard shad	<i>Dorosoma cepedianum</i>	-9.60	7.70	0.53	0.0089	4.40	Saylor et al. (2020)
Hybrid striped bass	<i>Morone saxatilis</i> x <i>M. chrysops</i>	-15.90	8.60	0.55	0.0089	6.40	Saylor et al. (2019)
Rainbow trout	<i>Oncorhynchus mykiss</i>	-12.33	7.06	0.54	0.0089	5.08	Saylor et al. (2019)

2.2.7 USE OF SURROGACY FOR BLADE STRIKE

All laboratory work related to the HydroPASSAGE project was directed by prioritization of species analysis and use of surrogates to represent the most at-risk groups of fishes. Most of prioritization relies on trait-based analyses that link common biological, ecological, and other life history traits to groups of taxonomically related fish and estimated entrainment risk (Čada and Schweizer 2012; Pracheil et al. 2016b). Species were chosen because they were affected by hydropower, broadly representative of each taxonomic group, easy to collect or purchase, were not considered threatened, and were reasonably easy to maintain in captivity. While the latter is justifiable from a logistical standpoint, little if any quantitative evidence has been produced to suggest surrogate species provide a proper substitute for blade strike biological response models. A recently published study was

directed at this very problem and tested surrogacy directly for salmonids and clupeids. It was concluded that surrogacy among salmonids was possible at the genus level—i.e., *Oncorhynchus* (rainbow trout) and *Salvelinus* (brook trout) responses to blade strike were not significantly different from one another and impact variables were more important predictors of mortality (Saylor et al. 2020). In contrast, however, size-based surrogacy within a species was ill-advised because the exact relationship between size and mortality has yet to be broadly applied to all species. Surrogacy among clupeids was also deemed possible so that fishes within the *Alosa* and *Dorosoma* genera could be considered together in a biological response model. This was the first instance of quantifiable support for blade strike surrogacy using biological response data and suggests that the biological response models can potentially be applied to other groups beyond the nine species tested to date.

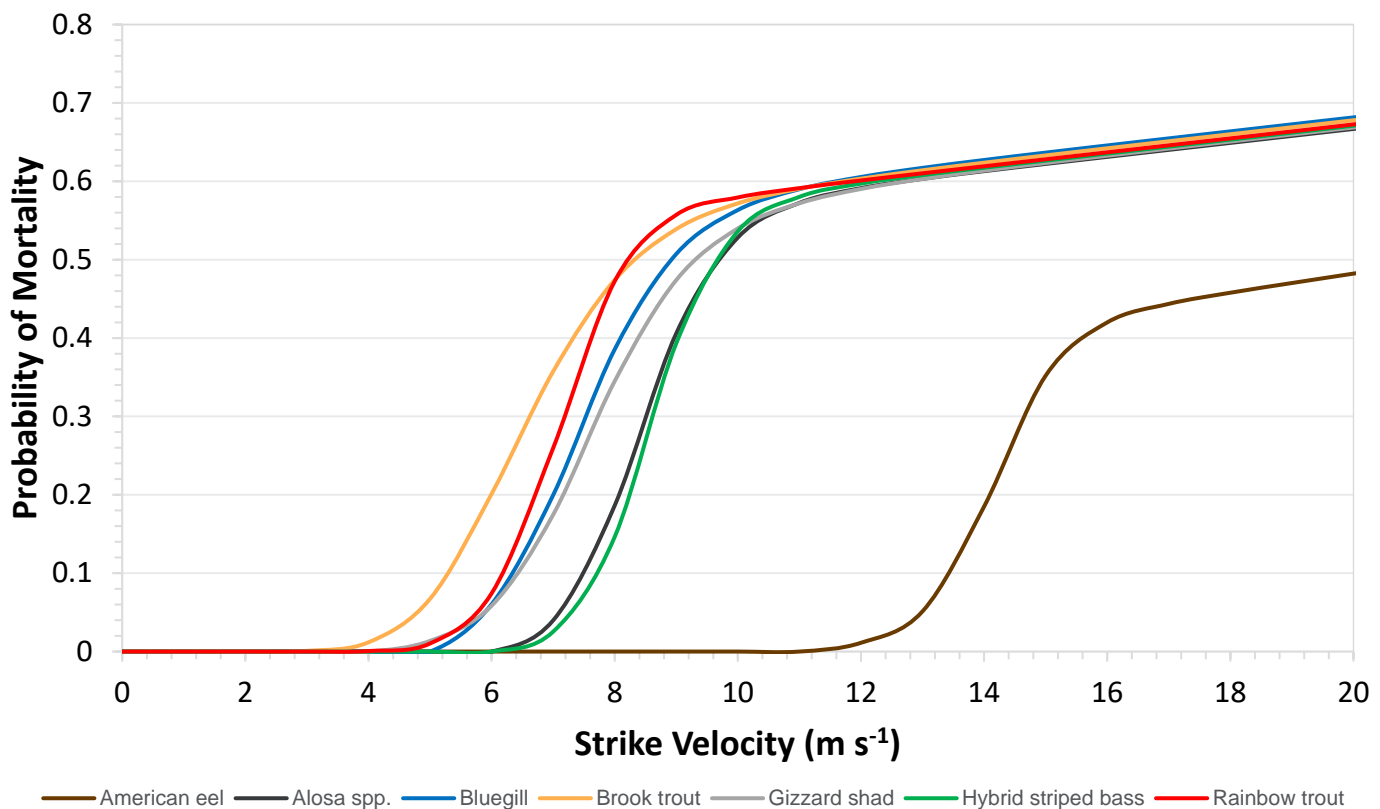


Figure 12. Comparison of the curvilinear biological response models for various species that have been integrated into the BioPA toolset and HBET. The lines represent the coefficients from Table 7 applied to Equation (10). Mortality estimates include functional and immediate mortality.

2.3 TRAITS AFFECTING SUSCEPTIBILITY TO BLADE STRIKE

Blade strike survival also depends on characteristics of the fish itself, its body shape, center of gravity, biomechanical traits (e.g., scales, skin, muscle, and skeleton), and size.

2.3.1 FISH SHAPE

Fish are the most taxonomically diverse group of vertebrates alive today; nearly 40,000 species have been described (Froese and Pauly 2020). Fish have evolved into a variety of unique shapes that are best adapted to suit their needs (e.g., interacting with the environment, use of resources, and other life history requirements). In biological terms, fish shape is most often linked with swim type—proportion of the body and fins involved with propulsion—which in turn relates to swimming performance based on the

biomechanics of movement (Blake 2004). Fish shape likely plays an important part in susceptibility to turbine passage-related injuries including blade strike impact. For example, many riverine species, including clupeids (shad/herring), centrarchids (sunfishes), moronids (temperate basses), and percids (perch-like fishes), have laterally compressed bodies that are much deeper than they are wide. In contrast, acipenserid (sturgeons), anguillid (true eels), ictalurid (North American freshwater catfishes), and catostomid (suckers) fishes are more rotund so that the disparity between body depth and width is reduced. The salmonid (salmon/trout), cyprinid (minnows), and esocid (pike/muskellunge) fishes have shapes that fall somewhere between these other groups. Regardless, it seems reasonable to assume that each shape, and the inherent biomechanical traits linked to shape, would also have unique susceptibility to blade strike. For example, laterally compressed fish have much less

musculature along their lateral flanks than other groups, which would not absorb as much energy after impact. Less muscle may cause more energy to transfer directly onto the skeletal system and organs, thereby causing higher rates of injury or mortality in these fishes. The exact relationship between body shape and susceptibility to blade strike injury or mortality has not been explicitly tested.

2.3.2 CENTER OF GRAVITY

Another species-related difference is consideration of fish as a physical object and variation in susceptibility to blade strike linked with disparities in their centers of gravity. Strike events occurring near the center of gravity, likely transfer more energy to the fish and potentially lead to higher injury and mortality rates. Early work by Turnpenny et al. (1992) found that impacts from a turbine blade were considered deflections unless the blade contacted the body close to the center of gravity. In this way, rates of injury and mortality are also likely linked to the proximity of impact to the center of gravity for many species. Paddlefish and American eel likely do not fit this trend because of the disproportionate influence of their head and tail, respectively, on their centers of gravity. To investigate this directly, two different groups of rainbow trout were exposed to blade strike impact with a 52 mm blade at velocities known to be nearly 100% lethal. We struck fish along their entire body length (head to tail) to link vertebral fractures to location of strike relative to center of gravity. In general, vertebral fractures seem to be more likely and severe (i.e., more than one fracture) because the impact occurs closer to the center of mass for both small and large rainbow trout (Figure 13). Interestingly, large rainbow trout also formed a separate cluster of internal decapitations linked with impacts to the head, but no such impacts caused comparable injuries in small rainbow trout. Internal decapitations were likely observed in large fish because their head has more mass compared to small fish, suggesting strikes near vulnerable points (e.g., the connection of vertebral column to the cranium) are more likely to cause fractures as well. While the latter may be true, uncertainty remains because the experiment has yet to be

replicated, but results do suggest that center of gravity is an important variable in estimates of severe injury among fish exposed to blade strike. Bevelhimer et al. (2019) showed similar trends in hybrid striped bass for which the highest number of mortalities were associated with strikes to the head and mid-body near what is likely the center of gravity for this species. Recent work from Alden Laboratories has also shown that mortality was higher when the blade struck the body near the center of gravity in rainbow trout (Amaral et al. 2020). Center of gravity has been reported to be from 0.37 to 0.48 (proportion of body from the head relative to standard length) according to species (Turnpenny et al. 1992), but the underlying relationship between species, center of gravity, and blade strike impact remains untested.

2.3.3 BIOMECHANICAL TRAITS

The biomechanical traits of fish, or the inherent physical properties related to the mechanical behavior of their entire body or vertebral column, may also account for differences in blade strike injury and mortality susceptibility among species. Fish are a complex, well-adapted, mixture of mucus, scales, skin, muscle, and skeleton—the exact size, shape, and proportion of each structure also vary by species. To date, data from blade strike trials suggest that mid-body, lateral strikes at 90° cause the highest incidence of severe injury and death compared to other conditions (EPRI 2008, 2011; Saylor et al. 2019; Bevelhimer et al. 2019; Saylor et al. 2020; Amaral et al. 2020). The high rates of mortality from lateral strikes is surprising considering that dorso-ventral flexion of the body and vertebral column is minimal even in particularly flexible anguillid eels. Likewise, medial-lateral movement of the fish body around the center of gravity is normal and may be quite profound for certain species. There are contrasting demands at play with fish that have evolved efficient shapes and rigid musculoskeletal systems to maximize swimming efficiency; however, the same adaptations also allow for extraordinary flexibility during escape responses to predators. The startle or escape response is characterized by the formation of a “C-shape” of the fish body when the head and tail curve toward one another prior to a spring-like

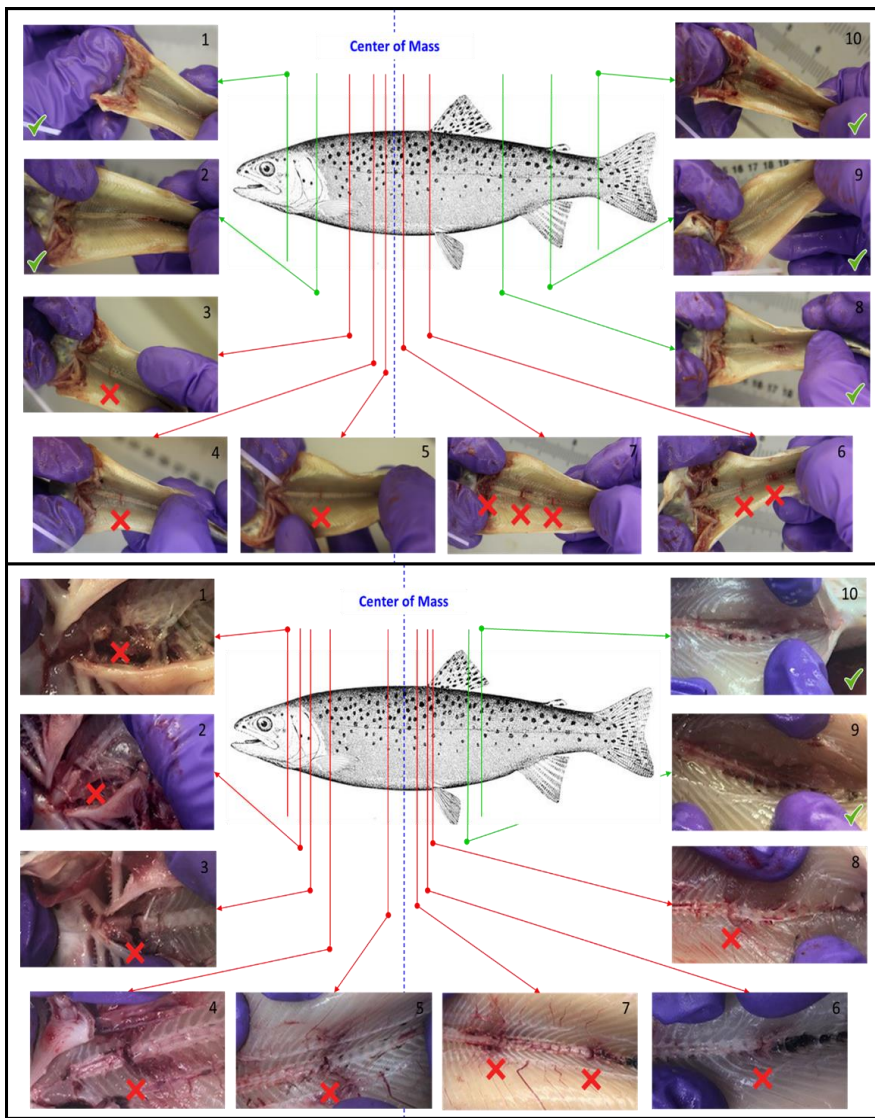


Figure 13. Results of blade strike impact trials on 10 juvenile (small, TL = 10.1–14.9 cm; top panel) and 10 subadult (large TL = 20.1–31.6 cm; bottom panel) rainbow trout. Trials include impacts to the mid-body, lateral surface at 90° with the 52 mm blade and ~9.0 m s⁻¹ (small) or 8.2 m s⁻¹ (large) impact velocity known to cause vertebral fractures. Center of mass was calculated as a proportion relative to standard length and was approximately 0.45 for small and 0.48 large rainbow trout. Red arrows and “X’s” represent fish observed with vertebral fractures, while green arrows and “✓’s” correspond to fish that were not observed to have any vertebral fractures. Rib fractures, clotting, and muscle contusions on small fish 6 and 10 (top panel) were not caused by blade strike impact and were linked to pinching between the blade and holding brackets following tail strikes. Internal decapitations were also observed in large rainbow trout (fish 1–3; bottom panel) and formed a separate cluster associated with head strikes.

motion in a new direction (Webb 1978; Blake 2004). Escape responses of fish occur within a few milliseconds during which the body returns to normal orientation but in the direction perpendicular to the stressful stimulus (Cada et al. 2003). The exact dimensions of the C-shape (i.e., how close the head gets to the tail) varies by species and condition of the fish tested (Cada et al. 2003; Ryon et al. 2004). These disparities among species have prompted use of this behavioral phenomenon as a latent indicator of stress caused by turbine passage (Cada et al. 2003; Ryon et al. 2004; Čada et al. 2006b), but no such link has been made with blade strike impact to date. Of particular interest is gaining a better understanding of how flexibility observed

during the startle response compares to the curvature caused by blade strike impact. Both the startle response and impact curvature appear to be approximately the same (R.K. Saylor *personal observation*) and occur over comparable time scales, but resistance to blade strike may only be partially related to flexibility.

2.3.4 FISH SIZE

The last and most debated fish characteristic is fish size and how it affects injury and mortality rates caused by blade strike. Fish size plays a role in nearly every part of fish passage starting with entrainment risk, which is highest for small fish (Coutant and Whitney 2000; Čada 2001).

There is no clear trend in injury or mortality rates linked with fish size that is true for every species tested.

Unlike other fish characteristics, there is no clear trend in injury or mortality rates linked with fish size that is true for every species tested. Turnpenny et al. (1992) also described a size effect, though their study emphasized fish mass in addition to standard length and related variation in the inertial effect to a higher probability of blade strike impact in larger versus smaller fish. More importantly, small fish were often pushed out of the way of the blade by the bow wave in front and pushed to the side of the approaching blade because these fish had masses <20 g (Turnpenny et al. 1992; Turnpenny 1998). Rainbow trout and *Alosa* spp. with an average mass below 20 g also moved more dramatically than larger individuals as the largest diameter blade (i.e., 76 mm) approached each fish (Saylor et al. 2020). Center of gravity and the movement of fish after blade strike impact are likely linked with inertia, which may partially explain why rates of injury and mortality differ among fish according to size. Susceptibility to blade strike impact is dependent on size, but size-based trends in one species does not necessarily translate to the other species, such as the differences observed between rainbow trout and bluegill.

Susceptibility to blade strike impact is dependent on size, but size-based trends in one species do not necessarily translate to other species.

More recent experimentation built upon work by Turnpenny et al. (1992), but also directly tested size effects. The first study to link fish size with rates of injury and survival were performed by Alden Laboratories starting in 2006 (EPRI 2008, 2011). The results of this study led to the creation of an L/t ratio (the ratio between fish length and blade thickness) that accounted for size within each treatment group of fish. As the L/t ratio increases, i.e., as the size of the blade decreased relative to the fish or as the size of fish increased relative to the size of the blade, the estimated survival decreased (Figure 14). In a similar way,

thinner blades that impact relatively larger fish were specifically injurious because the released energy and body curvature after strike are dissipated over a smaller area of the fish body (EPRI 2008, 2011). Treatment groups with L/t ratios near or below 1.0 correlate with blade thicknesses that nearly match fish length and also have notably higher survival (EPRI 2008). Fish struck with blades comparable to their own length bend less after impact and the energy of strike would be dissipated over a larger section of the fish body. This trend was true for species like rainbow trout, white sturgeon (*Acipenser transmontanus*), and American eel for L/t ratios of 25.0 and velocities up to 12.2 m s^{-1} (EPRI 2008, 2011). Studies performed at ORNL found that L/t ratios for rainbow trout (Bevelhimer et al. 2019) and American eel (Saylor et al. 2019) seemed to fit within the same predicted trends, although the overall fit was dependent on the treatment group tested (Figure 13) (Saylor et al. 2020). While trends in L/t ratio seem well supported, the estimates of mortality for some groups also contained fish that experienced decapitation as a result of the apparatus design and not blade strike specifically. There is no indication of how many individuals or for what treatments this was true, but the authors included these fish as a conservative estimate of mortality (EPRI 2008). This study also did not explicitly separate survival rates based on specific treatment conditions (i.e., location, orientation, and impact angle) so that survival rates for each L/t ratio include all fish in that group. Trials at ORNL suggest that mid-body, lateral strikes were more injurious and responses of fish to other blade strike treatment combinations must be separated to better estimate survival. The latter is especially true because data for other locations, orientations, or impact angles are usually not as thoroughly tested (EPRI 2008, 2011). Estimated survival did include individuals that experienced delayed mortality within 96 hr of strike, but no internal necropsies were performed to determine the actual cause of death of those fish. Lastly, no statistical tests were used to compare treatment groups to controls or other groups, which would help strengthen observed trends discussed by these authors. Trials at ORNL, performed from 2018 to 2020, were designed to control all aspects of blade

strike and also investigated the effects of size using a variety of statistical methods (Bevelhimer et al. 2019; Saylor et al. 2019; Saylor et al. 2020). In addition, we investigated size affects in a new species (e.g., bluegill sunfish) and analyzed rainbow trout in more detail. Trials investigating small= versus medium-size bluegill (Section 2.2.5.3) struck with the 52 mm blade over a range of exposure velocities suggested smaller fish were as susceptible, if not more so, to blade strike injury and mortality than larger fish (Saylor et al. 2019). This disparity is apparent when

comparing dose responses produced from immediate mortality versus mortality estimates that also included fish that survived exposure that cause vertebral fractures. The latter refers to “combined” mortality and also likely represents a more conservative estimate similar to EPRI (2008, 2011) adjusted survival.

Research on rainbow trout also found that large trout (20.1–31.6 cm) may experience slightly higher mortality rates than small rainbow trout (10.1–14.9 cm), but the disparity between the

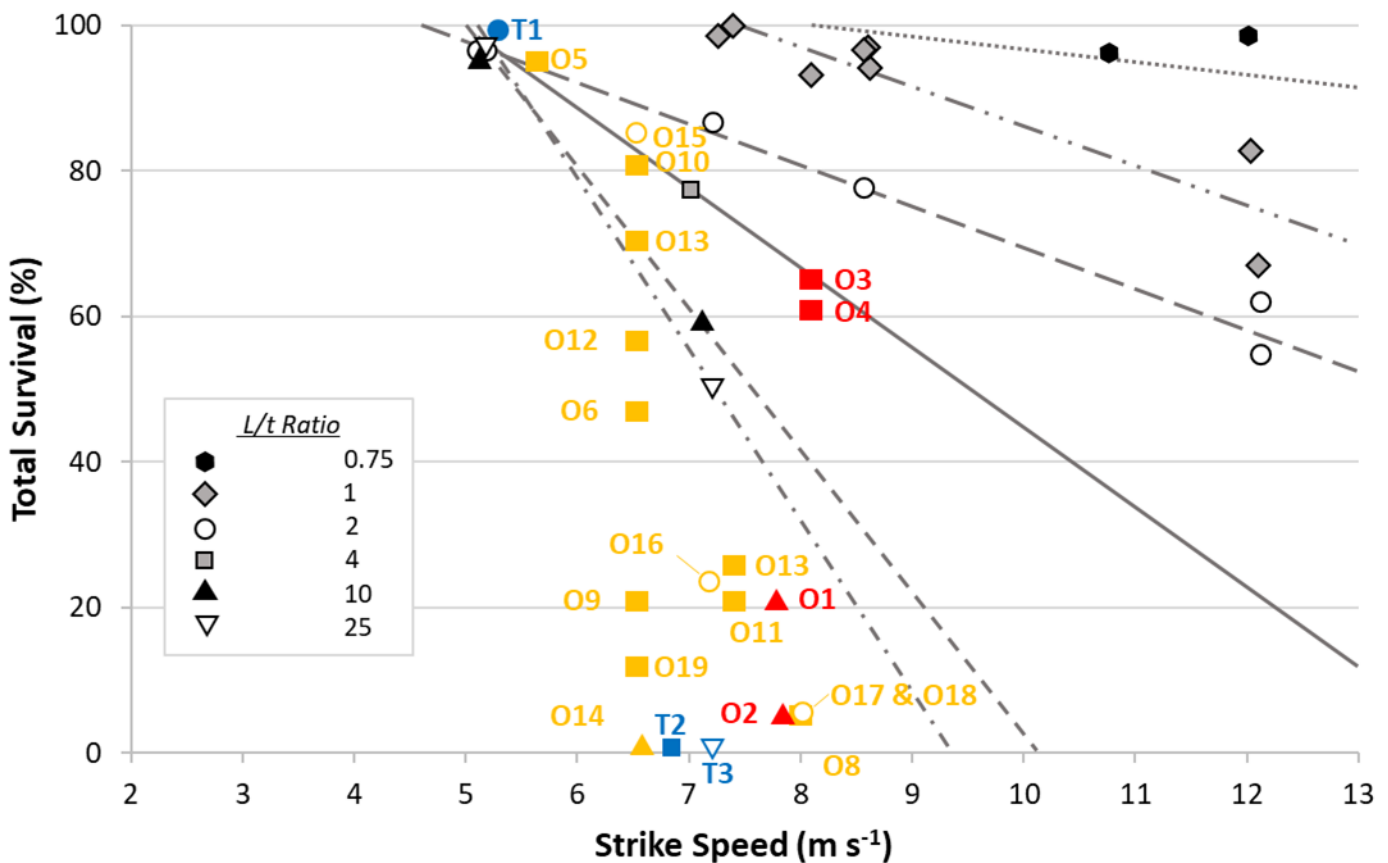


Figure 14. Comparison of L/t ratio for all published rainbow trout data, presented with original data from EPRI (2008). Figure is reproduced from a modified graph from Bevelhimer et al. (2017) where rainbow trout data from 2016 and 2017 (red shapes and text) trials were added. Additionally, for this report, rainbow trout data reported by Saylor et al. (2020; orange shapes and text) and brown trout data reported by Turnpenny et al. (1992; blue shapes and text). Treatment groups are distinguished by location (head, H; mid-body, M; or tail, T), orientation (dorsal, D; lateral, L; or ventral, V), and impact angle (45°, 90°, or 135°). Colored symbols include (1) ORNL 2016 and 2017 includes O1 (HL90; L/t=6.4), O2 (ML90; L/t=6.7), O3 (HL90; L/t=3.4), and O4 (ML90; L/t=3.3); or (2) ORNL 2020 including O5 – O8 (ML90; L/t=5.0), O9 (HD90; L/t=4.9), O10 & O11 (HL90; L/t=5.0), O12 (ML135; L/t=4.8), O13 (MV90; L/t=4.9), O14 (ML90; L/t=10.2), O15 – O18 (ML90; L/t=2.2), and O19 (ML90; L/t=4.4). Brown trout data were all mid-body hits with L/t ratios of 2.0 (T1), 4.0 (T2), and 20.2 (T3).

curves is small and confidence intervals overlapped, suggesting responses are not significantly different (Saylor et al. 2020). In addition, this work included a logistic regression of mortality in relation to blade width, velocity, and total length. In this way, individual estimates of total length were included in regression analysis and model selection. Our logistic regression indicated that within the sizes of fish we measured, fish size was not a significant predictor of mortality compared to blade width or velocity (Saylor et al. 2019; Saylor et al. 2020). Confidence intervals for our biological response curves suggest that bluegill size relationships may be more significant than size effects detected in rainbow trout. Interpretation of logistic regression is also limited by the number of treatment scenarios included in the analysis, which was mainly focused on the worst-case scenario of mid-body, lateral strikes at 90°. Total length is also included at an individual level in our analysis, whereas EPRI (2008, 2011) used average body length to represent each group: the main question is therefore related to how much variability is preferable when investigating size effects within a species. We suggest that disparate trends described by both the EPRI and ORNL studies are both true and reinforce the importance of species when estimating rates of mortality.

2.4 BLADE STRIKE DISCUSSION

Review of the previous 25 years of research on blade strike revealed a number of data limitations and has also helped identify future research needs, as described below.

2.4.1 DATA LIMITATIONS

In this report, we have highlighted many insights gained from laboratory trials for determining blade strike impacts over more than 25 years of active research. While this report summarizes the current knowledge of blade strike impacts to date, it is also important to explore some of the limitations associated with potential application and use of the biological response data. At least

half of the tested species are still in need of additional research to increase the understanding of the trends beyond worst case scenarios (i.e., mid-body, lateral strikes at 90°) available for species tested to date (Table 2). Our methods allowed us to separate rates of mortality among different locations, orientations, and impact angles that were addressed as extensively in previous studies. There are two potential limitations: determining which trials to prioritize and deciding how to balance uncertainty in the estimates with knowledge gained by having more treatment groups. Ideally, blade strike testing could continue for all species to confirm the assumptions about impact characteristics across a wider range of strike velocities. Small samples ($n < 25$ fish per treatment) may be viewed as a limitation, but treatment groups with at least 20 individuals were found to be sufficient with an estimated 95% confidence range of $\sim 0.5 \text{ m s}^{-1}$ for ED₅₀ values from biological response models (Figure 15). Moreover, using 100 fish to investigate five treatment scenarios is better than using them all in just one experiment with the main goal of limiting uncertainty and not gaining more relevant knowledge. We understand that uncertainty is an important consideration of turbine design, but the blade strike apparatus and experimental procedures used at ORNL are designed to maximize the replicability and utility of these biological response data. Surrogacy and its use with blade strike data specifically are only limited by how well one can argue two or more groups of species are similar or different. Most assumptions about surrogacy are based on similarities in biology or ecology and how other researchers have used surrogacy and trait-based data to successfully group related fishes. The only limitation in surrogacy that must be acknowledged is that size-based surrogacy within the same species is not advised unless no other data are available. We look forward to engaging with our industry partners to overcome these limitations and ensuring that our biological response data remain an integral part of designing new, efficient, and biologically inspired hydropower turbine technologies.

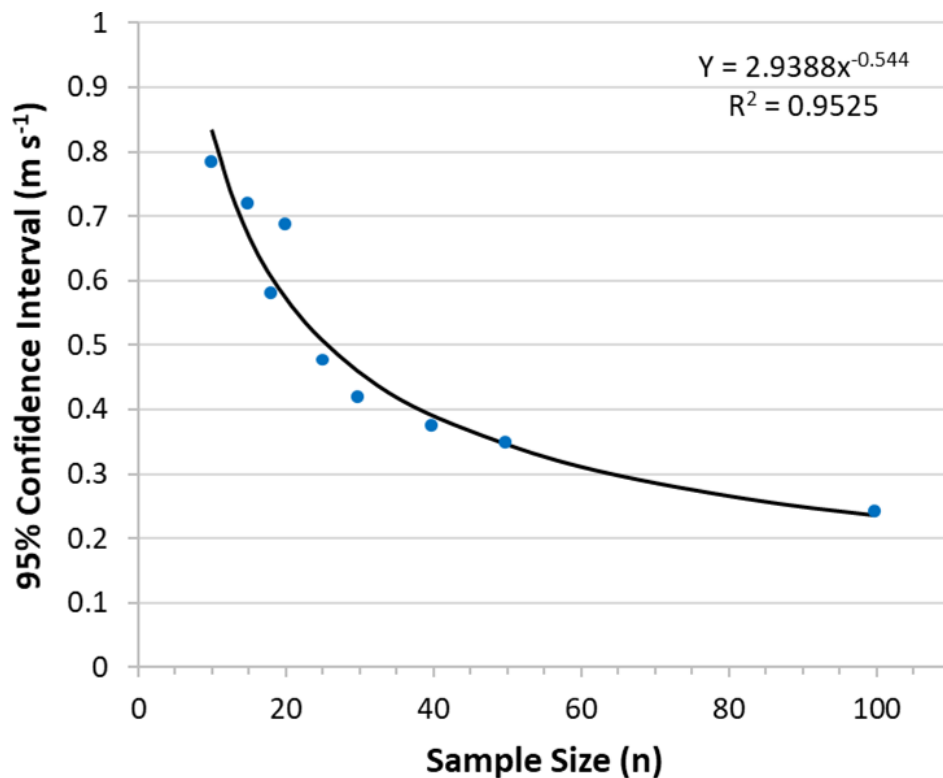


Figure 15. Estimated 95% confidence intervals versus the relative sample size of each treatment group. The resulting values were best described by a power function, which suggested sample size alone accounted for 95.3% of the total variation in this estimate. Use of 20 fish per treatment group is ideal because it will keep variability near 0.5 m s⁻¹ but also allows for inclusion of more test scenarios compared to higher sample sizes.

2.4.2 FUTURE RESEARCH NEEDS FOR BLADE STRIKE

As research on blade strike continues there are several areas in need of further research and additional species that need to be examined.

2.4.2.1 ADDITIONAL RESEARCH ON SPECIES FOUND IN THIS REPORT

Though significant advancements have been made, more research is needed to better understand how blade strike impact affects fish survival. To start, key gaps in available knowledge for species like American eel and paddlefish need to be filled to more completely understand how susceptible both species are to blade strike. It would be beneficial to test more American eel at much higher velocities (up to 15.0 m s⁻¹ or more) to determine the velocity and leading-edge blade width that causes 100% mortality for 90° lateral strikes. These data would be especially useful because eels are often severely injured by turbine passage and currently there is a lack of sufficient evidence to rule out blade strike impact as the main cause. Alternatively, no one has attempted to design a

study of the pinching or grinding of eel between the stators and rotors, which is presumed to be the main cause of amputation and mortality observed in subadult yellow- and silver-phase eels (Saylor et al. 2019). Research on American eel has broad international appeal because of comparable species like the European eel (*Anguilla anguilla*), which often becomes entrained in hydropower dams located throughout Europe. Paddlefish are of particular interest at dams throughout the Mississippi River Watershed because this species is often captured and found to exhibit obvious signs of turbine passage-related trauma, i.e., paddle disfigurement or complete amputation (Hoover et al. 2019). Observations of similar injuries during laboratory experimentation suggest blade strike is the most likely cause; however, previous experimental work was based on only ~100 individuals, so additional research focused on the effects of blade strikes to the head and paddle would be informative. The paddlefish reference biological response model was only based on three treatment groups and investigation of more scenarios would also be ideal when computing the whole-fish biological response model (Section 2.2.3).

2.4.2.2 ADDITIONAL SPECIES FOR BLADE STRIKE TESTING

The HydroPASSAGE project has been successful in leading efforts to test the most ecologically relevant species that are broadly representative of passage concerns in the U.S. However, only minimal laboratory testing of turbine passage-related stressors has been performed on cypriniform fishes (carps, minnows, suckers, and loaches) and no blade strike data are currently available. More laboratory studies of cypriniform fishes are especially important because they represent the most diverse order of freshwater fishes globally (Froese and Pauly 2020). In addition, most minnows and suckers found in this order are considered potamodromous—fish that migrate between upper and lower reaches of rivers and lakes but do not travel at any time to the marine environment (Grubbs and Kraus 2010; Binder et al. 2011). Most efforts to understand passage concerns at dams focus on anadromous salmonids (salmon, trout, and chars) or clupeids (herrings, shads, and sardines) and catadromous anguillids (eels), but largely ignore potamodromous cyprinids (carp) and catostomids (Silva et al. 2018a). Both families have unique body shapes, morphological traits, and attain a variety of sizes that likely make them very susceptible to turbine passage-related stressors as well. To date, no species with comparable traits have been tested to determine their susceptibility to blade strike and we suspect that these species will have a profoundly different response than other fishes tested so far. Outside of North America, groups of fish belonging to the Characiform (e.g., piranha and tetras) and Siluriform (catfish) orders should also be investigated because they are also unique and quite diverse in areas like South America and Southeast Asia where new hydropower development is occurring rapidly.

2.4.2.3 NOVEL RESEARCH OF INTEREST

Lastly, there is a need for novel research into the biomechanics of blade strike impact and how differences in fish size, shape, and morphological characteristics affect estimates of mortality. Studies of this nature would also allow us to use trait-based approaches by defining and grouping

fish based on shared biomechanical characteristics. The resulting “anatomorphic functional guilds” of fishes would provide additional opportunity to more broadly test the use of surrogacy among diverse assemblages of riverine fishes. Each species is uniquely suited to its riverine environment because of its unique anatomorphic adaptations; however, little is known about how the same adaptations may affect risk of mortality to a completely unnatural stressor like turbine passage. The effects of size also remain mostly unconfirmed for every species tested to date, and even well-studied species like rainbow trout have provided conflicting trends. We are most curious about whether size-based disparities are related simply to methodological differences, are truly a biological phenomenon based on changes in center gravity and other physical characteristics, or are a combination of both. Regardless, it is quite clear that fish size is an important variable given how rainbow trout and bluegill exhibited differences in size-effected mortality. While additional trials would be useful, the most current blade strike research will help inspire new technologies that simultaneously optimize power generation and maximize fish survivability during turbine passage.

2.5 BLADE STRIKE CONCLUSIONS

The purpose of this report is to review and clarify general trends for all current biological response data in a format that is easy to understand and to serve as a useful reference guide. We have also discussed each species’ biological responses in slightly more detail and refer the readers to the publications cited throughout for more specific detail if desired. To conclude this review of blade strike testing, we make the following recommendations and reiterate some important trends highlighted previously:

- Blade strike is likely the main cause of paddlefish injury because significant damage to the paddle observed in the field was nearly replicated during laboratory tests of blade strike impact.
- Young of the year *Alosa* spp. (i.e., American shad) may survive impacts up to 8.0 m s⁻¹ but their small size, presence at many dams

throughout their native range, and annual downstream migrations suggest these clupeids have a high likelihood of passage and interactions with turbine blades.

- American eel seems resistant to blade strike impacts, yet observations of whole-body amputations do occur, which may be caused by strikes from thinner blades (<19 mm) moving at higher velocities (>20 m s⁻¹), or is perhaps linked to pinching or grinding: both these scenarios remain untested.
- Mid-body lateral strikes at 90° are generally the most injurious and lethal and thus should always be included in laboratory experiments that aim to assess blade strike impacts.
- Thinner faster blades are always more detrimental than thicker slower blades, which is true even when evaluating incremental differences in blade leading-edge thicknesses that may only be 10 mm.
- All species we have tested so far generally do not survive mid-body, lateral blade strike impacts at 90° above 10.0 m s⁻¹ (except American eel), which makes testing faster velocities unnecessary.

- Modifications to turbines should include designs that have shallower impact angles, which would likely result in more strikes being deflected away from the fish's center of mass, thereby decreasing the rate of severe injury and increasing passage survival (Amaral et al. 2020).

Many of our assumptions related to experimental design and model derivation need to be supported by actual data. For example, we still lack data about the fundamental relationship of blade width to blade velocity that fish may encounter when passing through Francis and Kaplan turbines because these data are proprietary. Our data are meant to be broadly applicable to all turbines given trends in blade leading-edge width and strike impact velocity; however, more precise estimates based on actual blade geometry and operational specifications would be especially useful. Mutual data sharing of this nature will create stronger partnerships and allow us to better meet our industry partners' needs so that we may both inform the design of turbines that minimize environmental impacts.



3.0 PREDICTING THE EFFECTS OF EXPOSURE TO RAPID DECOMPRESSION ON FISH

Chapter authors: Brett D. Pflugrath, John R. Stephenson, and Alison H. Colotelo

Barotrauma may occur when fish are exposed to rapid decompression. Barotrauma refers to injuries that are caused by changes in ambient pressure and often occurs when pressures are reduced in a manner that does not allow the fish sufficient time to physiologically adjust. There are a few settings where this can occur, such as during commercial or recreational fishing when fish are brought to the surface from deep water, and passage through hydropower and other water management facilities where fish can move rapidly from deep to comparatively shallow water and fish may experience subatmospheric pressure due to the hydraulics of the structure.

Turbine passage is considered one of the more severe scenarios, because subatmospheric pressures often occur (up to 100% for some turbines), occasionally resulting in cavitation (the formation and violent collapse of vapor bubbles caused when local water pressure is reduced to the vapor pressure; Čada 1997). The occurrence of barotrauma in fish due to exposure to rapid decompression can be explained by two laws of physics, Boyle's law and Henry's law (Brown et al. 2012b).

Boyle's law states that under a constant temperature, pressure and volume are inversely

proportional, i.e., as pressure decreases, volume increases. Therefore, as fish are exposed to a rapid decrease in pressure, any gas within the fish will rapidly expand. This particularly affects fish that have a swim bladder—a gas-filled organ used to regulate buoyancy (Fänge 1966; Harvey 1963; Pflugrath et al. 2012; Brown et al. 2012b; Jones 1952). During decompression, the swim bladder can expand and rupture causing severe injuries to the fish (Brown et al. 2012b; Tsvetkov et al. 1972). Due its significance, swim bladder morphology is extremely important relative to a species' susceptibility to rapid decompression, and fish fall into three general categories: physoclistous (i.e., closed swim bladder), physostomous (i.e., open swim bladder), and fish with no swim bladder. Because of the significance of the physics described by Boyle's law on the occurrence of barotrauma, the equation has been adapted as a means of quantifying rapid decompression:

$$\frac{P_1}{P_2} = \frac{V_2}{V_1} \quad (11)$$

where P is pressure, V is volume, and the subscripts denote the initial (1) and the resulting (2) state of pressure and volume. Using this equation, the ratio of gas volume change within the fish (V_2/V_1) can be represented as P_1/P_2 , the RPC. For decompression studies, P_1 is often used to represent the acclimation pressure (i.e., the pressure at which the fish achieved neutral buoyancy prior to rapid decompression exposure) and P_2 is often used to represent the nadir pressure (i.e., the lowest pressure to which the fish is exposed during decompression). This calculation has been defined as the ratio of pressure change (RPC) and is often transformed using the natural log, creating the variable log ratio pressure change (LRP; Brown et al. 2012a).

Henry's law states that the amount of gas dissolved within a liquid is proportional to the pressure acting on the liquid. Therefore, as fish experience a rapid decrease in pressure, the amount of gas that can remain dissolved within the bodily fluids of the fish is reduced (Brown et al. 2012b). This can cause dissolved gases within the blood and other bodily fluids to come out of

suspension and form bubbles. Once these bubbles have formed, they are then affected by Boyle's law and can expand. If the bubbles become large enough, they can form emboli within the blood stream and restrict or stop the flow of blood to some areas of the fish. In addition, emphysema—abnormal presence of gas within bodily tissues—can occur when gas bubbles form within organs and other tissues, potentially causing hemorrhage and other damage as the bubbles expand.

3.1 DECOMPRESSION THROUGH TURBINES AND OTHER HYDRO STRUCTURES

The pressure exposure that a fish experiences starts in the forebay, where pressure is a function of water depth; i.e., the deeper a fish resides in the forebay, the greater the pressure. Once entrained, pressures within turbines typically increase within the intake and then rapidly decrease at the runner. As a fish passes through a turbine, pressures can fall in less than a second and to pressures less than atmospheric pressure (≈ 101.3 kPa; all pressures presented here are absolute pressures). After passing the turbine runner, pressures generally return to depth-equivalent ambient pressures within the draft tube and tailrace. Often the tailrace is much shallower than the forebay, and fish may not be able to seek deeper water (higher pressure) to help to alleviate some barotrauma that may have occurred during turbine passage.

Both the nadir and acclimation pressure, and therefore the RPC, that a fish experiences can vary significantly depending on the hydropower facility designs and species-specific traits. Acclimation depth is first limited to the physical restraints within the forebay, where a fish is restricted to a range of pressures from surface pressure to the pressure that is present at the bottom of the forebay. The acclimation depth is often further reduced because of species-specific traits, such as habitat or depth preferences and physiological limitations such as swim bladder morphology (Pflugrath et al. 2012). These species-specific traits may limit the physical

location that a species will or can inhabit at a state of neutral buoyancy.

The nadir pressure is greatly dependent on the turbine design and operation (discharge, forebay elevation, tailwater elevation), but is also dependent on where the fish enters the intake or passes the turbine runner. For example, the difference between turbine designs is apparent when comparing Sensor Fish data from three Francis turbines at Arrowrock (Boise River, Idaho), Detroit (North Santiam River, Oregon), and Cougar (South Fork McKenzie River, Oregon) dams, which had lower nadir pressures than an advanced hydropower Kaplan turbine design installed at Wanapum Dam (Columbia River, WA; Figure 14; Fu et al. 2016). In addition, Sensor Fish deployed through the Kaplan design installed at Wampum Dam show how operational settings such as flow can alter the nadir pressures (Figure 16). Lastly, the large range of nadir pressures recorded at each dam demonstrates the variance in nadir pressures that a fish may experience, even within the same turbine and operational settings, because of the

location at which the fish (or Sensor Fish) passes the turbine runner. It is obvious from these studies, that the nadir pressures that occur in turbines can vary from severe (near vapor pressure or just above 0 kPa) to likely benign (well above surface pressure).

In addition to turbines, other parts of hydropower facilities and other water regulation structures, including spillways and weirs, can cause rapid decompression (Pflugrath 2017; Deng et al. 2017). Weirs and spillways that take water from deep in the forebay can cause an immediate decompression to surface pressure as soon as the water passes the gate. The deeper the intake the more potential for the fish to be acclimated to deeper depths, and therefore a potential for greater RPCs.

3.2 DEVELOPING BIOLOGICAL RESPONSE MODELS FOR RAPID DECOMPRESSION

The effects of rapid decompression on fish, which can be applied to turbine passage, has been

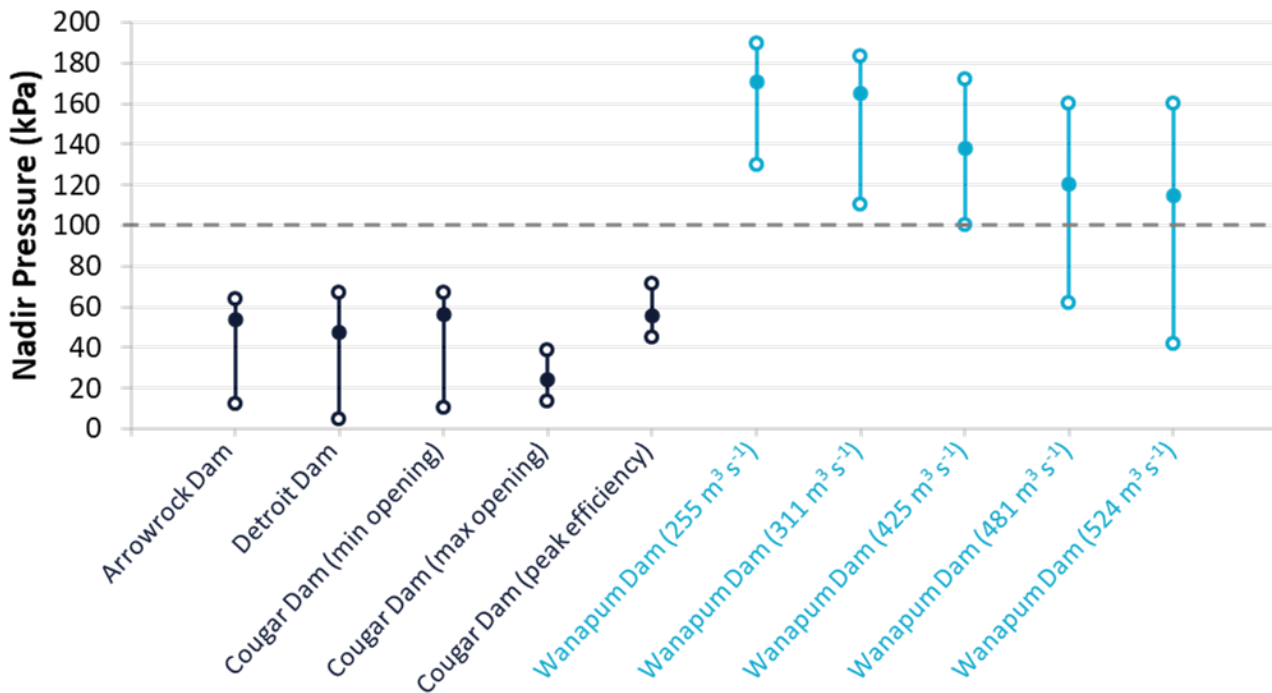


Figure 16. Median (solid dots) and range (open dots) of nadir pressures recorded during Sensor Fish releases through Francis turbines (dark blue) at Arrowrock, Detroit, and Cougar Dams, and an advanced hydropower Kaplan turbine (light blue) at Wanapum Dam. The horizontal dashed line represents surface pressure (approximately 101.3 kPa). Recreated from Fu et al. (2016).

examined in several species. These studies generally involve exposing fish to a rapid decompression using specialized testing apparatuses (refer to the Appendix for more details about testing apparatuses) and assessing fish for injuries, mortality, and often behavioral changes. Most studies conducted an examination or necropsy of the fish, which generally included an internal and external evaluation that looked for injuries including exophthalmia, gastrointestinal eversions, swim bladder rupture, and emboli, emphysema, and hemorrhaging within various organs and tissues. Many of the studies used these results to develop biological response models to predict the occurrence of injuries or mortalities.

3.2.1 FISH SPECIES EXAMINED FOR SUSCEPTIBILITY TO RAPID DECOMPRESSION

Many of the studies presented in this section produced biological response models for predicting the probability of injury or mortality when fish are exposed to various levels of rapid decompression. Studies that did not produce biological response models can still be used in providing an indication of susceptibility compared to other species, and in some cases it was possible to conduct further analyses as part of this review to develop new biological response models for direct comparison between species and for integration into the HBET and BioPA software tools.

Studies that have developed biological response models for rapid decompression have followed the same general methodology and this method was applied to the biological response models developed as part of this review. Results were analyzed to predict up to three potential endpoints: injury, mortal injury, and/or immediate mortality. Fish were considered injured if they were observed to have any barotrauma due to rapid decompression. Fish were considered mortally injured if they were observed to have sustained injuries that through statistical analysis were found to be highly associated (Odds ratio > 1 and Fisher's exact test $p < 0.05$) with and a significant predictor of mortality (stepwise

regression model $p < 0.05$; McKinstry et al. 2007). Immediate mortality included fish that died or exhibited moribund behavior within up to 30 min after exposure. Moribund behavior has included erratic or burst swimming, inability to regain equilibrium, or persistent cough-like behavior indicative of severe damage to the gills.

Each endpoint was then independently modeled (logistic regression) to predict the probability of occurrence at a given rapid decompression exposure:

$$P(X) = \frac{e^{\beta_0 + \beta_1 \cdot \ln(P_a/P_n)}}{1 + e^{\beta_0 + \beta_1 \cdot \ln(P_a/P_n)}} \quad (12)$$

where X is the selected endpoint (i.e., injury, mortal injury, or immediate mortality), β_0 and β_1 are specific coefficients for each endpoint determined by the logistic regression analysis, and P_a and P_n are acclimation and nadir pressures, which are combined to represent the ratio of pressure change from the decompression exposure (Equation (11)).

3.2.1.1 AMERICAN EEL – *ANGUILLA ROSTRATA*

Both yellow-phase ($n = 105$; $L = 230$ – 423 mm; $W = 17$ – 116 g) and silver-phase ($n = 108$; $L = 216$ – 686 mm; $W = 14$ – 507 g) American eel were exposed to rapid decompression using the PNNL aquatic barotrauma chambers (Appendix A, Section A.2.5) (Pflugrath et al. 2019). Eel were acclimated to a pressure of 172 kPa (depth equivalent ≈ 7.25 m) for about 1 day and exposed to nadir pressures ranging from 8.04 to 57.33 kPa. These exposures resulted in RPCs ranging from 3.0 to 21.4 (LRP = 1.10–3.06). No immediate mortality and minimal injuries were observed after exposure to rapid decompression, and, when statistically analyzed, there was no correlation between RPC and the occurrence of injuries or mortalities for either phase of American eel. American eel were observed to maintain a state of negative buoyancy and, when decompressed, were adept at quickly evacuating gas from their swim bladders. These two traits provide the eel with a resiliency to barotrauma. Because few injuries or mortality were observed,

the biological response models for injury (see Table 11 in Section 3.2.2.1), mortal injury (see Table 12 in Section 3.2.2.2), and immediate mortality (see Table 13 in Section 3.2.2.3) could not be fully developed and are designated as a minimal response over the tested range.

3.2.1.2 AMERICAN SHAD – *ALOSA SAPIDISSIMA*

Juvenile American shad were exposed to rapid decompression using the PNNL aquatic barotrauma chambers (Appendix A, Section A.2.5) (Pflugrath et al. 2020b). A total of 460 American shad, with lengths of 35–86 mm (median = 56) and masses of 0.3–5.9 g (median = 1.4 g), were exposed to various magnitudes of rapid decompression (138 of which were controls). Fish were acclimated to two acclimation pressures throughout the testing, 120 and 170 kPa (depth equivalent \approx 1.9 and 6.8 m), and nadir pressures ranged from 11.7 to 136.5 kPa, resulting in RPCs ranging from 1.2 to 14.5 (LRP = 0.2–2.7).

Biological response models were developed by following the previously described methods (Section 3.2.1) for the probability of injury (see in Section 3.2.2.1), mortal injury (see Table 12 in Section 3.2.2.2) and immediate mortality (see Table 13 in Section 3.2.2.3) (Pflugrath et al. 2020b). The mortal injury analysis classified six injuries and mortal injuries: swim bladder rupture, renal hemorrhaging, exophthalmia, renal embolism, dorsal fin emphysema, and right eye hemorrhaging. Swim bladder rupture was the most common injury and occurred in 88% of fish that were observed to have injuries (173 of 197).

3.2.1.3 AUSTRALIAN BASS – *PERCALATES NOVEMACULEATA*

Juvenile Australian bass ($n = 520$; $L = 73$ – 126 mm; $W = 6.7$ – 88.8 g) were examined using the New South Wales Department of Primary Industry (NSW DPI) barotrauma chambers (Appendix A, Section A.2.6) (Pflugrath et al. 2018). Throughout the study, fish were acclimated to pressures ranging from 100.9 to 200.6 kPa and exposed to nadir pressure ranging from 14.4 to 78.8 kPa. The RPC range was 1.3 to 10.6 (LRP = 0.25–2.36). Data from the rapid

decompression exposures were examined using the same methods previously described (Section 3.2.1), and biological response models were developed to predict the probability of injury (see Table 11 in Section 3.2.2.1) and mortal injury (see Table 12 in Section 3.2.2.2). Four injuries were classified as mortal injuries: heart hemorrhaging, gill emboli, exophthalmia, and subdermal emphysema. As part of this review, an additional analysis was conducted using the same methods and the original data (Pflugrath et al. 2018) to produce a biological response model for predicting immediate mortality for a given rapid decompression exposure (see Table 13 in Section 3.2.2.3).

3.2.1.4 BLUEGILL SUNFISH – *LEPOMIS MACROCHIRUS*

Several studies have been conducted to investigate the susceptibility of bluegill sunfish to rapid decompression (Hogan 1941). The mortality of bluegill due to decompression was first reported by Hogan (1941), where 6 of 10 blue gill died during a series of decompression tests that were conducted to better understand the effects of fish passage through a siphon tube.

A series of three studies of turbine passage were conducted on bluegill using the Turbine Passage System (Appendix A, Section A.2.5) (Abernethy et al. 2001, 2002, 2003). In addition to decompression, the effects of elevated total dissolved gas (TDG) were also examined for two of these studies. Three TDG levels were tested—100%, 120%, and 135%. For the first study, bluegill were acclimated to two pressures; half of the fish were acclimated to surface pressure (101 kPa) and the other half to 191 kPa (depth equivalent \approx 9 m). Fish were allowed to acclimate for 16–22 hr but their states of buoyancy prior to exposure were not reported. Precise nadir pressures were not reported, but chambers were programmed to reach a pressure of ≤ 10 kPa. Assuming a nadir of 10 kPa, RPCs of 10.1 and 19.1 (LRP = 2.3 and 2.9) would have occurred. For each trial, 20 fish were loaded into the chamber and three replicates were conducted per each of the six treatments, which were a combination of the three TDG levels and two acclimation depths. For the fish held at 100%

TDG, mortality rates were 2% for fish acclimated to surface pressure and 35% for fish acclimated to 191 kPa (Table 6).

The second study followed the same methods as the first but targeted a nadir of ≈ 50 kPa. Assuming a nadir of 50 kPa, RPCs of 2.0 and 3.8 (LRP = 0.7 and 1.3) would have occurred. For the fish held at 100% TDG, mortality rates were 5% for fish acclimated to surface pressure and 13% for fish acclimated to 191 kPa (Table 6).

The third study again acclimated half of the fish to surface pressure and the other half to 191 kPa. The chambers were programmed to expose fish to nadir pressures of 69 and 97 kPa, and testing was only conducted with 100% TDG. Again, precise nadir pressures were not reported, but assuming nadirs of 69 and 97 kPa, RPCs of 1.0, 1.5, 2.0, and 2.8 (LRP = 0.0, 0.4, 0.7, and 1.0) would have occurred. Of the 240 fish exposed to rapid decompression, only one mortality was observed (Table 6).

Table 6. Percent mortality of bluegill resulting from exposure to simulated turbine passage pressures at various acclimation and nadir pressures and total dissolved gas levels. Sixty fish were tested under each treatment.

Acclimation Pressure (kPa)	Nadir Pressure (kPa)	Total Dissolved Gas		
		100%	120%	135%
101	2–10	2%	7%	28%
191	2–10	35%	37%	43%
101	≈ 50	5%	0%	0%
191	≈ 50	13%	2%	18%
101	69	0%		
101	97	0%		
191	69	2%		
191	97	0%		

Because of the small sample size, high variability between trials, and imprecise reporting of the nadir pressures, no biological response models could be developed from these data.

A recent study of two Centrarchid species, largemouth bass (*Micropterus salmoides*) (Section 3.2.1.10) and bluegill, was conducted using the PNNL aquatic barotrauma chambers

(Appendix A, Section A.2.5) (Pflugrath et al. in prep-b). A total of 133 bluegill ranging in length from 80 to 117 mm were acclimated to a pressure of 140 kPa (depth equivalent = 4 m) and exposed to a range of nadir pressures from 9.7 to 139.9 kPa, resulting in RPCs ranging from 1.0 to 14.5 (LRP = 0 to 2.67). As the RPCs increased, so did the occurrence of injuries and mortality.

Data from the rapid decompression exposures were examined using the previously described methods (Section 3.2.1), and biological response models were developed to predict the probability of injury (see Table 11 in Section 3.2.2.1), mortal injury (see Table 12 in Section 3.2.2.2) and immediate mortality (see Table 13 in Section 3.2.2.3). Twenty-two different types of injuries were observed and five were classified as mortal injuries: swim bladder rupture, pharyngo-cleithral membrane (transparent tissue behind the gills enclosing the body cavity, often referred to as pericardial window or pericardial membrane) emphysema, hemorrhaging under the pharyngo-cleithral membrane, right eye hemorrhage, and torn mesentery.

3.2.1.5 CARP GUDGEON - *HYPSELEOTRIS* SP.

Carp gudgeon (*Hypseleotris*, sp.; $n = 510$; L = 23–50 mm; W = 0.1–1.6 g) were examined using the NSW DPI barotrauma chambers (Appendix A, Section A.2.6) (Pflugrath et al. 2018). Throughout the study, fish were acclimated to pressures ranging from 100.7 to 200.1 kPa and exposed to nadir pressure ranging from 4.1 to 78.7 kPa. The RPC range was 1.3 to 46.5 (LRP = 0.25–3.8). Data from the rapid decompression exposures were examined using the previously described methods (Section 3.2.1) and biological response models were developed to predict the probability of injury (see Table 11 in Section 3.2.2.1) and mortal injury (see Table 12 in Section 3.2.2.2). Three injuries were classified as mortal injuries: pharyngo-cleithral membrane emphysema, fin emphysema, and mesentery emphysema. As part of this review, an additional analysis was conducted using the same methods and original carp gudgeon data to produce a biological response model for predicting immediate mortality for a given rapid decompression exposure (see Table 13 in Section 3.2.2.3)

3.2.1.6 CHINOOK SALMON - *ONCORHYNCHUS TSHAWYTSCHA*

A series of three studies was conducted with juvenile fall Chinook salmon (*Oncorhynchus tshawytscha*; ~10 cm) in the same manner as the study conducted with bluegill to examine the effects of exposure to rapid decompression and elevated TDG (Abernethy et al. 2001, 2002, 2003; Becker et al. 2003). During these studies, fish were allowed to acclimate for 16–22 hr but were not provided an air pocket within the chambers. Because these fish are physostomous fish (see Section 3.3.1.1 for more details about physostomous fish) and do not have a highly active rete on the swim bladder, they must gulp air to fill their swim bladders; therefore, if these fish do not have access to the water surface or an air pocket, they will not be able to fill their swim bladders to achieve neutral buoyancy. No mortalities and only one injury were observed for fish from all acclimation and nadir treatments that were held at 100% TDG. All surface-acclimated fish held at 135% TDG died from gas bubble disease prior to decompression exposure (Table 7).

Because of the small sample size, no observed mortalities, only one injury observed, not providing an air pocket for fish to fill their swim bladder, and imprecise reporting of the nadir

pressures, no biological response models could be developed from these data.

A second series of studies was conducted using the PNNL aquatic barotrauma chambers to increase the understanding of juvenile fall Chinook salmon exposed to rapid decompression associated with turbine passage (Stephenson et al. 2010; Brown et al. 2012a). The first study examined how the state of buoyancy prior to exposure to rapid decompression affects the susceptibility of Chinook salmon (n = 1461; FL = 80–180; W = 6.0-71.5 g) to barotrauma (Stephenson et al. 2010). Fish were acclimated to 175.8 kPa (depth equivalent = 7.62 m) for at least 16 hr after the state of buoyancy was determined for individual fish by a visual examination within the chambers. Neutrally buoyant fish neither float nor sink; therefore, these fish can easily maintain a horizontal position in the water column with minimal swimming movement (Harvey 1963; Stephenson et al. 2010; Pflugrath et al. 2012). Negatively buoyant fish sink; therefore, to maintain a position in the water column, these fish must swim against gravity and therefore have elevated swimming efforts and exhibit a nose-up orientation. Once the state of buoyancy was determined, the fish were exposed to rapid decompression. Nadir pressures ranged from 12.1 to 127.9 kPa. A biological response model (logistic regression) was developed that predicted

Table 7. Percent mortality of fall Chinook salmon resulting from exposure to simulated turbine passage pressures at various acclimation and nadir pressures, and total dissolved gas levels. Sixty fish were tested under each treatment. Recreated from Abernethy et al. (2001).

Acclimation Pressure (kPa)	Nadir Pressure (kPa)	Injury			Mortality		
		Total Dissolved Gas			Total Dissolved Gas		
		100%	120%	135%	100%	120%	135%
101	2–10	0%	2%		0%	0%	
191	2–10	2%	2%	8%	0%	5%	5%
101	≈50	0%	3%		0%	0%	
191	≈50	0%	0%	0%	0%	0%	0%
101	69	0%			0%		
101	97	0%			0%		
191	69	0%			0%		
191	97	0%			0%		

immediate mortality based on nadir and state of buoyancy:

$$P(M) = \frac{e^{-1.132-0.450P_n+2.400b}}{1 + e^{-1.132-0.450P_n+2.400b}} \quad (13)$$

where M is immediate mortality, P_n is nadir pressure, and b is the state of buoyancy (binary: negative = 0, neutral = 1). As the nadir pressure decreased (resulting in increased RPCs) the probability of immediate mortality increased, and the likelihood of mortality was much lower for negatively buoyant fish (Figure 17).

The second study (Brown et al. 2012a) in this series conducted an extensive examination of the effects of simulated turbine passage pressures on juvenile Chinook salmon. Fish ($n = 5,713$; $L = 71$ – 205 mm; $W = 3.7$ – 134.0 g) were acclimated to pressures of 116.5 kPa (depth equivalent ≈ 1.5

m), 146.2 (depth equivalent ~ 4.6 m), or 175.8 (depth equivalent ~ 7.6 m) prior to rapid decompression (<1 s) to nadir pressures ranging from 6.4 to 144.8 kPa. Testing was conducted at a median temperature of 17.0°C (range = 15.8–17.9°C) and TDG levels were set to two levels, 115% (range = 112.7–118.2; $n = 3,533$) and 125% (range = 122.2–127.5; $n = 2,180$). Eight injuries were determined to be mortal injuries (McKinstry et al. 2007): hemorrhaging in the pericardium, liver, or kidney; ruptured swim bladder; blood or bile secretions from the vent; and emboli in the gills or pelvic fins. A mortal injury biological response model (see Table 12 in Section 3.2.2.2) was reported for juvenile Chinook salmon exposed to rapid decompression. In addition to LRP, the cofactors of TDG and RPCs were found to be significant predictors of mortal injury; however, these covariables combined to explain less than 1% of

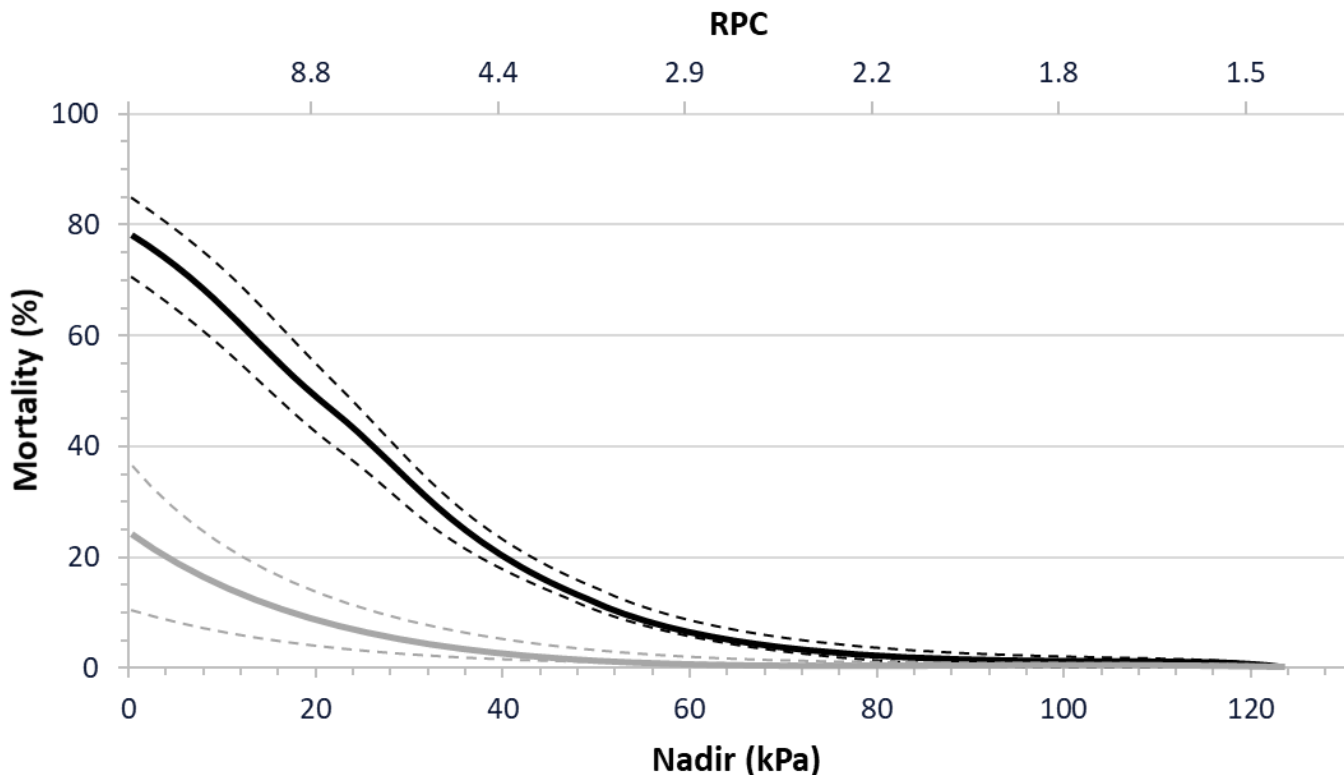


Figure 17. Neutrally buoyant (black line) juvenile Chinook salmon are more susceptible to rapid decompression than negatively buoyant (gray line) due to the amount of gas held within the swim bladder. Because of these differences, researchers should try to match the likely state of buoyancy that fish maintain within nature for application of biological response models. Chinook salmon were acclimated to 175.8 kPa, and percent mortality increases as nadir exposure decreases (RPC increases). Corresponding confidence intervals (95%) are shown with dotted lines.

the deviance in the model and were therefore removed from the model. As part of this review, an additional analysis was conducted using the same methods and the original data for juvenile Chinook salmon to produce biological response models for predicting the occurrence of injury (see Table 11 in Section 3.2.2.1) and immediate mortality (see Table 13 Section 3.2.2.3) at a given rapid decompression exposure (LRP).

3.2.1.7 COMMON SOLE - *SOLEA SOLEA*

Juvenile common sole (*Solea solea*; $n = 160$), along with several other species, were examined using the National Power Marine and Freshwater Biology Unit pressure system (Appendix A, Section A.2.4) to determine the potential effects of fish passing through tidal power turbines (Turnpenny et al. 1992). Testing of these fish was initiated at surface pressure and fish were exposed to nadir pressures ranging from 15 kPa to surface pressure (15, 30, 45, 60, 75, 90, and 100 kPa), resulting in RPCs ranging from 1 to 6.7 (LRP = 0.0–1.9). No injuries or mortalities were observed in the common sole after exposure to rapid decompression. This was attributed to the lack of swim bladder in this species because flat fish of the order Pleuronectiformes lose the swim bladder during metamorphosis from larva to juveniles (Ahlstrom et al. 1984; Desoutter-Meniger and Chanet 2009). Because no injuries or mortalities were observed, the biological response model for these fish has been designated as no response over the tested range (see Table 11–13 in Sections 3.2.2.1–3.2.2.3).

3.2.1.8 GOLDEN GRAY MULLET - *CHELON AURATA*

Juvenile golden gray mullet (*Chelon aurata*; $n = 65$) were tested along with common sole (Section 3.2.1.7) and several other species to determine the potential effects of fish passing through tidal power turbines (Turnpenny et al. 1992). Golden gray mullet tests were initiated at surface pressure and fish were exposed to nadir pressures ranging from 15 kPa to surface pressure (15, 30, 45, 60 kPa, and controls), resulting in an RPC range of 1.0 to 6.7 (LRP 0.0–1.9). Swim bladder rupture was only observed in fish exposed to the lowest nadir value of 15 kPa

(79%). A mortality rate of 6% was observed in fish exposed to a nadir of 30 and 40% for fish exposed to a nadir of 15 kPa. As part of this review, an additional analysis was conducted using the previously described methods and the reported data (Turnpenny et al. 1992) to produce a biological response model for predicting the immediate mortality of golden gray mullet for a given rapid decompression exposure (see Table 13 in Section 3.2.2.3).

3.2.1.9 SOCKEYE SALMON AND KOKANEE - *ONCORHYNCHUS NERKA*

A series of examinations were conducted on juvenile sockeye salmon (*Oncorhynchus nerka*) using a pressure chamber at the University of British Columbia (Appendix A, Section A.2.1; (Harvey 1963). These studies were conducted to better understand the response of sockeye salmon to changes in pressure, particularly the response of the swim bladder to regulate buoyancy. One of the experiments gradually decompressed 50 sockeye salmon to 16.7 kPa, and no mortality was observed (Harvey 1963). These decompressions were sufficiently slow that while experiencing decompression, fish were able to evacuate gas from the swim bladder and avoid barotrauma.

Juvenile kokanee (*O. nerka*) were tested in the PNNL aquatic barotrauma chambers (Appendix A, Section A.2.5) as part of a study examining the use of surrogacy species for testing susceptibility to the rapid decompression associated with turbine passage (Beirão et al. 2020). Kokanee were tested alongside rainbow trout (Section 3.2.1.14) and the results were compared to previously tested Chinook salmon (Section 3.2.1.6). A total of 200 kokanee were examined as part of the study; 179 were exposed to rapid decompression and the remaining 21 were controls. The fish had a median length of 136 mm (range = 113–166 mm) and weight of 26.7 g (range = 10.6–47.7 g). The acclimation pressure was 150 kPa (depth equivalent ~ 5 m) and nadir pressures reached as low as 11.7 kPa, resulting in RPCs ranging from 1 to 12.8 (LRP= 0–2.55).

As part of the surrogacy study, biological response models were developed using the

previously described method (Section 3.2.1) to predict the probability of mortal injury (see Table 12 in Section 3.2.2.2). Immediate mortality only occurred in five kokanee, which was insufficient for conducting a mortal injury analysis. Therefore, mortal injuries developed for Chinook salmon were used (Brown et al. 2012a; McKinstry et al. 2007). In addition, because of the low number of immediate mortalities, a biological response could not be developed with that endpoint. Swim bladder rupture was the most common injury; it occurred in 52 (29.1%) of the tested fish. As part of this review, an additional biological response model was developed using the kokanee data from the surrogacy study (Beirão et al. 2020) to predict the probability of injury due to rapid decompression (see Table 11 in Section 3.2.2.1).

3.2.1.10 LARGEMOUTH BASS – *MICROPTERUS SALMOIDES*

Multiple studies have examined the effects of decompression on largemouth bass. To understand the effects of exposure to a siphon tube, five largemouth bass were exposed to a decompression from surface pressure to 16.7 kPa and held for 15 s before pressures were restored to surface pressure (Hogan 1941). Mortality occurred in four of the five fish.

To understand the effects of angling from depth on largemouth bass ($n = 96$; $L = 150\text{--}380$), fish were exposed to pressure scenarios using the California Polytechnic State University chambers (Feathers and Knable 1983). Fish ranging in size from 150 to 380 mm (total length) were gradually (35 kPa d^{-1}) pressurized and allowed to acclimate to pressures of 101, 191, 281, and 370 kPa (depth equivalent = 0.0, 9.1, 18.3, and 27.4 m) and then rapidly ($<1 \text{ min}$) decompressed to surface pressure. This resulted in RPC values of 1.0, 1.9, 2.8, and 3.7 ($\text{LRP} = 0.00, 0.64, 1.02, \text{ and } 1.30$). Zero mortality was observed in the control treatment group (RPC 1.0). Immediate and delayed mortality was observed in the three other treatment groups (RPC = 1.9, 2.8 and 3.7), 4.4, 41.2, and 41.2% immediate mortality, and 25.0, 41.7, and 45.8% delayed mortality, respectively.

To understand the effects of turbine passage a recent study was conducted on two Centrarchid species, largemouth bass and bluegill, using the PNNL aquatic barotrauma chambers (Appendix A, Section A.2.5) (Pflugrath et al. in prep-b). A total of 308 juvenile largemouth bass ranging in length from 73 to 118 mm were acclimated to a pressure of 140 kPa (depth equivalent = 4 m) and exposed to a range of nadir pressures from 9.4 to 139.9 kPa, resulting in RPCs ranging from 1.0 to 14.5 ($\text{LRP} = 0 \text{ to } 2.7$). As RPCs increased, so did the occurrence of injuries and mortality.

Data from the rapid decompression exposures were examined using the previously described methods (Section 3.2.1) and biological response models were developed to predict the probability of injury (see Table 12 in Section 3.2.2.1), mortal injury (see in Section 3.2.2.2), and immediate mortality (see Table 13 in Section 3.2.2.3) (Pflugrath et al. in prep-b). Forty-nine different types of injuries were observed and six were classified as mortal injuries: pharyngo-cleithral membrane (transparent tissue behind the gills enclosing the body cavity) emphysema, gill emboli, eye emboli, caudal fin emphysema, posterior swim bladder rupture, and exophthalmia.

Pflugrath et al. (in prep-b) compared the results from these three studies by developing a biological response model following the previously described methods for immediate mortality (coefficients: $\beta_0 = -4.625$ and $\beta_1 = 3.115$) from the data reported by Feathers and Knable (1983), and charting the results of all three studies (Figure 18). Decompression results from the study of angling largemouth bass from depth indicated a very similar mortality rate when compared to additional testing conducted for turbine passage (Feathers and Knable 1983; Pflugrath et al. in prep-b). Additional details of this comparison can be found in the discussion of Rate of Pressure Change in Section 3.4.2.4, Confounding Variables.

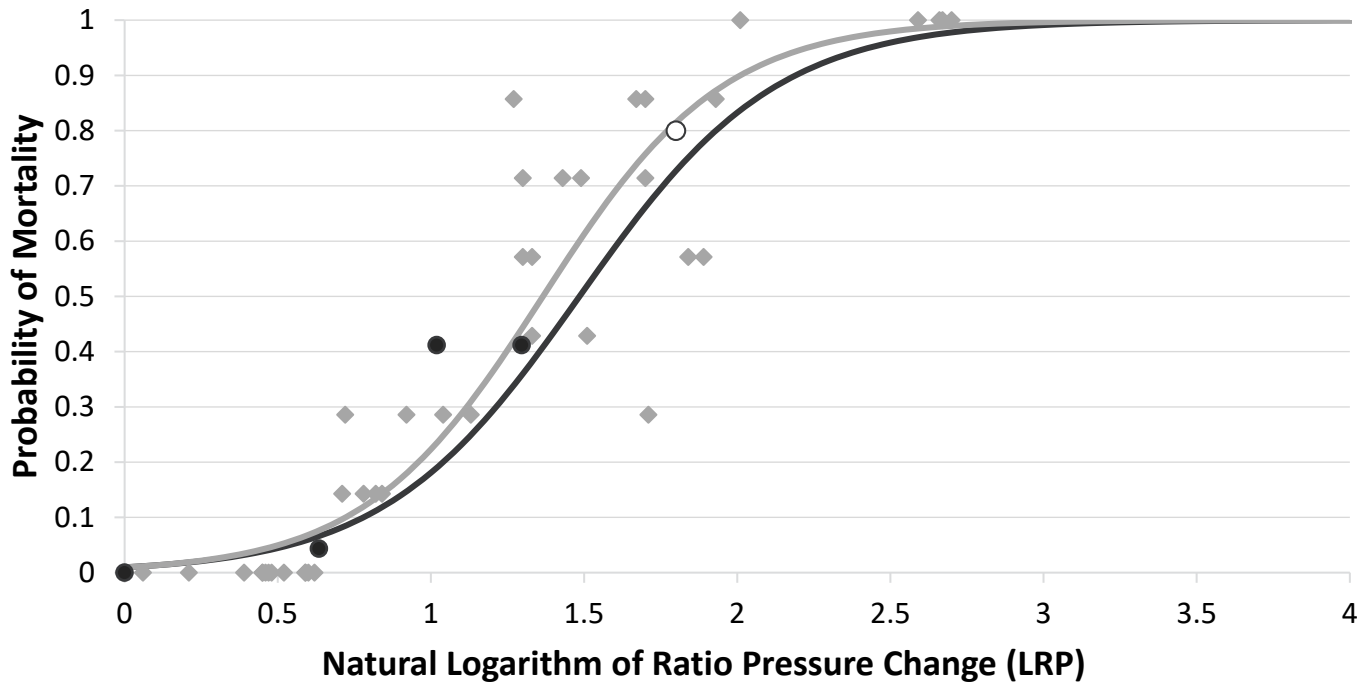


Figure 18. The results from three studies conducted on the susceptibility of largemouth bass to rapid decompression reported rates. The black open circle represents results from the single trial reported by Hogan (1941), the solid black circles represent the results of four treatment groups from Feathers and Knable (1983), and the gray diamonds represent results from Pflugrath et al. (in prep-b). The black line represents a biological response model developed from the data reported by Feathers and Knable (1983), and the gray line represents the biological response model from Pflugrath et al. (in prep-b). This figure was recreated from Pflugrath et al. (in prep-b).

3.2.1.11 MACQUARIE PERCH - *MACQUARIA AUSTRALASICA*

Juvenile Macquarie perch (*Macquaria australasica*; $n = 84$; TL = 33–53 mm; W = 0.4–1.7 g) were examined using the NSW DPI barotrauma chambers (Appendix A, Section A.2.6) (Pflugrath et al. in prep-a). Throughout the study, fish were acclimated to pressures ranging from 100.9 to 200.6 kPa and exposed to nadir pressures ranging from 14.4 to 78.8 kPa. The RPC range was 1.3 to 10.6 (LRP = 0.25–2.36). Data from the rapid decompression exposures were examined using the same methods previously described (Section 3.2.1) and biological response models were developed to predict the probability of injury (see Table 11 in Section 3.2.2.1), mortal injury (see Table 12 in Section 3.2.2.2), and immediate mortality (see Table 13 in Section 3.2.2.3). Five injuries were determined to be mortal injuries: internal

hemorrhaging, emboli in the gills, and emphysema in the pelvic fins, operculum, and body wall musculature.

3.2.1.12 MURRAY COD - *MACCULLOCHELLA PEELII*

Juvenile Murray cod (*Maccullochella peelii*; $n = 273$; L = 54–80 mm; W = 1.7–5.8 g) were examined using the NSW DPI barotrauma chambers (Appendix A, Section A.2.6) (Pflugrath et al. 2018; Boys et al. 2016b). Throughout the study, fish were acclimated to pressures ranging from 100.9 to 199.6 kPa and exposed to nadir pressures ranging from 6.0 to 79.3 kPa. The RPC range was 1.3 to 25.9 (LRP = 0.25–3.26). Data from the rapid decompression exposures were examined using the same methods previously described (Section 3.2.1) and biological response models were developed to predict the probability of injury (see Table 11 in Section 3.2.2.1) and mortal injury (see Table 12 in Section 3.2.2.2)

(Pflugrath et al. 2018). Only two injuries were classified as mortal injuries: heart emboli and eye emphysema. As part of this review, an additional analysis was conducted using the same methods and data to produce a biological response model for predicting immediate mortality for a given rapid decompression exposure (see Table 13 in Section 3.2.2.3).

3.2.1.13 PACIFIC LAMPREY - *ENTOSPHEBUS TRIDENTATUS*

A study was conducted to understand the susceptibility of lamprey to decompression, including juvenile Pacific lamprey (*Entosphenus tridentatus*; $n = 20$; L = 127–183 mm; W = 2.7–7.9 g), which were exposed to sustained decompression (Colotelo et al. 2012). Based on the results from simulated turbine passage on western juvenile brook lamprey (*Lampetra planeri*; Section 1.0) and because lamprey do not have a swim bladder, Pacific lamprey are not likely to sustain injuries due to the expansion of gases (Boyle's law; Section 1.0). Therefore, a test was conducted to increase the potential for injuries to occur due to dissolution of gases (Henry's law; Section; Section 1.0). Pacific lamprey were acclimated for 16–24 hr to 146.2 kPa (depth equivalent = 4.6 m) and then decompressed to 13.8 kPa over approximately 3 min, resulting in an RPC of 10.6 (LRP = 2.36). Pressures were maintained near 13.8 for approximately 17 min. Seven of the lamprey were euthanized and necropsied after exposure, two of which were x-rayed prior to necropsy. The remaining lamprey were held and monitored for up to 120 hr. No injuries or mortalities were observed in any fish, suggesting that Pacific lamprey are not susceptible to barotrauma when exposed to pressure scenarios far exceeding the ranges likely encountered during turbine passage. Biological response models for Pacific lamprey injury (see Table 11 in Section 3.2.2.1), mortal injury (see Table 12 in Section 3.2.2.2), and immediate mortality (see Table 13 in Section 3.2.2.3) are all designated as no response for the tested range.

3.2.1.14 RAINBOW TROUT - *ONCORHYNCHUS MYKISS*

The susceptibility of juvenile rainbow trout to rapid decompression associated with turbine passage and elevated gas levels was examined using the Turbine Passage System at PNNL (Abernethy et al. 2001). Several treatments were examined based on various combinations of acclimation pressure (101 and 191 kPa) and gas saturation (100, 120, and 135%). Chambers were set to expose fish to nadir pressures less than 10 kPa. No fish attained neutral buoyancy for trials where fish were acclimated to 191 kPa. No mortalities and minimal injuries were observed. Because of the small sample size, high variability between trials, negatively buoyant fish, and imprecise reporting of the nadir pressures, no biological response models could be developed from these data.

Juvenile rainbow trout (along with kokanee; Section 3.2.1.7) were tested in the PNNL aquatic barotrauma chambers (Appendix A, Section A.2.5) as part of a study examining the use of surrogacy species for testing susceptibility to rapid decompression associated with turbine passage (Beirão et al. 2020). Rainbow trout and kokanee were compared to previously tested Chinook salmon (Section 3.2.1.6). A total of 194 rainbow trout were examined as part of the study; 174 were exposed to rapid decompression and the remaining 20 were controls. Fish had a median length of 131 mm (range = 104–156) and weight of 26.4 g (range = 4.9–43.9). The acclimation pressure was 150 kPa (depth equivalent \approx 5 m) and nadir pressures reached as low as 11.7 kPa, resulting in RPCs ranging from 1 to 12.8 (LRP = 0–2.55).

As part of the surrogacy study (Beirão et al. 2020), biological response models were developed using the previously described method (Section 3.2.1) to predict the probability of mortal injury (see Table 12 in Section 3.2.2.2). Immediate mortality was not observed in rainbow trout; consequently, a mortal injury analysis could not be conducted. Therefore, mortal injuries developed for Chinook salmon were used. In addition, because no immediate mortalities were observed, a biological response could not be

developed with that endpoint. Swim bladder rupture was the most common injury; it occurred in 38 (21.8%) of the tested fish. As part of this review, an additional biological response model was developed using the rainbow trout data from the surrogacy study (Beirão et al. 2020) to predict the probability of injury due to rapid decompression (see Table 11 in Section 3.2.2.1).

3.2.1.15 SILVER PERCH - *BIDYANUS BIDYANUS*

Juvenile silver perch (*Bidyanus bidyanus*; $n = 390$; $L = 45\text{--}112$ mm; $W = 0.9\text{--}19.6$ g) were examined using the NSW DPI barotrauma chambers (Appendix A, Section A.2.6) (Pflugrath et al. 2018; Boys et al. 2016b). Throughout the study, fish were acclimated to pressures ranging from 101.7 to 201.0 kPa and exposed to nadir pressures ranging from 5.9 to 79.1 kPa. The RPC range was 1.3 to 22.7 (LRP = 0.25–3.12) (Pflugrath et al. 2018). Data from the rapid decompression exposures were examined using the same methods previously described (Section 3.2.1) and biological response models were developed to predict the probability of injury (see Table 11 in Section 3.2.2.1) and mortal injury (see Table 12 in Section 3.2.2.2) (Pflugrath et al. 2018). Three injuries were classified as mortal injuries: pharyngo-cleithral membrane emphysema, fin emphysema, and mesentery emphysema. As part of this review, an additional analysis was conducted using the same methods and data to produce a biological response model for predicting immediate mortality for a given rapid decompression exposure (see Table 13 in Section 3.2.2.3).

3.2.1.16 TIGER MUSKIE - *ESOX MASQUINONGY* × *E. LUCIUS*

A preliminary study of the effects of pressures associated with turbine passage was conducted on three species of fish, including tiger muskie (Brown et al. 2016) using the PNNL aquatic barotrauma chambers (Appendix A, Section A.2.5) (Stephenson et al. 2010). Tiger muskie were selected as a surrogate for northern pike (*Esox lucius*). Fifty juvenile tiger muskie, with a mean fork length of 187 mm (range = 122–259) and mean weight of 41.1 g (range = 8.2–103.6 g), were exposed to rapid (<1 s) decompression,

simulating passage through a hydropower turbine (Brown et al. 2016). Fish were acclimated for 16–24 hr to 146.2 kPa (depth equivalent = 4.6 m) and exposed to nadir pressures ranging from 13.1 to 73.8 kPa. This resulted in RPCs ranging from 1.7 to 11.2 (LRP = 0.53–2.42). Prior to the exposure to rapid decompression, fish were slowly decompressed to determine the pressure at which any negatively buoyant fish were neutrally buoyant. This was done so they could be included in the analysis by adjusting their RPCs using the pressure of neutral buoyancy as the acclimation pressure. Once the state of buoyancy was determined, the pressure was returned to 146.2 and the exposure was initiated.

Few injuries were observed, but they included swim bladder rupture ($n = 11$), emphysema in the pharyngo-cleithral membrane ($n = 1$), and hemorrhaging in the fins ($n = 8$) and liver ($n = 1$). No immediate mortalities were observed; therefore, a mortal injury analysis could not be conducted. At the time this study was conducted, juvenile Chinook salmon were the only species for which a mortal injury analysis had been conducted and the resulting mortal injuries from that analysis were used to develop a mortal injury biological response model for tiger muskie (see Table 12 in Section 3.2.2.2). Further research conducted on other species has shown that what is considered a mortal injury can vary between species, and this must be considered when applying any model that does not use mortal injuries developed specifically for that species.

As part of this review, an additional analysis was conducted using the previously described methods (Section 3.2.1) with the reported data on tiger muskie (Brown et al. 2016) to produce a biological response model for predicting injury at a given rapid decompression exposure (see Table 11 in Section 3.2.2.1). This analysis was conducted using the adjusted RPC to account for pressure of neutral buoyancy.

3.2.1.17 WALLEYE - *SANDER VITREUS*

Walleye (*Sander vitreus*) were examined using PNNL aquatic barotrauma chambers (Appendix A, Section A.2.5) as part of a preliminary study along with tiger muskie (Section 3.2.1.16) and

white sturgeon (Section 3.2.1.19) (Brown et al. 2016). The same methods used for tiger muskie were used to examine walleye ($n = 56$; $L = 178\text{--}319$ mm; $W = 40.9\text{--}272.4$ g), including the 16–24 hr acclimation to 146.2 kPa, and exposure to rapid decompression (nadir = 6.9–73.1 kPa). The resulting RPCs ranged from 1.6 to 20.0 (LRP = 0.47–3.00). As with tiger muskie (Section 3.2.1.16), walleye were slowly decompressed prior to exposure to determine the pressure of neutral buoyancy, so that the RPC could be adjusted.

Fourteen injuries were observed in walleye; swim bladder rupture ($n = 11$) and emphysema in the pharyngo-cleithral membrane ($n = 17$) were the most common injuries. As with tiger muskie, no immediate mortalities were observed; therefore, a mortal injury analysis could not be conducted. Mortal injuries determined for Chinook salmon were instead used to develop the mortal injury biological response model (see Table 12 in Section 3.2.2.2) for walleye and this methodology must be considered when applying this model.

As part of this review, an additional analysis was conducted with the walleye data, and using the previously described methods (Section 3.2.1), a biological response model for predicting injury at a given rapid decompression exposure was developed (see Table 11 in Section 3.2.2.1). This analysis was conducted using the adjusted RPC to account for pressure of neutral buoyancy.

3.2.1.18 WESTERN BROOK LAMPREY - *LAMPETRA PLANERI*

Western brook lamprey were examined as part of a study to determine the susceptibility of lamprey to decompression (Colotelo et al. 2012), which also included Pacific lamprey (Section 3.2.1.13), using the PNNL aquatic barotrauma chambers (Appendix A, Section A.2.5) (Stephenson et al. 2010). Juvenile western brook lamprey ammocoetes ($n = 15$; $L = 80\text{--}124$ mm; $W = 0.8\text{--}3.3$ g) were exposed to two pressure scenarios, rapid decompression and sustained decompression (Colotelo et al. 2012). For the rapid decompression exposure, three lamprey were acclimated for 16–24 hr to 146.2 kPa prior to a rapid (<1 s) decompression to 13.8 kPa for

an RPC of 10.6 (LRP = 2.36). All three lamprey were necropsied after exposure, one of which was first x-rayed, and no injuries or mortalities were observed. For the sustained decompression test, the same methods previously described for Pacific lamprey (Section 3.2.1.13) were used. The sustained decompression period ranged from 13.0–20.0 min for western brook lamprey and no injuries or mortalities were observed. The lack of injuries and mortalities observed in western brook lamprey indicate an extreme resilience to rapid decompression. The injury, mortal injury, and immediate mortality biological response models for western brook lamprey are all designated as no response over the tested range.

3.2.1.19 WHITE STURGEON - *ACIPENSER TRANSMONTANUS*

Juvenile white sturgeon ($n = 46$; $L = 145\text{--}338$ mm; $W = 17.4\text{--}236.4$ g) were included as one of three species that were examined as part of a preliminary study of the effects of rapid decompression on fish using the PNNL aquatic barotrauma chambers (Appendix A, Section A.2.5) (Brown et al. 2016). Fish were acclimated to 146.2 kPa (depth equivalent = 4.6 m) for 16–24 hr, but no fish attained neutral buoyancy. Fish were then exposed to a rapid decompression to nadir pressures ranging from 12.4 to 71.0 kPa, which resulted in RPCs ranging from 2.1 to 11.8 (LRP = 0.72–2.47).

Sixteen of the white sturgeon were injured due to decompression; emphysema that occurred in the head sinus ($n = 9$) and pharyngo-cleithral membrane (reported using the term pericardial window; $n = 8$) were the most common injuries. No mortalities were observed; therefore, no analysis could be conducted to determine mortal injuries. No biological response models were reported in this study; however, as part of this review, the reported data were analyzed to develop an injury biological response model for white sturgeon (see Table 11 in Section 3.2.2.1). This model neglects state of buoyancy and assumes that white sturgeon will not attain neutral buoyancy, because doing so is not likely advantageous for benthic species, but rather, they will maintain a state of negative buoyancy (see Section 3.3.1.4 for further discussion of

buoyancy behavior) (Pflugrath et al. 2019; Silva et al. 2018b; Beirão et al. 2018). In addition, because no mortality was observed, the biological response model for mortality is designated as no response over the tested range (see Table 13 in Section 3.2.2.3).

3.2.1.20 OTHER SPECIES NOT INCLUDED IN HBET OR THE BIOPA TOOLSET

A variety of other species have been examined, but because of incomplete testing or because certain variables were not reported or were reported imprecisely, no biological response models could be developed for these species. There are, however, some inferences about susceptibility that can be gained by examining the data.

HOGAN (1941)

Hogan (1941) conducted various tests on several species to gain an understanding of the potential effects of passage through three large siphon tubes on the lower St. Francis River in Arkansas. In addition to the previously described tests on bluegill (Section 3.2.1.4) and largemouth bass (Section 3.2.1.10), tests were also conducted on golden shiner (*Notemigonus crysoleucas*), crappie (*Pomoxis* sp.), common carp (*Cyprinus carpio*), bullhead catfish (*Ameiurus* sp.), and long-nosed gar (*Lepisosteus osseus*).

Golden shiner (yearling: $n = 20$, adult: $n = 10$) were decompressed from surface pressure (≈ 101 kPa) to 16.8 kPa (RPC = 6.0; LRP = 1.80) for 30 s and no mortality was observed (Table 8). Two exposures were completed on crappie. For

the first, four crappie ($L \approx 10$ cm) were decompressed from surface to 40.5 kPa (RPC = 2.5; LRP = 0.91) for 55 s and mortality occurred in all four fish. For the second exposure, two adult crappie were decompressed from surface to 16.8 kPa and mortality was observed in one of the two fish (Table 8). During this decompression, bruising was observed in the fish and milt and eggs were expelled from the fish. Two yearling common carp ($L \approx 20$ -25 cm) were decompressed from surface pressure to 16.8 kPa (RPC = 6.0; LRP = 1.80) for 30 s and no mortality was observed. Four bullhead catfish ($W = 110$ -450 g) were decompressed from surface pressure to 16.8 kPa (RPC = 6.0; LRP = 1.80) for 25 s with no observable effect. Lastly, a single long-nosed gar was decompressed from surface pressure to 16.8 kPa (RPC = 6.0; LRP = 1.80) for 45 s. The fish expelled gas from its swim bladder during decompression but showed no signs of injury (Table 8). After the initial test, the long-nosed gar filled its swim bladder and after 8 min was then exposed again. The long-nose gar again expelled gas from its swim bladder and had no observable injuries.

The rate of decompression is not reported for these species, though for bluegill it was reported as taking 15 s for the vacuum to build. Assuming a similar period for the other species, this would provide sufficient time for physostomous fish to release gas from the swim bladder and avoid barotrauma. Therefore, these tests on physostomes are likely not applicable for the pressures fish are likely to experience when passing through turbines. However, crappie, which along with bluegill and largemouth bass (Sections 3.2.1.4 and 3.2.1.10) is a physoclistous

Table 8. Mortality rates reported by Hogan (1941) for various fish species exposed to a vacuum simulating passage through a siphon tube.

Common Name	Scientific Name	Age Class	Size	n	Nadir (kPa)	Mortality (%)
Golden shiner	<i>Notemigonus crysoleucas</i>	yearling		20	16.8	0
		adult		10	16.8	0
Crappie	<i>Pomoxis</i> sp.		≈ 10 cm	4	40.5	100
		adult	≈ 340 g	2	16.8	100
Common carp	<i>Cyprinus carpio</i>	yearling	20-25 cm	2	16.8	0
Bullhead catfish	<i>Ameiurus</i> sp.		110-450 g	4	16.8	0
Long-nosed gar	<i>Lepisosteus osseus</i>		29 cm	1	16.8	0

species(see Section 3.3.1.2 for more details about physoclistous fish), would not be able to adjust the swim bladder sufficiently over this time period and this is likely what caused the high mortality rates that were observed.

TSVETKOV ET AL. (1972)

Several species of Eurasian fish were decompressed using the Union of Soviet Socialist Republics Academy of Sciences pressure system (Appendix A, Section A.2.2) (Tsvetkov et al. 1972). These fish were acclimated to pressures

Table 9. Mortality rates reported by Tsvetkov et al. (1972) for several species exposed to varying rapid decompression treatments. Fish were decompressed to surface pressure (≈ 101 kPa) from acclimation pressures ranging from 200–700 kPa.

Common Name	Scientific Name	Length (mm)	<i>n</i>	Rate of Decompression (kPa s ⁻¹)	Mortality (%)
Atlantic salmon	<i>Salmo salar</i>	90	34	100-600	0 ^(a)
		60–80	36	200	20
		Parr	—	300	50
Common minnow	<i>Phoxinus</i>	60–70	11	200	60
Common roach	<i>Rutilus rutilus</i>	20–25	30	10	10
		20–25	50	10–50	40–72
		20–25	10	300	100
		60	8	40	0 ^(a)
		60	2	75	100 ^(a)
		60	1	100	0 ^(a)
Crucian carp	<i>Carassius carassius</i>	60	3	150	100 ^(a)
		86	14	70	0 ^(a)
		86	2	100	100 ^(a)
		86	2	110	0 ^(a)
		86	2	120	100 ^(a)
European cisco	<i>Coregonus albula</i>	86	10	130	100 ^(a)
		130	1	250	100 ^(a)
European perch	<i>Perca fluviatilis</i>	25–30	7	—	0 ^(a)
		25–30	10	—	70
Grayling	<i>Thymallus thymallus</i>	150	2	300	100 ^(a)
Russian sturgeon	<i>Acipenser guldenstadti</i>	90	28	30–600	0 ^(a)
Siberian sturgeon	<i>Acipenser baeri</i>	18–30	30	100–300	100 ^(a)
		30	4	250	0 ^(a)
Sunbleak	<i>Leucaspius delineatus</i>	15–25	22	10	4.5
		15–25	64	10–40	4.7
		15–25	16	150–200	69
		33–60	38	70	0 ^(a)
		33–60	20	100	45
		33–60	5	110	0 ^(a)
		33–60	5	120	40
33–60	20	130	85		

(a) Mortality rates reported as 0 or 100% were originally reported as nonlethal and lethal, respectively.

ranging from 200 to 700 kPa and decompressed to surface pressure at rates of 10 to 1 kPa s⁻¹. Because the acclimation pressure was not precisely reported, biological response models for these fish cannot be developed, but some inferences can be made. For instance, Russian sturgeon (*Acipenser guldenstadtii*) and Siberian sturgeon (*Acipenser baeri*) were observed to have no mortality for fish over 30 mm in length (Table 9). This indicates that these species may have a tolerance for rapid decompression similar to white sturgeon. However, for Siberian sturgeon that were 18–30 mm, 100% mortality was observed (Table 9). Because precise acclimation pressures were not reported, it is difficult to determine if these fish were exposed to a more extreme decompression than the larger fish, or if there is some period of high susceptibility for this species in the early life stages. An additional inference can be made about crucian carp (*Carassius carassius*), which were reported to have high mortality rates across the various treatments, indicating the potential for a high susceptibility to rapid decompression. Additional species were also reported with various treatments and mortality rates (Table 9).

TURNPENNY ET AL. (1992)

In addition to common sole (Section 3.2.1.7) and golden gray mullet (Section 3.2.1.7), Turnpenny et al. (1992) examined several other species of fish for susceptibility to rapid decompression associated with tidal power turbines: Atlantic herring (*Clupea harengus*), Atlantic salmon (*Salmo salar*), brown trout (*Salmo trutta*), dragonet (*Callionymus lyra*), European bass (*Dicentrarchus labrax*), sand smelt (*Atherina boyeri*), twait shad (*Alosa fallax*), and whiting (*Merlangus merlangus*). Two pressure series experiments were conducted, a high-pressure series and a low-pressure series. No injuries or mortalities were observed for the high-pressure series and, because this series did not represent passage through a turbine, only the low-pressure series is discussed in this report. For the low-

pressure series, fish were loaded into the pressure chambers and the pressure simulation was initiated from surface pressure. Pressure was increased to 400 kPa over 10 s and maintained for an additional 5 s. Fish were then rapidly decompressed. Nadir pressures were varied between seven different treatments within the series: 15, 30, 45, 60, 75, 90, and 100 kPa. The resulting RPCs ranged from 1 to 6.7 (LRP = 0.0–1.9). No immediate mortalities were observed for any of the fish species tested by Turnpenny et al. (1992). Delayed mortality was recorded after holding fish for 7 days, but only three species (brown trout, dragonet, and sand smelt) had delayed mortality rates for treatment fish that would likely differ from controls (Table 10). The occurrences of four injuries were also reported: swim bladder rupture and hemorrhaging in the eyes, lateral line, and fins (Table 10). However, no occurrences of hemorrhaging in the lateral line were observed.

BEIRÃO ET AL. (2018)

Pictus catfish (*Pimelodus pictus*; $n = 35$) were exposed to varying magnitudes of rapid decompression simulating passage through a turbine (Beirão et al. 2018). Pictus catfish did not attain neutral buoyancy during the acclimation period. Several different injuries were observed, including swim bladder rupture, gastrointestinal rupture, hemorrhaging (internal and external), emboli, exophthalmia, and intestinal eversion. Swim bladder rupture was the most common injury, occurring in 81% of fish, closely followed by internal hemorrhaging (79%) and emboli (64%). Fish were anesthetized during the testing and immediately euthanized after testing; therefore, mortalities could not be determined. No biological response models were developed from this study because individual fish data were not reported for injuries. However, an analysis of specific injuries was conducted and showed that intestinal rupture and emboli were more likely to occur at faster rates of decompression.

Table 10. Mortality rates and rates for specific observed injuries, including swim bladder rupture (SB rupture, eye hemorrhage (eye hem), and fin hemorrhage (fin hem), reported by Turnpenny et al. (1992) for several fish species exposed to rapid decompression simulating passage through a tidal power turbine.

Common Name	Scientific Name	<i>n</i>	Nadir (kPa)	SB Rupture	Eye Hem	Fin Hem	7 Day Mortality	% Mortality
Atlantic herring	<i>Clupea harengus</i>	25	Control	0	0	0	2	8.0
		19	90	0	0	0	0	0.0
		19	75	0	0	0	0	0.0
		19	60	0	0	0	0	0.0
		35	45	0	14	2	0	0.0
		32	30	0	10	0	0	0.0
		33	15	1	7	0	3	9.1
Atlantic salmon	<i>Salmo salar</i>	20	Control	0	0	0	0	0.0
		20	90	0	0	0	0	0.0
		20	75	0	0	0	1	5.0
		20	60	0	0	0	0	0.0
		20	45	0	0	0	0	0.0
		20	30	0	0	0	0	0.0
		20	15	3	0	0	0	0.0
Brown trout	<i>Salmo trutta</i>	20	Control	0	0	0	0	0.0
		10	100	0	0	0	0	0.0
		10	90	0	0	0	0	0.0
		10	75	0	0	0	0	0.0
		10	60	0	0	0	0	0.0
		10	45	2	0	0	0	0.0
		10	30	3	0	0	0	0.0
		30	15	5	0	0	3	10.0
Dragonet	<i>Callionymus lyra</i>	7	Control	0	0	0	0	0.0
		10	15	0	0	0	3	30.0
European bass	<i>Dicentrarchus labrax</i>	30	Control	0	0	0	0	0.0
		13	30	2	0	0	0	0.0
		17	15	16	0	0	0	0.0
Sand smelt	<i>Atherina boyeri</i>	10	Control	0	0	0	0	0.0
		7	30	0	0	0	0	0.0
		14	15	14	2	2	2	14.3
Twait shad	<i>Alosa fallax</i>	9	100	0	0	0	0	0.0
		9	90	0	0	0	0	0.0
		9	75	0	0	0	0	0.0
		9	60	0	0	0	0	0.0
		9	45	0	0	0	0	0.0
		9	30	0	0	0	0	0.0
		9	15	0	0	0	0	0.0
Whiting	<i>Merlangus</i>	20	Control	0	0	0	3	15.0
		20	45	2	0	0	4	20.0
		10	30	0	1	0	0	0.0
		10	15	8	0	0	2	20.0

3.2.2 RAPID DECOMPRESSION BIOLOGICAL RESPONSE MODELS

Biological response models for predicting injury, mortal injury, or immediate mortality for fish exposed to rapid decompression, have been gathered from the literature or developed as part of this review from previously conducted research and are reported in the following sections (3.2.2.1–3.2.2.3).

3.2.2.1 PROBABILITY OF INJURY DUE TO RAPID DECOMPRESSION

Biological response models have been developed to predict the probability of injury occurring in fish when exposed to rapid decompression associated with passage through hydropower facilities. These models predict the likelihood that

Injury susceptibility ranged from no susceptibility for fish without swim bladders (common sole, Pacific lamprey, and western brook lamprey) to high susceptibility for selected physoclistous fish (bluegill, largemouth bass, and Macquarie perch)

a fish will sustain any injury when exposed to a given ratio pressure change. A total of 18 models have been developed for different fish species (Table 11). Susceptibility ranged from no susceptibility for fish without swim bladders (common sole, Pacific lamprey, and western brook lamprey) to high susceptibility for selected physoclistous fish (bluegill, largemouth bass, and Macquarie perch; Figure 19).

Table 11. Coefficients for rapid decompression biological response models predicting the probability of injury. Model coefficients to be used with Equation (12).

Species	Scientific Name	Coefficients		Citation
		β_0	β_1	
American eel	<i>Anguilla rostrata</i>	∅	∅	Pflugrath et al. (2019)
American shad	<i>Alosa sapidissima</i>	-5.301	4.921	Pflugrath et al. (2020)
Australian bass	<i>Percales novemaculeata</i>	-3.710	3.520	Pflugrath et al. (2018)
Bluegill sunfish	<i>Lepomis macrochirus</i>	-3.402	8.594	Pflugrath et al. (in prep-b)
Carp gudgeon	<i>Hypseleotris</i> sp.	-3.940	3.220	Pflugrath et al. (2018)
Common sole	<i>Solea solea</i>	∅	∅	Turnpenny et al. (1992)
Chinook salmon ^(a)	<i>Oncorhynchus tshawytscha</i>	-4.735	3.485	Brown et al. (2012a)
Kokanee ^(a)	<i>Oncorhynchus nerka</i>	-6.180	4.885	Beirão et al. (2020)
Largemouth bass	<i>Micropterus salmoides</i>	-3.245	7.591	Pflugrath et al. (in prep-b)
Macquarie perch	<i>Macquaria australasica</i>	-6.282	12.353	Pflugrath et al. (in prep-a)
Murray cod	<i>Maccullochella peelii</i>	-4.250	3.230	Pflugrath et al. (2018)
Pacific lamprey	<i>Entosphenus tridentatus</i>	∅	∅	Colotelo et al. (2012)
Rainbow trout ^(a)	<i>Oncorhynchus mykiss</i>	-4.956	3.276	Beirão et al. (2020)
Silver perch	<i>Bidyanus bidyanus</i>	-3.700	4.110	Pflugrath et al. (2018)
Tiger muskie	<i>Esox masquinongy</i> x <i>E. lucius</i>	-4.491	2.581	Brown et al. (2016)
Walleye ^(a)	<i>Sander vitreus</i>	-3.526	3.196	Brown et al. (2016)
Western brook lamprey	<i>Lampetra planeri</i>	∅	∅	Colotelo et al. (2012)
White sturgeon ^(a)	<i>Acipenser transmontanus</i>	-4.625	2.062	Brown et al. (2015)

(a) Model developed as part of this review using data from the cited source.

∅ denotes models of which minimal or no injuries were observed over the tested range.

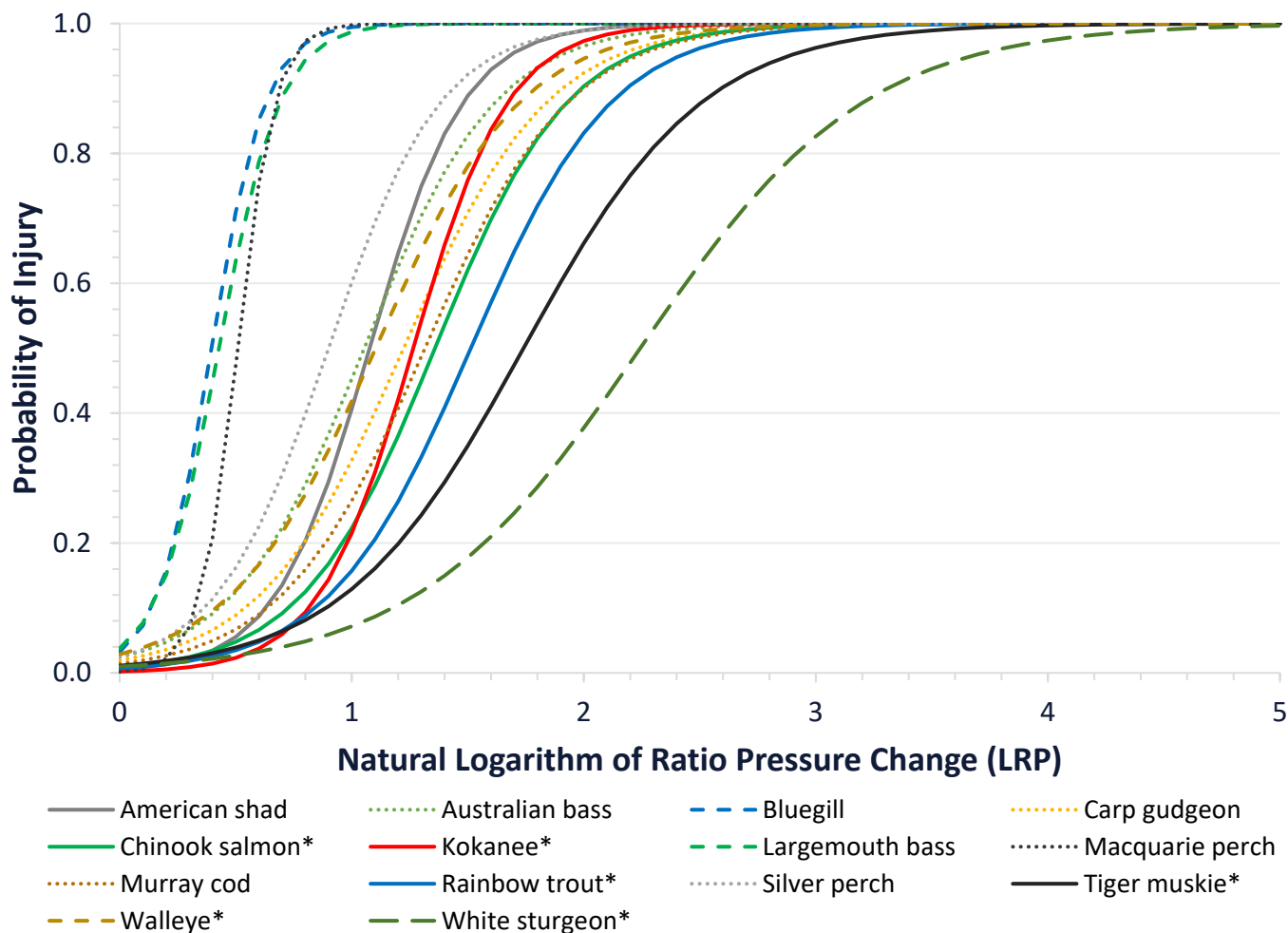


Figure 19. Probability of injury biological response models for rapid decompression using coefficients from Table 11 with Equation (12). Solid lines represent physostomous species, short dash lines represent physoclistous species, and dotted lines represent Australian species. Models developed as part of this review from previously reported data are indicated with an asterisk (*).

3.2.2.2 PROBABILITY OF MORTAL INJURY DUE TO RAPID DECOMPRESSION

Biological response models have been developed to predict the probability of mortal injury occurring in fish when exposed to rapid decompression associated with passage through hydropower facilities. These models predict the likelihood that a fish will sustain a mortal injury when exposed to

a given RPC. Mortal injuries are injuries that have been found to be highly associated with and a significant predictor of immediate mortality (McKinstry et al. 2007). A total of 17 models have been developed for different fish species (Table 12). Susceptibility ranged from no susceptibility for fish without swim bladders (common sole, Pacific lamprey, and western brook lamprey) to high susceptibility for select physoclistous fish (bluegill and largemouth bass; Figure 20).

Table 12. Coefficients for rapid decompression biological response models predicting the probability of mortal injury. Model coefficients to be used with Equation (12).

Species	Scientific Name	Coefficients		Citation
		β_0	β_1	
American eel	<i>Anguilla rostrata</i>	Ø	Ø	Pflugrath et al. (2019)
American shad	<i>Alosa sapidissima</i>	-5.301	4.825	Pflugrath et al. (2020)
Australian bass	<i>Percales novemaculeata</i>	-5.720	2.680	Pflugrath et al. (2018)
Bluegill sunfish	<i>Lepomis macrochirus</i>	-3.308	6.195	Pflugrath et al. (in prep-b)
Carp gudgeon	<i>Hypseleotris</i> sp.	-5.700	1.990	Pflugrath et al. (2018)
Common sole	<i>Solea solea</i>	Ø	Ø	Turnpenny et al. (1992)
Chinook salmon	<i>Oncorhynchus tshawytscha</i>	-5.560	3.850	Brown et al. (2012a)
Kokanee	<i>Oncorhynchus nerka</i>	-6.506	4.669	Beirão et al. (2020)
Largemouth bass	<i>Micropterus salmoides</i>	-3.937	5.723	Pflugrath et al. (in prep-b)
Macquarie perch	<i>Macquaria australasica</i>	-8.926	3.994	Pflugrath et al. (in prep-a)
Murray cod	<i>Maccullochella peelii</i>	-7.330	2.790	Pflugrath et al. (2018)
Pacific lamprey	<i>Entosphenus tridentatus</i>	Ø	Ø	Colotelo et al. (2012)
Rainbow trout	<i>Oncorhynchus mykiss</i>	-5.118	2.927	Beirão et al. (2020)
Silver perch	<i>Bidyanus bidyanus</i>	-3.910	1.390	Pflugrath et al. (2018)
Tiger muskie	<i>Esox masquinongy</i> × <i>E. lucius</i>	-3.926	1.957	Brown et al. (2016)
Walleye	<i>Sander vitreus</i>	-4.957	2.838	Brown et al. (2016)
Western brook lamprey	<i>Lampetra planeri</i>	Ø	Ø	Colotelo et al. (2012)

Ø denotes models of which minimal or no injuries were observed over the tested range.

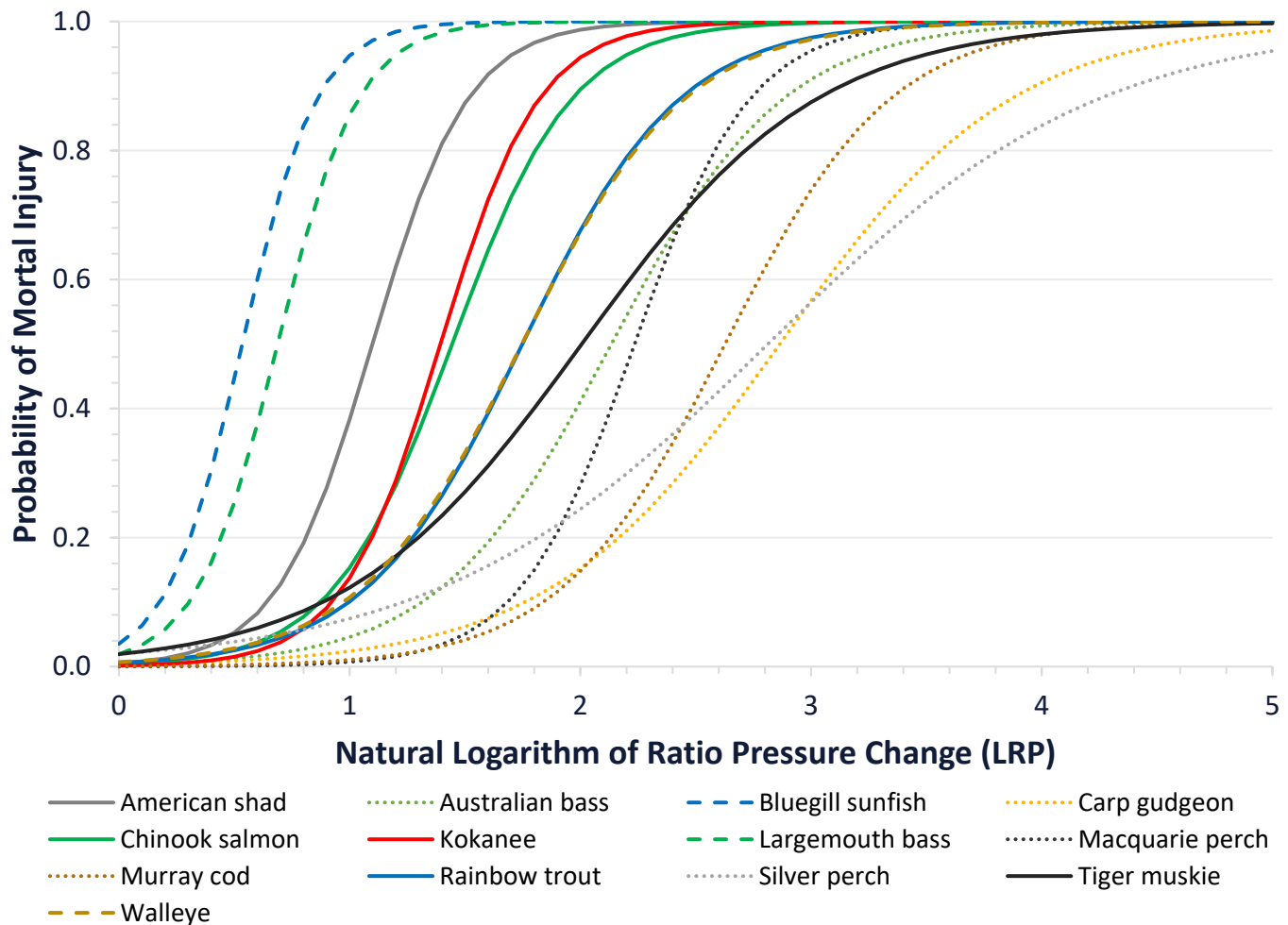


Figure 20. Probability of mortal injury biological response models for rapid decompression using the coefficients from Table 12 and Equation (12). Solid lines represent physostomous species, dashed lines represent physoclistous species, and dotted lines represent species not native to the U.S.

3.2.2.3 PROBABILITY OF IMMEDIATE MORTALITY DUE TO RAPID DECOMPRESSION

Biological response models have been developed to predict the probability of immediate mortality occurring in fish when exposed to rapid decompression associated with passage through hydropower facilities. These models predict the

likelihood that a fish will sustain immediate mortality when exposed to a given RPC. A total of 14 models have been developed for different fish species (Table 13). Susceptibility ranged from no susceptibility for fish without swim bladders (common sole, Pacific lamprey, and western brook lamprey) to high susceptibility for select physoclistous fish (bluegill and largemouth bass; Figure 21).

Table 13. Coefficients for rapid decompression biological response models predicting the probability of immediate mortality. Model coefficients to be used with Equation (12).

Species	Scientific Name	Coefficients		Citation
		β_0	β_1	
American eel	<i>Anguilla rostrata</i>	∅	∅	Pflugrath et al. (2019)
American shad	<i>Alosa sapidissima</i>	-4.431	2.617	Pflugrath et al. (2020)
Australian bass	<i>Percales novemaculeata</i>	-8.573	2.979	Pflugrath et al. (in prep-a)
Bluegill sunfish	<i>Lepomis macrochirus</i>	-8.802	5.097	Pflugrath et al. (in prep-b)
Carp gudgeon	<i>Hypseleotris</i> sp.	-7.220	1.977	Pflugrath et al. (in prep-a)
Common sole	<i>Solea solea</i>	∅	∅	Turnpenny et al. (1992)
Chinook salmon ^(a)	<i>Oncorhynchus tshawytscha</i>	-7.700	3.878	Brown et al. (2012a)
Golden gray mullet ^(a)	<i>Chelon aurata</i>	-7.710	3.820	Turnpenny et al. (1992)
Largemouth bass	<i>Micropterus salmoides</i>	-4.657	3.410	Pflugrath et al. (in prep-b)
Macquarie perch	<i>Macquaria australasica</i>	-6.019	1.825	Pflugrath et al. (in prep-a)
Murray cod	<i>Maccullochella peelii</i>	-6.592	1.488	Pflugrath et al. (in prep-a)
Pacific lamprey	<i>Entosphenus tridentatus</i>	∅	∅	Colotelo et al. (2012)
Silver perch	<i>Bidyanus bidyanus</i>	-5.438	1.126	Pflugrath et al. (in prep-a)
Western brook lamprey	<i>Lampetra planeri</i>	∅	∅	Colotelo et al. (2012)
White sturgeon ^(a)	<i>Acipenser transmontanus</i>	∅	∅	Brown et al. (2016)

(a) Model developed as part of this review using data from the cited source.

∅ denotes models of which no immediate mortality was observed over the tested range.

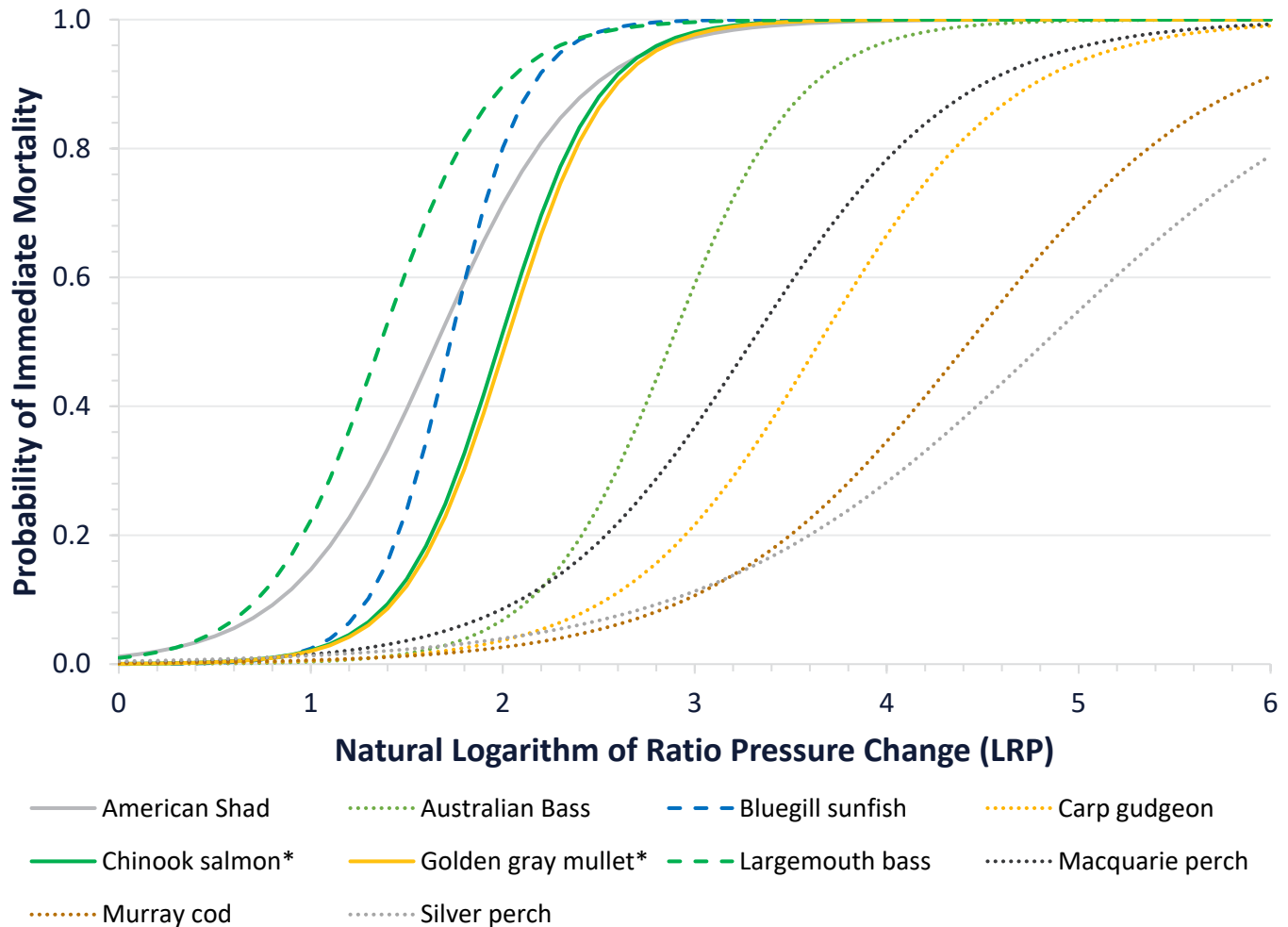


Figure 21. Probability of immediate mortality biological response models for rapid decompression using the coefficients from Table 13 and Equation (12). Solid lines represent physostomous species, dashed lines represent physoclistous species, and dotted lines represent species not native to the U.S. Models developed as part of this review from previously reported data are indicated with an asterisk (*).

3.3 TRAITS AFFECTING BAROTRAUMA

A fish's susceptibility to barotrauma associated with turbine passage can be attributed to several fish characteristics. The most significant trait associated with susceptibility to barotrauma is likely swim bladder morphology. Life stage and fish behavior, both of which are indirectly related to swim bladder morphology or state, also can affect barotrauma susceptibility. Swim bladder morphology is known to change during fish development, and different behaviors may alter the state of buoyancy and amount of gas within the swim bladder.

3.3.1 SWIM BLADDER MORPHOLOGY

Swim bladder morphology is likely the most important factor affecting the susceptibility of fish to barotrauma. The swim bladder most often holds the greatest amount of gas within the fish and is noticeably affected by the physics described by Boyle's law. In addition, the swim bladders of several fish species have sections that can connect or come near the inner ear to aid in hearing. Because of the proximity of these sections of the swim bladder to the brain and the prevalence of this trait, it may significantly increase susceptibility to barotrauma. The ability to withstand or prevent the expansion of the swim

bladder during decompression can greatly protect fish from barotrauma. Swim bladders can be divided into two main types: physostomous (open swim bladder) and physoclistous (closed swim bladder), and a third group of fish has no swim bladder.

Swim bladder morphology is likely the most important factor affecting the susceptibility of fish to barotrauma.

3.3.1.1 PHYSOSTOMES

Physostomes, such as salmon, eel, and shad, are a group of fish that have open swim bladders, meaning the swim bladder is connected to the gastrointestinal tract via a pneumatic duct. This allows physostomes to fill and empty their swim bladders relatively quickly, ranging from a few seconds to minutes. Physostomes have a significant advantage during decompression because they can evacuate gas from the swim bladder and potentially avoid over-expansion and rupture. However, during rapid decompression, the expansion may still occur more quickly than the fish can compensate for, resulting in rupture. But any gas that does escape through the pneumatic duct would reduce the total expansion of the gases within the swim bladder and likely reduce the occurrence and magnitude of barotraumas.

There are several types of physostomous swim bladders, and they can vary by the location of the pneumatic duct, number of chambers, wall thickness, and the abundance of vasculature (rete mirabile; Fänge 1966). Some fish, such as cypriniformes and characiformes, have multiple chambers within their swim bladders, and preliminary testing indicates that swim bladder rupture may occur more often in the anterior chamber (Pflugrath et al. in press). Because the pneumatic duct is located on the posterior chamber, the anterior chamber is likely more susceptible because gas must pass through the additional constriction. Therefore, it is possible that physostomous fish with multiple chambers may be more susceptible to barotrauma during

decompression than physostomous fish with only one chamber, but further testing is needed.

Several physostomous fish, including American eel, American shad, Chinook salmon, kokanee, rainbow trout, tiger muskie, and white sturgeon, have biological response models. These species tend to have lower injury rates than physoclistous species, but their mortality rates do not necessarily follow the same trend. Several Australian physoclistous species were found to have lower mortality rates than the tested physostomes even though the injury rates were mostly greater than physostomes, suggesting that these fish are hardier and able to withstand some injuries without mortality.

3.3.1.2 PHYSOCLISTS

Physoclistous species have a closed swim bladder and rely solely on blood gas exchange to add or remove gas from the swim bladder. Because physoclists cannot rapidly remove gas from their swim bladders through a pneumatic duct, these fish are likely more susceptible to barotrauma during decompression. However, other variables, such as swim bladder tensile strength, can have a significant effect on the likelihood of a swim bladder rupture, because stronger swim bladders may avoid rupture. When comparing the biological response models, physoclistous fish, in general, were more likely to be injured by decompression. However, this was not the case for some physoclistous species when comparing mortal injury and immediate mortality biological response models. This indicates that some physoclistous fish, though more likely to be injured than physostomes, may be more resilient and able to survive the injuries.

3.3.1.3 NO SWIM BLADDER

Some species of fish, such as those from the Chondrichthyes class (sharks, rays, skates, sawfishes, and chimeras) and the orders Myxiniformes (hagfishes) and Petromyzontiformes (lampreys), do not have a swim bladder. These fishes use other measures to maintain buoyancy, such as fats or oils and upward lift generated by their fins (most often pectoral fins) as water passes over and under the

fins. Some of these fishes also use the state of negative buoyancy to easily remain on the substrate. Pacific lamprey and western brook lamprey have been examined for susceptibility to barotrauma and were found to have a tolerance to decompression that far exceeded what would likely be encountered during turbine passage and even exceeded the limits of the testing apparatus. In addition, the common sole, which belongs to a genus of fish that lose the swim bladder when transitioning from larvae (Ahlstrom et al. 1984; Desoutter-Meniger and Chanet 2009), were observed to have no injuries when exposed to severe decompression (Turnpenny et al. 1992). Therefore, current literature about fish without swim bladders indicates a very high tolerance to rapid decompression and a correspondingly low susceptibility to barotrauma during passage through hydropower facilities.

Fish without swim bladders have low to no susceptibility to rapid decompression.

3.3.1.4 BEHAVIOR

The behavior of fish can potentially affect barotrauma susceptibility due to rapid decompression. This primarily pertains to behaviors that influence the amount of gas within the swim bladder such as the depth the fish inhabit. For example, studies have found that benthic fish species (i.e., American eel, white sturgeon, and pictus catfish) do not become neutrally buoyant when allowed to acclimate within pressure chambers (Beirão et al. 2018; Pflugrath et al. 2019). The state of negative buoyancy is likely advantageous for these species that typically remain at the bottom of the water column, often resting on the sediment. This state of negative buoyancy means that the swim bladder is frequently under-inflated, which can provide a significant advantage when exposed to rapid decompression.

Surface-oriented fish also have an advantage over fish that become neutrally buoyant at deeper depths when it comes to rapid decompression. When fish inhabit shallower depths, less pressure is acting on the swim bladder and therefore less gas is needed to attain neutral buoyancy. This

provides a significant advantage over fish that attain neutral buoyancy at greater depths. It is assumed that fish that reside within the water column maintain a state of neutral buoyancy, but the observed depth of a fish may not be the same as the depth at which they are neutrally buoyant. Further research is needed to determine the state of buoyancy of fish, including physiological limits, prior to downstream passage through hydropower facilities.

3.3.2 LIFE STAGE

Several life stages have been examined for susceptibility to barotrauma, and a majority of the studies focused on juveniles. A study conducted on golden perch, Murray cod, and silver perch showed that eggs were not susceptible to barotrauma, likely because no gas pockets are present in their eggs (Brown et al. 2013). However, long-term effects were not examined and could be present; for example, pressure shock to eggs is a known practice for producing infertile triploid fish (Tiway et al. 2004).

Larval fish have also been examined and are susceptible to barotrauma upon swim bladder inflation (Boys et al. 2016a). When compared to more developed fish, larval fish may be more susceptible because they have been observed to have greater difficulty in releasing gas from the swim bladder (Tsvetkov et al. 1972). In addition, white sturgeon were found to have a potential period of increased susceptibility caused by the production of gases within the gastrointestinal tract during the first exogenous feedings (Brown et al. 2013). Compared to other life stages, many larval fish are more fragile especially once the swim bladder is inflated.

3.3.3 RAPID DECOMPRESSION SURROGACY

Traits based or phylogenic-based surrogacy have been suggested as a means of implying susceptibility to a group of fish species, based on a species that has been examined. Depending on the accuracy that is needed, this may be a viable option for implying the susceptibility of species that have not been tested. Beirão et al. (2020) compared three species from the genus *Oncorhynchus* to the validity of applying

surrogacy to rapid decompression testing. Kokanee and rainbow trout were examined and the results were compared to those for previously tested Chinook salmon (Brown et al. 2012a). When the results were applied in the BioPA toolset for passage through a Kaplan turbine, kokanee and rainbow trout had mortal injury rates similar to those of Chinook salmon. However, use of caution was emphasized when applying surrogacy for rapid decompression, especially if the applications require precise estimates.

In addition, Brown et al. (2016) examined tiger muskie as a surrogate for northern pike (*Esox lucius*). Tiger muskie are a hybrid of northern pike and muskellunge. The validity of this application was not examined, but a hybrid of two species from the same genus would be expected to have susceptibility to rapid decompression very similar to the parent species. However, in this case, hybrid vigor may need to be considered, and future research on hybrid susceptibility to rapid decompression is needed because it could potentially result in a higher tolerance for the hybrids.

3.4 RAPID DECOMPRESSION DISCUSSION

As research into the effects of rapid decompression due to passage through hydropower facilities has progressed, the method set forth by Brown et al. (2012a) has become the standard. Brown et al. (2012a) first reported a mortal injury biological response model, but as research has continued, these models have also been reported for injury and immediate mortality (Pflugrath et al. 2020b; 2018; in prep-b; in prep-a). So that species can continue to be accurately compared for susceptibility to barotrauma, it is advisable to continue applying this methodology. As research in this area increases, several areas need to be further explored to fully understand limitations and applicability of these models. Additional fish species also need to be examined to provide a better understanding of how different traits may affect susceptibility.

3.4.1 LIMITATIONS OF CURRENT RAPID DECOMPRESSION DATA

Many of the studies were conducted on a preliminary basis with a minimal number of fish tested. These studies provide a good indication of susceptibility for the reported species, but for cases where more accurate estimates are needed, additional research is advisable. This is particularly important if there is a high likelihood that, for the desired application, RPCs are likely to occur at a point where approximately 50% of fish are likely to respond with the selected endpoint (i.e., injury, mortal injury, or immediate mortality). This is because, when small sample sizes are used, the biological response models have the most variation at the point around a 50% response. If, however, the likelihood of RPCs occurring in this region is low, the models will likely be more accurate.

3.4.2 FUTURE RESEARCH NEEDS FOR RAPID DECOMPRESSION

As research into the effects of rapid decompression continues, several areas need to be considered, such as confounding variables, additional species, and delayed effects. Gaining a better understanding in these areas will help to create more accurate biological response models and determine the most appropriate application for the models.

3.4.2.1 THE EFFECTS OF MULTIPLE EXPOSURE

A majority of fish that pass through hydropower facilities do so during a migration, and during these migrations there is potential for fish to encounter several dams. Therefore, a percentage of fish are likely to be exposed to rapid decompression multiple times. As with decompression sickness in humans (Moon et al. 1989), once a fish has suffered barotrauma, if not lethal, there is potential for the fish to be more susceptible to barotrauma during future exposures. Therefore, because of the prevalence and continued development of hydropower facilities, there is a need to better understand the likelihood and effects of multiple exposures to rapid decompression.

3.4.2.2 REPRODUCTION AFTER EXPOSURE

During migrations, fish are more likely to encounter and pass through hydropower facilities. This may be of particular concern for spawning migrations. Though it has not been examined specifically, studies have observed the expulsion of eggs or milt from fish during decompression (Hogan 1941; Pflugrath et al. 2020a). As the swim bladder expands within the fish, it presses up against the internal organs, including the gonads. The effect of this has not been quantified, but it is extremely likely that the reproduction success of these fish was likely affected when the fish were exposed to rapid decompression. Future research is needed to better assess the effects on reproductive organs and reproductive success after exposure to rapid decompression.

3.4.2.3 ADDITIONAL SPECIES FOR RAPID DECOMPRESSION TESTING

Additional species may need to be tested and these tests are likely to occur because of site-specific needs. A good variety of species with different morphological features has been examined thus far for exposure to rapid decompression. These initial studies have focused on some at-risk and common species. Previous efforts could be expanded upon by examining additional at-risk species and selecting species that may have different morphological features. For example, one significant group of fish has had minimal testing conducted and warrants further examination—Cyprinids.

Cyprinids have been underrepresented for rapid decompression testing, and there is a significant concern for these fish around the world, particularly in areas such as the Mekong and Amazon River basins (Brown et al. 2014). These fish represent the largest and most diverse family of fish and approximately 300 species are native to North America (Nelson et al. 2016; Schofield 2005). Several of these species such as the humpback chub (*Gila cypha*), which is federally protected within the U.S., have been listed on the International Union for Conservation of Nature (IUCN) Red List. Another notable cyprinid, the Oregon chub (*Oregonichthys crameri*) which is

native to the Willamette River drainage, was previously listed as endangered on the Endangered Species Act-listed but became the first fish to be taken off the list. Very little is known about the susceptibility of these fishes to barotrauma, but preliminary studies indicate that the multiple-chambered swim bladder of cyprinids may make them more susceptible to barotrauma when passing through turbines (Pflugrath et al. 2020a). Additionally, because of the migrational behavior of many Cyprinids, particularly Catostomids (suckers), there is significant chances of encounter hydropower facilities (Cooke et al. 2005).

3.4.2.4 CONFOUNDING VARIABLES

Several variables likely influence the probability of barotrauma occurring in fish that experience rapid decompression, however little research has been done in this area. Such variables include water temperature, TDG, RPC, and swimming activity.

TEMPERATURE

Temperature may play an important role in how a fish responds to rapid decompression. Cooler temperatures tend to slow reflexes in cold-blooded animals such as fish. Therefore, cooler temperatures may reduce a fish's capacity to evacuate gas from the swim bladder quickly and therefore make fish more susceptible. However, cooler temperatures can slow processes such as metabolic and heart rates, and if fish are injured, cooler temperatures may provide them more time to recover from an injury.

TOTAL DISSOLVED GAS

The effects of increased TDG have been examined during several studies of the effects of rapid decompression on fish associated with passage through hydropower facilities. Elevated gas levels can cause gas bubble disease, which is a result of excess gas being absorbed into the fish from the water. This can cause the formation of bubbles under the epidermis, including in the skin, eyes, and gills. This disease can be fatal by itself, but if fish are suffering mild gas bubble disease, they may be more susceptible to rapid decompression because these micro bubbles will

expand as pressure is reduced. Brown et al. (2012a) exposed fish to a range of TDG levels (114.8–127.5%) for 16–24 hr prior to exposure to rapid decompression. The TDG levels were found to be a significant predictor of mortality in juvenile Chinook salmon, but they explained less than 1% of the deviation in the analysis. This suggests that TDG likely influences the susceptibility of fish to rapid decompression, but the ratio of decompression has a much greater effect. Further research on other species is needed to better understand the influence of elevated TDG on fish. This may be particularly important when fish are exposed to extreme TDG levels within the tailrace of a dam, where fish may not be able to take refuge in deeper water, which has been found to prevent or relieve the symptoms of gas bubble disease.

RATE OF PRESSURE CHANGE

The rate at which the pressure is reduced can have a significant impact on the probability of injury for fish. This particularly applies to physostomous fish, which, if the decompression occurs slowly enough, can evacuate expanding gas from the swim bladder. Physoclistous fish would require a considerably slow pressure change in order to compensate; therefore, mortality rates are not likely to differ because of the rate of decompression even if the decompression occurs over a period of up to a several minutes. For example, Chinook salmon that were decompressed from 146.3 to 13.8 kPa over 3 min had no signs of barotrauma (Brown et al. 2012b). The same results were observed for sockeye salmon when gradually decompressed to 16.7 kPa (Harvey 1963) and also for several Eurasian species decompressed from up to 600 kPa to surface pressure (Tsvetkov et al. 1972). This differs greatly from physostomous fish that were similarly decompressed, but in less than 1 s, which had significant amounts of barotrauma and mortality (Brown et al. 2012a; Pflugrath et al. 2020b; Tsvetkov et al. 1972). In addition,

experiments on the pictus catfish (*Pimelodus pictus*) found that intestinal rupture and emboli were significantly more likely to occur when the decompression occurred in less than 0.1 s than when decompression occurred in more than 0.2 s (Beirão et al. 2018). Physoclistous fish, however, have not been seen to have significant differences in mortality rates when compared for decompressions ranging in occurrence from nearly instantaneously to over a few minutes (Tsvetkov et al. 1972; Hogan 1941; Feathers and Knable 1983; Pflugrath et al. in prep-b).

The RPC was included as a variable in the extensive study conducted on juvenile Chinook salmon and was found to be a significant variable, but when compared to the RPC, the rate of decompression added very little to the predictability of the model; therefore, it was not included (Brown et al. 2012a). Based on the results from slow decompression of Chinook salmon, expanding the range in decompression rates would likely increase the effect of this variable for the Chinook salmon model and likely other physostomous fish as well.

When considering the RPC, how the RPC is calculated must also be taken into account. Because fish are most affected by the RPC rather than a pressure differential, it may not be optimal to calculate the rate using a differential. For instance, if a fish is decompressed from 200 to 100 kPa in 1 s, the rate of decompression is 100 kPa s⁻¹ and the result of this decompression is an RPC of 2. But if a fish is decompressed from 100 to 50 kPa in 1 s, the RPC is still 2 but the rate of decompression is half, 50 kPa s⁻¹. Therefore, a more relevant calculation of the rate of decompression may be needed. This issue also highlights the fact that the effects of decompression essentially accelerate as pressures decrease (limited by vapor pressure), due to the exponential nature of Boyle's law (Figure 22).

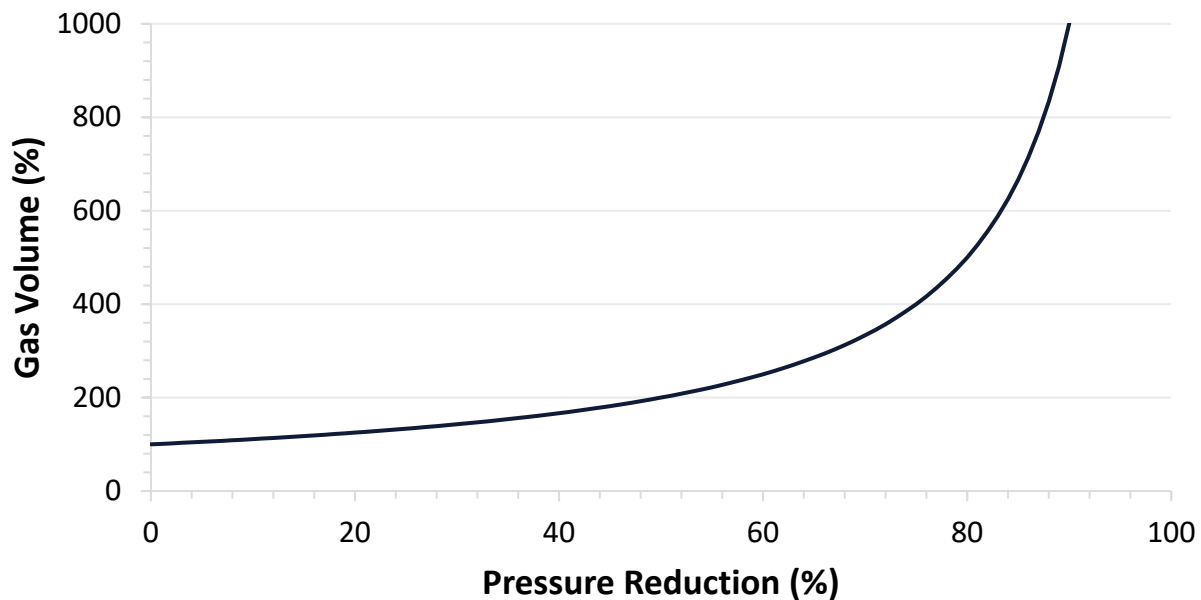


Figure 22. The relationship between pressure reduction and gas volume according to Boyle's law under constant temperature. Gas within fish will respond close to this relationship and this relationship is particularly important to the swim bladder.

SWIMMING ACTIVITY

A preliminary study was conducted to determine if active swimming affected susceptibility to rapid decompression. For a majority of the studies conducted on the rapid decompression of fish, the fish are held in chambers with minimal water flow. These fish therefore have minimal swimming activity during decompression. Swimming actively, as would be expected during entrainment into a turbine, can cause physiological changes in fish and may affect a fish's susceptibility to barotrauma (Pflugrath 2017). Pflugrath (2017) installed swim tubes in the New South Wales Department of Primary Industry pressures system and exposed two species (Murray cod and Australian bass) to rapid decompression while fish were exposed to elevated flow velocities. The two species responded differently; the swimming Murray cod had a lower occurrence of injury than non-swimming Murray cod, and swimming Australian bass had a higher occurrence of injury than non-swimming Australian bass. This change in susceptibility was potentially attributed to the production of nitric oxide within the blood stream, which can reduce nucleation sites (areas where

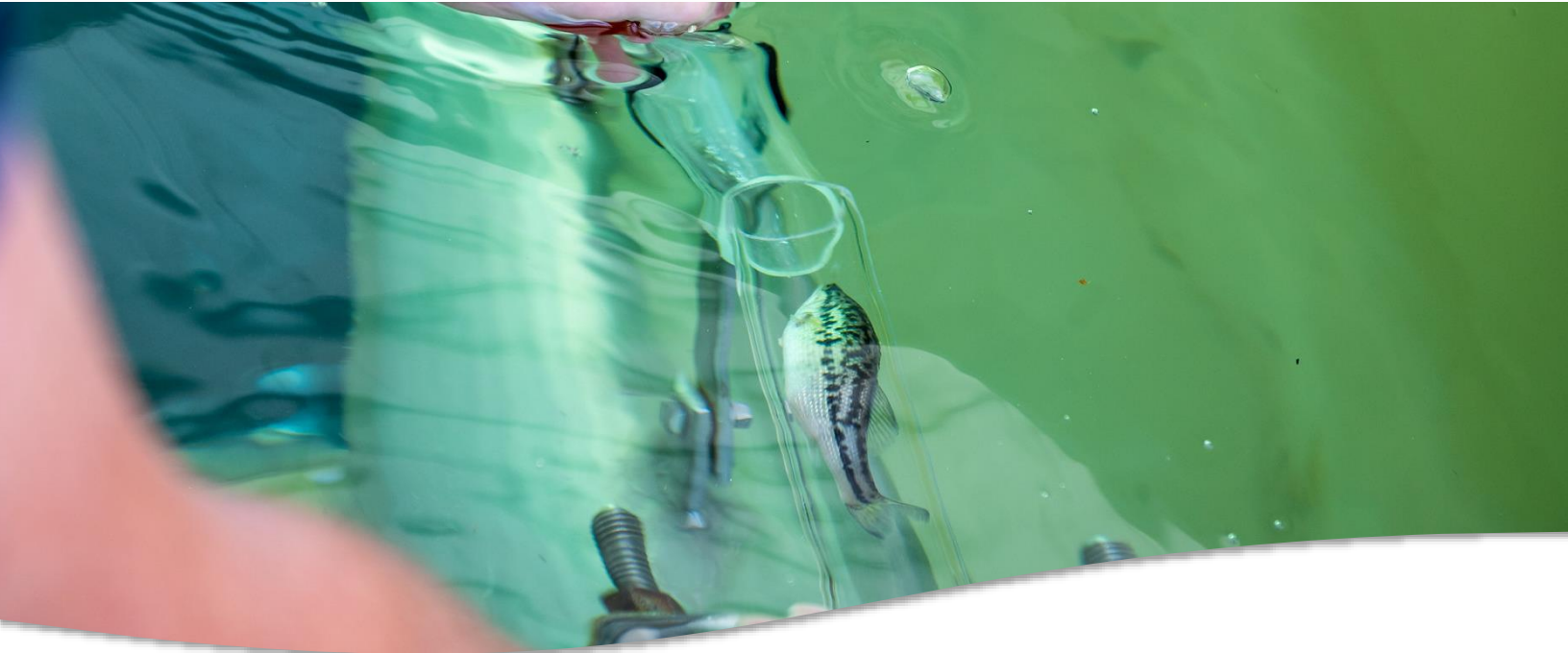
gas bubbles form in a solution) and consequently reduce the occurrence of emboli and/or emphysema (Pflugrath et al. 2012). As blood flow is increased during elevated swimming efforts, nucleation sites are formed. A good analogy to this is that when a carbonated beverage is shaken prior to being opened, it forms many nucleation sites and this is why the gas is rapidly released when the beverage is opened. The release of nitric oxide is a physiological reaction to prevent this phenomenon from occurring within the blood stream. However, the amount of nitric oxide that is released and the timing of that release can differ between species and is likely why Australian bass and Murray cod had different responses. Research is needed to further examine this variable beyond this preliminary examination.

3.5 RAPID DECOMPRESSION CONCLUSIONS

Several studies have developed methods for exposing fish to rapid decompression and have examined the effects of those exposures. From those studies, a total of 46 biological response models (injury, mortal injury, and immediate

mortality) have been developed for 16 fish species. The results from these studies have demonstrated that different species can have very different responses to rapid decompression. Several conclusions can be made from this collection of research:

- In general, as the RPC increases, fish are more likely to sustain injury or mortality when passing through hydropower facilities. The RPC increases as the nadir pressure decreases and/or the acclimation pressure increases.
- For fish species without swim bladders (common sole, Pacific lamprey, and western brook lamprey), barotrauma is not likely to occur because of rapid decompression associated with passage through hydropower facilities.
- Physoclistous fish (with a closed swim bladder, where gases cannot be rapidly released) are more likely to be injured by rapid decompression. Mortality (mortal injury or immediate mortality) is more likely to occur for some physoclistous species (e.g., bluegill and largemouth bass); however, research indicates some physoclistous species (e.g., Australian Bass and Murray cod) are hardier and are able to sustain those injuries without mortality.
- Several research topics need to be addressed as research on rapid decompression continues, including the effects of multiple exposures, temperature, rates of decompression, swimming activity during decompression, and reproduction success after exposure to rapid decompression.
- Research is needed on additional species that have morphemically different traits than those previously examined. This includes cyprinids, the most diverse family of fish, which have been minimally researched and have unique characteristics that have not been fully examined, such as a multiple-chambered physostomous swim bladder.



4.0 PREDICTING THE EFFECTS OF EXPOSURE TO FLUID SHEAR ON FISH

Chapter authors: Kristin Engbrecht, Brett D. Pflugrath, Robert P. Mueller, and Alison H. Colotelo

Fluid shear exposure ensues when fish pass the interface of two masses of water moving in different directions or at different velocities. Naturally occurring shear in rivers and streams is usually less than 100 N/m^2 during normal flows and most often causes few, if any, injuries to fish (Fausch and White 1981; Costa 1987; Statzner and Müller 1989). Generally, fish develop natural adaptations to these levels of shear. Fish also experience shear exposure during passage at hydropower structures, usually at higher levels than naturally occurring shear, potentially resulting in a variety of injuries and mortality to

fish. Levels of shear in the draft tube of a bulb turbine have been estimated to range from 500 to over $5,000 \text{ N/m}^2$, although the periods during which shear levels between $4,000$ and $5,000 \text{ N m}^{-2}$ are experienced by fish are usually brief (McEwen and Scobie 1992). In some ways, exposure to high shear levels can be comparable to exposure to the friction forces generated by two solid surfaces contacting and sliding against each other (Čada et al. 2006a). Common injuries resulting from high levels of shear are loss of mucous layer, descaling, tissue tearing or bruising, and decapitation (Cada et al. 2007).

Two locations where elevated shear forces are frequently seen during downstream fish passage routes are spillways and turbines (Čada et al. 2006a). Numerous factors have been shown to affect injury severity, including fish size, morphology, life history stage, and turbine type (Pracheil et al. 2016a).

Previous studies testing the susceptibility of fish to fluid shear used a variety of specialized apparatuses to expose fish to a range of fluid shear levels. On average, water velocities through turbines can vary from 3 to 12 m s⁻¹ depending on the amount of flow present (Cada 1991). For each species, it is important to determine the shear environments in which injuries and mortality occur. The development of biological response models for fish exposed to fluid shear are advantageous for several reasons, such as giving recommendations or tolerance values for turbine development or modification; decreasing the possibility that fish are exposed to harmful levels of fluid shear; and where the magnitude and frequency of shear is known, it allows the rates of injury and mortality to be estimated. Biological response models were provided in most studies discussed in this review and sometimes upon further analyses in this review new biological response models were produced for some studies. Regardless of whether biological response models are available, every study performed has moved us one step closer to understanding the effects of harmful fluid shear.

4.1 FLUID SHEAR THROUGH TURBINES AND OTHER HYDRO STRUCTURES

The magnitude and occurrence of shear events can vary between not only turbine types and designs, but also between different installations and operations of the same turbine. For Sensor Fish deployments, the magnitude of a shear event has been categorized as a slight event if the acceleration magnitude is $\geq 245 \text{ m s}^{-2}$ and $< 490 \text{ m s}^{-2}$, a moderate event if the acceleration magnitude is $\geq 490 \text{ m s}^{-2}$ and $< 932 \text{ m s}^{-2}$, and a severe event if the acceleration magnitude is $\geq 932 \text{ m s}^{-2}$ (Deng et al. 2005a). Sensor Fish deployed through turbines have recorded the

The magnitude and occurrence of shear events can vary between not only turbine types and designs, but also between different installations and operations of the same turbine

occurrence of shear events ranging from very few percent to 100% during passage through the entire penstock to draft tube. For example, three hydropower facilities were examined with Sensor Fish and two of the turbines (Detroit and Cougar Dams) recorded severe strike events in 100% of the deployments, while one turbine (Arrowrock Dam) only recorded severe events in 40% of deployments (Fu et al. 2016). These turbines differed greatly from a Kaplan turbine (Wanapum Dam), which only recorded severe shear events in 1% of Sensor Fish deployments (Fu et al. 2016; Deng et al. 2014). These results serve as a general reference, not as a direct comparison between Francis and Kaplan turbines due to differences in flow and power generation of these turbines (Fu et al. 2016). However, mortality rates of fish passing through Kaplan turbines are frequently lower than the mortality rates of fish passing through Francis turbines (EPRI 1992). A review of 22 studies involving Francis turbines revealed a fish mortality range from 5% to 50% compared to a range from 4% to 15% for fish passing through Kaplan turbines with an adjustable blade propeller (Franke et al. 1997; Eicher et al. 1987).

4.2 DEVELOPING BIOLOGICAL RESPONSE MODELS FOR EXPOSURE TO FLUID SHEAR

The effects of exposure to fluid shear on fish, which are associated with turbine passage, have been examined in several species. These studies generally involve exposing fish to a gradient of high-velocity water using specialized testing apparatuses and assessing fish for injuries, mortality, and often behavioral changes after exposure. Many of the studies have used these results to develop biological response models to predict the occurrence of injuries of mortality.

4.2.1 FISH SPECIES EXAMINED FOR SUSCEPTIBILITY TO FLUID SHEAR

Biological response models that predict the probability of injury or mortality when exposed to various levels of fluid shear have been produced in several of the studies discussed in this section. Important information about species vulnerability to fluid shear exposure can still be provided from studies that did not produce biological response models. Direct comparison between tested species and integration of biological response models into HBET and BioPA software tools were still possible with some studies by performing additional analyses to produce biological response models.

The same general methodology that was used by the studies to produce biological response models was also used in this review to develop additional biological response models. Three potential endpoints of minor injury, major injury, and/or mortality were predicted based on the results analyzed. Fish were classified as having minor injuries if the observed injuries were not life-threatening like small bruises (<0.5 cm in diameter) or descaling that was less than 20% on one side. To be classified as having major injuries, fish needed to exhibit a life-threatening injury like spinal fractures, eye damage (bulged, hemorrhaged, or missing), excessive descaling (>20% on one side), lacerations with visible bleeding, large bruises (>0.5 cm in diameter), or operculum and gill damage. Mortality included both immediate and delayed mortality after testing as well as any fish showing signs of moribund behavior within up to 30 min after exposure. Moribund behavior was defined as any fish swimming erratically or experiencing prolonged loss of equilibrium. The probability of fish sustaining a minor injury, major injury, or immediate mortality when exposed to a fluid shear event (S) associated with turbine passage can be represented as follows:

$$P(X) = \frac{e^{\beta_0 + \beta_1 \cdot \ln(S)}}{1 + e^{\beta_0 + \beta_1 \cdot \ln(S)}} \quad (14)$$

where the response—minor injury, major injury, or immediate mortality—for the desired species is

represented by X , and β_0 and β_1 are the corresponding species-specific coefficients determined by logistic regression analysis. Fluid shear severity is represented by S and for this report will be expressed as strain rate ($\text{cm s}^{-1} \text{cm}^{-1}$, abbreviated as s^{-1}).

Strain rate is calculated by mapping the flow velocities downstream of the jet. This has been accomplished using a heavy-duty pitot tube, where measurements were conducted along a grid at several locations downstream of the jet (Neitzel et al. 2000). Once the flow fields were characterized, the strain rate (S) was estimated using the equation

$$S = \frac{\Delta \bar{v}}{\Delta y} \quad (15)$$

where \bar{v} is the mean water velocity (cm s^{-1}) and y is the distance (cm) perpendicular to force. The Δy is an arbitrary number that can have a significant effect on the calculation. For instance, if a Δy of 50 cm was selected for a $\Delta \bar{v}$ of 1,000 cm s^{-1} , the resulting strain rate would be 20 s^{-1} . If, however, the same $\Delta \bar{v}$ occurred over 5 cm, the resulting strain rate would be 200 s^{-1} . Therefore, it is important to consider what Δy is most applicable. Neitzel et al. (2000) selected 1.8 cm for the change in distance (Δy) for calculating the exposure strain rate, which is based on representing the width of the test fish. Because other experiments were conducted with similarly sized fish, all biological response models are based on the precedence of 1.8 cm for Δy set by Neitzel et al. (2000). To conduct these calculations, the jet flow field was characterized using a heavy-duty pitot tube (Neitzel et al. 2000).

Because Sensor Fish measure acceleration, which is then attributed to exposure to fluid shear, a correlation was required to adapt the biological response models so that they could be integrated into HBET. This correlation was accomplished by releasing Sensor Fish into the PNNL shear flume using the same methods as those used for live fish. Acceleration due to exposure to fluid shear was then correlated to strain rate calculations (Neitzel et al. 2000) for the same jet velocity (Figure 23).

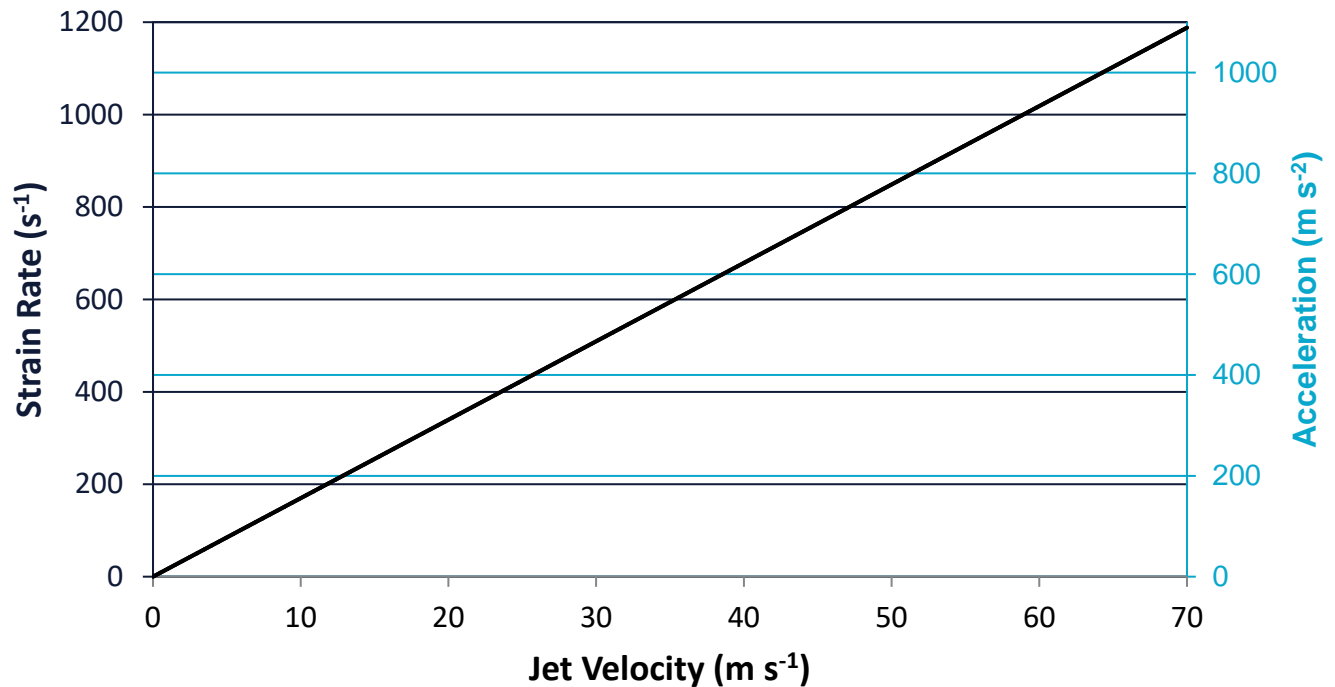


Figure 23. Jet velocity correlates to strain rate and acceleration measured by Sensor Fish for exposure to fluid shear.

4.2.1.1 AMERICAN EEL - *ANGUILLA ROSTRATA*

Using the PNNL Fluid Shear Testing Facility (FSTF; 7.0A.3.3), yellow-phase American eel ($n = 45$, $L = 265\text{--}453$ cm, $W = 24.0\text{--}112.0$ g) were exposed to jet velocities of 15 m s^{-1} and 18 m s^{-1} (strain rate equivalent to 833 and $1,000\text{ s}^{-1}$, respectively; Pflugrath et al. in prep-c). Eel had no observable injuries or behavioral changes immediately after exposure to fluid shear or 48 hours after exposure, although there was noticeable slime sluff-off during and prior to the exposures. The production of slime was likely not due to exposure to fluid shear, but a possible stress response to handling. Although the removal of slime during exposure to fluid shear did not appear to affect the fish, it may cause increased disease susceptibility. Because of the high tolerance to fluid shear exposure, all American eel had no response in the biological response models over the tested range (Table 14–Table 16).

American eel were found to have high tolerance to fluid shear and no biological response model could be developed for the examined fluid shear range.

4.2.1.2 AMERICAN SHAD - *ALOSA SAPIDISSIMA*

Several studies conducted at the PNNL FSTF have looked at the susceptibility of American shad to fluid shear. Collectively, all of the studies determined shad are exceptionally susceptible to fluid shear exposure.

Neitzel et al. (2000; 2004) conducted two very similar studies, both exposing juvenile shad ($n = 150$ each, mean $FL = 100$ mm) headfirst to jet velocities ranging from 3 m s^{-1} to 21 m s^{-1} (strain rate equivalent of 168 to $1,008\text{ s}^{-1}$). Significant injury and mortality occurred at a strain rate of 517 s^{-1} (Neitzel et al. 2000) and 10% of the population experienced injury and mortality at strain rates of 400 and 578 s^{-1} , respectively (Neitzel et al. 2004). Both studies had 100% mortality with exposure to the highest strain rate

American Shad are the exceptionally susceptible to fluid shear exposure.

tested ($1,008 \text{ s}^{-1}$) and also documented a 20% mortality rate in control fish within the first 48 hr post handling, further demonstrating the sensitivity of shad to handling stress. For the Neitzel et al. (2000) study, biological response models were developed to predict the probability of minor injuries (see Table 14 in Section 4.2.2.1), major injuries (see Table 15 in Section 4.2.2.2), and mortality (see Table 16 in Section 4.2.2.3).

Juvenile American shad ($n = 420$, FL = 53–85 mm, W = 0.3–5.9 g) were exposed to jet velocities ranging from 0 m s^{-1} to 18 m s^{-1} (strain rate equivalent of 0 to $1,000 \text{ s}^{-1}$) using the PNNL aquatic shear tank (Pflugrath et al. 2020b). When exposed to jet velocities of 9 m s^{-1} (500 s^{-1}), all but two fish were injured, and once jet velocities reached 15 m s^{-1} (833 s^{-1}) all fish had major injuries. When subjected to the highest jet velocity of 18 m s^{-1} ($1,000 \text{ s}^{-1}$), 100% mortality occurred in all fish. The most prevalent injury observed was descaling, and injuries to the eyes and operculum also were very common. At strain rates of 350 s^{-1} and 400 s^{-1} , both major injuries and mortalities began to occur, respectively. Biological response models were developed to predict the occurrence of minor injuries (Table 14), major injuries (Table 15), and mortality (Table 16).

4.2.1.3 ATLANTIC HERRING - *CLUPEA HARENGUS*

Juvenile Atlantic herring ($n = 57$) were tested at multiple jet velocities (5.4 to 20.9 m s^{-1}), for which Neitzel et al. (2000) calculated the equating strain rates to be 297 to $1,153 \text{ s}^{-1}$ (Turnpenny et al. 1992). Testing in an apparatus comparable to the PNNL aquatic shear tank resulted in 100% mortality at every jet velocity after 7 days. Common injuries seen at 16.4 and 20.9 m s^{-1} (908 and $1,153 \text{ s}^{-1}$) were major descaling, eye removal (60% at both velocities), damaged and hemorrhaging gills (40 and 20%), and torn operculum and jaw (20 and 60%). High mortality was likely due to osmotic shock caused by damage to the mucous and epithelial layers. The predicted occurrence of minor injuries (Table 14), major injuries (Table 15), and mortality (Table

16). was the product of additional analysis done in this review to create biological response models.

4.2.1.4 ATLANTIC SALMON - *SALMO SALAR*

Using an apparatus similar to the one used by PNNL, Turnpenny et al. (1992) exposed 2-year-old Atlantic salmon ($n = 125$) to jet velocities ranging from 5.4 to 20.9 m s^{-1} (estimated strain rates of 297 to $1,153 \text{ s}^{-1}$ calculated by Neitzel et al. (2000)). After testing, some fish were held for 7 days and the highest mortality (12%) was observed after exposure to the highest velocity of 20.9 m s^{-1} ($1,153 \text{ s}^{-1}$). Injuries consisted of minor descaling present at all of the jet velocities and both eye damage (28%–32%) and loss of mucous cover only occurring at jet velocities of 16.4 and 20.9 m s^{-1} (908 and $1,153 \text{ s}^{-1}$). As part of the review, a biological response model was produced with the reported data, which predicted the occurrence of injuries (Table 14), major injuries (Table 15), and mortality (Table 16).

4.2.1.5 BALA SHARK - *BALANTIOCHEILUS MELANOPTERUS*

The Mekong river runs through six countries in Southeast Asia and is experiencing rapid hydropower development. Two studies have been conducted on the fluid shear susceptibility of three Mekong river species—blue gourami (*Trichogaster trichopterus*), iridescent shark (*Pangasianodon hypophthalmus*), and bala shark (*Balantiocheilus melanopterus*; also commonly called silver shark) have been examined (Colotelo et al. 2018; Baumgartner et al. 2017). Baumgartner et al. (2017) examined the susceptibility of bala shark to fluid shear using the NSW DPI fluid shear testing system (Appendix A, Section A.3.4) (Boys et al. 2014a). Juvenile bala shark ($n = 120$, mean FL = 64–66 mm, mean W = 4.68–5.14 g) entered the shear environment tailfirst and were exposed to strain rates ranging from 18 to $1,296 \text{ s}^{-1}$. Immediate mortality was observed when strain rates exceeded 600 s^{-1} and at the highest strain rate there was 50% mortality and 100% of the fish were injured. Some of the common injuries were scale loss (95%), operculum damage (70%), fin damage (20%), and spinal injuries (20%). Injuries were also

reported in control fish, where scale loss occurred in 25% and fin damage in 15% of fish.

Biological response models were reported for injury (Table 14) and mortality (Table 16) (Baumgartner et al. 2017), though a handling effect based on the occurrence of injuries in the control fish was not factored into the injury model. As part of this report an additional model was developed by analyzing injuries to the operculum as an indication of major injuries (Table 15). Individual data were not reported; therefore, a more precise analysis could not be conducted, but injuries to the operculum, which did not occur in control fish, was the most common injury after scale loss and fin damage, which were prevalent throughout control fish.

4.2.1.6 BLUE GOURAMI - *TRICHOGASTER TRICHOPTERUS*

Adult blue gourami ($n = 90$, $L = 45\text{--}72$ mm, $W = 1.6\text{--}6.2$ g) were exposed to fluid shear using the PNNL FSTF (Colotelo et al. 2018). Fish were subjected to jet velocities ranging from 3 to 21.3 m s^{-1} (strain rate equivalent of 168 to 1,185 s^{-1}), and resulted in more pronounced behavioral effects, injuries, and mortality at higher strain rates. Erratic swimming and equilibrium loss were first observed after exposure to strain rates of 688 s^{-1} and higher and 852 s^{-1} and higher, respectively. At the highest strain rate of 1,185 s^{-1} , the most common injuries were descaling (32.5%); eye (46.7%) and operculum (86.7%) damage; and bruises, cuts, and fin frays (60%). The highest total mortality (40%) was observed after exposure to the highest strain rate (1,185 s^{-1}). Biological response models reported in this study predicted the probability of injury (Table 14) and mortality (Table 16).

4.2.1.7 BROWN TROUT - *SALMO TRUTTA*

Turnpenny et al. (1992) tested 1- and 2-year-old brown trout ($n = 40$) at jet velocities of 10.4, 16.4, and 20.9 m s^{-1} (equating to strain rates of 603, 908, 1,153 s^{-1} , calculated by Neitzel et al. 2000) using an apparatus similar to the one used by PNNL. Some injuries observed were minor scale loss, corneal ruptures (20%), and damaged and hemorrhaging gills (10%). The highest mortality

(20%) was observed at 16.4 m s^{-1} (908 s^{-1}). Additional analysis done in this report allowed for the development of a biological response model for predicting the occurrence of minor injuries (Table 14), major injuries (Table 15), and mortality (Table 16).

4.2.1.8 CHINOOK SALMON - *ONCORHYNCHUS TSHAWYTSCHA*

A series of studies have been performed looking at the susceptibility of Chinook salmon to fluid shear. Two studies conducted by Johnson (1970a, 1972) exposed juvenile Chinook salmon to fluid shear using a high-velocity jet submerged in a large tank. The first study subjected Chinook salmon ($n = 250$, $L = 127\text{--}178$ mm) to a jet velocity of 17.5 m s^{-1} or an estimated strain rate of about 974 s^{-1} (Johnson 1970a). Fish experienced violent body distortions but had no apparent injuries or mortalities. In a similar apparatus, Johnson (1972) exposed Chinook salmon to jet velocities of 17.5, 20, 24, and 28 m s^{-1} (estimated strain rates of 974, 1,135, 1,312, and 1,558 s^{-1}). Chinook salmon ($n = 1,700$, $L = 76\text{--}229$ mm) had no mortalities at 17.5 m s^{-1} , 5.4% at 20 m s^{-1} , 3.7% at 24 m s^{-1} , and 25.8% at 28 m s^{-1} . Some of the injuries observed included decapitation, torn operculum, eye damage, and broken vertebral columns. At the highest velocity, larger fish experienced the lowest mortalities. Johnson (1972) acknowledges cavitation from the apparatus used to create the fluid shear environment could have also contributed to the injuries and mortalities observed, especially at the 24 and 28 m s^{-1} jet velocities.

Neitzel et al. (2000; 2004) also examined the effects of fluid shear on a variety of fish species, including Chinook salmon at the PNNL FSTF (Appendix A, Section A.3.3). The first study (Neitzel et al. 2000) exposed smolt spring Chinook salmon ($n = 170$, mean FL = 145 mm) and pre-smolt ($n = 180$, mean FL = 85 mm) and smolt ($n = 300$, mean FL = 140 mm) fall Chinook salmon headfirst to jet velocities ranging from 0 to 18.3 m s^{-1} (strain rate equivalent of 0 to 1,008 s^{-1}) using the PNNL aquatic shear tank. The pre-smolt fall Chinook salmon began showing major injuries and mortalities at a strain rate of approximately 852 s^{-1} , and the smolt fall and

spring Chinook salmon showed major injuries and mortalities at a lower strain rate of 688 s^{-1} . At the highest strain rate, both the pre-smolt fall Chinook and spring Chinook mortality rates were about 10%, and the smolt fall Chinook mortality rate was about 40%. Smolt fall ($n = 130$, mean FL = 140 mm) and spring ($n = 130$, mean FL = 145 mm) Chinook were also exposed tailfirst to strain rates of 688 to $1,008 \text{ s}^{-1}$, primarily just sustaining minor injuries and no significant proportions of major injuries and mortalities.

Similarly, up to 180 pre-smolt (L = 85–95 mm) and smolt (L = 123–152 mm) fall Chinook and juvenile spring Chinook (L = 135–154 mm) per test series were exposed to fluid shear using the same apparatus, jet velocities, and corresponding strain rates as the previous Neitzel studies (Neitzel et al. 2004; Neitzel et al. 2000). Results were reported in the form of strain rates at which 10% of the population would be affected (LC-10). The LC-10 for pre-smolt and smolt fall Chinook salmon introduced headfirst were 913 s^{-1} and 734 s^{-1} for major injuries and $>1,008$ and 863 s^{-1} for mortalities, respectively. When introduced headfirst into a shear environment, the LC-10 for spring Chinook for major injury and mortality occurred at strain rates of 805 and 991 s^{-1} . Smolt fall Chinook and spring Chinook were also introduced into the apparatus tailfirst. For the smolt fall Chinook, the LC-10 for major injuries and mortalities was predicted to occur above or at a strain rate of $1,008 \text{ s}^{-1}$, with no major injuries or mortalities occurring at any strain rates for the spring Chinook. Overall, it was observed that the larger, fall Chinook salmon smolt had an increased susceptibility to fluid shear relative to the smaller, pre-smolt fall Chinook salmon. Fish that were introduced headfirst into the shear environment had higher injury and mortality rates than fish introduced tailfirst.

The PNNL FSTF was used to expose subyearling fall Chinook salmon ($n = 147$, L = 93–128 mm, W = 8.1–23.5 g) to jet velocities ranging from 12.2 to 19.8 m s^{-1} , and a control group was subjected to a velocity of 3 m s^{-1} (Deng et al. 2005a). The onset of minor and major injuries and mortalities began at jet velocities of 12.2, 13.7, and 16.8 m s^{-1} (estimated strain rates of 677, 761, and 933 s^{-1}), respectively. Exposure to

jet velocities of 16.8 m s^{-1} and greater resulted in 40–50% of fish experiencing eye injuries, bruising, and loss of equilibrium. Operculum damage was the most common injury; it occurred in 70–90% of fish exposed to a jet velocity of 15.2 m s^{-1} or higher.

In the Neitzel et al. (2004) and Deng et al. (2005b) studies, biological response models were already developed to predict the occurrence of minor injuries (Table 14), major injuries (Table 15), and mortality (Table 16). Additional analyses were necessary in this review for the Neitzel et al. (2000) and Johnson (1972) papers in order to create biological response models that predicted the occurrence of minor injuries (Table 14), major injuries (Table 15), and mortality (Table 16).

4.2.1.9 COHO SALMON - *ONCORHYNCHUS KISUTCH*

Johnson (1972) exposed juvenile coho salmon (*Oncorhynchus kisutch*) to jet velocities of 20, 24, and 28 m s^{-1} (estimated strain rates of 1,135, 1,312, and $1,558 \text{ s}^{-1}$) using an apparatus similar to the one used earlier by Johnson (1970). Coho salmon ($n = 1,560$, L = 76–229 mm) had mortalities at 20 m s^{-1} (2.0%), 24 m s^{-1} (10.3%), and 28 m s^{-1} (78%). Some of the injuries observed included decapitation, torn operculum, eye damage, and broken vertebral columns. It should be noted the apparatus used also had high occurrences of cavitation, especially at the 24 and 28 m s^{-1} jet velocities, which likely contributed to the injuries and mortalities observed. As part of this review, an additional analysis was done to produce a biological response model for predicting injuries (Table 14 and Table 15) and mortality (Table 16).

4.2.1.10 COMMON SOLE - *SOLEA SOLEA*

Using an apparatus comparable to the PNNL aquatic shear facility, juvenile common sole ($n = 160$) were tested at velocities of 10.4, 16.4, and 20.9 m s^{-1} (Turnpenny et al. 1992). Neitzel et al. (2000) calculated the estimated strain rates of these velocities to be 603, 908, and $1,153 \text{ s}^{-1}$, respectively. The primary injury observed was loss of mucous coating, which likely caused the fungal infections and delayed mortality of 65 to

75% of fish exposed to the two highest velocities. As part of this review, the reported data were analyzed using the previously described methods to develop a biological response model to predict the occurrence mortality (Table 16).

4.2.1.11 COMMON SUNFISHES - *LEPOMIS MACROCHIRUS* AND *L. GIBBOSUS*

Juvenile *Lepomis* species, bluegill and pumpkinseed (*L. gibbosus*; $n = 98$ [85 bluegill and 13 pumpkinseed], $L = 75\text{--}117$ mm, $W = 7.3\text{--}34.5$ g) were also exposed to fluid shear using the PNNL FSTF (Engbrecht et al. in prep). Bluegill and pumpkinseed are morphologically similar and are frequently used as surrogates for one another. Fish were exposed to jet velocities ranging from 3 to 21 m s^{-1} (strain rate equivalent of 167 to 1,167 s^{-1}). The incidences of altered swimming behavior, injuries, and immediate mortality increased as the jet velocities increased. Altered swimming behavior rapidly increased from exposure to jet velocities ranging from 15 to 18 m s^{-1} (833 to 1,000 s^{-1}) and the most frequent major injuries were descaling and damaged branchiostegal rays. Modeling indicates that major injuries and immediate mortality began to occur when fish were exposed to a strain rate of approximately 520 s^{-1} and 860 s^{-1} , respectively. Exposure to the highest strain rate of 1,167 s^{-1} resulted in 100% mortality. Biological response models were developed to predict the occurrence of minor injuries (Table 14), major injuries (Table 15), and mortality (Table 16).

4.2.1.12 EUROPEAN EEL - *ANGUILLA ANGUILLA*

Adult European eels ($n = 100$) were tested at velocities ranging from 5.4 to 20.9 m s^{-1} (estimated strain rates of 297 to 1,153 s^{-1}) calculated by Neitzel et al. (2000) using an apparatus similar to the PNNL FSTF (Turnpenny et al. 1992). Similarly, there were no mortalities or obvious injuries, except for some loss of mucous coating resulting in some discoloration. Because of the high tolerance to fluid shear exposure, biological response models were not developed for European eel.

4.2.1.13 IRIDESCENT SHARK - *PANGASIANODON HYPOPHthalmus*

Juvenile iridescent sharks ($n = 60$, $L = 43\text{--}67$ mm, $W = 1.5\text{--}4.3$ g) were exposed to fluid shear using the PNNL FSTF (Colotelo et al. 2018). Sharks were exposed to jet velocities ranging from 3 to 21.3 m s^{-1} (equating to strain rates of 168 to 1,185 s^{-1}), with an additional 15 larger sharks ($L = 70\text{--}86$ mm, $W = 4.7\text{--}10.5$ g) also tested at 21.3 m s^{-1} (1,185 s^{-1}). Altered swimming behavior, injuries, and mortality rates were positively correlated with strain rates. At the highest strain rate, 53.3% of the smaller sharks experienced equilibrium loss after fluid shear exposure, while only 6.7% of the larger sharks were observed to have equilibrium loss. This indicates the ability to swim in turbulent environments may be easier for large individuals. For all of the sharks, bruises, cuts, and fin frays were the most common injuries, followed by operculum damage, which was seen in the same percentage (73.3%) of large and small sharks at the highest strain rate. Mortality rates were lower for the larger sharks (33%) than for the smaller sharks (67%) when exposed to the highest strain rates, which may be due to the increased hardiness of the larger sharks. Biological response models reported in this study predicted the occurrence of injuries (Table 14) and mortality (Table 16).

4.2.1.14 LARGEMOUTH BASS - *MICROPTERUS SALMOIDES*

Using the PNNL FSTF, juvenile largemouth bass ($n = 196$, $L = 94\text{--}136$ mm, $W = 12.7\text{--}33.0$ g) were exposed to jet velocities ranging from 3 to 21 m s^{-1} (equating to strain rates of 167 to 1,167 s^{-1} ; Engbrecht et al. in prep). Altered swimming behavior began to occur at 12 m s^{-1} (677 s^{-1}) and steadily increased with higher jet velocity exposures. Common major injuries observed were bruising (head, operculum, body), gill hemorrhaging, and torn isthmus, and immediate mortality occurred in 23% and no delayed mortality occurred after testing. This study also predicted the occurrence of minor (Table 14) and major injuries (Table 15) and mortality (Table 16) using biological response models.

4.2.1.15 STEELHEAD AND RAINBOW TROUT – *ONCORHYNCHUS MYKISS*

Juvenile steelhead (*Oncorhynchus mykiss*; $n = 967$, $L = 76\text{--}305$ mm) were subjected to fluid shear using a high-velocity jet submerged in a large tank (Johnson 1972). Mortality rates for each of the jet velocities of 20, 24, and 28 m s^{-1} (estimated strain rates of 1,135, 1,312, and 1,558 s^{-1}) were 0.7%, 23%, and 30.1%, respectively. Common injuries included decapitation, torn operculum, eye damage, and broken vertebral columns. It should be noted the apparatus used to create the fluid shear environment also created cavitation, especially at the 24 and 28 m s^{-1} (1,312, and 1,558 s^{-1}) jet velocities, which could have also contributed to the injuries and mortality observed.

Neitzel et al. (2000) exposed yearling rainbow trout ($n = 170$, mean FL = 155 mm) and steelhead smolts ($n = 170$, mean FL = 215 mm) using the PNNL FSTF. They were all introduced headfirst at the edge of the jet stream (slow-fish-to-fast-water scenario) and exposed to velocities ranging from 0 to 18.3 m s^{-1} (equating to strain rates of 0 to 1,008 s^{-1}). Major injuries only occurred at strain rates of 852 (6%) and 1,008 s^{-1} (7%) for rainbow trout and at strain rates of 852 s^{-1} (7%) for steelhead. No mortalities occurred during or after testing for both species. Steelhead smolts ($n = 80$, mean FL = 145 mm) were also exposed (852 and 1,008 s^{-1}) to fluid shear by a tailfirst orientation. Twenty percent of the fish had minor injuries at the highest strain rate and no major injuries or mortalities were observed. Rainbow trout ($n = 200$, mean FL = 120 mm) were also exposed to strain rates of 688 to 1,150 s^{-1} . They were introduced upstream of the jet stream (fast-to-slow-water scenario) and major injuries occurred in 10% of fish tested at strain rates of 1,008 and 1,150 s^{-1} with no significant rates of mortality. Head and body bruising and gill hemorrhaging were some of the injuries associated with this test group. Overall, results indicate juvenile rainbow trout and steelhead smolts are rather resistant to fluid shear environments.

Using the same apparatus as used in the previous Neitzel (2000) study, up to 180 fish per

test series were also exposed to jet velocities ranging from 3 to 18.3 m s^{-1} (equating to strain rates of 0 to 1,008 s^{-1} ; Neitzel et al. 2004). Results demonstrate both juvenile steelhead (FL = 175–232 mm) and rainbow trout (FL = 147–173 mm) have a high tolerance to shear environments. For each test group and response variable, strain rates were estimated at which 10% of the population would be affected (LC-10). The LC-10 for major injuries for rainbow trout and steelhead introduced headfirst into the shear environment was predicted to occur at strain rates above 1,008 s^{-1} . Steelhead introduced tailfirst had no major injuries at any strain rates up to 1,008 s^{-1} . There were no mortalities for any of the steelhead or rainbow trout tested.

Biological response models were already developed by Neitzel et al. (2004) to predict the occurrence of minor injuries (Table 14), major injuries (Table 15), and mortality (Table 16). In this review, additional analyses were done for the Neitzel et al. (2000) and Johnson (1972) papers in order to create biological response models that predicted the occurrence of minor injuries (Table 14), major injuries (Table 15) and mortality (Table 16).

4.2.1.16 PACIFIC LAMPREY – *ENTOSPHEMUS TRIDENTATUS*

Juvenile Pacific lamprey ($n = 210$, $L = 110\text{--}165$ mm) were exposed to jet velocities ranging from 0 to 18 m s^{-1} (equating to strain rates of 0 to 1,830 s^{-1}) using the PNNL FSTF (Moursund et al. 2000). Juvenile Pacific lamprey were very resistant to the effects of fluid shear; they experienced no immediate mortalities or injuries. Biological response models were not developed for Pacific lamprey because of their high tolerance to fluid shear exposure.

No injuries or mortalities were observed during fluid shear testing of juvenile Pacific lamprey, and no biological response models were developed for these fish.

4.2.1.17 SPECIES NOT INCLUDED IN HBET AND THE BIOPA TOOLSET

Dose-response models could not be developed for all fluid shear experiments found in the literature because of a variety of factors, including imprecise reporting and shear exposure quantified in different measurement forms than those accepted by HBET and the BioPA toolset, such as newtons per square meter (N m^{-2}) or dynes per square centimeter (dynes cm^{-2}). Although, they are not included in HBET and the BioPA toolset they still help to enable a better understanding of different fish susceptibility in general.

MISCELLANEOUS SPECIES

Juvenile common carp (*Cyprinus carpio*, $n = 20$, TL = 16–32 mm) were exposed to fluid shear via a scale model of a towboat propeller (Killgore et al. 2001). Fluid shear was reported as shear stress (dynes/cm^{-2}), which could not be converted to strain rate without additional velocity measurements of the flow field. Common carp were subjected to shear levels of 1,613 and 4,743 dynes cm^{-2} and experienced 7% and 26% total mortality, respectively. Results indicate the size of the fish, not the species, is the primary determining factor for mortality susceptibility.

Čada et al. (1981) tested juvenile mosquitofish (*Gambusia affinis*, $n = 728$, L = 30–35 mm) at a jet velocity of 2.4 m s^{-1} using a power plant simulator constructed at ORNL. Mortality was not significantly different than the controls and was usually less than 2%.

Johnson (1970a) exposed juvenile Chinook salmon ($n = 250$, L = 127–178 mm) and coho salmon ($n = 250$, L = 178–203 mm) to fluid shear using a high-velocity jet submerged in a large tank. A jet velocity of 17.5 m s^{-1} or an estimated strain rate of about 974 s^{-1} resulted in no apparent injuries and no mortalities, although fish did experience violent body distortions.

One of the earliest studies looked at the combined effects of fluid shear on Chinook, coho, and sockeye salmon (Groves 1972). Over the course of three tests, juvenile salmon ($n = 1,403$,

L = 30–135 mm) were exposed to jet velocities ranging from 9 to 37 m s^{-1} , with the corresponding strain rates calculated to range from 508 to $2,032 \text{ s}^{-1}$ (Neitzel et al. 2000). Fish were unaffected by exposure to 11.9 m s^{-1} and noticeable injuries began around exposure to velocities of 15 m s^{-1} . Some of the most common injuries observed were torn gills, damaged operculum, and damage to the eyes (bulging or missing). Normal swimming behavior was regained 5 to 30 min after fluid shear exposure caused disorientation and there were no visible injuries. As jet velocities increased, so did the altered swimming behavior, injuries, and mortality. Injury rates were inversely related to the size of the fish; the smaller fish received more injuries regardless of the jet velocities used. The difference in injury rates is likely due to the proportion of the fish's surface area struck by the jet; larger fish had a smaller portion of their bodies contacted by the jet than the smaller fish.

TURNPENNY'S SPECIES

Turnpenny et al. (1992) used an apparatus similar to that used by PNNL to expose fish to fluid shear with jet velocities ranging from 5.4 to 20.9 m s^{-1} (Neitzel et al. (2000)). Morphologically related species were used as models when the available numbers of the primary species was limited. It should be noted that some fish were anesthetized or euthanized prior to exposure to fluid shear, which could alter, likely underestimate, the occurrence of injuries. Unspecified numbers of some fish were also tested alive to observe any delayed mortality after testing. However, the condition of each species prior to testing is unclear.

One-year-old rainbow trout ($n = 280$) were exposed to velocities of 16.4 and 20.9 m s^{-1} (908 and $1,153 \text{ s}^{-1}$). Minor scale and mucous coating loss occurred at both velocities, and eye damage (0.3%) and gill damage and hemorrhaging (2%) occurred only at the highest velocity. No rainbow trout were held after testing, indicating perhaps that they were euthanized prior to testing.

A small group of juvenile twaite shad (*Allosa fallax*, $n = 5$) was tested at 20.9 m s^{-1} ($1,153 \text{ s}^{-1}$) resulting in 100% mortality. The injuries observed

were torn jaws and opercula (40%), torn gills (20%), major scale loss, and eye removal (40%).

A small number of European bass (*Dicentrarchus labrax*, age 0, $n = 65$) and whiting (*Merlangius merlangus*, 1 year old, $n = 120$) were tested at 0, 16.4, and 20.9 m s^{-1} . At the highest velocity, the bass experienced eye damage, scale and mucous loss (10%), and gill hemorrhaging (8%). Whiting that were exposed to the highest velocities were each passed through the apparatus 10 times, resulting in eye damage and loss of scales and mucous coating. Once the scale loss began, subsequent exposure to the shear environment allowed scales to more easily be lifted and removed. After 10 passes at 20.9 m s^{-1} , descaling on each fish ranged from 20–90%. Mortality was not reported for either of these species.

AUSTRALIAN SPECIES

Two studies looked at the susceptibility of juvenile and adult fish species within the Murray-Darling Basin in Australia to fluid shear environments (Baumgartner et al. 2013; Boys et al. 2014a). Within the Murray-Darling Basin an estimated 10,000 dams and weirs have contributed to widespread declines of native fish (Baumgartner 2005).

Baumgartner et al. (2013) sought to understand the impacts of two irrigation weir types, overshoot and undershot, on seven native fish species. Larvae, juvenile, and adult golden perch (*Macquaria ambigua*, $L = 246\text{--}565$ mm, $W = 192\text{--}3,208$ g), Murray cod ($L = 304\text{--}456$ mm, $W = 190\text{--}787$ g), and silver perch ($L = 242\text{--}440$ mm, $W = 228\text{--}1,049$ g) were tested. Overall, adult mortality for all species was relatively low for both weirs, and the golden perch had the highest mortality (under 10%, overshoot weirs) among all species. Silver perch and Murray cod adults had no overshoot mortalities and mortalities for undershot weirs were less than 5%. There were no consistent patterns of juvenile mortality rates overall for species or weir type. Golden perch and Murray cod had higher rates of mortality during passage through undershot weirs, but mortality rates overall for both weirs were the lowest for Murray cod. Silver perch suffered about half as

much mortality when passed through undershot weirs. Adult Australian smelt (*Retropinna semoni*, $L = 25\text{--}49$ mm, $W = 0.08\text{--}0.5$ g), Murray-Darling rainbowfish (*Melanotaenia fluviatilis*, $L = 35\text{--}84$ mm, $W = 0.4\text{--}6.1$ g), unspotted hardyhead (*Craterocephalus stercusmucarum*, $L = 20\text{--}54$ mm, $W = 0.06\text{--}0.98$ g) and carp gudgeon ($L = 26\text{--}50$ mm, $W = 0.14\text{--}0.87$ g) were also tested. All species experienced higher mortality rates when passing through undershot weirs. Rainbowfish and carp had the lowest mortality rate for both overshoot and undershot weirs. Overshoot weirs have an estimated strain rate of 150–200 s^{-1} , whereas undershot weirs have strain rates measured at 400 s^{-1} or higher, so it is not surprising that passage through overshoot weirs had fewer deaths than undershot weirs. Results suggest the safest conditions for most fish sizes and species would be to construct overshoot weirs with deep plunge pools. Higher values of shear, turbulence, and pressure changes were a characteristic of undershot weirs as determined by CFD.

Juvenile golden perch ($n = 180$, $L = 30\text{--}50$ mm, $W = 0.2\text{--}1.6$ g), Murray cod ($n = 180$, $L = 36\text{--}49$ mm, $W = 0.4\text{--}1.2$ g), and silver perch ($n = 180$, $L = 23\text{--}38$ mm, $W = 0.2\text{--}1.0$ g) susceptibility to fluid shear was tested using the NSW DPI fluid shear testing system (Appendix A, Section A.3.4) (Boys et al. 2014a). The jet velocities used ranged from 3.13 to 10.01 m s^{-1} , equating to strain rates of 18.2 to 1,296.87 s^{-1} . The occurrence and type of injuries were fairly consistent for all of the species, with the most common injuries being fin damage (39%) and scale loss (14%). No mortality was observed with Murray cod and golden perch and the probability of mortality for silver perch was around 20%. The orientation of the fish into the shear environment was not restricted to any specific orientation (headfirst or tailfirst) and most fish entered in a tailfirst orientation, which potentially caused the low numbers of major injuries and no mortality.

4.2.2 FLUID SHEAR BIOLOGICAL RESPONSE MODELS

Biological response models for predicting injury, major injury, or mortality for fish exposed to fluid shear have been gathered from the literature or

developed as part of this review from previously conducted research and are reported in the following sections (4.2.2.1–4.2.2.3).

4.2.2.1 PROBABILITY OF INJURY DUE TO EXPOSURE TO FLUID SHEAR

Biological response models have been developed to predict the probability of injury occurring in fish when exposed to fluid shear associated with

passage through hydropower facilities. These models predict the likelihood that a fish will sustain any injury when exposed to a given strain rate. A total of 14 models have been developed for different fish species (Table 14). Susceptibility ranged from no susceptibility for fish without scales and absent and/or reduced vulnerable structures (American eel, European eel, and Pacific lamprey) to high susceptibility for select fish (American shad; Figure 24).

Table 14. Probability of injury due to exposure to fluid shear (strain rate: s⁻¹) biological response model coefficients to be used with Equation (14).

Species	Scientific Name	Coefficients		Citation
		β_0	β_1	
American eel	<i>Anguilla rostrata</i>	∅	∅	Pflugrath et al. in prep-c
American shad	<i>Alosa sapidissima</i>	-8.418	0.023	Pflugrath et al. 2020
Bala shark	<i>Balantiocheilos melanopterus</i>	-0.261	0.002	Baumgartner et al. 2017
Blue gourami	<i>Trichopodus trichopterus</i>	-4.535	0.007	Colotelo et al. 2018
Bluegill and pumpkinseed	<i>Lepomis macrochirus and L. gibbosus</i>	-6.081	0.011	Engbrecht et al. in prep
Chinook salmon (fall/subyearling)	<i>Oncorhynchus tshawytscha</i>	-8.272	0.01	Neitzel et al. 2004
Chinook salmon (fall/yearling)	<i>Oncorhynchus tshawytscha</i>	-7.148	0.010	Neitzel et al. 2004
Chinook salmon (spring)	<i>Oncorhynchus tshawytscha</i>	-9.845	0.014 4	Neitzel et al. 2004
European eel	<i>Anguilla anguilla</i>	∅	∅	Turnpenny et al. 1992
Iridescent shark	<i>Pangasianodon hypophthalmus</i>	-18.14	0.016	Colotelo et al. 2018
Largemouth bass	<i>Micropterus salmoides</i>	-13.623	0.020	Engbrecht et al. in prep
Pacific lamprey	<i>Entosphenus tridentatus</i>	∅	∅	Moursund et al. 2000
Rainbow trout	<i>Oncorhynchus mykiss</i>	-5.352	0.005	Neitzel et al. 2004
Steelhead	<i>Oncorhynchus mykiss</i>	-12.73	0.016	Neitzel et al. 2004

∅ denotes models of which minimal or no susceptibility was observed.

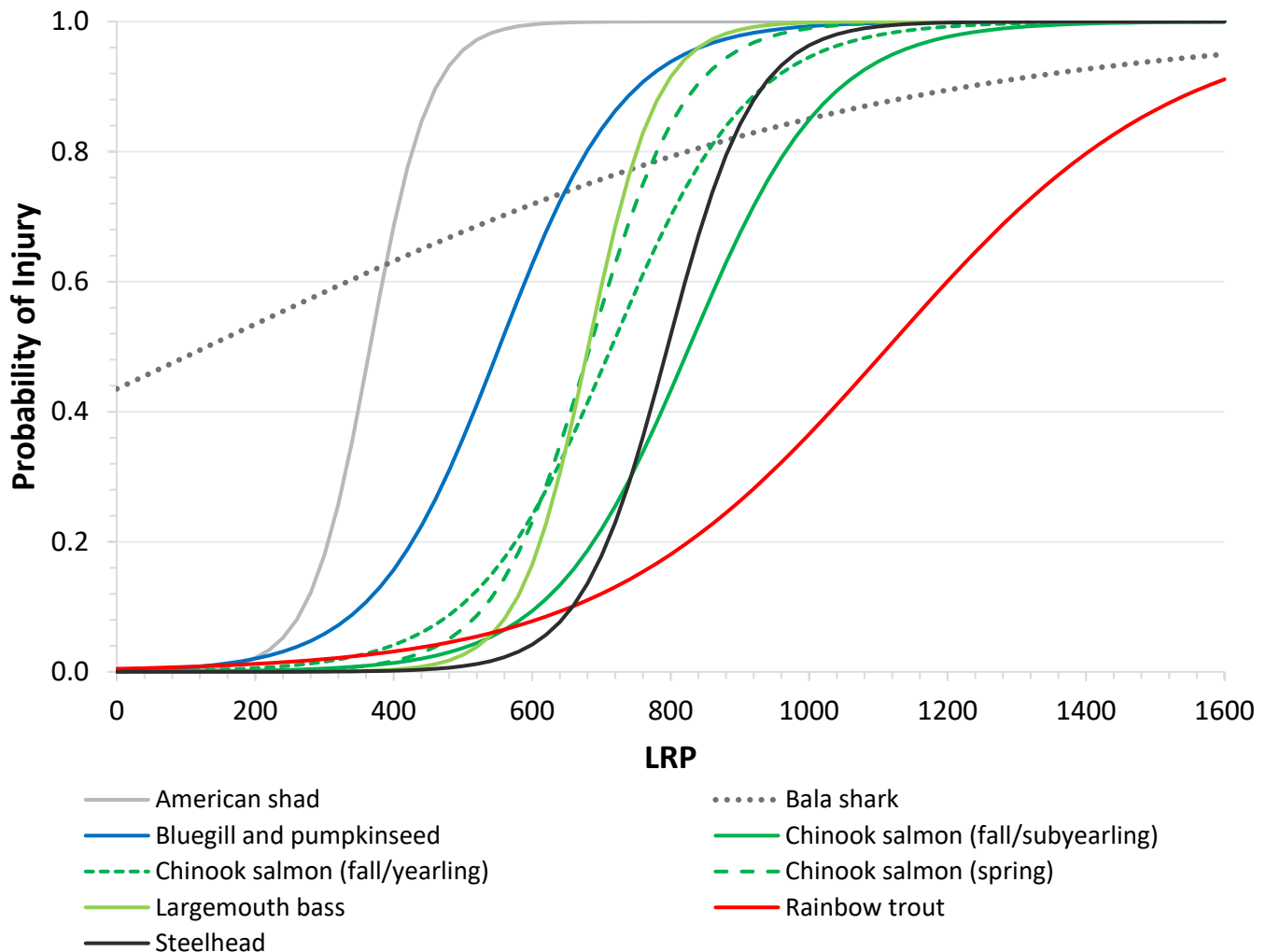


Figure 24. Probability of injury biological response models for exposure to fluid shear using the coefficients from Table 14 and Equation (14). Dashed lines represent different subspecies from the same species all represented by the same color, and dotted lines represent Mekong River species.

4.2.2.2 PROBABILITY OF MAJOR INJURY DUE TO EXPOSURE TO FLUID SHEAR

Biological response models have been developed to predict the probability of major injury occurring in fish when exposed to fluid shear associated with passage through hydropower facilities. These models predict the likelihood that a fish will sustain any injury when exposed to a given strain

rate. Major injuries are those injuries likely to result in mortality either directly or indirectly (i.e., disease or predation). A total of 12 models have been developed for different fish species (Table 15). Susceptibility ranged from no susceptibility for fish without scales and absent and/or reduced vulnerable structures (American eel, European eel, and Pacific lamprey) to high susceptibility for select fish (American shad; Figure 25).

Table 15. Probability of major injury due to exposure to fluid shear biological response model coefficients to be used with Equation (14).

Species	Scientific Name	Coefficients		Citation
		β_0	β_1	
American eel	<i>Anguilla rostrata</i>	Ø	Ø	Pflugrath et al. in prep-c
American shad	<i>Alosa sapidissima</i>	-8.515	0.015	Pflugrath et al. 2020
Bala shark	<i>Balantiocheilos melanopterus</i>	-6.663	0.006	Baumgartner et al. 2017
Bluegill and pumpkinseed	<i>Lepomis macrochirus and L. gibbosus</i>	-8.093	0.010	Engbrecht et al. in prep
Chinook salmon (fall/subyearling)	<i>Oncorhynchus tshawytscha</i>	-27.534	0.028	Neitzel et al. 2004
Chinook salmon (fall/yearling)	<i>Oncorhynchus tshawytscha</i>	-10.502	0.011	Neitzel et al. 2004
Chinook salmon (spring)	<i>Oncorhynchus tshawytscha</i>	-10.053	0.010	Neitzel et al. 2004
European eel	<i>Anguilla anguilla</i>	Ø	Ø	Turnpenny et al. 1992
Largemouth bass	<i>Micropterus salmoides</i>	-12.838	0.016	Engbrecht et al. in prep
Pacific lamprey	<i>Entosphenus tridentatus</i>	Ø	Ø	Moursund et al. 2000
Rainbow trout	<i>Oncorhynchus mykiss</i>	-9.156	0.0068	Neitzel et al. 2004
Steelhead	<i>Oncorhynchus mykiss</i>	-9.668	0.0071	Neitzel et al. 2004

Ø denotes models of which minimal or no susceptibility was observed.

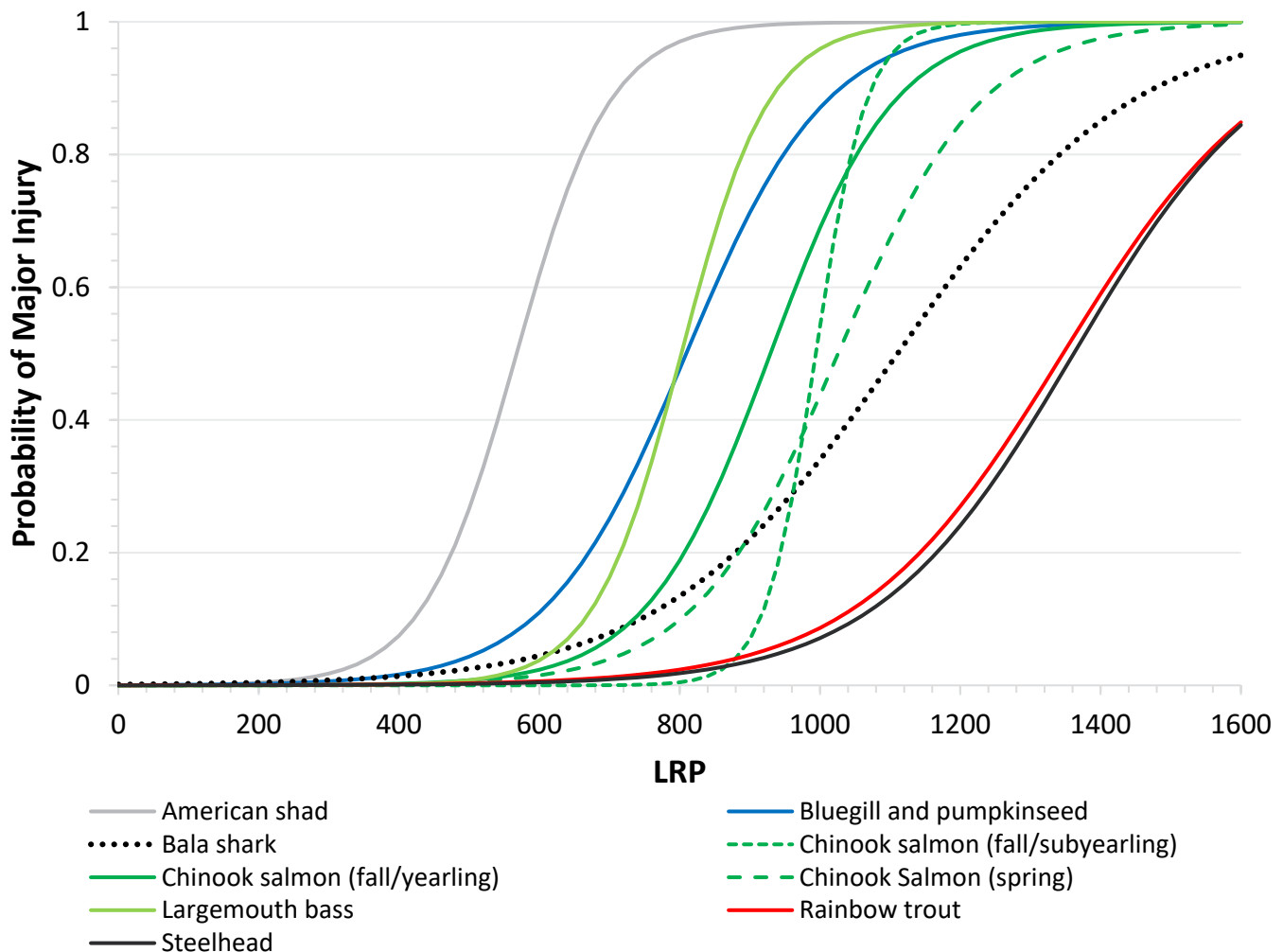


Figure 25. Probability of major injury biological response models for exposure to fluid shear using the coefficients from Table 15 and Equation (14). Dashed lines represent different subspecies from the same species all represented by the same color, and dotted lines represent Mekong River species.

4.2.2.3 PROBABILITY OF MORTALITY DUE TO EXPOSURE TO FLUID SHEAR

Biological response models have been developed to predict the probability of mortality occurring in fish when exposed to fluid shear associated with passage through hydropower facilities. These

models predict the likelihood that a fish will sustain any injury when exposed to a given strain rate. A total of 19 models have been developed for different fish species (Table 16). Susceptibility ranged from no susceptibility (American eel, European eel, Pacific lamprey, rainbow trout, and steelhead) to high susceptibility (American shad, Atlantic herring; Figure 26).

Table 16. Probability of mortality due to exposure to fluid shear biological response model coefficients to be used with Equation (14).

Species	Scientific Name	Coefficients		Citation
		β_0	β_1	
American eel	<i>Anguilla rostrata</i>	∅	∅	Pflugrath et al. in prep-c
American shad	<i>Alosa sapidissima</i>	-6.877	0.01	Pflugrath et al. 2020
Atlantic salmon ^(a)	<i>Salmo salar</i>	-7.555	0.005	Turnpenny et al. 1992
Atlantic herring ^(a)	<i>Clupea harengus</i>	-22.752	0.151	Turnpenny et al. 1992
Bala shark	<i>Balantiocheilos melanopterus</i>	-9.095	0.007	Baumgartner et al. 2017
Blue gourami	<i>Trichopodus trichopterus</i>	-1.946	0.001	Colotelo et al. 2018
Bluegill and pumpkinseed	<i>Lepomis macrochirus and L. gibbosus</i>	-20.027	0.02	Engbrecht et al. in prep
Brown trout ^(a)	<i>Salmo trutta</i>	-5.087	0.003	Turnpenny et al. 1992
Coho salmon ^(a)	<i>Oncorhynchus kisutch</i>	-12.588	0.008	Johnson 1972
Common sole ^(a)	<i>Solea solea</i>	-6.654	0.007	Turnpenny et al. 1992
Chinook salmon (fall/subyearling)	<i>Oncorhynchus tshawytscha</i>	-40.981	0.039	Neitzel et al. 2004
Chinook salmon (fall/yearling)	<i>Oncorhynchus tshawytscha</i>	-10.251	0.009	Neitzel et al. 2004
Chinook salmon (spring)	<i>Oncorhynchus tshawytscha</i>	-13.992	0.012	Neitzel et al. 2004
European eel	<i>Anguilla anguilla</i>	∅	∅	Turnpenny et al. 1992
Iridescent shark	<i>Pangasianodon hypophthalmus</i>	-3.811	0.003	Colotelo et al. 2018
Largemouth bass	<i>Micropterus salmoides</i>	-14.642	0.015	Engbrecht et al. in prep
Pacific lamprey	<i>Entosphenus tridentatus</i>	∅	∅	Moursund et al. 2000
Rainbow trout	<i>Oncorhynchus mykiss</i>	∅	∅	Neitzel et al. 2004
Steelhead	<i>Oncorhynchus mykiss</i>	∅	∅	Neitzel et al. 2004

(a) Model developed as part of this review using data from the cited source. ∅ denotes models for which minimal or no susceptibility was observed.

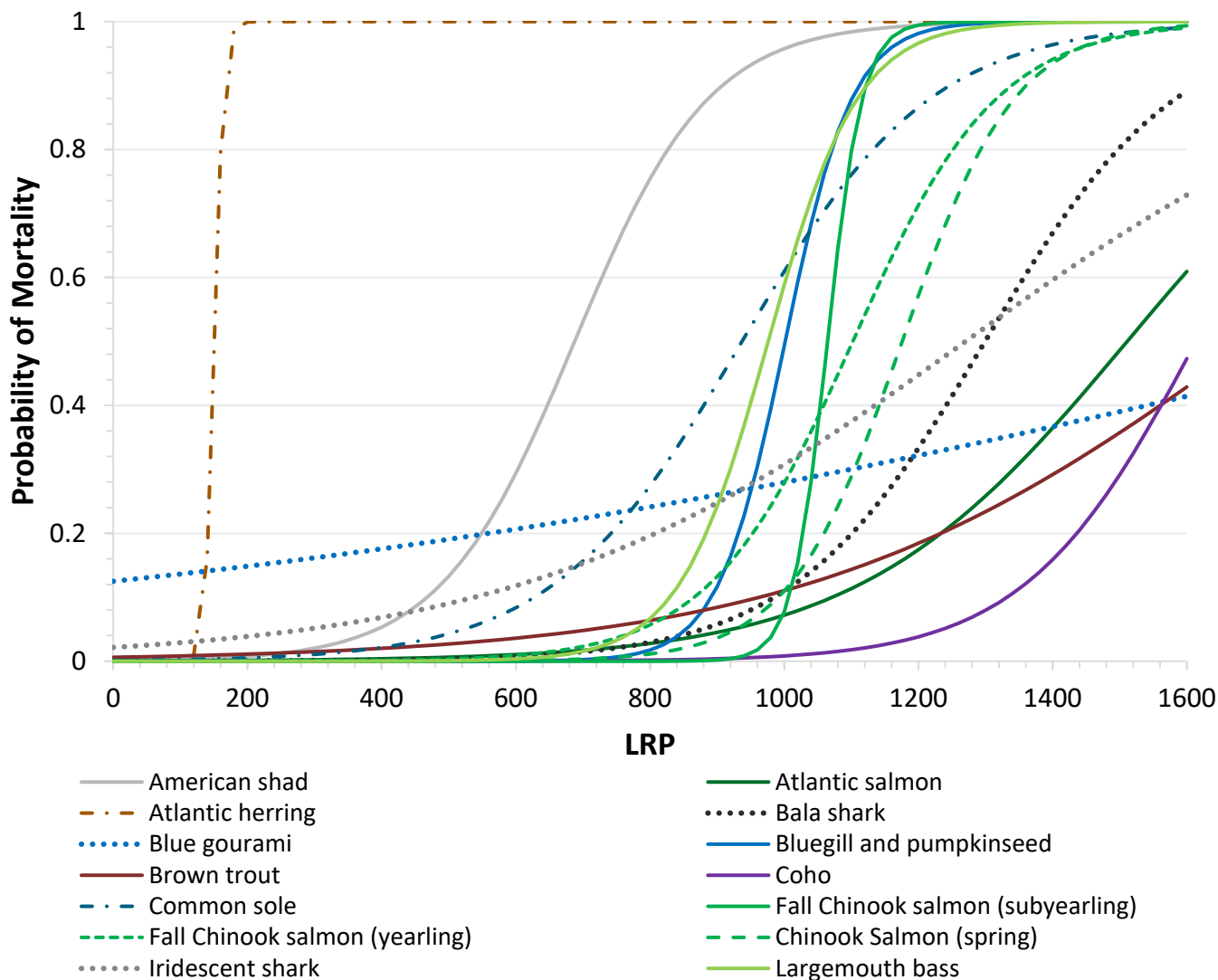


Figure 26. Probability of mortality biological response models for exposure to fluid shear using the coefficients from Table 16 and Equation (14). Dashed lines represent different subspecies from the same species all represented by the same color, dotted lines represent Mekong River species, and lines alternating dots and long dashes are saltwater or brackish water species.

4.3 TRAITS AND VARIABLES AFFECTING SHEAR-RELATED TRAUMA

Collectively, it is clear that several traits and variables contribute to increased or decreased susceptibility to fluid shear. Specific physical characteristics and life stages have been shown

to be useful in predicting susceptibility, but further research is warranted because the current literature on these topics is helpful, but sparse. Studies have shown exposure mechanisms and fish orientation during fluid shear testing are also valuable for understanding more about species vulnerability.

4.3.1 MORPHOLOGY

Categorizing fish by morphology can be an informative, noninvasive way to make inferences about potential susceptibility to fluid shear. A literature review of studies exposing juvenile and adult fish to fluid shear led to some understanding of how certain physical characteristics can make certain species more susceptible. Currently, results have suggested morphological features of the scales, eyes, operculum, and body shape are valuable indicators of fluid shear susceptibility. These conclusions may be subject to change as a greater variety of species are studied.

Morphological features of the scales, eyes, operculum, and body shape are valuable indicators of fluid shear susceptibility.

4.3.2 SCALES

Descaling is a quick, effective way to determine the general quality of health for fish. Scale loss can occur for multiple reasons, whether from predator attacks or passage through hydropower facilities. Substantial scale loss can lead to increased stress response, disease susceptibility, predation, and mortality, and as little as 10% descaling can result in life-threatening osmotic stress and high acute mortality in some species (Bouck and Smith 1979; Noga 2000; Turnpenny et al. 1992; Neitzel et al. 2000; 2004; Deng et al. 2005a; Gadomski et al. 1994). Scale size, type, overlap, and number also play a role in the susceptibility of scale loss, so species-specific differences must be addressed (Saylor et al. 2017).

Saylor et al. (2017) subjected adult rainbow trout, gizzard shad (*Dorosoma cepedianum*), and hybrid striped bass (striped bass [*Morone saxatilis*] × white bass [*M. chrysops*]) to varying levels of fluid shear from jet velocities ranging from 0 to 11 m s⁻¹. Rainbow trout, gizzard shad, and hybrid striped bass were chosen because they are a good representative of salmonidae, clupeidae, and moronidae, respectively. When exposed to all velocities, the rainbow trout were more resistant to descaling than the gizzard shad

and hybrid striped bass. Modeling predicted 50% scale loss to occur for gizzard shad, hybrid striped bass, and rainbow trout at velocities of 5.6, 6.5, and 9.5 m s⁻¹, respectively. These results may be explained by looking at the types of scales each of these species has. Rainbow trout have cycloid scales, that are smaller and more densely compacted (Roberts 1993) and hybrid striped bass have ctenoid scales that overlap more than gizzard shad scales, perhaps allowing hybrid striped bass to be slightly more resistant to descaling from fluid shear (Lagler 1947; Roberts 1993). In addition, gizzard shad easily lose scales because they are deciduous, have little overlap, and are not firmly attached to the skin (Lagler 1947).

This is all further complicated by the fact most species of fish have multiple types of scales across different sections of their bodies and little research has been done describing this for most species (Wainwright and Lauder 2016). For this reason, future studies should focus not just on the percentage of descaling present, but also the location of the descaling on fish.

4.3.3 EYES AND OPERCULA

Eyes and opercula are valuable organs that are frequently affected by fluid shear environments. An overview of past studies has shown the susceptibility of injuries to these organs can depend on the morphological differences based on the species tested. American shad have relatively large, slightly protruding eyes compared to their body, which makes them vulnerable to being injured by fluid shear (Pflugrath et al. 2020b). They also have reasonably large opercula, which extend vertically across an estimated 80% of their heads (Pflugrath et al. 2020b). American shad exposed to the highest strain rate (1,000 s⁻¹) by Pflugrath et al. (2020b) resulted in eye and operculum injuries being the second (85%) and third (68%) most common injuries observed. American eel are quite the opposite, having small opercula and embedded eyes. When exposed to a strain rate of 1,000 s⁻¹, no injuries to the eyes or opercula were observed (Pflugrath et al. in prep). Studies examining the effects of fluid shear on eyes and opercula help to better understand specific species susceptibility.

4.3.4 BODY SHAPE AND OVERALL TRENDS

Currently, species with the highest susceptibility to fluid shear can be divided into two body types: fusiform, elongated bodies and laterally compressed, truncated bodies. Each body type appears to have susceptibility to different injuries sustained from fluid shear exposure.

Study results indicate that fish with fusiform, elongated bodies tend to experience an increase in bruising and lacerations. The species included in HBET and the BioPA toolset that have this body type are salmonids (Chinook salmon, rainbow trout, and steelhead), iridescent shark, and largemouth bass. Multiple studies have exposed these fish (headfirst) to similar strain rates ranging from 0 to around $1,185 \text{ s}^{-1}$ using the PNNL shear apparatus (Neitzel et al. 2000; Neitzel et al. 2004; Deng et al. 2005a; Colotelo et al. 2018; Engbrecht et al. in prep). The most common of the major injuries seen in largemouth bass and iridescent shark were bruises and/or lacerations (Colotelo et al. 2018; Engbrecht et al. in prep). Out of all of these species, iridescent sharks experienced a considerable number of bruises and lacerations compared to the rest. Exceptions to this general trend are rainbow trout and steelhead, which experienced very few major injuries and no mortalities in either of the Neitzel et al. studies (2000; 2004). This is possibly due to the fact they have small, more densely compacted cycloid scales that potentially protect against the bruises and cuts associated with fluid shear environments (Roberts 1993; Saylor et al. 2017). However, Chinook salmon have scales that are similar to those of rainbow trout and steelhead, but they still experienced up to 50% bruising (Deng et al. 2005a). Many factors could cause this difference; the scale type among salmonids may be more different than previously thought or a fish size effect may have been present because the Chinook salmon from these studies were smaller than the rainbow trout and steelhead tested (Neitzel et al. 2000; 2004).

The second body type, fish laterally compressed with truncated bodies, appears to be more susceptible to descaling and operculum damage. American shad, blue gourami, and bluegill are included in HBET and the BioPA toolset and all

represent this body type. They have been tested at similar strain rates using the same shear apparatus, allowing for a more thorough comparison of their susceptibility to fluid shear (Neitzel et al. 2000; 2004; Pflugrath et al. 2020b; Colotelo et al. 2018; Engbrecht et al. in prep). The most common injuries for blue gourami and bluegill were operculum damage and descaling, respectively. American shad are unique in that they have both a laterally compressed and fusiform body, but it seems their body type is most similar to this second group of body types. Multiple studies have shown shad are susceptible to operculum injuries and especially susceptible to descaling (Pflugrath et al. 2020b). It is important to acknowledge American shad are also highly sensitive to basic handling stress, as supported by the 20% mortality rate observed in the controls of the Neitzel et al. (2004) study.

Interestingly, studies have shown that American and European eel and Pacific lamprey exposed to fluid shear had no observable injuries or mortalities (Moursund et al. 2000; Pflugrath et al. in prep-c; Turnpenny et al. 1992). This may be due to their unique physical characteristics; for example, their flexible, streamlined bodies; lack of scales; small, heavily recessed eyes; and the absence and/or reduction of vulnerable structures frequent injured by fluid shear like opercula, gills, and jaws.

More studies of a broader variety of morphologically different species would be valuable to help confirm and develop these preliminary trends observed. Understanding more about how certain species characteristics lead to increased or decreased susceptibility can allow us to get a better idea of the susceptibility of other morphologically similar species.

4.3.5 LIFE STAGE

While this review primarily focuses on juvenile fish susceptibility to fluid shear, studies have shown both larvae and eggs are more susceptible to fluid shear and encounter it often by drifting from spawning grounds or nursery areas to rearing habitats. Even at exposure to low strain rates, normal hatching of eggs is prevented because of the easy tearing of the chorion and

subsequent disruption of cellular contents, thereby demonstrating the exceptional vulnerability of eggs (Navarro et al. 2019). Specifically, damage to the eggs has been shown to occur via separation of the developing embryo from the yolk or a breakup of the yolk droplet (Morgan et al. 1976). Larvae are especially susceptible during a specific stage in development—the transition from endogenous nutrition (yolk absorption) to exogenous feeding when new functions in the body are beginning and most organs are underdeveloped (Sifa and Mathias 1987). As larvae grow, the risk of yolk sac rupture decreases as their internal organs and outer protective layer become less fragile.

Overall, a review of the current literature indicates that as fish develop from eggs to increasingly older larvae, they normally become more resistant to fluid shear. However, the level of susceptibility of larvae and eggs appears to be dependent on a number of factors like the species type, age, and size at which shear exposure occurs, and the type of spawning environment. For example, after testing multiple larval species the results from the Killgore et al. (2001) study indicate the size of the fish, not the species, is the primary determining factor for mortality susceptibility. Also, when exposed to elevated levels of fluid shear, paddlefish larvae were found to be far more susceptible than they were as eggs (Killgore et al. 2001). Paddlefish eggs are spawned in riffle environments where rapid acceleration and elevated shear levels may be present, which may be the reason their eggs have some protection against deformation by having a flexible outer chorion (Killgore et al. 2001; Payne et al. 1990). Interestingly, golden perch and silver perch spawn in lowland rivers where lower shear may be encountered, and results show their eggs experience much higher rates of mortality after fluid shear exposure than larvae (Navarro et al. 2019). It is clear many factors influence the susceptibility of larvae and eggs to fluid shear, thus making it challenging to generalize the effects fluid shear environments may have on larvae and eggs.

4.3.6 FISH LENGTH

Fish length may also affect susceptibility to shear exposure. Although, many of the species tested were selected at a size and life stage that was associated with a higher likelihood of entrainment, like American shad, Pacific salmon, and eel, several other species, including, largemouth bass and bluegill, can be entrained at any time. Currently, testing has been limited to relatively small fish, and mostly juveniles, with very little variability in the length of fish tested among species. As fish size increases, it may be necessary to alter how we calculate strain rate by changing Δy (in Equation (15)) from 1.8 cm, which was the precedent set by Neitzel et al. (2000). There is a potential that susceptibility to shear exposure may be similar to blade strike in that as the L/t ratio decreases, the likelihood of injury or mortality increases. In the case of fluid shear, t would represent thickness of the fluid shear transition rather than blade thickness, where a thinner transition would create a more acute exposure to the fish. In addition, as fish grow so do vulnerable physical structures like scales, opercula, and eyes. Interestingly, this may magnify their potential for fluid shear to act upon these features or it may not affect them at all because as these structures increase in size they also likely increase in strength. Future research is needed to tease apart and understand the undetermined effects shear exposure potentially has on larger fish.

4.3.7 FISH ORIENTATION AND SUSCEPTIBILITY DURING EXPOSURE

Little is known about fish behavior and orientation as they enter turbine environments, primarily because of the difficulty in accessing these challenging environments with the necessary equipment. As a result, researchers are often restricted to conducting fluid shear laboratory experiments using scale models of various turbine designs. Studies have shown fish tend to have an increased chance of severe injuries when introduced into fluid shear environments headfirst compared to fish entering in a tailfirst orientation (Neitzel et al. 2000; Neitzel et al. 2004). Furthermore, fish can be subjected to

shear environments via two different scenarios: slow-fish-to-fast-water and fast-fish-to-slow-water where fish are introduced to the edge of the jet stream or within and upstream of the jet stream, respectively.

4.3.7.1 HEADFIRST VS TAILFIRST

The primary conclusions from current studies show that introducing fish to the fluid shear environment headfirst (slow-to-fast-water) results in more severe injuries, primarily occurring in the head and operculum regions (Neitzel et al. 2000; Neitzel et al. 2004). Observations indicate that rainbow trout introduced into a small-scale turbine facility quickly orient themselves facing upstream (tailfirst) before and after passage through the facility, while facing downstream (headfirst) as they first enter the turbine region (Cook et al. 2003).

Introducing fish to the fluid shear environment headfirst results in more severe injuries, primarily occurring in the head and operculum regions

Injuries were shown to be more severe in juvenile salmonids introduced into fluid shear environments in a headfirst orientation compared to fish introduced tailfirst (Neitzel et al. 2000; Neitzel et al. 2004). Salmonids would seem to be more resistant to injury when introduced in a headfirst orientation versus a tailfirst orientation because of their streamlined fusiform bodies. However, a force directed toward the head, in a headfirst orientation, could dislodge scales because they imbricate in a backward direction, likely prying the scales off. Headfirst orientation also increases the opportunity for gill damage because a jet can lift the operculum up and perhaps bend or tear it. Neitzel et al. (2004) found the LC-10 or response was lower when the fish entered the shear zone headfirst versus tailfirst (i.e., 529 s⁻¹ versus 865 s⁻¹ for spring Chinook salmon, and 659 s⁻¹ versus 955 s⁻¹ for steelhead). Observations revealed a majority of the headfirst injuries occurred immediately after contact with the shear zone, and damage to the operculum and isthmus was facilitated by a bending or twisting action.

4.3.7.2 EXPOSURE SCENARIOS

Two exposure scenarios—slow-fish-to-fast-water and fast-fish-to-slow-water—have direct implications for understanding fish injury and mortality rates during passage and entrainment at hydropower dams. It is crucial to understand the mechanism to which fish are exposed because each creates profoundly different exposures to a shear environment (Neitzel et al. 2000).

Usually, slow-fish-to-fast-water scenarios slowly allow fish to swim down the introduction tube only to be rapidly accelerated once it reaches the shear environment created by the submerged jet. Injuries are normally on a small portion of the body as a result of a very confined, but severe force. Conversely, the fast-fish-to-slow-water scenarios usually place a fish in a pipe upstream of the jet nozzle allowing the fish to slowly accelerate to the nozzle exit velocity. Upon exiting, the jet spreads out in the mixing zone of the flume subjecting the fish to the shear environment. Comparatively, fish are less likely to experience fluid shear under this scenario and test results usually indicated fewer localized injuries. This scenario is frequently observed in the bulk flow within a turbine and especially in the draft tube and tailrace.

Laboratory studies indicate injuries from fish exposed via slow-fish-to-fast-water were more severe than those exposed through fast-fish-to-slow-water scenarios (Neitzel et al. 2000; 2004; Deng et al. 2010). Common injuries from fish being exposed via slow-fish-to-fast-water include exophthalmia, eye removal, torn operculum and isthmus, and scale loss as opposed to fast-fish-to-slow-water scenarios, which had fewer localized injuries and included head and body bruising, damaged and/or bleeding gills, minor isthmus tears, and loss of equilibrium (Neitzel et al. 2000).

The onset of injuries occurs at different jet velocities depending on the mechanism of fish entry into the shear environment. Juvenile fish exposed to the slow-fish-to-fast-water entry mechanism were found to not be injured until jet velocities reached 9.1 m s⁻¹ or higher (Groves 1972; Neitzel et al. 2000). The onset of minor,

major, and mortal injuries of subyearling fall Chinook salmon exposed to the slow-fish-to-fast-water entry mechanism occurred at lower jet velocities of 12.2, 13.7, and 16.8 m s⁻¹, respectively (Deng et al. 2005b). Using similar fast-fish-to-slow-water entry mechanisms, Johnson et al. (2003) and (1972) reported no injuries for juvenile salmonids at jet entry velocities of up to 15.2 m s⁻¹ and 17.4 m s⁻¹, respectively. (Deng et al. 2010) also found the threshold of minor and major injuries for juvenile fall Chinook salmon introduced via fast-fish-to-slow-water mechanism to occur at 15.2 and 21.3 m s⁻¹, respectively.

4.3.8 FLUID SHEAR SURROGACY

The use of surrogacy species for testing is beneficial because it allows researchers to imply susceptibility to different fish species that are not as readily available for testing, based on the examination of a species that has similar traits or phylogeny. Unlike blade strike and rapid decompression, no studies have been conducted of the use of surrogacy for fluid shear. Based on the results of the studies discussed and conclusions made about fish susceptibility based on morphology in this review, it may be possible to apply surrogacy. For example, shear testing on three Centrarchid species (largemouth bass, bluegill, and pumpkinseed) found similar injury and mortality rates and there is not much morphological variation across species within the *Micropterus* and *Lepomis* genera. Because variation in susceptibility to fluid shear is expected to be less within a genus of fish than within a family and because of similar morphology, bluegill and pumpkinseed are likely suitable surrogates for the genus *Lepomis*, and largemouth bass are likely an appropriate surrogate for the genus *Micropterus*. Of course, the use of surrogates would likely provide an approximation of susceptibility and is not recommended if precise estimates are needed for certain applications.

4.4 FLUID SHEAR DISCUSSION

As the effects of fluid shear due to passage through hydropower turbines continue to be

examined and more biological response models are developed, the method set forth by (Neitzel et al. 2004) has become the standard. Future studies should consider following this methodology so that species can continue to be accurately compared for susceptibility to fluid shear. There are several areas in which this research can be expanded to address the limitations and applicability of these models. The examination of additional fish species and life stages is also needed to provide a better understanding of how different traits may affect susceptibility.

4.4.1 FLUID SHEAR LIMITATIONS OF THE CURRENT DATA

While a number of comprehensive studies have been completed, it is sometimes difficult to make direct comparisons between them. Some studies have measured shear levels in dynes/cm² making it difficult to compare their results to the results of studies that measure shear levels in jet velocity (m s⁻¹) or strain rate (s⁻¹). In addition, studies generally categorize and report the results in different ways. Certain studies only reported mortality data with no information about injuries observed and several others measured injury severity differently. Although this can be insightful in various ways, it makes it hard to draw conclusions about species or the effects of varying levels of fluid shear. Other limitations of the current data are the inadequate ranges or only low levels of shear tested, different shear testing facilities used, and low numbers of fish tested that make it challenging to find significance in the data. Perhaps, a solution to these limitations could be to have future testing follow a standardized method. For example, methods listed in the Neitzel et al. papers (2000, 2004) have been repeatedly used by other researchers because they expose fish to a broad range of jet velocities using a reliable testing apparatus and they categorize injuries based on levels of severity.

4.4.2 FUTURE RESEARCH NEEDS FOR FLUID SHEAR

A significant amount of research has been completed in this field allowing our knowledge about the susceptibility of species exposed to varying levels of fluid shear to expand. While this is an excellent start, there is still much research to be done to build on what we already know about fluid shear.

Future studies could examine a greater variety of fish sizes and morphologically diverse species. This would help develop new or refine the current trends of susceptibility observed based on the physical characteristics of each fish tested. Solidifying appropriate surrogates for testing would be helpful for future studies, especially if certain species of interest are not readily available. A more in-depth evaluation of the physiological effects of shear exposure via necropsies or stress hormone analysis would not only be interesting, but likely insightful. Altered swimming behavior can indicate the effects on many body systems and more severe underlying injuries; therefore, finding a correlation between certain types of behavior and injuries could be a quick way to determine fish susceptibility or potential mortality.

Most species of fish encounter several hydropower facilities during migration, so it would be useful if future studies could also focus on performing repeated fluid shear testing to simulate passage through multiple dams. Along the lines of replicating an accurate portrayal of what fish experience in the wild, studying how shear exposure and altered swimming behavior affect the ability of fish to avoid predation would also be valuable. Doing so would help us understand more about the indirect effects of fluid shear exposure.

4.4.2.1 ADDITIONAL SPECIES FOR FLUID SHEAR TESTING

The HydroPASSAGE project has focused attention on species of conservation concern that encounter hydropower facilities often, but many species remain to be tested, such as fish from the Acipenseridae, Ictaluridae, and Polyodontidae

families. As is true for rapid decompression and blade strike, cyprinids have also been minimally tested for fluid shear. As discussed in previous chapters, cyprinids are highly prevalent around the world and conservation concerns are known for many of these species. Many of these species likely encounter hydropower structures through downstream migration, so it is imperative to understand more about the susceptibility of fish in this family. A large portion of the aforementioned species have barbells and ventrally oriented mouths, two traits about which little is known relative to susceptibility to fluid shear. Examining the susceptibility of more morphologically diverse species would help develop more definitive trends about what physical characteristics make some species more vulnerable than others to fluid shear.

4.5 FLUID SHEAR CONCLUSIONS

The effects of fluid shear exposure during passage through hydropower facilities has been examined and reported by several studies. Specialized flumes and submerged water jets were used to conduct this research. From those studies, a total of 45 biological response models (injury, major injury, and immediate mortality) have been developed for 16 fish species (19 when including subspecies). The results from these studies have demonstrated that the response to fluid shear can vary significantly between different species such as little to no susceptibility for eel and lamprey (Turnpenny et al. 1992; Moursund et al. 2000; Pflugrath et al. in prep-c) and highly susceptible for shad and herring. Several conclusions can be drawn from this collection of research:

- Overall, fish susceptibility to injury or mortality increases as strain rate or acceleration increase during passage through hydropower facilities.
- All levels of fluid shear associated with hydropower facilities are not likely to affect species that have no scales and no and/or reduced sizes of vulnerable organs (e.g., eyes, opercula, and gills) regularly injured by shear (e.g., American eel, European eel, and Pacific lamprey).

- Current literature suggests fish with fusiform, elongated bodies tend to suffer increased bruising and cuts, and fish laterally compressed with truncated bodies appear to be more susceptible to descaling and operculum damage.
- Fish with different morphological features of the scales, eyes, opercula, and body shape are valuable indicators of fluid shear susceptibility and testing new, more morphologically diverse fish would help develop more understanding about specific susceptibility.
- Future research should focus on the effects of multiple fluid shear exposures, selection of appropriate surrogates for testing, examination of more of the physiological effects caused by fluid shear, and understanding of the indirect effects of fluid shear, like potential increased predation.



5.0 APPLICATION OF BIOLOGICAL RESPONSE MODELS

The biological response models compiled and developed for the HydroPASSAGE project can be applied to evaluate various hydropower designs using the software tools the BioPA toolset and HBET. Once data have been either developed through CFD or gathered by Sensor Fish, the BioPA toolset and HBET can be used with the integrated biological response models to predict the likelihood of injuries and mortality caused by the main stressors and make relative fish passage comparisons (Richmond et al. 2014b; Hou et al. 2018). These software tools were developed primarily to be used for turbines, but they can be and have also been used for several other applications such as spillways and irrigation weirs (Deng et al. 2017; Pflugrath 2017).

5.1 HYDROPASSAGE TOOL EXAMPLE

To demonstrate the use of the BioPA toolset and HBET, two generalized turbines (based on values observed through various turbines; (Fu et al. 2016) were compared—a Kaplan turbine and a Francis turbine. These turbines represent a generalized form of each turbine type and are not intended to imply injury or survival rates for any specific turbine. For this demonstration, the BioPA toolset was used, but the same analysis can be conducted using HBET if the data were gathered using Sensor Fish. Rainbow trout, bluegill, and American Eel were selected for demonstration purposes, because these three species differ morphologically and all three have biological response models for each of the main stressors. These fish also represent a range of susceptibility to the stressors.

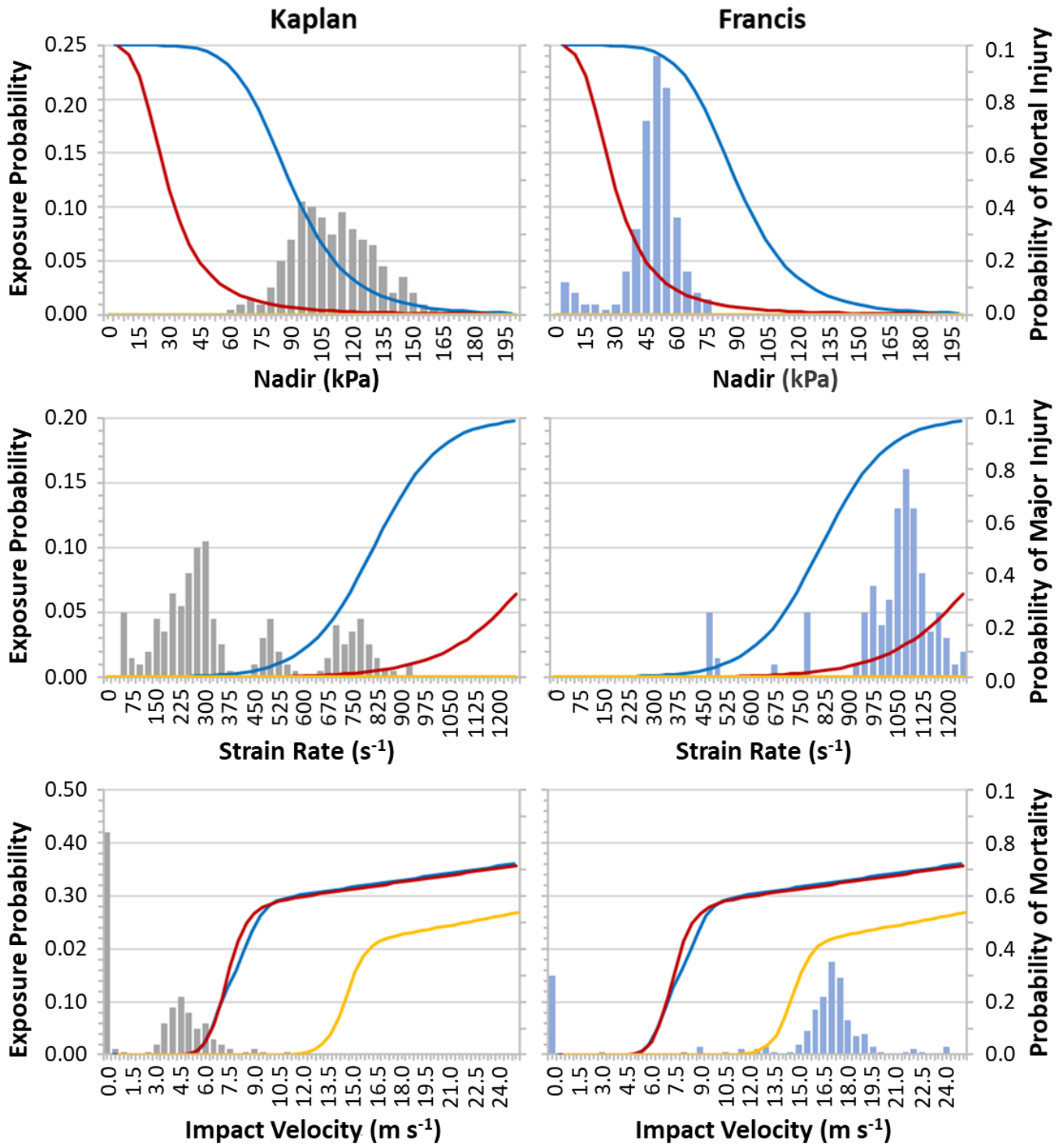


Figure 27. Probability of exposure distributions of rapid decompression (nadir), fluid shear (strain rate), and collision (impact velocity) for fish passing through generalized Kaplan (gray bars) and Francis (light blue bars) turbines. Biological dose-response models are overlain exposure distributions for bluegill (blue line), rainbow trout (red line), and American eel (gold line).

Exposure distributions for each stressor were generated for each turbine (Figure 27). For exposure to rapid decompression, the acclimation pressure was set to 150 kPa, which is a depth equivalent of approximately 5 m. An acclimation pressure must be selected when using the BioPA toolset or HBET because this value is used to determine the RPC based on nadir pressures calculated from the CFD models or measured by Sensor Fish. Once the exposure distributions (probability of exposure, P_E) have been generated, the biological response models (probability of response, P_R) are applied to calculate the probability of adverse passage (P_A):

$$P_E \times P_R = P_A \tag{16}$$

The probability of adverse passage is the likelihood that a fish will experience a stressor and respond to that stressor. The response is based on the selected biological response model. For this demonstration the response for exposure to rapid decompression is mortal injury, the response for fluid shear is major injury, and the response for collision is mortality.

The results from the BioPA analysis indicate that American eel had the lowest likelihood of adverse passage for all three stressors when compared to

bluegill and rainbow trout (Figure 28). Bluegill had the highest likelihood of adverse passage due to rapid decompression and fluid shear but had a likelihood similar to that of rainbow trout for collision. For American eel, the biological response models for rapid decommission and fluid shear are no response. In addition, the Kaplan turbine would not likely expose American eel to impact velocities likely to cause mortality. Therefore, American eel are only likely to encounter an adverse passage due to collision when passing through the generic Francis turbine.

The BioPA toolset combines the probability of adverse passage and gives each turbine a relative performance score for each species (known as the Passage Quality Index [PQI]). These scores provide a relative comparison of turbine passage because stressor interactions (i.e., how a fish might respond when exposed to multiple stressors) are currently unknown. PQI scores can range from 0 to 500, with 500 being the best possible score and indicating a very low likelihood of adverse passage. Scores closer to zero indicate a high likelihood of adverse passage for that species. The Kaplan turbine had higher scores for all three species and is likely to provide a significantly lower chance of adverse passage than the Francis turbine (Figure 29).

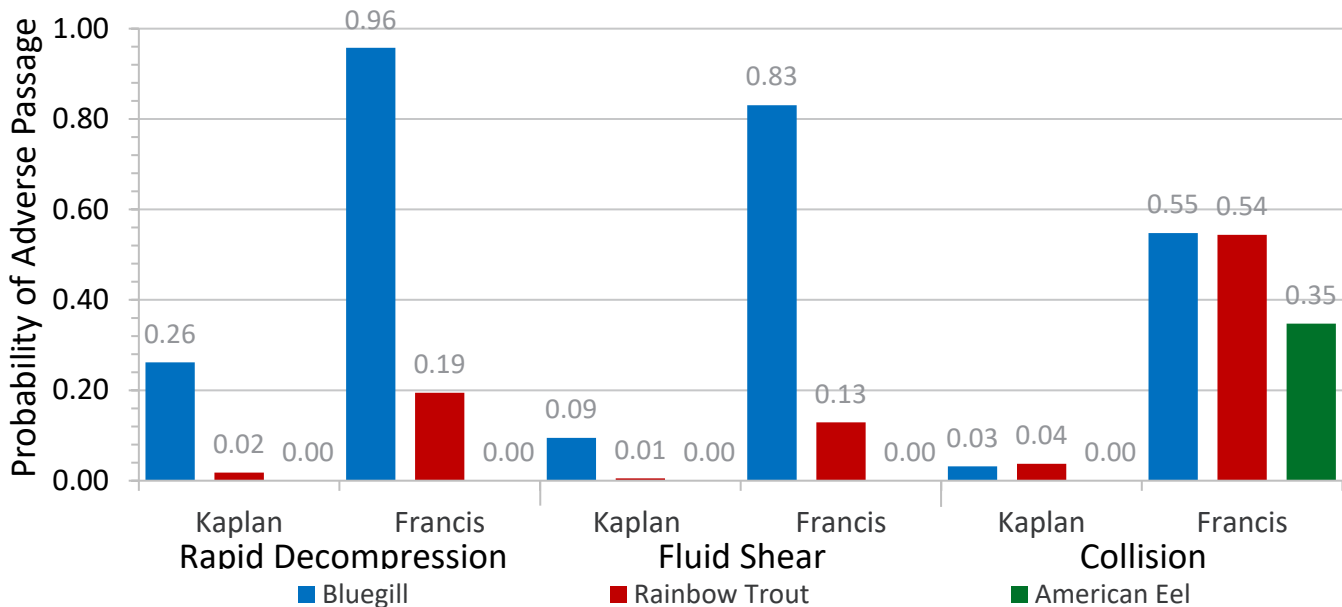


Figure 28. Comparison of the probability of adverse passage for bluegill, rainbow trout, and American eel passing through a generic Kaplan and Francis turbine.

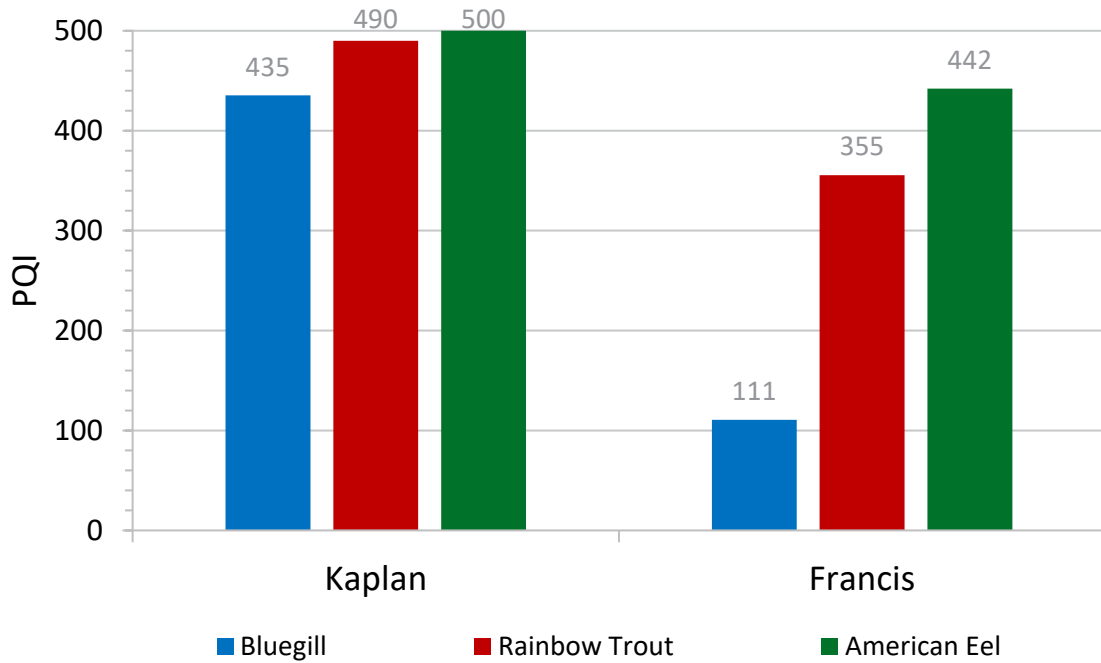


Figure 29. BioPA PQI scores (relative performance scores) for bluegill, rainbow trout, and American eel passing through a generic Kaplan and Francis turbine. Scores range from 0 to 500, with 500 representing a likelihood of no adverse passage.



6.0 CONCLUSION

The use of biological response models, integrated with the HBET and BioPA software tools, provides valuable information for the design and operation of hydropower that will promote the safe passage of fish. A total of 99 biological response models for exposure to blade strike, fluid shear, or rapid decompression have been developed or collected from the literature, including models for 31 different species of fish. In addition to the stressor-specific conclusions previously mentioned, a few general conclusions can be drawn from this assemblage of research:

- Considerable variation in susceptibility from one species to another has been reported for exposure to blade strike, fluid shear, and rapid decompression, and susceptibility to one stressor does not necessarily indicate similar susceptibility to another stressor.
- Biological response models can be and have been applied through HBET and the BioPA toolset for numerous applications to better understand the potential for injury and mortality to occur during fish passage.
- Future research related to these stressors needs to examine additional species, such as cyprinid species, that have different morphological traits, and how different environment and physical variables may affect the severity of these stressors.

As hydropower is continually developed to meet the electricity needs of society, tools such as HBET and the BioPA toolset, with the integrated biological response models, will aid in the development of technologies and strategies that avoid, minimize, mitigate, or manage environmental effects.

7.0 REFERENCES

This list contains references cited in the main narrative and in Appendix A.

- Abernethy, C. S., Amidan, B. G. & Čada, G. F. 2001. Laboratory Studies of the Effects of Pressure and Dissolved Gas Supersaturation on Turbine-Passed Fish. Pacific Northwest National Laboratory.
- Abernethy, C. S., Amidan, B. G. & Čada, G. F. 2002. Simulated Passage Through a Modified Kaplan Turbine Pressure Regime: A Supplement to "Laboratory Studies of the Effects of Pressure and Dissolved Gas Supersaturation on Turbine-Passed Fish". Pacific Northwest National Laboratory.
- Abernethy, C. S., Amidan, B. G. & Čada, G. F. 2003. Fish Passage Through a Simulated Horizontal Bulb Turbine Pressure Regime: A Supplement to "Laboratory Studies of the Effects of Pressure and Dissolved Gas Supersaturation on Turbine-Passed Fish". Pacific Northwest National Laboratory.
- Ahlstrom, E., Amaoka, K., Hensley, D., Moser, H. & Sumida, B. 1984. Pleuronectiformes: development. *Ontogeny and systematics of fishes*. Allen Press Lawrence.
- Amaral, B. S., Hecker, G., Metzger, M. & Cook, T. 2003. 2002 Biological Evaluation of the Alden / Concepts NREC Turbine. 2003 2003 Buffalo. HCI Publications, 1-12.
- Amaral, S. V., Watson, S. M., Schneider, A. D., Rackovan, J. & Baumgartner, A. 2020. Improving survival : injury and mortality of fish struck by blades with slanted , blunt leading edges. *Journal of Ecohydraulics*.
- Baumgartner, L. 2005. Effects of dams and weirs on fish migrations in the Murray-Darling Basin. *University of Canberra, Canberra*.
- Baumgartner, L., Mcpherson, B., Doyle, J., Cory, F., Cinotti, N. & Hutchison, J. 2013. Quantifying and mitigating the impacts of weirs on downstream passage of native fish in the Murray-Darling Basin.
- Baumgartner, L. J., Thorncraft, G., Phonekhampheng, O., Boys, C., Navarro, A., Robinson, W., Brown, R. & Deng, Z. 2017. High fluid shear strain causes injury in silver shark: preliminary implications for Mekong hydropower turbine design. *Fisheries Management and Ecology*, 24, 193-198.
- Becker, J. M., Abernethy, C. S. & Dauble, D. D. 2003. Identifying the Effects on Fish of Changes In Water Pressure during Turbine Passage. *Hydro Review*, 22, 11.
- Beirão, B., Pflugrath, B. D., Harnish, R. A., Harding, S. F., Richmond, M. C. & Colotelo, A. H. 2020. Empirical Investigation into the Applicability of Surrogacy for Juvenile Salmonids (*Oncorhynchus* spp.) Exposed to Hydropower Induced Rapid Decompression. *Ecological Indicators*.
- Beirão, B. V., Silva, L. G., Brown, R. S. & Walker, R. W. 2018. Determining barotrauma in the Pictus catfish, *Pimelodus pictus*, experimentally exposed to simulated hydropower turbine passage. *Marine and Freshwater Research*, 69, 1913-1921.
- Bevelhimer, M. S., Pracheil, B. M., Fortner, A. M. & Deck, K. L. 2017. An Overview of Experimental Efforts to Understand the Mechanisms of Fish Injury and Mortality Caused by Hydropower Turbine Blade Strike. *ORNL/TM-2017/731*, Medium: ED; Size: 29 p.-Medium: ED; Size: 29 p.
- Bevelhimer, M. S., Pracheil, B. M., Fortner, A. M., Saylor, R. & Deck, K. L. 2019. Mortality and Injury Assessment for Three Species of Fish Exposed to Simulated Turbine Blade Strike. *Canadian Journal of Fisheries and Aquatic Sciences*.
- Binder, T. R., Cooke, S. J. & Hinch, S. G. 2011. Physiological Specializations of Different Fish Groups: Fish Migrations. *In: FARRELL, A. P., CECH JR, J. J., RICHARDS, J. G. & STEVENS, E. D. (eds.)* 1 ed. San Diego: Elsevier Inc.
- Blake, R. W. 2004. Review Paper: Fish functional design and swimming performance. *Journal of Fish Biology*, 65, 1193-1193.

- Bouck, G. R. & Smith, S. D. 1979. Mortality of Experimentally Descaled Smolts of Coho Salmon (*Oncorhynchus kisutch*) in Fresh and Salt Water. *Transactions of the American Fisheries Society*, 108, 67-69.
- Boys, C., Baumgartner, L., Miller, B., Deng, Z., Brown, R. & Pflugrath, B. 2013. Protecting downstream migrating fish at mini hydropower and other river infrastructure. *Fisheries Final Report Series*, 137.
- Boys, C., Navarro, A., Robinson, W., Fowler, T., Chilcott, S., Miller, B., Pflugrath, B., Baumgartner, L., Mcpherson, J. & Brown, R. 2014a. Downstream fish passage criteria for hydropower and irrigation infrastructure in the Murray–Darling Basin. *Fisheries Final Report Series*.
- Boys, C. A., Navarro, A., Robinson, W., Fowler, A. C., Chilcott, S., Miller, B., Pflugrath, B. D., Baumgartner, L. J., Mcpherson, J., Brown, R. S. & Deng, Z. D. 2014b. Downstream fish passage criteria for hydropower and irrigation infrastructure in the Murray-Darling Basin. *Fisheries Final Report*. NSW Department of Primary Industries.
- Boys, C. A., Robinson, W., Miller, B., Pflugrath, B. D., Baumgartner, L., Navarro, A., Brown, R. S. & Deng, Z. D. 2016a. How low can they go when going with the flow? Tolerance of egg and larval fishes to rapid decompression. *Biology Open*, bio. 017491.
- Boys, C. A., Robinson, W., Miller, B., Pflugrath, B. D., Baumgartner, L. J., Navarro, A., Brown, R. S. & Deng, Z. D. 2016b. A piecewise regression approach for determining biologically relevant hydraulic thresholds for the protection of fishes at river infrastructure. *Journal of fish biology*, 88, 1677-1692.
- Brown, R. S., Carlson, T. J., Gingerich, A. J., Stephenson, J. R., Pflugrath, B. D., Welch, A. E., Langeslay, M. J., Ahmann, M. L., Johnson, R. L., Skalski, J. R., Seaburg, A. G. & Townsend, R. L. 2012a. Quantifying mortal injury of juvenile Chinook salmon exposed to simulated hydro-turbine passage. *Transactions of the American Fisheries Society*, 141, 147-157.
- Brown, R. S., Colotelo, A. H., Pflugrath, B. D., Boys, C. A., Baumgartner, L. J., Deng, Z. D., Silva, L. G. M., Brauner, C. J., Mallen-Cooper, M., Phonekhampeng, O., Thorncraft, G. & Singhanouvong, D. 2014. Understanding barotrauma in fish passing hydro structures: a global strategy for sustainable development of water resources. *Fisheries*, 39, 108-122.
- Brown, R. S., Cook, K. V., Pflugrath, B. D., Rozeboom, L. L., Johnson, R. C., Mclellan, J. G., Linley, T. J., Gao, Y., Baumgartner, L. J., Dowell, F. E., Miller, E. A. & White, T. A. 2013. Vulnerability of larval and juvenile white sturgeon to barotrauma: can they handle the pressure? *Conservation Physiology*, 1, 1-9.
- Brown, R. S., Pflugrath, B. D., Colotelo, A. H., Brauner, C. J., Carlson, T. J., Deng, Z. D. & Seaburg, A. G. 2012b. Pathways of barotrauma in juvenile salmonids exposed to simulated hydrotrubine passage: Boyle's law vs Henry's law. *Fisheries Research*, 121-122, 43-50.
- Brown, R. S., Walker, R. W. & Stephenson, J. R. 2016. A Preliminary Assessment of Barotrauma Injuries and Acclimation Studies for Three Fish Species. Pacific Northwest National Lab.(PNNL), Richland, WA (United States).
- Cada, G. F. 1991. Effects of hydroelectric turbine passage on fish early life stages. Oak Ridge National Lab., TN (USA).
- Čada, G. F. 1997. Shaken, Not Stirred: The Recipe for a Fish-Friendly Turbine. *Waterpower*. American Society Civil Engineers.
- Čada, G. F. 2001. The development of advanced hydroelectric turbines to improve fish passage survival. *Fisheries*, 26, 14-23.
- Cada, G. F., Garrison, L. A. & Fisher, R. K. 2007. Determining the effect of shear stress on fish mortality during turbine passage. *Hydro Review*, 26, 52.
- Čada, G. F., Loar, J., Garrison, L., Fisher, R., Jr. & Neitzel, D. 2006a. Efforts to reduce mortality to hydroelectric turbine-passed fish: locating and quantifying damaging shear stresses. *Environ Manage*, 37, 898-906.
- Čada, G. F., Ryon, M. G., Smith, J. G. & Luckett, C. A. 2006b. The Effects of Turbine Passage on C-Start Behavior of Salmon at the Wanapum Dam, Washington Wind and Hydropower Technologies. Oak Ridge.
- Cada, G. F., Ryon, M. G., Wolf, D. A. & Smith, B. T. 2003. Development of a New Technique to Assess Susceptibility to Predation Resulting from Sublethal Stresses (Indirect Mortality). Oak Ridge.

- Čada, G. F. & Schweizer, P. E. 2012. The Application of Traits-Based Assessment Approaches to Estimate the Effects of Hydroelectric Turbine Passage on Fish Populations. Oak Ridge.
- Čada, G. F., Suffern, J. S., Kumar, K. D. & Solomon, J. A. 1981. Investigations of entrainment mortality among larval and juvenile fishes using a power plant simulator. Oak Ridge National Lab.
- Calles, O. & Greenberg, L. 2009. Connectivity is a two - way street—the need for a holistic approach to fish passage problems in regulated rivers. *River Research and Applications*, 25, 1268-1286.
- Çelebioğlu, K. & Kaplan, A. 2019. Development and Implementation of a Methodology for Reverse Engineering Design of Francis Turbine Runners. *Pamukkale University Journal of Engineering Sciences*, 25, 430-439.
- Colotelo, A., Mueller, R., Harnish, R., Martinez, J., Phommavong, T., Phommachanh, K., Thorncraft, G., Baumgartner, L., Hubbard, J. & Rhode, B. 2018. Injury and mortality of two Mekong River species exposed to turbulent shear forces. *Marine and Freshwater Research*, 69, 1945-1953.
- Colotelo, A. H., Goldman, A. E., Wagner, K. A., Brown, R. S., Deng, Z. D. & Richmond, M. C. 2017. A comparison of metrics to evaluate the effects of hydro-facility passage stressors on fish. *Environmental Reviews*, 25, 1-11.
- Colotelo, A. H., Pflugrath, B. D., Brown, R. S., Brauner, C. J., Mueller, R. P., Carlson, T. J., Deng, Z. D., Ahmann, M. L. & Trumbo, B. A. 2012. The effect of rapid and sustained decompression on barotrauma in juvenile brook lamprey and Pacific lamprey: implications for passage at hydroelectric facilities. *Fisheries Research*, 129-130, 17-20.
- Cook, T. C., Hecker, G. E., Amaral, S. V., Stacy, P. S., Lin, F. & Taft, E. P. 2003. Pilot Scale Tests Alden/Concepts NREC Turbine. Alden Research Laboratory (US).
- Cooke, S. J., Bunt, C. M., Hamilton, S. J., Jennings, C. A., Pearson, M. P., Cooperman, M. S. & Markle, D. F. 2005. Threats, conservation strategies, and prognosis for suckers (Catostomidae) in North America: insights from regional case studies of a diverse family of non-game fishes. *Biological Conservation*, 121, 317-331.
- Costa, J. E. 1987. Hydraulics and basin morphometry of the largest flash floods in the conterminous United States. *Journal of hydrology*, 93, 313-338.
- Coutant, C. C. & Whitney, R. R. 2000. Fish Behavior in Relation to Passage through Hydropower Turbines : A Review. *Transactions of the American Fisheries Society*, 129, 351-380.
- Deng, Z., Duncan, J., Arnold, J., Fu, T., Martinez, J., Lu, J., Titzler, P., Zhou, D. & Mueller, R. 2017. Evaluation of Boundary Dam spillway using an autonomous Sensor Fish device. *Journal of Hydro-environment Research*, 14, 85-92.
- Deng, Z., Guensch, G. R., Mckinstry, C. A., Mueller, R. P., Dauble, D. D. & Richmond, M. C. 2005a. Evaluation of fish-injury mechanisms during exposure to turbulent shear flow. *Canadian Journal of Fisheries and Aquatic Sciences*, 62, 1513-1522.
- Deng, Z., Mueller, R. P., Richmond, M. C. & Johnson, G. E. 2010. Injury and mortality of juvenile salmon entrained in a submerged jet entering still water. *North American Journal of Fisheries Management*, 30, 623-628.
- Deng, Z. D., Guensch, G. R., Mckinstry, C. A., Mueller, R. P., Dauble, D. D. & Richmond, M. C. 2005b. Evaluation of fish-injury mechanisms during exposure to turbulent shear flow. *Canadian Journal of Fisheries and Aquatic Sciences*, 62, 1513-1522.
- Deng, Z. D., Lu, J., Myjak, M. J., Martinez, J. J., Tian, C., Morris, S. J., Carlson, T. J., Zhou, D. & Hou, H. 2014. Design and implementation of a new autonomous sensor fish to support advanced hydropower development. *Review of Scientific Instruments*, 85, 115001.
- Desoutter-Meniger, M. & Chanut, B. 2009. The swim bladder of the adult soleids [Acanthomorpha: Pleuronectiformes, Soleidae]: fact or fiction. *Cahier d'Anatomie Comparée*, 40-49.
- Eicher, G. J., Bell, M., Campbell, C., Craven, R. & Wert, M. 1987. Turbine-related fish mortality: review and evaluation of studies.
- Engbrecht, K., Pflugrath, B. D., Mueller, R. P., Stephenson, J. R., Deters, K. A. & Colotelo, A. H. in prep. The Susceptibility of Juvenile Centrarchids to Fluid Shear Exposure Associated with Simulated Hydroturbine Passage.
- Epri 1992. Fish entrainment and turbine mortality review and guidelines. *Report TR - 101231, Project 2694 - 01*.

- Epri 2008. Electric Power Research Institute. Evaluation of the Effects of Turbine Blade Leading Edge Design on Fish Survival. Palo Alto.
- Epri 2011. Electric Power Research Institute. 2010 Tests Examining Survival of Fish Struck By Turbine Blades. Palo Alto.
- Fänge, R. 1966. Physiology of the swimbladder. *Physiological reviews*, 46, 299-322.
- Fausch, K. D. & White, R. J. 1981. Competition between brook trout (*Salvelinus fontinalis*) and brown trout (*Salmo trutta*) for positions in a Michigan stream. *Canadian Journal of Fisheries and Aquatic Sciences*, 38, 1220-1227.
- Feathers, M. G. & Knable, A. E. 1983. Effects of Depressurization Upon Largemouth Bass. *North American Journal of Fisheries Management*, 3, 86-90.
- Franke, G., Webb, D., Fisher, R., Mathur, D., Hopping, P., March, P., Hedrick, M., Laczko, I., Ventikos, Y. & Sotiropoulos, F. 1997. Development of environmentally advanced hydroturbine system concepts. *Report prepared for the Department of Energy under Contract DE-AC07-96ID13382*.
- Froese, R. & Pauly, D. 2020. Fishbase.
- Fu, T., Deng, Z. D., Duncan, J. P., Zhou, D., Carlson, T. J., Johnson, G. E. & Hou, H. 2016. Assessing hydraulic conditions through Francis turbines using an autonomous sensor device. *Renewable Energy*, 99, 1244-1252.
- Gadomski, D. M., Mesa, M. G. & Olson, T. M. 1994. Vulnerability to predation and physiological stress responses of experimentally descaled juvenile chinook salmon, *Oncorhynchus tshawytscha*. *Environmental Biology of Fishes*, 39, 191-199.
- Ghosh, T. K. & Prelas, M. A. 2011. Energy Resources and Systems. 1 ed. New York: Springer Science+Business media, LLC.
- Groves, A. B. 1972. Effects of Hydraulic Shearing Actions on Juvenile Salmon: Summary Report.
- Grubbs, R. D. & Kraus, R. T. 2010. Fish Migration. In: BREED, M. D. & MOORE, J. (eds.) 1 ed. San Diego: Elsevier Academic Press.
- Harvey, H. H. 1963. *Pressure in the early life history of Sockeye Salmon. Doctoral Dissertation*. PhD Doctoral Dissertation, University of British Columbia.
- Hecker, G. E. & Cook, T. C. 2005. Development and Evaluation of a New Helical Fish-Friendly Hydroturbine. *Journal of Hydraulic Engineering*, 131, 835-844.
- Hogan, J. 1941. The effects of high vacuum on fish. *Transactions of the American Fisheries Society*, 70, 469-474.
- Hoover, J. J., Bailey, P., Januchowski-Hartley, S. R., Lyons, J., Pracheil, B. & Zigler, S. 2019. Anthropogenic Obstructions to Paddlefish Movement and Migration. American F ed. Bethesda: American Fisheries Society.
- Hostetter, N. J., Evans, A. F., Roby, D. D., Collis, K., Hawbecker, M., Sandford, B. P., Thompson, D. E. & Loge, F. J. 2011. Relationship of External Fish Condition to Pathogen Prevalence and Out-Migration Survival in Juvenile Steelhead. *Transactions of the American Fisheries Society*, 140, 1158-1171.
- Hou, H., Deng, Z., Martinez, J., Fu, T., Duncan, J., Johnson, G., Lu, J., Skalski, J., Townsend, R. & Tan, L. 2018. A hydropower biological evaluation toolset (HBET) for characterizing hydraulic conditions and impacts of hydro-structures on fish. *Energies*, 11, 990.
- Johnson, G. E., Ebberts, B. D., Dauble, D. D., Giorgi, A. E., Heisey, P. G., Mueller, R. P. & Neitzel, D. A. 2003. Effects of jet entry at high-flow outfalls on juvenile Pacific salmon. *North American Journal of Fisheries Management*, 23, 441-449.
- Johnson, R. 1970a. Fingerling fish mortalities at 57.5 fps. *Fourth Progress Report on Fisheries Engineering Research Program, 1966-1972*, 14.
- Johnson, R. 1970b. Fingerling fish research effect of mortality of 67 fps velocity.
- Johnson, R. 1972. Fingerling fish research, high-velocity flow through four-inch nozzle.
- Jones, F. H. 1952. THE SWIMBLADDER AND THE VERTICAL MOVEMENTS OF TELEOSTEAN FISHES: II. THE RESTRICTION TO RAPID AND SLOW MOVEMENTS. *Journal of Experimental Biology*, 29, 94-109.
- Killgore, K. J., Maynard, S. T., Chan, M. D. & Morgan, R. P. 2001. Evaluation of propeller-induced mortality on early life stages of selected fish species. *North American Journal of Fisheries Management*, 21, 947-955.

- Knable, A. E. & Feathers, M. G. 1983. Device for examining the effects of pressure changes on fish. *The Progressive Fish-Culturist*, 45, 16-18.
- Lagler, K. F. 1947. Lepidological studies 1. Scale characters of the families of Great Lakes fishes. *Transactions of the American Microscopical Society*, 66, 149-171.
- Martinez, J. J., Deng, Z. D., Titzler, P. S., Duncan, J. P., Lu, J., Mueller, R. P., Tian, C., Trumbo, B. A., Ahmann, M. L. & Renholds, J. F. 2019. Hydraulic and biological characterization of a large Kaplan turbine. *Renewable Energy*, 131, 240-249.
- Mathur, D., Heisey, P. G., Skalski, J. R. & Kenney, D. R. 2000. Salmonid smolt survival relative to turbine efficiency and entrainment depth in hydroelectric power generation. *Journal of the American Water Resources Association*, 36, 737-747.
- Mathur, D., Heisey, P. G., Terry Euston, E., Skalski, J. R. & Hays, S. 1996. Turbine passage survival estimation for chinook salmon smolts (*Oncorhynchus tshawytscha*) at a large dam on the Columbia River. *Canadian Journal of Fisheries and Aquatic Sciences*, 53, 542-549.
- Mcewen, D. & Scobie, G. 1992. Estimation of the hydraulic conditions relating to fish passage through turbines. *NPC001. National Engineering Laboratory, East Kilbride, Glasgow.*
- Mckinstry, C. A., Carlson, T. J. & Brown, R. S. 2007. Derivation of a mortal injury metric for studies of rapid decompression of depth-acclimated physostomous fish. Pacific Northwest National Laboratory.
- Moon, R., Camporesi, E. & Kisslo, J. 1989. Patent foramen ovale and decompression sickness in divers. *The Lancet*, 333, 513-514.
- Morgan, R. P., Ulanowicz, R. E., Rasin Jr, V. J., Noe, L. A. & Gray, G. B. 1976. Effects of shear on eggs and larvae of striped bass, *Morone saxatilis*, and white perch, *M. americana*. *Transactions of the American Fisheries Society*, 105, 149-154.
- Moursund, R., Dauble, D. & Bleich, M. 2000. Effects of John Day Dam bypass screens and project operations on the behavior and survival of juvenile Pacific lamprey (*Lampetra tridentata*). *US Army Corps of Engineers, Portland, Oregon.*
- Mueller, M., Pander, J. & Geist, J. 2017. Evaluation of external fish injury caused by hydropower plants based on a novel field - based protocol. *Fisheries Management and Ecology*, 24, 240-255.
- Navarro, A., Boys, C. A., Robinson, W., Baumgartner, L. J., Miller, B., Deng, Z. D. & Finlayson, C. M. 2019. Tolerable ranges of fluid shear for early life-stage fishes: implications for safe fish passage at hydropower and irrigation infrastructure. *Marine and Freshwater Research*, 70, 1503-1512.
- Neitzel, D. A., Dauble, D. D., Čada, G. F., Richmond, M. C., Guensch, G. R., Mueller, R. P., Abernethy, C. S. & Amidan, B. G. 2004. Survival Estimates for Juvenile Fish Subjected to a Laboratory-Generated Shear Environment. *Transactions of the American Fisheries Society*, 133, 8.
- Neitzel, D. A., Richmond, M. C., Dauble, D. D., Mueller, R. P., Moursund, R. A., Abernethy, C. S. & Guensch, G. R. 2000. Laboratory studies on the effects of shear on fish. Pacific Northwest National Lab.(PNNL), Richland, WA (United States).
- Nelson, J. S., Grande, T. C. & Wilson, M. V. 2016. *Fishes of the World*, John Wiley & Sons.
- Noga, E. J. 2000. Skin ulcers in fish: Pfiesteria and other etiologies. *Toxicologic Pathology*, 28, 807-823.
- Payne, B. S., Killgore, K. J. & Miller, A. C. 1990. *Mortality of yolk-sac larvae of paddlefish entrained in high-velocity water currents*, Mississippi Academy of Sciences.
- Pflugrath, B. 2017. *Quantifying Stressors and Predicting Injury and Mortality in Fish Passing Downstream Through Weirs and Turbines*. Doctor of Philosophy, University of New South Wales.
- Pflugrath, B. D., Boys, C. A. & Cathers, B. 2018. Predicting hydraulic structure-induced barotrauma in Australian fish species. *Marine and Freshwater Research*, 69(12), 1954-1961.
- Pflugrath, B. D., Boys, C. A. & Fowler, A. C. in prep-a. Preliminary testing suggests high susceptibility to injury for Macquarie perch exposed to rapid decompression.

- Pflugrath, B. D., Brown, R. S. & Carlson, T. J. 2012. Maximum neutral buoyancy depth of juvenile Chinook salmon: implications for survival during hydroturbine passage. *Transactions of the American Fisheries Society*, 141, 520-525.
- Pflugrath, B. D., Brown, R. S. & Dowell, F. E. 2020a. Using transparent fish to observe barotrauma associated with downstream passage through turbines. *River Research and Applications*.
- Pflugrath, B. D., Engbrecht, K., Beirão, B. V., Mccann, E. L., Stephenson, J. R. & Colotelo, A. H. in prep-b. The Susceptibility of Bluegill and Largemouth bass to Rapid Decompression Exposure Associated with Simulated Hydroturbine Passage.
- Pflugrath, B. D., Harnish, R., Rhode, B., Beirao, B., Engbrecht, K., Stephenson, J. R. & Colotelo, A. H. 2019. American eel state of buoyancy and barotrauma susceptibility associated with hydroturbine passage. *Knowledge & Management of Aquatic Ecosystems*, 20.
- Pflugrath, B. D., Harnish, R. A., Rhode, B., Engbrecht, K., Beirão, B., Mueller, R. P., Mccann, E. L., Stephenson, J. R. & Colotelo, A. H. 2020b. The Susceptibility of Juvenile American Shad to Rapid Decompression and Fluid Shear Exposure Associated with Simulated Hydroturbine Passage. *Water*, 12, 586.
- Pflugrath, B. D., Mueller, R. P., Engbrecht, K. & Colotelo, A. H. in prep-c. American eel resilience to fluid shear associated with passage through hydroturbines.
- Pracheil, B. M., Derolph, C. R., Schramm, M. P. & Bevelhimer, M. S. 2016a. A fish-eye view of riverine hydropower systems: the current understanding of the biological response to turbine passage. *Reviews in Fish Biology and Fisheries*, 26, 153-167.
- Pracheil, B. M., Mcmanamay, R. A., Bevelhimer, M. S., Derolph, C. R. & Čada, G. F. 2016b. A traits-based approach for prioritizing species for monitoring and surrogacy selection. *Endangered Species Research*, 31, 243-258.
- Pracheil, B. M., Mestl, G. E. & Pegg, M. A. 2014. Movement through dams facilitates population connectivity in a large river. *River Research and Applications*, 31, 517-525.
- Richmond, M. C., Serkowski, J. A., Ebner, L. L., Sick, M., Brown, R. S. & Carlson, T. J. 2014a. Quantifying barotrauma risk to juvenile fish during hydro-turbine passage. *Fisheries Research*, 154, 152-164.
- Richmond, M. C., Serkowski, J. A., Rakowski, C., Strickler, B., Weisbeck, M. & Dotson, C. 2014b. Computational tools to assess turbine biological performance. *Hydro Review*, 33(6), 10.
- Ritz, C., Baty, F., Streibig, J. C. & Gerhard, D. 2015. Dose-response analysis using R. *PLOS ONE*, 10, 1-13.
- Roberts, C. D. 1993. Comparative morphology of spined scales and their phylogenetic significance in the Teleostei. *Bulletin of marine science*, 52, 60-113.
- Ryon, M. G., Cada, G. F. & Smith, J. G. 2004. Further Tests of Changes in Fish Escape Behavior Resulting from Sublethal Stresses Associated with Hydroelectric Turbine Passage. Oak.
- Salalila, A., Deng, Z. D., Martinez, J. J., Lu, J. & Baumgartner, L. J. 2019. Evaluation of a fish-friendly self-cleaning horizontal irrigation screen using autonomous sensors. *Marine and Freshwater Research*, 70, 1274-1283.
- Saylor, R., Bevelhimer, M., Fortner, A. M. & Pracheil, B. M. 2017. Species-specific Susceptibility to Scale Loss: Using Simulated Shear to Understand Among Species Differences in Turbine Passage Injury. Oak Ridge National Lab.(ORNL), Oak Ridge, TN (United States).
- Saylor, R., Fortner, A. & Bevelhimer, M. 2019. Quantifying mortality and injury susceptibility for two morphologically disparate fishes exposed to simulated turbine blade strike. *Hydrobiologia*, 842, 55-75.
- Saylor, R., Sterling, D., Bevelhimer, M. & Pracheil, B. 2020. Within and Among Fish Species Differences in Simulated Turbine Blade Strike Mortality : Limits on the Use of Surrogacy for Untested Species. *Water*, 12, 1-27.
- Schofield, P. J. 2005. *Foreign nonindigenous carps and minnows (Cyprinidae) in the United States: a guide to their identification, distribution, and biology*, US Department of the Interior, US Geological Survey.
- Sifa, L. & Mathias, J. 1987. The critical period of high mortality of larvae fish—a discussion based on current research. *Chinese Journal of Oceanology and Limnology*, 5, 80-96.
- Silva, A. T., Lucas, M. C., Castro-Santos, T., Katopodis, C., Baumgartner, L. J., Thiem, J. D., Aarestrup, K., Pompeu, P. S., O'brien, G. C., Braun, D. C., Burnett, N. J., Zhu, D. Z., Fjeldstad, H. P., Forseth, T., Rajaratnam, N., Williams,

- J. G. & Cooke, S. J. 2018a. The future of fish passage science, engineering, and practice. *Fish and Fisheries*, 19, 340-362.
- Silva, L. G., Beirão, B. V., Falcão, R. C., De Castro, A. L. & Dias, E. W. 2018b. It'sa catfish! Novel approaches are needed to study the effects of rapid decompression on benthic species. *Marine and Freshwater Research*, 69, 1922-1933.
- Statzner, B. & Müller, R. 1989. Standard hemispheres as indicators of flow characteristics in lotic benthos research. *Freshwater Biology*, 21, 445-459.
- Stephenson, J. R., Gingerich, A. J., Brown, R. S., Pflugrath, B. D., Deng, Z., Carlson, T. J., Langeslay, M. J., Ahmann, M. L., Johnson, R. L. & Seaburg, A. G. 2010. Assessing barotrauma in neutrally and negatively buoyant juvenile salmonids exposed to simulated hydro-turbine passage using a mobile aquatic barotrauma laboratory. *Fisheries Research*, 106, 271-278.
- Tiwary, B. K., Kirubakaran, R. & Ray, A. K. 2004. The biology of triploid fish. *Reviews in Fish Biology and Fisheries*, 14, 391-402.
- Tsvetkov, V. I., Pavlov, D. S. & Nezdoliy, V. K. 1972. Changes in hydrostatic pressure lethal to the young of some freshwater fish. *Journal of Ichthyology*, 307-318.
- Turnpenny, A., Clough, S., Hanson, K., Ramsay, R. & Mcewan, D. 2000. *Risk assessment for fish passage through small, low-head turbines*, Atomic Energy Research Establishment, Energy Technology Support Unit, New
- Turnpenny, A. W., Davis, M., Fleming, J. & Davies, J. 1992. Experimental Studies Relating to the Passage of Fish and Shrimps Through Tidal Power Turbines.
- Turnpenny, A. W. H. 1998. Mechanisms of Fish Damage in Low Head Turbines: An Experimental Appraisal. *In*: JUNGWIRTH, M., SCHMUTZ, S. & WEISS, S. (eds.) 1 ed. Malden: Blackwell Publishing Ltd.
- Uria-Martinez, R., Johnson, M. M., O'connor, P. W., Samu, N. M., Witt, A. M., Battey, H., Welch, T., Bonnet, M. & Wagoner, S. 2018. 2017 Hydropower Market Report. Oak Ridge.
- Wainwright, D. K. & Lauder, G. V. 2016. Three-dimensional analysis of scale morphology in bluegill sunfish, *Lepomis macrochirus*. *Zoology*, 119, 182-195.
- Webb, P. W. 1978. Fast-Start Performance and Body Form in Seven Species of Teleost Fish. *Journal of Experimental Biology*, 74, 211-226.

Appendix A – Experimental Apparatuses

Apparatuses for blade strike testing, rapid decompression testing, and fluid shear testing are described in the following sections.

A.1 BLADE STRIKE TESTING APPARATUSES

Apparatuses for blade strike testing have been developed by the National Power Marine and Freshwater Biology Unit, the Electric Power Research Institute (EPRI), and Oak Ridge National Laboratory (ORNL), as described below.

A.1.1 NATIONAL POWER MARINE AND FRESHWATER BIOLOGY UNIT BLADE STRIKE TESTING SYSTEM

The first apparatus designed to simulate blade strike impact was used by Turnpenny et al. (1992) and enabled controlled exposure of blade strike impact for individual fish (Figure A.1). The setup included a linear platform and used stored energy in springs to power blade movement along guide rails through an open, water-filled flume to impact fish. Trials also included blades of different shapes, leading-edge thicknesses between 10 to 100 mm, and the realized strike velocity was 5 to 7 m s⁻¹ (Turnpenny et al. 1992; Turnpenny 1998). The blade moved along a linear trajectory from left to right and the impact was viewed through an observation window on the left side. All impacts were video-recorded for later analysis and fish were held in place along the mid-sagittal plane with their snouts pointing toward the viewing window with a fine thread, though it was not possible to control fish orientation completely during impact (Bevelhimer et al. 2017). In this orientation, the blade would make contact with the fish along the frontal plane (Table A.1); i.e., a fish divided into a dorsal and ventral half, which was considered a positive strike (Turnpenny et al. 1992). Two different trial types were performed: (1) mortality estimates for live brown trout, European eel, and European bass, and (2) probability of strike trials on freshly euthanized fish including the previous species as well as rainbow trout and sand smelt (Table A.1). Mortality estimates were made during a 1 hr observation period after blade strike impact to measure instantaneous mortality. No biological response models are available for this work because there were too few treatment groups to properly model mortality.

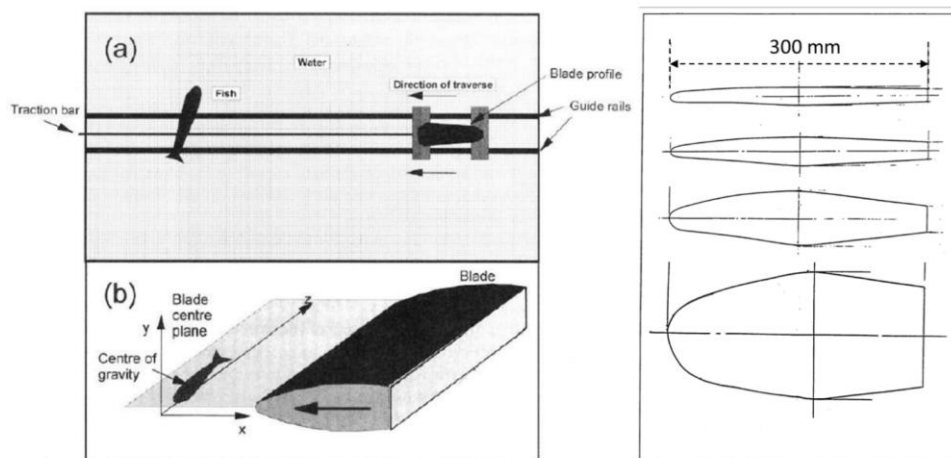


Figure A.1. Blade strike apparatus used by Turnpenny et al. (1992) and also described by Turnpenny (1998). The left panel includes a diagram that highlights fish location and orientation relative to the blade that is guided along tracks. The right panel includes diagram schematics of the blades tested in this study with a reference length of 300 mm. (Original Source: Turnpenny 1998.)

Table A.1. Review of simulated blade strike laboratory experiments on all live fishes published to date between 1992 and 2020. Models include different strike locations [including head (H), mid-body (M), and tail (T)], different impact angles, (including 90°, 45°, and 135°), and fish orientation [including dorsal (D), lateral (L), and Ventral (V)]. Families are arranged according to phylogeny, while species are in alphabetical order within each family. Variable questions are answered yes with a check mark. External assessments include visual inspection of fish but do not include internal necropsy in their protocol. Fish lengths are reported as total lengths unless marked otherwise.

Family	Species	1 hr Mortality	Functional Mortality	Latent Mortality	External Assessment	Internal Necropsy	Fish Length (cm)	Blade Width (mm)	Realized Blade Strike Velocity (m s ⁻¹)	Strike Location			Impact Angle			Fish Orientation			Source
										H	M	T	90°	45°	135°	D	L	V	
Acipenseridae	White sturgeon (<i>Acipenser transmontanus</i>)	✓		✓	✓		10.5–16.8 ^(a)	50, 100	10.7, 12.2	✓	✓	✓	✓			✓	✓	✓	EPRI 2008
		✓		✓	✓		20.6–21.7 ^(a)	25, 50	12.0, 12.2	✓	✓	✓	✓	✓		✓	✓	✓	EPRI 2011
Polydontidae	American paddlefish (<i>Polyodon spathula</i>)	✓	✓		✓	✓	5.10–10.3 ^(b)	26, 52	5.3–9.4	✓	✓		✓			✓	✓		ORNL unpublished
Anguillidae	European eel (<i>Anguilla anguilla</i>)			✓	✓	✓	32.0–70.0 ^(c)	10, 20, 40 & 100	5.2–7.1	✓	✓	✓	✓				✓		Turnpenny et al. 1992
	American eel (<i>Anguilla rostrata</i>)	✓		✓	✓		28.5–79.5 ^(a)	25, 50 & 150	10.7, 12.2	✓	✓	✓	✓			✓	✓	✓	EPRI 2008
		✓	✓		✓	✓	53.9	19, 26	12.0, 13.6	✓	✓		✓			✓	✓	✓	Saylor et al. 2019
Clupeidae	American shad (<i>Alosa sapidissima</i>)	✓	✓		✓	✓	8.5	52	7.1–9.7		✓		✓				✓		Saylor et al. 2020
	Blueback herring (<i>Alosa aestivalis</i>)	✓	✓		✓	✓	7.2	26, 52, 76	7.1–9.7		✓		✓				✓		Saylor et al. 2020

Family	Species	1 hr Mortality	Functional Mortality	Latent Mortality	External Assessment	Internal Necropsy	Fish Length (cm)	Blade Width (mm)	Realized Blade Strike Velocity (m s ⁻¹)	Strike Location			Impact Angle			Fish Orientation			Source	
										H	M	T	90°	45°	135°	D	L	V		
Clupeidae	Atlantic herring (<i>Clupea harengus</i>)				✓	✓	7.0 ^(c)	10, 20, 40 & 100	5.2–7.1		✓		✓				✓		Turnpenny et al. 1992	
	American gizzard shad (<i>Dorosoma cepedianum</i>)	✓	✓		✓	✓	19.3	26, 52	7.4–8.3	✓	✓	✓	✓	✓	✓	✓	✓	✓	Bevelhimer et al. 2019	
		✓	✓		✓	✓	16.0	52	4.7–8.1		✓		✓					✓	Saylor et al. 2020	
Salmonidae	Rainbow trout (<i>Oncorhynchus mykiss</i>)				✓	✓	50.2 – 61.6 ^(c)	10, 20, 40 & 100	5.2–7.1		✓		✓				✓		Turnpenny et al. 1992	
		✓		✓	✓		10.7 – 26.4 ^(a)	10, 25, 50, 100 & 150	3.0–12.2	✓	✓	✓	✓			✓	✓	✓	EPRI 2008	
		✓		✓	✓		12.7 – 25.5 ^(a)	25, 50 & 100	7.3, 12.2	✓	✓	✓	✓	✓			✓	✓	EPRI 2008	
		✓	✓		✓	✓	17.4	26, 52	8.0, 8.3	✓	✓	✓	✓					✓		Bevelhimer et al. 2019
		✓	✓		✓	✓	11.4, 25.8	26, 52	5.5–9.4	✓	✓		✓		✓	✓	✓	✓	✓	Saylor et al. 2020
		✓		✓	✓	✓	11.0 – 23.6 ^(a)	100	10.0	✓	✓	✓	✓	✓				✓		Amaral et al. 2020
	Atlantic salmon (<i>Salmo salar</i>)				✓	✓	15.0 – 100.0 ^(c)	10, 20, 40 & 100	5.2–7.1		✓		✓					✓		Turnpenny et al. 1992
	Brown trout (<i>Salmo trutta</i>)			✓	✓	✓	18.0 – 23.8 ^(c)	10, 20, 40 & 100	5.2–7.1	✓	✓	✓	✓					✓		Turnpenny et al. 1992
Brook trout (<i>Salvelinus fontinalis</i>)	✓	✓		✓	✓	24.2	52	4.9–7.3	✓	✓		✓		✓	✓	✓	✓		Saylor et al. 2020	

Family	Species	1 hr Mortality	Functional Mortality	Latent Mortality	External Assessment	Internal Necropsy	Fish Length (cm)	Blade Width (mm)	Realized Blade Strike Velocity (m s ⁻¹)	Strike Location			Impact Angle			Fish Orientation			Source
										H	M	T	90°	45°	135°	D	L	V	
Gadidae	Whiting (<i>Merlangius merlangius</i>)				✓	✓	20.0 ^(c)	10, 20, 40 & 100	5.2–7.1		✓		✓				✓		Turnpenny et al. 1992
Atherinidae	Sand smelt (<i>Atherina presbyter</i>)				✓	✓	6.1 – 9.0 ^(c)	10, 20, 40 & 100	5.2–7.1		✓		✓				✓		Turnpenny et al. 1992
Moronidae	European bass (<i>Dicentrarchus labrax</i>)			✓	✓	✓	15.0 – 38.0 ^(c)	10, 20, 40 & 100	5.2–7.1	✓	✓	✓	✓				✓		Turnpenny et al. 1992
	Hybrid striped bass (<i>Morone saxatilis</i> × <i>M. chrysops</i>)	✓	✓		✓	✓	17.1	26, 52	6.4–10.1	✓	✓	✓	✓	✓	✓	✓	✓	✓	Bevelhimer et al. 2019
Centrarchidae	Bluegill (<i>Lepomis macrochirus</i>)	✓	✓		✓	✓	11.8, 16.0 & 17.5	26, 52	4.7–9.1	✓	✓	✓	✓	✓	✓	✓	✓	✓	Saylor et al. 2019

^(a) Fork length from mid-eye

^(b) Fork length

^(c) Standard length

A.1.2 ELECTRIC POWER RESEARCH INSTITUTE

Work at Alden Laboratories was similar to Turnpenny et al. (1992) work, but their system used larger blades and could attain faster impact velocities. Like Turnpenny et al. (1992), the system employed by Alden used blades that moved in a linear trajectory through a water-filled flume until they impacted fish at the opposite end (Figure A.2). Early work tested elliptical and semicircular leading-edge shapes, but most studies focused on semicircular blades with leading-edge thicknesses between 10 to 150 mm for live fish trials. The blade was attached to a carriage that moved along a track on the back wall of the flume, but, unlike the system used by Turnpenny et al. (1992), the blade was moved by a motorized belt-driven mechanism (Bevelhimer et al. 2017). The new modification allowed the thickest, 100 and 150 mm blades to achieve velocities $>7.0 \text{ m s}^{-1}$ and provided a blade strike velocity range of 3.0 to 12.2 m s^{-1} (EPRI 2008, 2011; Amaral et al. 2020). This study also used view windows and high-speed videography to film impacts for later visual inspection to confirm exact strike impact characteristics. Fish were held in place using monofilament line and Styrofoam braces that were designed to allow the fish to move freely after contact with the blade. Each fish was held in a vertical position so that the body was oriented, head-up with the ventral surface pointing toward the viewing window perpendicular to the blade. The exact position was also difficult to maintain using this method and, in some cases, led to mortal injuries as a result of interactions with the monofilament line (EPRI 2008). In all studies using this apparatus, only live fish were tested including rainbow trout, white sturgeon, and American eel (Table A.1; EPRI 2008, 2011; Amaral et al. 2020). Both instantaneous (1 hr) and delayed (96 hr) mortality were estimated for each treatment group and for all species tested. Adjusted mortality rates were reported for each species that included delayed mortality and were adjusted for control deaths if observed (EPRI 2008). Biological response models were based on adjusted mortality rates, grouped according to the fish body length to blade thickness ratio (L/t ratio), and formed linear relationships with blade strike velocity.

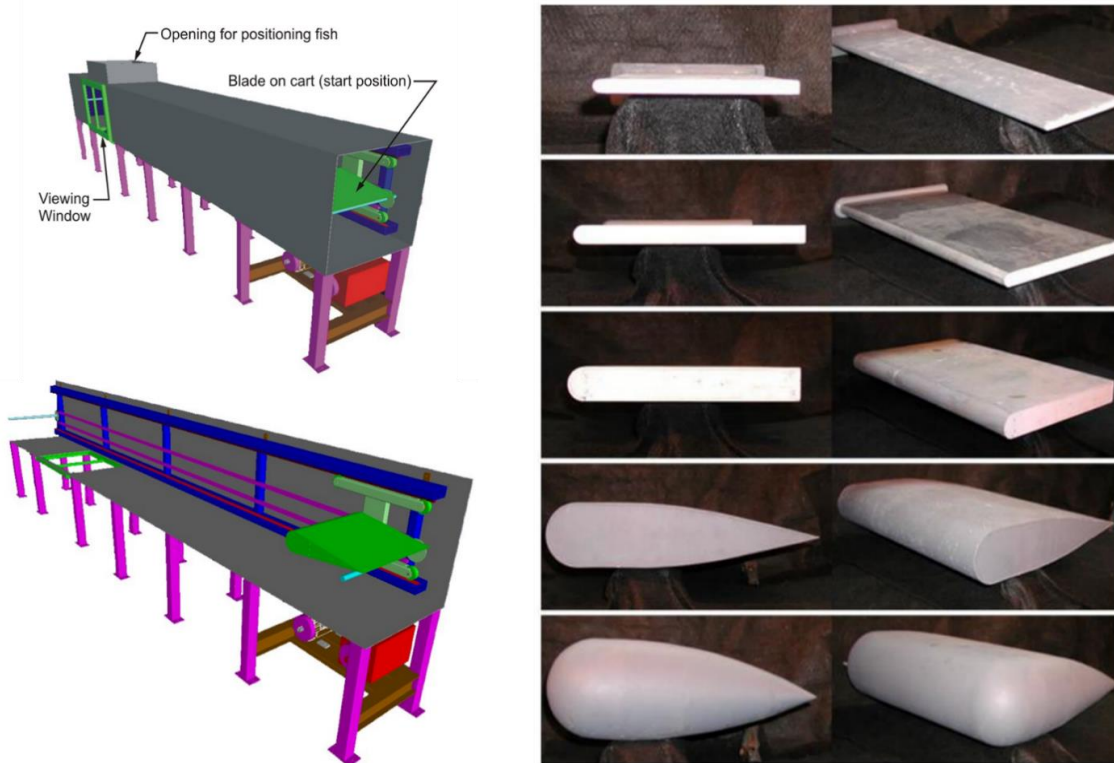


Figure A.2. Blade strike apparatus used by Alden Laboratories and reported by EPRI (2008, 2011) and Amaral et al. (2020). The left panel includes a labeled diagram of major features including the viewing window and guide rail that held and moved the blade. The right panel is a compilation of pictures showing blades of varying leading-edge thicknesses. (Original Source: EPRI 2008).

A.1.3 OAK RIDGE NATIONAL LABORATORY

The apparatus used for ORNL laboratory experiments was designed based on insights gained from all previous work. These insights enabled a reduction of the overall size of the blade simulation system and increased control of fish positioning. This system also relied on stored energy from a single spring that was loaded and released using a safety release trigger. The spring assembly was attached to the blade arm that extends down into a 0.324 m³ stainless-steel tank that could hold up to 320 L of water (Figure A.3). Turbine blades in this system were made of aluminum, had a semicircular cross section, and also had a blade shaft that extended upward from the blade itself. The blade shaft slid inside the blade arm where it could be securely fastened. The blade was “loaded” by extending the spring connected to the blade arm and when it was triggered, it moved in an arc toward the front side of the tank where it would hit a rubber stopper and come to rest. Blades with leading-edge thicknesses of 19, 26, 52, and 76 mm were used, although most of these trials used the 26 and 52 mm blades. Blade strike velocity ranged from 5.0 to 15.0 m s⁻¹, but the exact velocity range generated was dependent on blade leading-edge thickness. Velocity was changed by adjusting the tension on the spring using the bolt tensioner or changing the slot position where the spring attached to the blade arm. In addition, up to three pieces of flexible tubing could be secured around the blade arm to reduce blade strike velocities. Standard curves were created for 26, 52, and 78 mm blades according to bolt setting, slot position, and average strike velocity for quick reference (Figure A.4). Fish

were held in place on two mounting brackets that hung down into the tank along the front wall and were angled such that the blade would make contact with the fish body perpendicular to its mid-sagittal axis. Fish were secured to the brackets using flexible tubing that gently held the fish in place while still allowing the fish to move freely once struck. This system allowed for quick modifications to the brackets to account for the angle of strike and to accommodate each species. Impacts on the fish were filmed through a viewing port using high-speed videography at 1,000 frames per second to confirm exact strike conditions and estimate blade strike

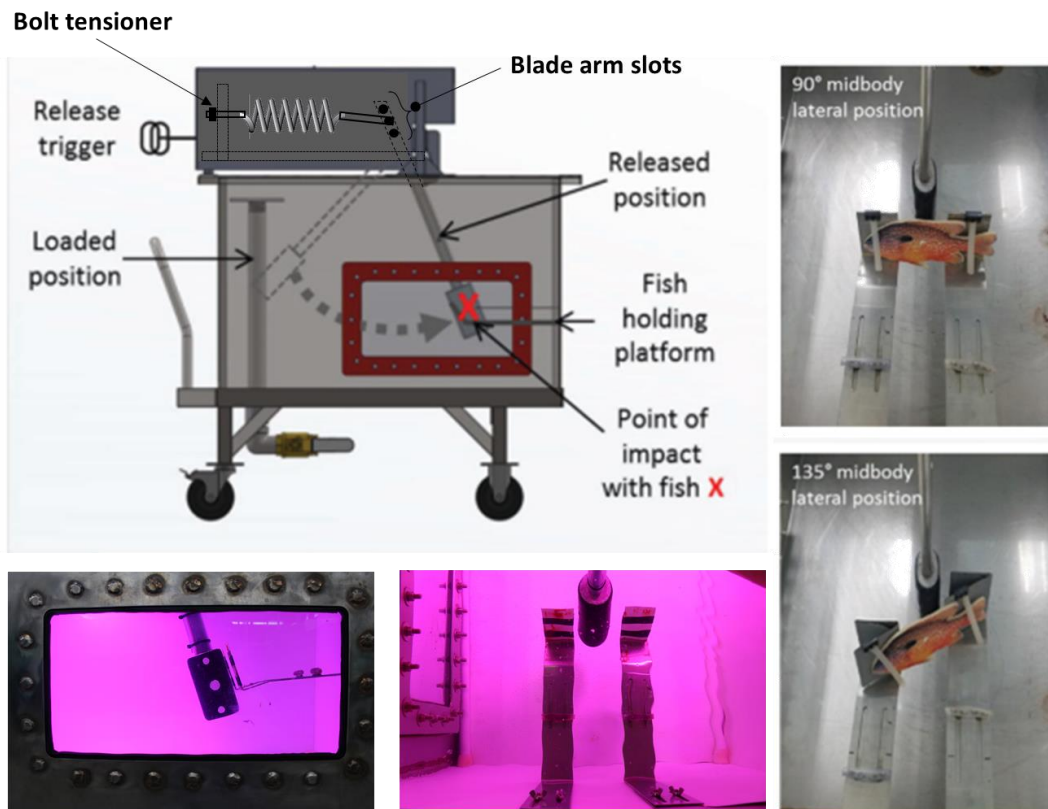


Figure A.3. Blade strike apparatus used by researchers at ORNL and reported by Bevelhimer (2019) and Saylor et al. (2019, 2020). The top-left panel is a diagram showing the spring assembly, test tank, and mobile carriage that enabled the system to be moved as needed. The bottom left pane shows the viewing port; the middle panel is a top-down look at the brackets designed to hold fish and the relative location of approach for the blade. The right-most panels also showcase the holding brackets that secured the fish and also allowed for easy modification of the impact angle.

velocity. To date, live tests have been conducted on nine species including paddlefish, American eel, gizzard shad, American shad, blueback herring, rainbow trout, brook trout, hybrid striped bass, and bluegill sunfish (Table A.1; Bevelhimer et al. 2019; Saylor et al. 2019, 2020; and ORNL unpublished data). We estimated instantaneous mortality rates but also created a combined mortality metric that incorporated insights from internal necropsies. Biological response models were reported as rates of combined mortality versus blade strike velocity and were published for every species except paddlefish.

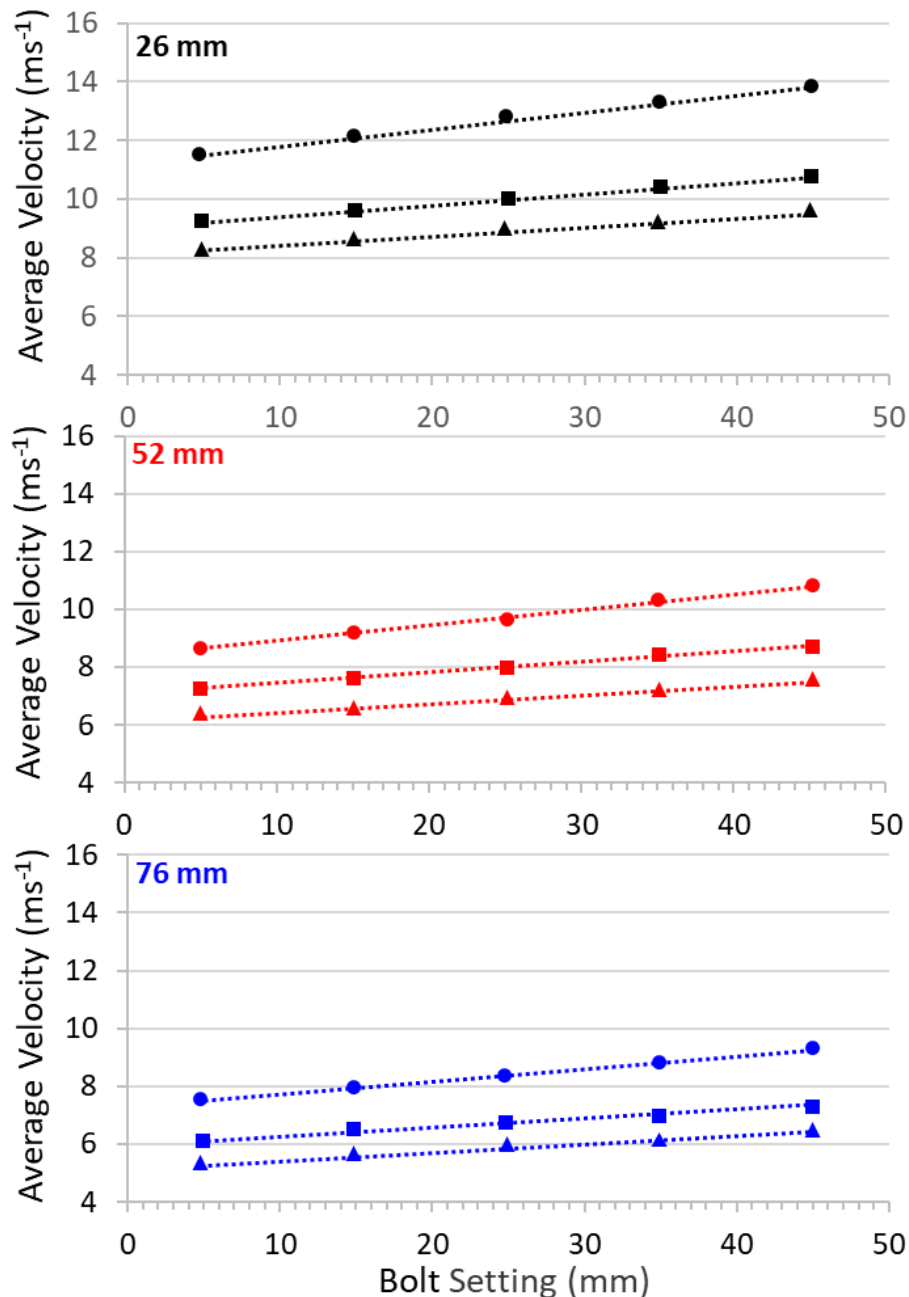


Figure A.4. Standard curves of average velocity ($m s^{-1}$) against bolt setting (mm) for each of three blade leading-edge thicknesses (26, 52, and 76 mm) used in ORNL laboratory studies of blade strike impact. Shapes correspond to different slot locations (middle or top) and/or springs (original or new) used to generate sufficient velocity. Triangles refer the original spring in the middle slot, squares represent the original spring in the top slot, and circles represent the new spring in the top slot.

A.2 RAPID DECOMPRESSION TESTING APPARATUSES

Several apparatuses have been designed to simulate pressures that fish may experience during turbine passage, including both pressurizations associated with the draft tube and rapid decompression as fish pass the turbine runner. Many of the apparatuses also allow for an acclimation period, during which a steady pressure is maintained and flow-through water is passed through the system to maintain water quality parameters such as temperature and total dissolved gas (TDG). During this period, fish can regulate their buoyancy by filling or removing gas from their swim bladder.

A.2.1 UNIVERSITY OF BRITISH COLUMBIA

A pressure system was developed by the International Pacific Salmon Fisheries Commission for studies to be conducted at the University of British Columbia (Harvey 1963). The purpose of this pressure system was to investigate the effects of pressure and pressure changes when sockeye salmon make vertical movements. Some of these effects are tolerance to positive pressure, decompression, filling of the swim bladder, and maintenance of neutral buoyancy (Harvey 1963).

The pressure vessel consisted of a steel cylinder 91.4 cm long and 30.5 cm in diameter (Figure A.5). Metallic end plates were fitted with 15.2 cm diameter plastic ports to allow observation inside the chamber. The internal space of the chamber was accessed by a removable bolted flange end plate. A smaller vacuum tank was attached to the top of this vessel to perform testing of pressure below atmospheric. When in operation, the cylinder had a capacity of 67 liters of water (Harvey 1963).

Pressure was applied within the chamber by means of a centrifugal pump. The pressure was regulated by adjusting valves. A bypass valve (range 0 to 2,070 kPa) safely relieved pressure in the event of over-pressurization. To achieve pressure below atmospheric pressure a smaller cylinder connected to the top of the pressure chamber induced a vacuum using a second pump. A range of subatmospheric pressures could be achieved, from near vapor pressure to surface pressure. Pressure within the chamber was measured by means of a pressure transducer electrically connected to a recording oscillograph (range of 0 to 3450 kPa; Harvey 1963).

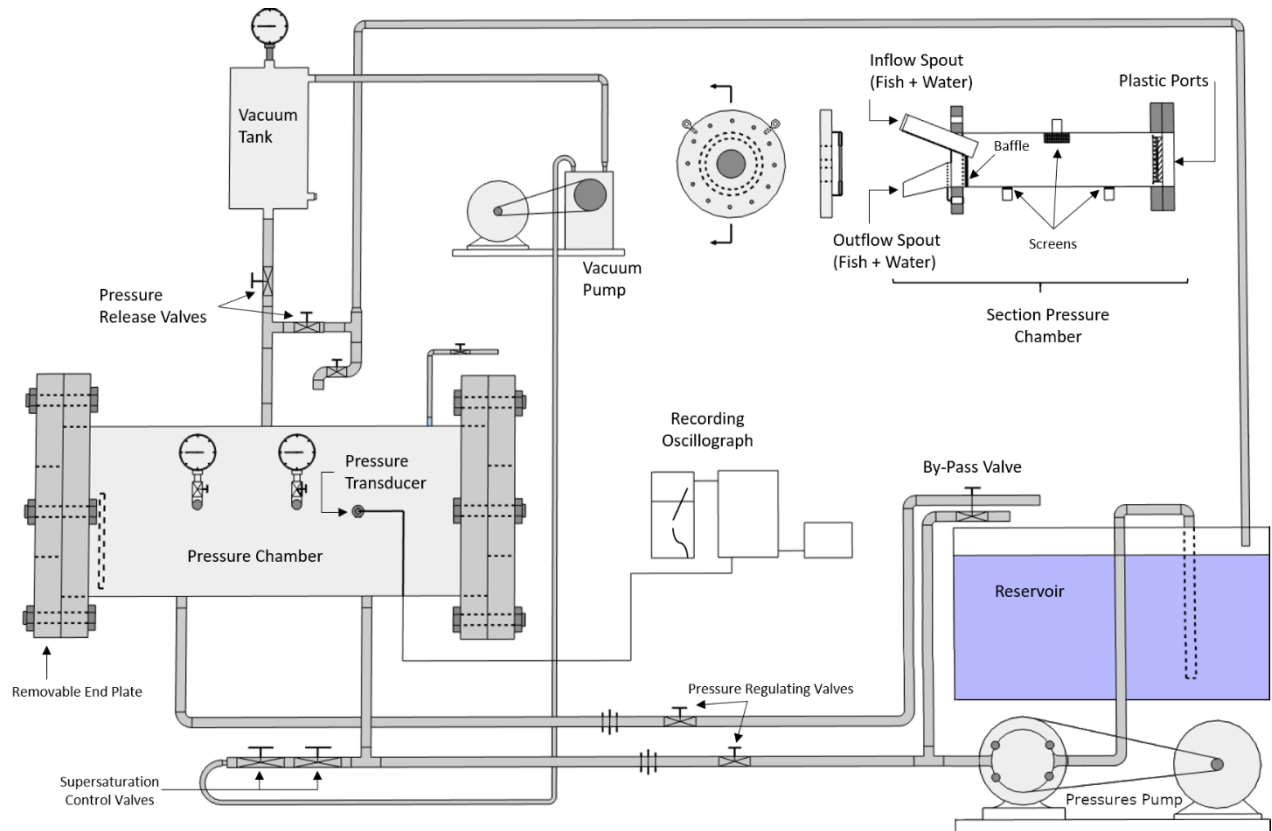


Figure A.5. Pressure chamber schematic for exposing fish to a range of pressure scenarios. Recreated from Harvey (1963).

Pressure capabilities within the chamber could range between atmospheric pressure and 2.070 kPa in intervals of 0.02, 0.2, 2.0, 20, and 200 s. A rate of pressure change of 103,420, 10,340, 1,034; 103, and 10 kPa s⁻¹ could be achieved. TDG in the chamber could be manipulated by pumping air under pressure into the bottom of the chamber. The TDG could be regulated to 140 percent of air saturation (Harvey 1963). A standard test consisted of fish being introduced into the chamber and the pressure being raised to 345 kPa from atmospheric in 50 s for a period of 5 min. The pressure was then released in 0.02 s to a 3.1 kPa maintained for 1.0 s (Harvey 1963).

A.2.2 UNION OF SOVIET SOCIALIST REPUBLICS ACADEMY OF SCIENCES

A pressure system was developed by the Union of Soviet Socialist Republics Academy of Sciences, in Moscow, for studies to be conducted at the Laboratory of the Orientation and Signaling Systems of Lower Vertebrates. The purpose of this pressure system was to investigate the effects of hydrostatic pressure change (magnitude and rate) associated with hydropower turbines on juvenile fish species (Tsvetkov et al. 1972). In addition, this system highlighted the toxic effects of high concentrations of dissolved gases on fishes.

The pressure vessel consisted of a glass cylinder with removable metal caps that could be bolted in place on each end (Tsvetkov et al. 1972). The dimensions of the vessel were not reported but, based on the image, the cylinder is estimated to be approximately 60 cm in length with a diameter of 10 to 15 cm. Based on these dimensions, the volume of the cylinder would be 4.5 to 10.5 L. Pressure was applied within the vessel using a centrifugal pump (up to 700 kPa). The pressure was regulated by opening the drain valve or

by piercing a rubber bung with a syringe needle. Pressure in this apparatus reduced at a rate of approximately 10 to 600 kPa s⁻¹. The rate of pressure reduction was calculated by monitoring a pressure gauge that was installed on the top flange of the vessel and recording the dissipation time with a stopwatch (Tsvetkov et al. 1972).

A standard test consisted of fish being introduced into the chamber, which was then pressurized to approximately 100 to 600 kPa over a period of 2 to 5 min. Fish were then allowed to acclimate for an extended period, sometimes up to a few days. The pressure was then released to surface pressure at various rates ranging from 10 to 1 kPa s⁻¹ (Tsvetkov et al. 1972).

A.2.3 CALIFORNIA POLYTECHNIC STATE UNIVERSITY

A grant from California Polytechnic State University and California Fish and Game funded the construction of a pressure system that was built to investigate the effects of rapid decompression from deep water angling on largemouth bass (Knable and Feathers 1983). The 853.1 L pressure vessel consisted of a 6.4 mm thick steel cylinder 200 cm long and 70 cm in diameter with ends composed of 4.8 mm steel. The cylinder was fitted with three removable ports: one 29.9 cm diameter by 3.2 cm thick plexiglass window for chamber observation; one 31 cm diameter by 12.7 mm thick solid steel plate access port designed for rapid entry to the internal space of the chamber; and a third access port of unreported dimensions installed in the center of the back of the chamber. When all ports were removed the water remaining in the tank was approximately 21.8 cm deep. To facilitate drainage of the chamber a 5.0 cm gate valve was installed on the underside of the tank.

Pressure was applied within the chamber using a vane-type roller pump. Pressure was regulated by adjusting a 19 mm relief valve installed on the outlet of the tank and a safety valve was set at 490 kPa to relieve pressure in the event of over-pressurization. The chamber was designed to operate at a range between atmospheric pressure and 520 kPa and was unable to produce subatmospheric pressure scenarios. Therefore, fish were able to be depth acclimated and then decompressed to surface pressure. Pressure within the chamber was measured by means of a pressure gauge (range of 0 to 690 kPa; Knable and Feathers 1983). TDG could also be monitored in the chamber (YSI model 57 oxygen meter), but could not be manipulated by this system (Knable and Feathers 1983).

A standard test consisted of fish being introduced into the chamber and the pressure being increased daily in 35 kPa increments to allow acclimation of the fish. The pressure was then released at a rate of 10 to 600 kPa s⁻¹ to surface pressure conditions (Knable and Feathers 1983).

A.2.4 NATIONAL POWER MARINE AND FRESHWATER BIOLOGY UNIT DECOMPRESSION TESTING SYSTEM

The National Power (United Kingdom) and the Energy Technology Support Unit (United Kingdom) jointly funded the construction of a pressure system to investigate and define hydraulic conditions expected to occur within low head hydro-turbines and their effects on fish passage (Turnpenny et al. 1992). The pressure vessel consisted of a 140 L stainless-steel chamber that was pressure rated from 0 to 500 kPa (Figure A.6). An accessory plexiglass observation chamber was added to the pressure vessel to allow observation of fish. The internal space of the chamber could be accessed by a removable bolted lid and the accessory viewing chamber could be accessed by a threaded cap (Turnpenny et al. 1992).

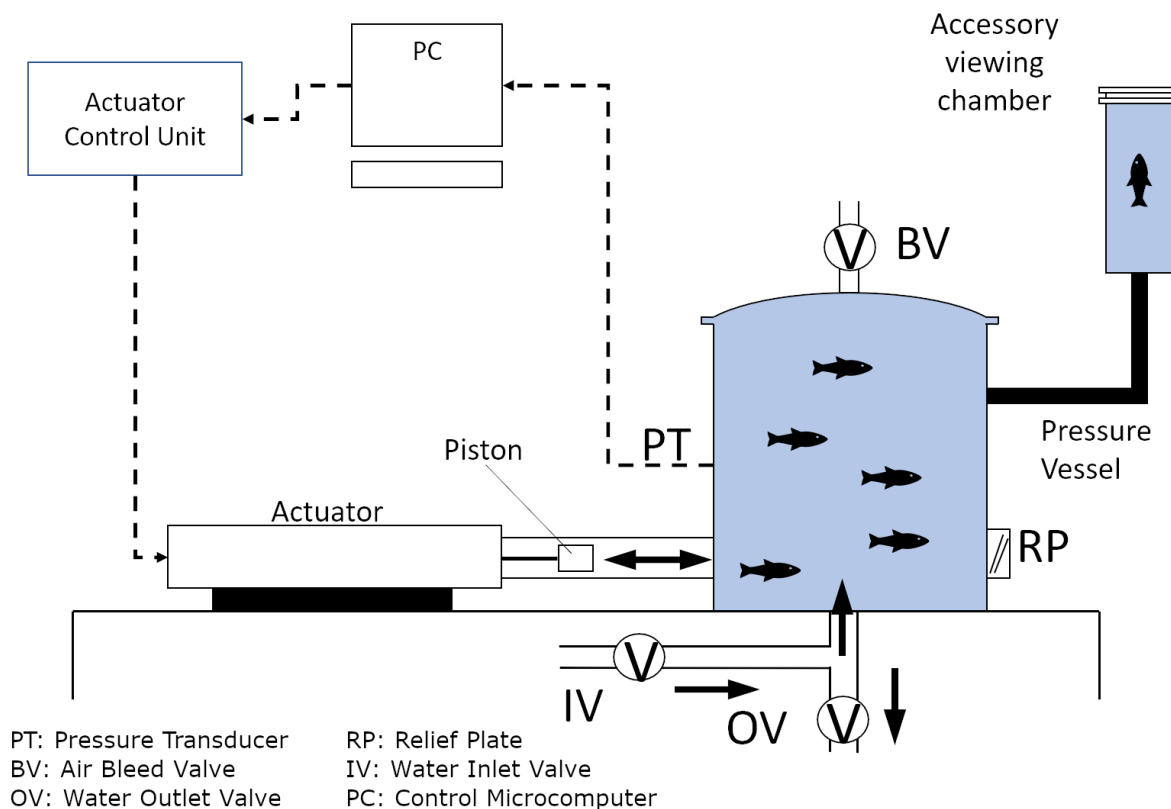


Figure A.6. Configuration of the National Power Marine and Freshwater Biology Unit pressure system. Figure recreated from Turnpenney et al. (1992).

Acclimation pressure was applied within the chamber by means of a centrifugal pump and regulated by adjusting an inlet valve and a bleed valve. Pressure flux within the chamber was adjusted by the movement of a piston (displacement 900 cm³) within a cylinder open at one end into the pressure vessel. Piston movement was achieved using a hydraulic actuator and control unit coupled to a computer data acquisition card. A pressure transducer was attached to the pressure vessel and wired to the data acquisition card. A control program allows the pressure-time series to be defined and stored to generate repeatable patterns of pressure flux. The system can achieve pressure changes from 400 kPa maximum and 10 kPa minimum. The program displays the targeted curve and achieved curve for comparison controlled to within 5% of the target value. A spring-loaded pressure relief plate was set to release pressure at 500 kPa. The system can sustain pressures from total vacuum to ~40 m water depth equivalent (Turnpenney et al. 1992).

A.2.5 PACIFIC NORTHWEST NATIONAL LABORATORY

Two pressure testing systems have been developed and operated at Pacific Northwest National Laboratory (PNNL). The first system was funded by the U.S. Department of Energy's (DOE's) Advanced Hydropower Turbine Systems Program (a predecessor to the Water Power Technologies Office). The purpose of this pressure system (depicted in Figure A.7) was to investigate the effects of rapid decompression associated with hydropower turbine passage and dissolved gas supersaturation (Abernethy et al. 2001). The pressure vessel comprised two separately controlled chambers, each 55 cm long with a diameter of 27.5 cm and a capacity of 34 L. The internal space of each chamber can be accessed via removable end plates (Abernethy et al. 2001).

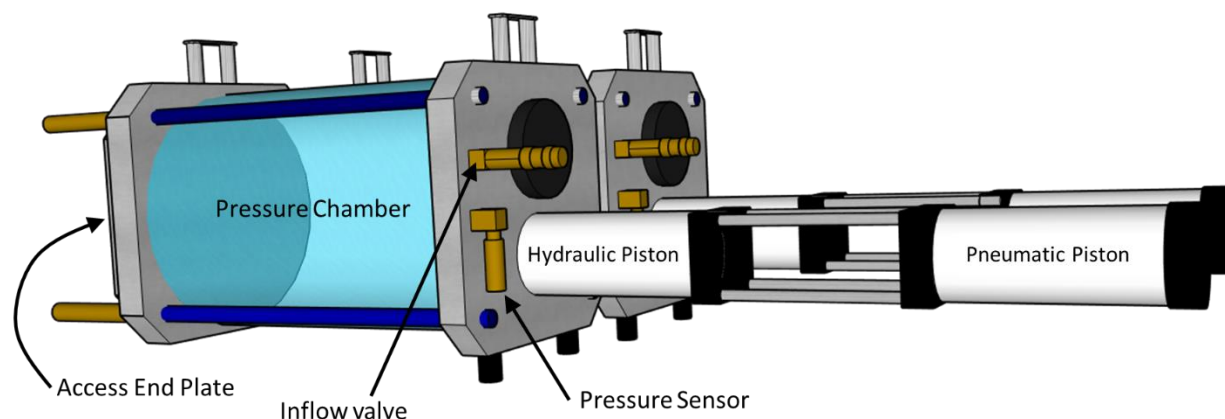


Figure A.7. Diagram of the major components of the pressure system developed by PNNL for the U.S. Department of Energy's Advanced Hydropower Turbine Systems Program to examine the effects of pressure on fish. Not pictured is the outflow valve, which is attached to the access end plate, the pump that connects to the inflow, and the air compressor and valves that control the airflow to the pneumatic piston.

Pressure was applied within the chamber by means of a centrifugal pump during the acclimation phase and regulated by adjusting water exiting gate valve orifices. A computer program with a graphical user interface (GUI) controlled pressure sequences to produce a preprogrammed nadir following a typical Kaplan turbine pressure scenario. The automated program controlled pressure flux (both pressurized or depressurized) within the chamber by adjusting the movement of a pneumatic piston, which in turn was connected to a hydraulic piston open at one end into the pressure vessel (Abernethy et al. 2001). The maximum pressure of the chamber was 30 m of head (≈ 400 kPa) and the pressure could be decompressed to nearly the vapor pressure of water (≈ 2 – 10 kPa) in 0.1 s (Abernethy et al. 2001). In addition, a pressurized packed cell column was used to generate the desired TDG levels within the water during testing (Abernethy et al. 2001).

A standard test consisted of fish being introduced into the chamber and allowed to acclimate in the partially filled chamber for approximately 24 hr. After this time, the chamber was filled and the inflow and outflow valves were sealed in preparation to run the pressure flux program. The system controlled the pneumatic piston to alter the pressure within the chamber following a preprogrammed pressure scenario.

The second, more advanced system was developed by PNNL with funding provided by the U.S. Army Corps of Engineers (USACE) as part of their Turbine Survival Program (Brown et al. 2012a; Stephenson et al. 2010). A fully automated system included four separately computer-controlled aquatic barotrauma chambers intended to investigate the effects of rapid decompression associated with hydropower turbine passage and dissolved gas supersaturation (Brown et al. 2012a).

The pressure vessels had dimensions of 45.7 cm inside diameter and 31.2 cm high, giving an interior volume of 51.2 L. The chambers are made of 3.0 cm thick acrylic glass and are sealed at the top and bottom by 5.1 cm thick aluminum. The internal space of each chamber can be accessed via 30.5 cm diameter removable hatches that are securely dogged down for a tight seal. The chamber is surrounded by an acrylic lens that is flat on all sides. The void between the lens and the chamber is filled with water, allowing for non-distorted viewing (Stephenson et al. 2010)

Pressure is applied within the chambers by means of a centrifugal pump and controlled by a computer program with a GUI. The user can adjust the flow rate (± 0.95 L min^{-1} of target) through the GUI allowing the chambers to hold a constant acclimation pressure indefinitely while maintaining dissolved oxygen and the

desired water quality parameters. Pressures can be maintained during the acclimation period between surface pressure (≈ 101.3 kPa) and 414 kPa (depth equivalent ≈ 32 m). The system can drop the pressure from 414 kPa to close to the vapor pressure of water in 0.1 s. Because each chamber is controlled separately, the flow and acclimation pressures can be unique to each chamber simultaneously. A packed injection column was installed with the system and can be used to control the total dissolved atmospheric gas levels within the water up to 150% before it is transferred to the chambers (Stephenson et al. 2010).

A standard test consisted of fish being introduced into the chambers and allowed to acclimate in the partially filled chamber for approximately 24 hr. After this time, the program completely fills the chamber and closes the inflow and outflow in preparation to run the pressure flux program. A pressure change scenario is initiated by directing the program to load the predetermined pressure simulation profile. This process activates a servo motor that controls a piston and subsequently initiates a pressure profile. The GUI displays the complete exposure instantaneously and saves the pressure measurements sampled at 1,000 Hz. Upon completion of the pressure simulation, profile air slowly enters while water is removed from the chamber to a depth of 2.54 cm without disrupting the surface pressure conditions (Stephenson et al. 2010).

A.2.6 NEW SOUTH WALES DEPARTMENT OF PRIMARY INDUSTRY

The New South Wales Department of Primary Industry (NSW DPI) (Port Stephens, New South Wales, Australia) oversaw the construction of a pressures system to investigate fish passage and hydraulic conditions of undershot irrigation weirs and rapid decompression conditions present at mini hydropower facilities (Boys et al. 2013). The system consists of two rectangular pressure chambers measuring 0.7 m x 0.4 m x 0.4 m giving an interior volume of 88 L (Figure A.8). The internal space of each chamber can be accessed through a lockable lid on the top. The top, bottom, and ends are constructed of stainless steel. Flat glass windows at the front and back allow for viewing of the internal space. The chambers are designed to achieve a maximum decompression from 200 kPa to 20 kPa absolute. The system can also accommodate the nadir pressures expected at mini hydropower facilities as well as those expected in Kaplan turbines at high head hydropower dams (Boys et al. 2013).

Pressure is applied within each chamber by means of a dedicated centrifugal pump and controlled by a dedicated computer program with a GUI. The GUI controls an actuated outlet valve downstream to control flow and water pressure in the chambers. This allows chambers to hold acclimation pressure constant and enables water to continually flow through the chambers, maintaining dissolved oxygen and water quality levels (Boys et al. 2013).

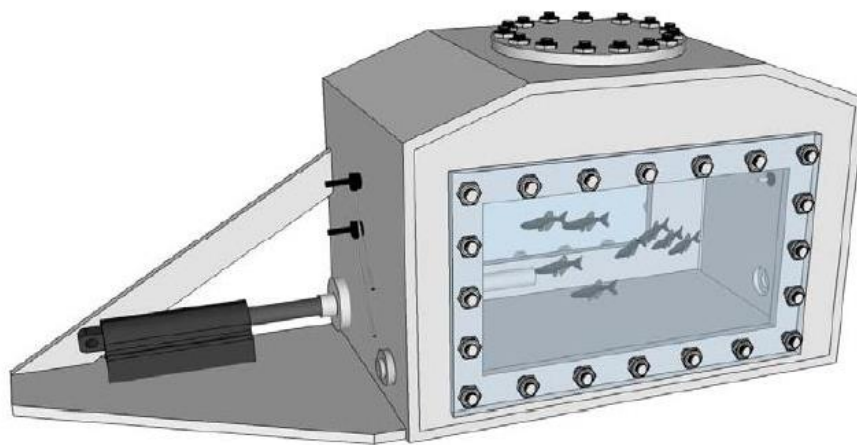


Figure A.8. Model of the NSW DPI pressure chambers. Image from Boys et al. (2013).

A standard test is conducted similarly to tests conducted in the PNNL aquatic barotrauma chambers. Fish are introduced into the chambers and allowed to acclimate in the partially filled chamber for approximately 24 hr. After this time, chamber filling is initiated from the GUI and the inlet and outlet are closed in preparation for running the pressure flux program. A pressure change scenario is initiated by directing the GUI to load the predetermined pressure simulation profile. This process activates an electromagnetic actuator with a 20 mm rod moving approximately 100 mm in about 0.25 s that controls a piston and subsequently initiates a pressure profile. The GUI displays the complete exposure instantaneously and saves the actual pressure measurements sampled. Upon completion of the pressure simulation, profile air slowly enters while water is removed from the chamber to a depth of 2.54 cm without disrupting the surface pressure conditions. Sensors automatically monitor water pressure, dissolved gas pressure, and temperature within the chambers and send these data to the control software (Boys et al. 2013).

A.3 FLUID SHEAR TESTING APPARATUSES

Several apparatuses have been designed and operated to simulate exposure to the fluid shear that fish may experience during turbine passage. In general, a submerged jet powered by a pump is used to generate the flow and fluid shear. Fish are introduced into the zone of fluid shear and then recaptured after exposure for examination.

A.3.1 U.S. ARMY CORPS OF ENGINEERS NORTH PACIFIC DIVISION FLUID SHEAR APPARATUS

A testing apparatus located at the USACE facility at the North Pacific Division Hydraulic Laboratory (Bonneville, Oregon) was developed to conduct fluid shear experiments on Chinook and coho salmon smolts (Johnson 1970b, 1972). The test system consisted of a tank measuring 6.1 m wide, 12.2 m long, and 1.8 m deep with a submerged jet nozzle at a depth of 0.6 m at one end of the tank. Two sized nozzles were used on the jet, a 10 cm and a 15.2 cm diameter nozzle. Exit velocities ranged from 17.5 to 28.0 m s⁻¹. Fish were released initially into a 15.2 cm pipe and then into a 35.5 cm pipe just prior to being ejected into the test tank through the nozzle. High-speed video was used to document fish exposures at the nozzle entry location. Fish exited the tank in a random orientation (headfirst, tailfirst, or broadside).

A.3.2 NATIONAL POWER MARINE AND FRESHWATER BIOLOGY UNIT SHEAR TESTING SYSTEM

The fluid shear testing system was located at the National Engineering Laboratories (East Kilbride, United Kingdom). Hydraulic shear effects on fish were investigated using a high-velocity water jet submerged in a flume tank. The apparatus generated a shear region where fish were injected. The jet flows and dimensions were designed to generate shear stresses of comparable magnitude to those generated by the trailing edge of turbine blades.

The system consisted of a 5.5 kVA centrifugal pump that had a maximum discharge of approximately 25 m³ s⁻¹. The discharge from the pump was measured on the flow indicator and could be regulated by a combination of the throttle and bypass valves (Figure A.9). Pumped water was discharged to a flume tank, measuring 8 m long x 1.5 m wide x 1 m height, with a water depth of 0.6 m. The jet comprised a flat nozzle (rectangular opening), with opening dimensions of 50.8 mm (width) x 6.35 mm (height). This was positioned at mid-width in the flume section and at a depth of 20 cm below the water surface. The maximum estimated shear stress value of 3,410 N m⁻² (strain rate = 1153 cm s⁻¹ converted by Neitzel et al. 2000) can be attained at a jet exit velocity of 20 m s⁻¹ (1.33 jet widths downstream of the jet). The jet is oriented along the long axis of the tank, parallel to the tank walls and floor. Fish were introduced into the jet via an induction tube system, with an exit close to the nozzle (Figure A.10). The fish induction system comprised an outer sleeve to facilitate induction tubes of various sizes corresponding to the size of the fish to be tested. A small volume of water was injected inside the tube to act as a lubricant to facilitate fish

passage. A plexiglass chamber (35 x 62 cm) was constructed to provide a camera viewing window above the jet (Turnpenny et al. 1992).

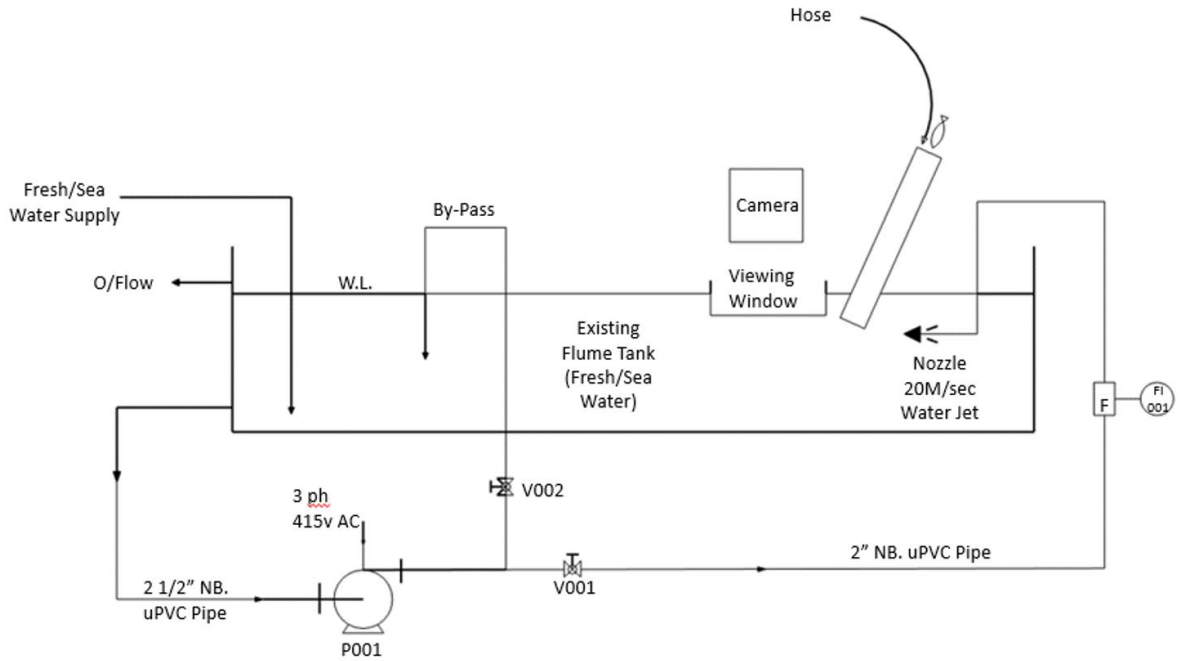


Figure A.9. Side view diagram of the National Power Marine and Freshwater Biology Unit Shear Testing System. Image recreated from Turnpenny et al. (1992).

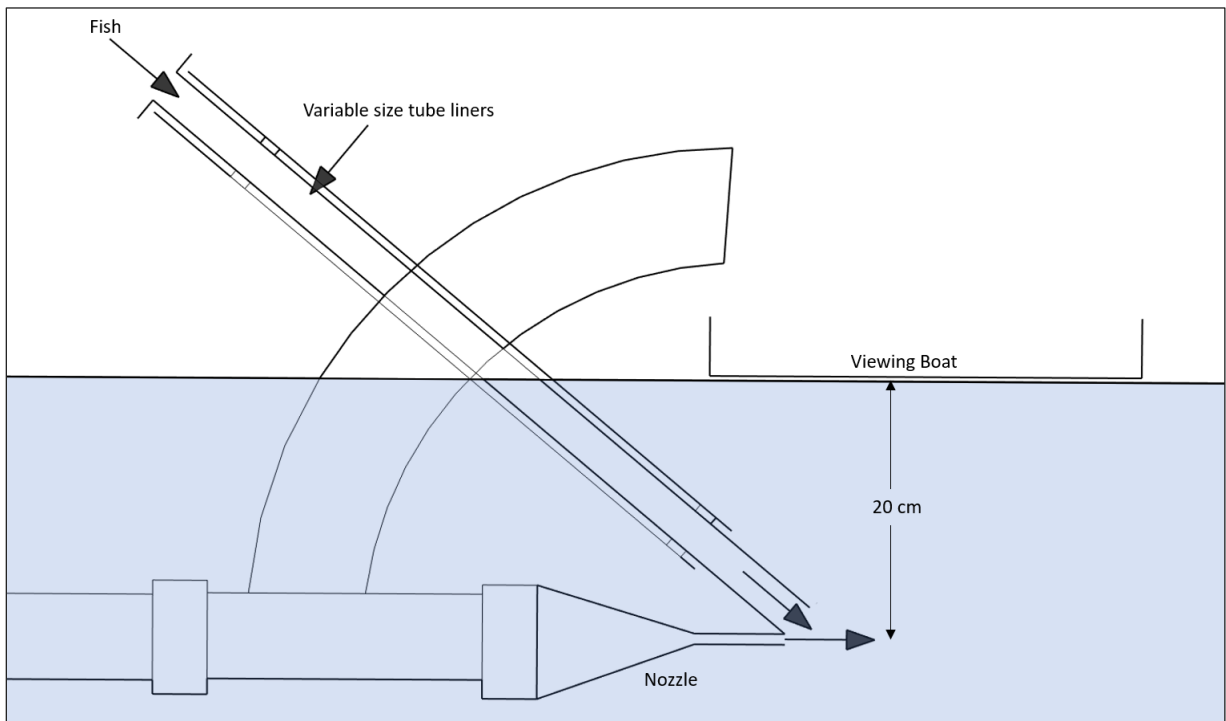


Figure A.10. Diagram of the fish induction system, water jet nozzle and viewing boat from the National Power Marine and Freshwater Biology Unit Shear Testing System. Image recreated from Turnpenny et al. (1992).

A.3.3 PACIFIC NORTHWEST NATIONAL LABORATORY FLUID SHEAR TESTING FACILITY

The PNNL Fluid Shear Testing Facility (FSTF) was constructed in 1998 as part of research supported by the DOE Advanced Hydropower Turbine System Program. The facility consists of a rectangular flume containing a submerged water jet to create a quantifiable shear environment consistent with conditions expected within a hydroelectric turbine. The modular fiberglass flume is 9 m long by 1.2 m wide by 1.2 m deep (Neitzel et al. 2004). A conical stainless-steel nozzle that begins at 25.4 cm diameter and is constricted to a circular 6.35 cm diameter over 50.8 cm in length is bolted to a flange inside the flume (Figure A.11). This nozzle configuration provided a contraction ratio of 5:1 that effectively accelerated flow and reduced non-uniformity in the inlet velocity distribution. The pump/nozzle system is capable of creating exit velocities in excess of 20 m s^{-1} and strain rates of $1,185 \text{ s}^{-1}$ ($\Delta y = 1.8 \text{ cm}$). A flow conditioner is incorporated upstream of the nozzle to reduce inlet turbulence. Clear acrylic ports are located on the side and bottom at the nozzle end of the flume to facilitate high-speed videography as fish enter and exit the shear environment. The nozzle exit is submerged under $\sim 0.6 \text{ m}$ of water. For the slow-fish-to-fast-water entry mechanism, test fish are introduced into the jet through 60 cm long various diameter polycarbonate deployment tubes fastened above the nozzle at an angle of 30° (Figure A.12). The terminus of the deployment tube is just above the terminus of the nozzle and has a 1 cm horizontal separation width. This separation width prevents fish from exiting the test without being subjected to the shear environment. Fish can also be introduced within the nozzle by inserting fish into a 1 m long section of 25.4 cm diameter acrylic tube located upstream from the conical section (Figure A.12). For this scenario, fish are projected out the terminal end at a desired exit velocity and used to simulate shear impacts in the periphery of an elevated waterway into the receiving pool (Johnson et al. 2003). In addition, fish can be projected from inside the nozzle into stationary structures to simulate strike impacts. Some of the strike impacts tested include simulated flip lips (used at the base of spillways to dissipate TDG) or strike with turbine runner or blades.

A 75 hp electric pump (ITT model 150) controlled by a BALDOR Adjustable Speed Drive, ID15H460-EOTM3 variable-speed motor drive is used to circulate water through the flume. The system is capable circulating up to $11,356 \text{ L m}^{-1}$ of water through a 25.4 cm polyvinyl chloride (PVC) pipe. For most shear-related experiments, water is constricted through a 6.35 cm nozzle. A remote keypad is used to program the operating frequency (Hz) to achieve the desired velocity at the nozzle. The pump, controller, and flume were designed to create conditions simulating the shear environment that may occur within a hydroelectric turbine.

The downstream section of the flume can be segregated with barrier netting to confine a group of predator fish so that tested fish can be exposed by removing a mesh screen to determine post exposure susceptibility to predation (Neitzel et al. 2004).

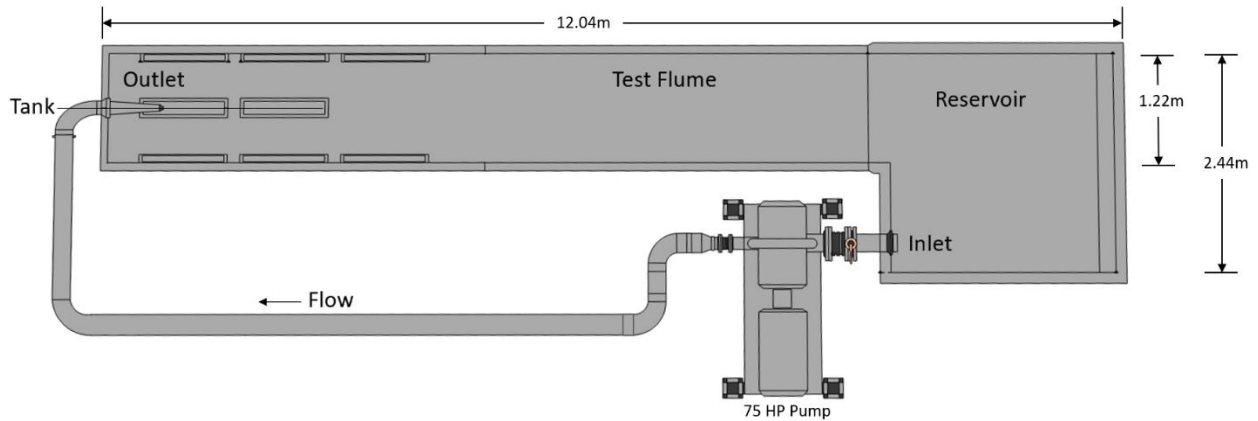


Figure A.11. Top view diagram of the PNNL FSTF, highlighting the flume, reservoir, pump and outlet (water jet nozzle). Figure recreated from Neitzel et al. (2000).

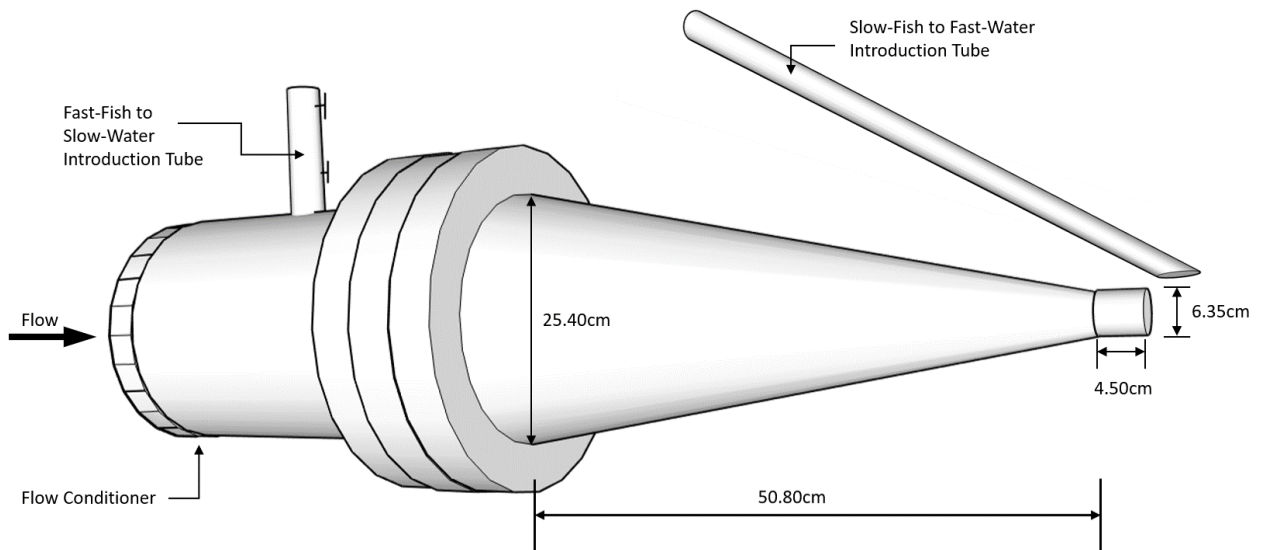


Figure A.12. Diagram of the water jet nozzle and fish introduction tubes for the PNNL FSTF. Figure recreated from (Deng et al. 2010).

A.3.4 NEW SOUTH WALES DEPARTMENT OF PRIMARY INDUSTRY FLUID SHEAR TESTING SYSTEM

The NSW DPI fluid shear testing system was constructed in 2012 at the University of New South Wales Water Research Laboratory. The system comprises a transparent cylindrical plexiglass flume, 1.95 m long and 0.44 m in diameter, and has been used to determine critical tolerances of fish to different magnitudes of fluid shear. It is a closed circular system with water circulated using an electric pump (Grundfos NBG 125, 3-phase, Max discharge 153 m). The maximum water velocity through a 5 cm nozzle diameter is 18.3 m s^{-1} . The flume was connected at one end to a fiberglass reservoir tank (2.10 m long x 2.10 m wide x 0.9 m in depth; Figure A.13). The remaining loop consists of 15 cm diameter PVC pipe. At the entrance to the cylindrical flume, a conical plastic nozzle was installed to reduce the diameter flow from 15 cm to 5 cm (Figure A.13). The restriction caused by this reduction created a high-velocity submerged jet when the pump was operated. The approach generates a quantifiable shear environment where water from the flume becomes entrained in the jet stream. A shut-off valve is installed within the circulating line to reduce the pump output and enable flow rate manipulation at the nozzle. A clear polycarbonate tube was fixed above the submerged jet at an angle of 30° and was used to introduce fish within 30 mm of the submerged jet

(Figure A.14). A flow meter (Wollman Silver Turbo Water Meter, ARAD Waterworks) was used to calculate overall pump discharge and a pitot tube was used to conduct velocity measurements at the point where fish were released, just above the nozzle terminus.

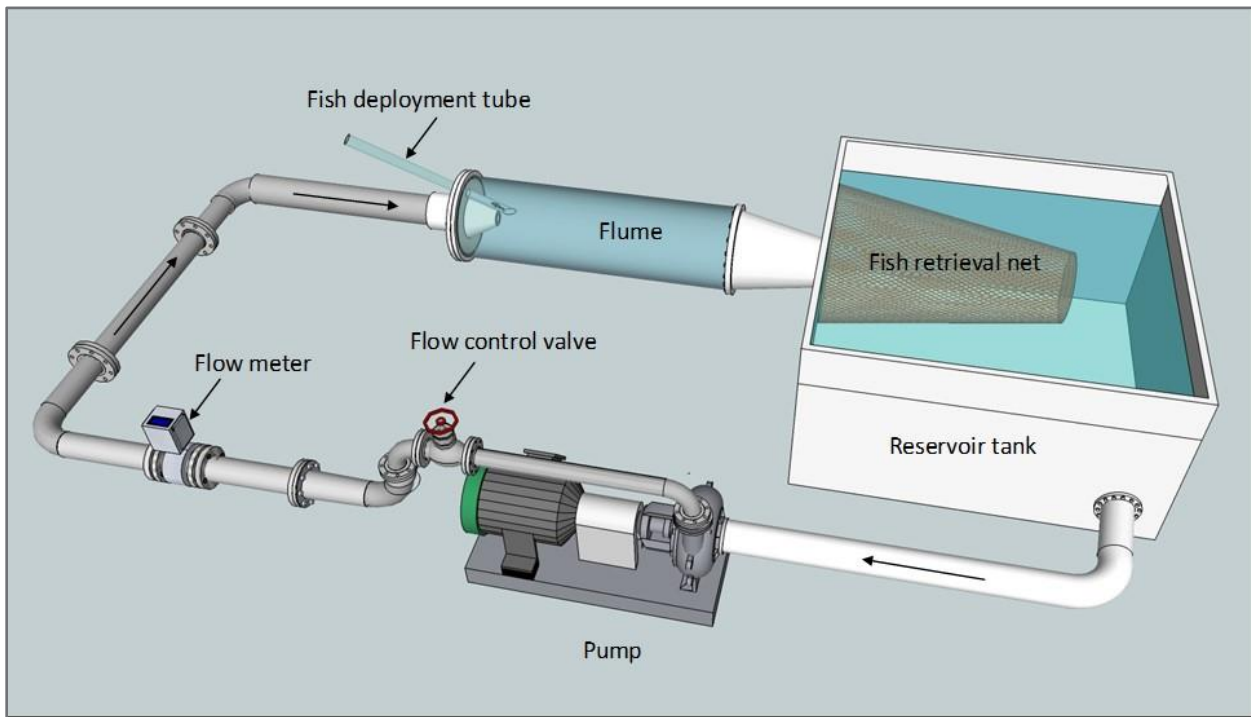


Figure A.13. Schematic of the shear flume. Fish are released in the fish deployment tube, exposed to a jet in the flume, then collected in the retrieval net, before being transferred to holding facilities. Image from Boys et al. (2014b).

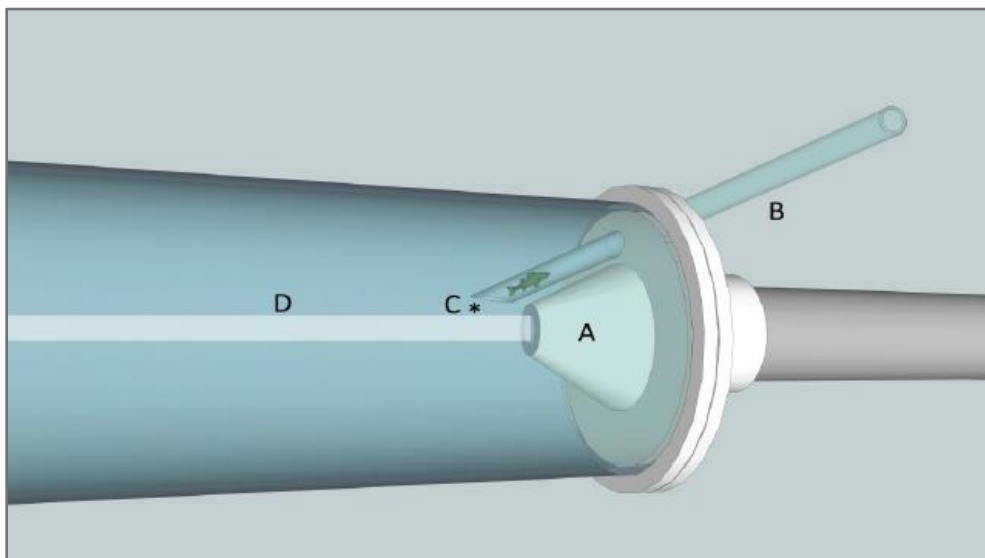


Figure A.14. Plan view of the jet in the test facility that shows the schematic of the flow establishment zone of the flume, showing the nozzle (A), the deployment tube (B), the edge of the jet and fish exposure point (C) and location of the flow establishment zone (D). Image from Boys et al. (2014b).

HYDROPASSAGE

U.S. DEPARTMENT OF ENERGY

U.S. DEPARTMENT OF
ENERGY

Energy Efficiency &
Renewable Energy



*For information about licensing the
BioPA toolset, HBET, and Sensor Fish:*

Sara Hunt

PNNL Commercialization Manager
206.528.3535 | Sara.Hunt@pnnl.gov

For technical information:

HydroPASSAGE@pnnl.gov

HYDROPASSAGE.ORG